



RHODES UNIVERSITY
Where leaders learn

**RECOVERY AND MOLECULAR IDENTIFICATION OF
AICHI VIRUS 1, ENTERIC HUMAN BOCAVIRUSES AND
ENTERIC HUMAN ADENOVIRUSES IN UNTREATED
SEWAGE AND MUSSEL SAMPLES COLLECTED IN THE
EASTERN CAPE PROVINCE OF SOUTH AFRICA**

Thesis submitted in the fulfilment of the requirements of the degree

Master of Science (Microbiology)

At Rhodes University

BY

OIKWATHAILE ONOSI

Department of Biochemistry and Microbiology, Rhodes University,
Grahamstown 6140, South Africa.

March 2018

Abstract

Gastroenteritis, commonly known as diarrhoeal disease, is one of the top killers responsible for substantial human morbidity and mortality especially in third world countries where most people do not have access to potable water and where hygiene levels are low. Many bacterial, viral and protozoal agents are known causes of gastroenteritis and viral gastroenteritis is responsible for over 70% of cases. Rotaviruses are the main causes of viral gastroenteritis and are responsible for most of the cases worldwide. Other viral agents associated with this disease include human noroviruses, Aichi virus 1, enteric human bocavirus, enteric human adenovirus and many other emerging viral agents such as klassivirus, Saffold virus, cosavirus and others. In 2009 the South African government introduced a rotavirus vaccine, RotaRix™ into the expanded programme on immunisation (EPI). More than a 50% decrease in diarrhoea related morbidity and mortality due to rotavirus infections was noted during surveillance studies on the efficacy of the vaccine. However, over 40% of cases of gastroenteritis are of unknown aetiology. The present study aimed to perform a preliminary study to investigate the presence of Aichi virus 1 and enteric human bocaviruses in the Eastern Cape Province by the use of molecular techniques. Furthermore, the study aimed to add to the limited molecular data about enteric adenoviruses in South Africa. Samples used in this study were swab samples collected from Belmont Valley Wastewater Treatment Plant in Grahamstown, South Africa, as well as mussel samples collected from the Swartkops River in Port Elizabeth, South Africa. Both raw sewage and shellfish give a broad idea of what microbes are circulating in the communities. In the present study, twenty swabs and twenty mussel samples were prepared by centrifugation, sonication and filtration. Samples were then subjected to transmission electron microscopy (TEM) analysis, for which the electron micrographs revealed presence of viral particles with diameters ranging from around 20 nm to just over 100 nm. Viral nucleic acids were extracted from 140 µL of the twenty swabs and twenty mussels samples using the QIAamp® Viral RNA Mini Kit, following manufacturer's instructions. For detection of Aichi virus 1 from the swab and mussel samples three reverse transcriptase- polymerase chain reaction (RT-PCR) assays using the Verso 1-Step RT-PCR Hot-Start Kit were developed. The first RT-PCR assay targeted amplification of the highly conserved 5' UTR using published primers. However, despite many amplification attempts no positive results were obtained from both swab and mussel samples. It was only after the addition

of DMSO (to a final concentration of 10%) that one swab sample was positive for this assay. In addition, a 2-step RT-PCR was developed using the Maxima H Minus First Strand cDNA Synthesis Kit. By using this 2-step RT-PCR assay, an additional swab sample was positive for the Aichi virus 1 5' UTR. Using Basic Logarithm Alignment Search Tool (BLAST) analysis these two samples were 98% identical to an Aichi virus isolate from South Korea. The second one-step RT-PCR assay targeted amplification of the 266 bp partial 3CD coding region of Aichi virus 1 using published primers. By using this assay, positive results were obtained from both the swab and mussel samples, which when analysed by BLAST were all 99% identical to various Aichi virus 1 isolates in GenBank. A phylogenetic tree constructed based on this region showed that isolates from the present study clustered with Genotype B isolates in GenBank. The third assay was a semi-nested RT-PCR assay that targeted amplification of the hypervariable VP1 coding region of Aichi virus 1 using a combination of published primers and those designed in the present study. Amplicons which were 472 bp in size were produced from two swab samples. When analysed by BLAST, these two swab samples had percentage identities of 98% to an Aichi virus isolate from South Korea. A phylogenetic tree constructed based on this region showed that isolates from the present study clustered with Genotype B isolates in GenBank. This was consistent with phylogenetic results discussed above which were based on the partial 3CD region. For detection of enteric human bocaviruses from the swab and mussel samples a nested polymerase chain reaction (PCR) assay, using the Ampliqon Taq PCR kit (Ampliqon Bio Reagents and Molecular Diagnostics, Denmark) was developed based on PCR amplification of the 382 bp partial VP1/VP2 coding region using published primers. A total of six swab samples and six mussel samples were analysed for which five swabs and six mussel samples gave positive results. When analysed by BLAST, the swab samples had percentage identities of between 98% and 99% to an enteric human bocavirus 3 strain from China while the mussel samples were all 99% identical to an enteric human bocavirus 2 isolate from Australia. A phylogenetic tree constructed based on this VP1/VP2 region showed that isolates from the present study clustered with human bocavirus 2 and human bocavirus 3 isolates in GenBank for those isolated from swab samples and mussel samples respectively. Lastly, for detection of enteric human adenoviruses from the swab and mussel samples a nested PCR assay, using the Ampliqon Taq PCR kit (Ampliqon Bio Reagents and Molecular Diagnostics, Denmark) was developed. This reaction was based on PCR amplification of the 168 bp partial hexon coding region using published primers for which ten swab samples gave

positive results. When analysed by BLAST, the swab samples had percentage identities of between 96% and 99% to enteric human adenoviruses in GenBank. A phylogenetic tree constructed based on the hexon coding region showed that isolates from the present study clustered with subtypes C, D and F which are associated with gastroenteritis worldwide. Despite several amplification attempts no positive results were obtained from mussel samples. The results from the present study show that Aichi virus 1, enteric bocaviruses and enteric adenoviruses are present in the Eastern Cape Province of South Africa. These viruses could possibly be responsible for enteric infections in South Africa. Although only a few samples were analysed, this study is the first to confirm the presence of Aichi virus 1 and enteric bocaviruses in South Africa and provides a platform for further investigation into prevalence and epidemiology of these viruses in the country.

Table of Contents

Abstract	i
List of Figures	x
List of Tables	xiv
List of abbreviations	xvi
Units and symbols	xvii
Acknowledgements	xix
Chapter 1: Literature Review	1
1.1 Introduction	1
1.2 Health and economic burden of gastroenteritis	1
1.3 Agents of gastroenteritis.....	4
1.4 Viral gastroenteritis	6
1.4.1 Rotaviruses as etiological agents of viral gastroenteritis.....	7
1.4.1.1.1 RotaRix™	9
1.4.2 Human noroviruses as agents of gastroenteritis	10
1.4.2.1 Genome structure.....	10
1.4.2.2 Detection and genotyping of HuNoVs	11
1.4.2.3 Geographical distribution and prevalence of HuNoVs.....	13
1.4.3 Aichi virus 1 as an etiological agent of gastroenteritis.....	14
1.4.3.1 Genome structure.....	14
1.4.3.2 Molecular detection and genotyping of AiV-1	16
1.4.3.3 GenBank data on AiV-1	19
1.4.3.4 Geographical distribution and prevalence of AiV-1.....	19
1.4.4 Enteric human bocaviruses as aetiological agents of gastroenteritis.....	21
1.4.4.1 Genome structure.....	21
1.4.4.2 GenBank data on enteric HBoV	25
1.4.4.3 Geographical distribution and prevalence of enteric HBoVs	25
1.4.5 Enteric human adenoviruses as agents of gastroenteritis	27
1.4.5.1 Genome structure.....	27
1.4.5.2 Molecular detection and typing of enteric HAdVs.....	29
1.4.5.3 GenBank data on enteric HAdVs	31
1.4.5.4 Geographic distribution and prevalence of enteric HAdVs.....	31
1.5 Pathways of Transmission for agents of gastroenteritis	34
1.5.1 Faecal-oral as the major transmission mode.....	34
1.5.2 Sewage polluted water as a primary vehicle of transmission of enteric viruses.....	35

1.5.3 Shellfish (Oysters, mussels and others) as primary vehicles of transmission of enteric viruses.....	36
1.6 Motivation, aims and objectives.....	37
1.6.1 Motivation	37
1.6.2 Study Design	38
Chapter 2: Development of sample preparation techniques for PCR assays	40
2.1 Introduction	40
2.2 Materials and methods.....	43
2.2.1 Sample collection- Swabs and mussels	43
2.2.2 Preparation of swab samples for morphological characterisation and nucleic acid extraction	46
2.2.3 Preparation of mussel samples for morphological characterisation of viral particles and nucleic acid extraction.....	48
2.2.4 Determination of morphological features of viral particles from swab and mussel samples by transmission electron microscopy.....	50
2.2.5 Nucleic acid extraction from swab and mussel samples	51
2.2.6 Primers for RT-PCR of HuNoV GII N/S domain of capsid VP1 protein- 342 bp product	51
2.2.7 Preparation of positive control RNA and RT-PCR of HuNoV GII N/S domain of capsid VP1 protein- 342 bp product	53
2.2.7.1 In vitro transcription and RNA clean-up	53
2.2.7.2 Application of a one-step RT-PCR assay for amplification of the N/S domain of the capsid VP1 coding region for the HuNoV GII T7 transcribed Control RNA	53
2.2.7.3 Sensitivity of the Thermo Scientific Verso 1-Step RT-PCR Hot-Start Kit versus the Thermo Scientific Maxima H Minus First Strand cDNA Synthesis Kit	54
2.2.8 Development of a one-step RT-PCR assay for amplification of the N/S junction of the capsid VP1 coding region of HuNoV GII from mussel and swab samples.....	56
2.2.9 Cloning purified PCR products into pJET 1.2/blunt	56
2.2.10 Transformation of competent cells	57
2.2.11 Plasmid extraction and restriction analysis	58
2.2.12 Sequencing of plasmids and BLAST analysis of resultant sequences.....	58
2.3 Results	58
2.3.1 Positive control.....	58
2.3.1.1 Confirmation of positive control plasmid DNA by restriction analysis	58
2.3.1.2 RNA synthesis by In vitro transcription and RT-PCR of positive control RNA.....	59
2.3.1.3 Sensitivity of the Verso 1-Step RT-PCR Hot-Start Kit versus Maxima H Minus First Strand cDNA Synthesis system	60
2.3.2 Swab samples	61
2.3.2.1 Determination of morphological features of viral particles by TEM- Swab samples	61
2.3.2.2 RNA extraction from swab samples	62
2.3.2.3 RT-PCR and gel purification of PCR products from swab samples	63

2.3.2.4 Cloning of RT-PCR products from swab samples into pJET 1.2/blunt vector and restriction analysis of plasmid DNA	64
2.3.3 Mussel samples.....	65
2.3.3.1 Determination of morphological features of viral particles by TEM- mussel samples	65
2.3.3.2 RNA extraction from mussel samples	66
2.3.3.3 RT-PCR and gel purification of PCR products from mussel samples.....	67
2.3.3.4 Cloning of RT-PCR products from mussel samples into pJET 1.2/blunt vector and restriction analysis of plasmid DNA	68
2.3.3.5 BLAST analysis of HuNoV GII PCR products from swab and mussel samples	69
2.4 Discussion	70
Chapter 3: Development of RT-PCR assays for molecular identification of Aichi virus 1 from swab and mussel samples	73
3.1 Introduction	73
3.2 Materials and methods.....	76
3.2.1 Primers for RT-PCR of AiV-1 5' UTR, 3CD coding region and VP1	76
3.2.2 Preparation of positive control RNA and RT-PCR of AiV-1 5' UTR and 3CD junction.....	80
3.2.2.1 <i>In vitro</i> transcription and RNA clean-up	80
3.2.2.2 Application of a one-step RT-PCR assay for amplification of the 5' UTR region of AiV-1 Control T7 transcribed RNA	81
3.2.2.3 Application of a one-step RT-PCR assay for amplification of the AiV-1 partial 3CD Control T7 transcribed RNA.....	82
3.2.3 Development of one-step RT-PCR Assays for swab and mussel samples	83
3.2.3.1 Samples	83
3.2.3.2 RNA extraction.....	85
3.2.3.3 Amplification of the 5' UTR of AiV-1 from mussel and swab samples.....	85
3.2.3.4 Amplification of AiV-1 partial 3CD coding region from swab and mussel samples	86
3.2.3.5 Amplification of AiV-1 partial VP1 from swab and mussel samples	87
3.2.4. PCR clean-up and cloning PCR products into pJET 1.2/blunt vector	88
3.2.5 Transformation of competent cells	89
3.2.6 Plasmid extraction and restriction enzyme analysis	89
3.2.7 Sequencing and BLAST analysis	89
3.2.8 Multiple sequence analysis and phylogeny	89
3.3 Results	90
3.3.1 Positive controls	90
3.3.1.1 AiV- 1 5' UTR	90
3.3.1.1.1 Confirmation of positive control plasmid DNA by restriction Analysis	90
3.3.1.1.2 RNA synthesis by <i>In vitro</i> transcription and RT-PCR of positive control RNA (AiV-1 5' UTR)	91

3.3.1.2 AiV-1 partial 3CD coding region	92
3.3.1.2.1 Confirmation of positive control Plasmid DNA by restriction analysis	92
3.4.1.2.2 RNA synthesis by <i>In vitro</i> transcription and RT-PCR of positive control RNA (AiV-1 partial 3CD)	93
3.3.2 Swab samples	94
3.3.2.1 AiV-1 5' UTR RT-PCR and gel purification	94
3.3.2.2 Cloning of AiV-1 5' UTR RT-PCR products from swab samples into pJET 1.2/blunt vector and restriction analysis of plasmid DNA	96
3.3.2.3 BLAST analysis and multiple sequence alignment of AiV-1 5' UTR PCR products from swab samples	97
3.3.2.4 AiV-1 3CD RT-PCR and gel purification	98
3.3.2.5 AiV-1 partial 3CD coding region (266 bp)- Cloning into pJET 1.2/blunt vector and restriction analysis of plasmid DNA	100
3.3.2.6 AiV-1 partial 3CD coding region- BLAST results	101
3.3.2.7 AiV-1 partial VP1 RT-PCR and gel purification	102
3.3.2.8 AiV-1 partial VP1 coding region- Cloning into pJET 1.2/blunt vector and restriction analysis of plasmid DNA	104
3.3.2.9 AiV-1 partial VP1 coding region- BLAST results	105
3.3.3 Mussel samples	106
3.3.3.1 AiV-1 5' UTR RT-PCR and gel purification	106
3.3.3.2 AiV-1 partial 3CD coding region- RT-PCR and gel purification	106
3.3.3.3 AiV-1 partial 3CD coding region- Cloning into pJET 1.2/ blunt vector and restriction analysis of plasmid DNA	107
3.3.3.4 AiV-1 partial 3CD coding region- BLAST results	108
3.3.3.5 AiV-1 partial VP1 coding region- RT-PCR and gel purification	109
3.3.4 AiV-1 multiple sequence analysis and phylogeny- 3CD region	109
3.4 Discussion	113
Chapter 4: Development of a nested PCR assay for molecular identification of enteric human bocaviruses from swabs and mussel samples.....	117
4.1 Introduction	117
4.2 Materials and methods	119
4.2.1 Primers for PCR amplification of the VP1/VP2 region of the HBoV genome	119
4.2.2 Development of a nested PCR assay for amplification of the VP1/VP2 region of enteric HBoVs	120
4.2.2.1 Samples	120
4.2.2.2 Nucleic acid extraction	121
4.2.2.3 Amplification of the VP1/VP2 region of enteric HBoVs	121
4.2.2.4 Cloning PCR products into pJET 1.2/blunt vector	122
4.2.2.5 Transformation of competent cells	123

4.2.2.6 Plasmid extraction and restriction enzyme analysis	123
4.2.2.7 Sequencing of plasmids and BLAST analysis of resultant sequences.....	123
4.2.2.8 Multiple sequence analysis and phylogeny	123
4.3 Results	124
4.3.1 Swab samples	124
4.3.1.1 Enteric HBoV VP1/VP2 PCR and gel purification	124
4.3.1.2 Cloning of PCR products into pJET 1.2/blunt vector and restriction analysis of plasmid DNA.....	125
4.3.1.3 BLAST analysis of enteric HBoV VP1/VP2 PCR products from swab samples.....	126
4.3.2 Mussel samples.....	127
4.3.2.1 Enteric HBoV VP1/VP2 RT-PCR and gel purification.....	127
4.3.2.2 Cloning of PCR products into pJET 1.2/blunt vector and restriction analysis of plasmid DNA.....	128
4.3.3 BLAST analysis of enteric HBoV VP1/VP2 PCR products from mussel samples.....	129
4.3.4 Multiple sequence analysis and phylogeny	129
4.4 Discussion	132
Chapter 5: Development of a nested PCR for molecular identification of enteric human adenoviruses from swab and mussel samples.....	134
5.1 Introduction	134
5.2 Materials and methods.....	137
5.2.1 Primers for PCR amplification of the hexon gene.....	137
5.2.2 Positive control.....	138
5.2.3 Samples	138
5.2.4 Nucleic acid extraction	138
5.2.5 Nested PCR assay for amplification of the hexon gene	139
5.2.6 Cloning of purified PCR products into pJET 1.2/ blunt vector	140
5.2.7 Transformation of competent cells.....	140
5.2.8 Plasmid extraction and restriction enzyme analysis	140
5.2.9 Sequencing of plasmids and BLAST analysis.....	141
5.2.10 Multiple sequence analysis and phylogeny	141
5.3 Results	141
5.3.1 Positive control.....	141
5.3.1.1 Confirmation of insert by restriction analysis with Xho 1 and Xba1	141
5.3.2 Swab samples	142
5.3.2.1 Enteric HAdV hexon gene PCR and gel purification	142
5.3.2.2 Cloning of PCR products into pJET 1.2/blunt vector and restriction analysis of plasmid DNA.....	144
5.3.2.3 BLAST analysis of enteric HAdV hexon gene PCR products from swab samples	145

5.3.3 Mussel samples.....	147
5.4 Multiple sequence analysis and phylogeny	147
5.5 Discussion	149
Chapter 6: General conclusions and future work.....	152
6.1 Introduction	152
6.2 Distribution and prevalence of Aichi virus 1, human bocaviruses and human adenoviruses	152
6.3 Sample preparation, virus purification and virus detection	154
6.4 Implications for effluent treatment and river water quality.....	158
6.5 Conclusion and future perspectives.....	159
References	161
Supplementary materials	191

List of Figures

Chapter 1

Figure 1.1: Global mortality rates due to diarrhoea in 2005	2
Figure 1.2: Global mortality rates due to diarrhoea in 2015	3
Figure 1.3: A) TEM of rotavirus particles. B) Schematic representation of a rotavirus particle	8
Figure 1.4: Pictorial representation of a HuNoV genome.	11
Figure 1.5: A) Pictorial representation of AiV-1 genome. B) Schematic representation of an AiV-1 virion	14
Figure 1.6: Schematic representation of post translational polyprotein processing of AiV-1 compared to other Picornaviruses.....	15
Figure 1.7: A) Schematic representation of an enteric HBoV genome.	22
Figure 1.8: A) TEM images of HAdV virions. B) Schematic representation of an HAdV virion.....	27
Figure 1.9: Pictorial representation of HAdV hexon protein.....	28
Figure 1.10: Pathways of transmission for agents of gastroenteritis..	35
Figure 1.11: Flow diagram of the study design	39

Chapter 2

Figure 2.1: A) Satellite image of the Belmont Wastewater Treatment Plant, Grahamstown, South Africa. B) Separation grids at the plant where samples were collected.	45
Figure 2.2: A) Satellite image of the Swartkops River. B) Mussels clumped together attached to rocks	46
Figure 2.3: Swab samples (10) pooled to make a single sample	47
Figure 2.4: Mussel samples sorted, dissected and homogenised in glycine buffer.	49

Figure 2.5: The Zeiss Libra 120 transmission electron microscope.	51
Figure 2.6: Schematic representation of the HuNoV N/S domain primer binding sites as on the complete genome of the Lordsdale virus.	52
Figure 2.7: Pictorial representation of pJET1.2/blunt Cloning Vector.	57
Figure 2.8: A) Plasmid map of the HuNoV GII insert (shown in red) cloned into pGEM [®] -T Easy. B) 1% agarose gel electrophoresis of uncut and cut HuNoV GII positive control plasmid DNA.	59
Figure 2.9: A) 1% agarose gel electrophoresis of positive control T7 synthesised RNA of the HuNoV GII N/S domain of the capsid VP1 protein. B) 1% agarose gel electrophoresis of the positive control RT-PCR product (342 bp) of the HuNoV N/S domain of the capsid VP1 protein	60
Figure 2.10: A) 1% agarose gel electrophoresis of RT-PCR products of the HuNoV GII N/S domain of capsid VP1 protein produced using the Maxima H Minus First Strand cDNA Synthesis Kit. B) 1% agarose gel electrophoresis of RT-PCR products of the NoV GII N/S domain of capsid VP1 protein produced using the Verso 1-Step RT-PCR Hot-Start Kit.....	61
Figure 2.11: TEM images of viral particles from swab samples	62
Figure 2.12: 1% agarose gel electrophoresis of nucleic acids extracted from swab samples.....	63
Figure 2.13: 1% agarose gel electrophoresis of RT-PCR products of the HuNoV N/S domain of the capsid VP1 coding region from swab samples.	64
Figure 2.14: A) 1% agarose gel electrophoresis of plasmid DNA from swab sample 2 (S2). B) 1% agarose gel electrophoresis of restriction digest products of the plasmids.....	65
Figure 2.15: TEM images from mussel samples (large mussels)	66
Figure 2.16: 1% agarose gel electrophoresis of nucleic acids..	67
Figure 2.17: 1% agarose gel electrophoresis of RT-PCR products of the HuNoV N/S domain of the capsid VP1 coding region from mussel samples.	68
Figure 2.18: A) 1% agarose gel electrophoresis of plasmid DNA from large mussel sample 1. B) 1% agarose gel electrophoresis of cut and uncut plasmids	69

Chapter 3

Figure 3.1: Schematic representation of the AiV-1 5' UTR primer binding sites on the AiV-1 genome.....	77
Figure 3.2: Schematic representation of the AiV-1 3CD primer binding sites.....	78

Figure 3.3: Schematic representation of the AiV-1 VP1 primer binding sites.	79
Figure 3.4: A) Plasmid map of the AiV-1 5' UTR positive control plasmid DNA. B) 1% agarose gel electrophoresis of uncut and cut AiV-1 5' UTR positive control plasmid DNA.	91
Figure 3.5: A) 1% Agarose gel electrophoresis of positive control T7 synthesised RNA of the AiV-1 5' UTR. B) 1% agarose gel electrophoresis of the positive control PCR product (approximately 1008 bp) of the AiV-1 5' UTR	92
Figure 3.6: A) 1% agarose gel electrophoresis of positive control plasmid DNA consisting of an insert approximately 266 bp of the AiV-1 partial 3CD junction cloned into pGEM [®] -T Vector B) 1% agarose gel electrophoresis of uncut and cut AiV-1 3CD positive control plasmid DNA.	93
Figure 3.7: A) 1% agarose gel electrophoresis of positive control T7 synthesised RNA of the AiV-1 partial 3CD coding region. B) 1% agarose gel electrophoresis of the positive control PCR product (approximately 266 bp) of the AiV-1 partial 3CD coding region	94
Figure 3. 8: A) 1% agarose gel electrophoresis of RT-PCR products of the AiV-1 5' UTR from swab sample 3. B) 1% agarose gel electrophoresis of RT-PCR product of the AiV-1 5' UTR from swab 9.....	96
Figure 3.9: A) 1% agarose gel electrophoresis of plasmid DNA from swab sample 3. B) 1% agarose gel electrophoresis of cut and uncut plasmids.....	97
Figure 3.10: A) 1% agarose gel electrophoresis of RT-PCR products of the AiV-1 partial 3CD coding region from swab samples 1 to 5. B) 1% agarose gel electrophoresis of RT-PCR products of the AiV-1 partial 3CD coding region from swab samples 6 to 10.....	100
Figure 3.11: A) 1% agarose gel electrophoresis of plasmid DNA from swab sample 1. B) 1% agarose gel electrophoresis of cut and uncut plasmids.....	101
Figure 3. 12: 1% Agarose gel electrophoresis of second round PCR products of the AiV-1 partial VP1 coding region from swab samples 6, 7, 9, 11 and 12.	104
Figure 3.13: A) 1% agarose gel electrophoresis of plasmid DNA from swab sample 9. B) 1% agarose gel electrophoresis of cut and uncut plasmids.....	105
Figure 3.14: A) 1% agarose gel electrophoresis of PCR products of the AiV-1 partial 3CD coding region from mussel samples ML1 to ML4. B) 1% agarose gel electrophoresis of PCR products of the AiV-1 partial 3CD coding region from mussel samples ML5 to ML7.....	107
Figure 3.15: A) 1% agarose gel electrophoresis of plasmid DNA from mussel sample 2 (ML2). B) 1% agarose gel electrophoresis of cut and uncut plasmids	108

Figure 3.16: Molecular Phylogenetic analysis of AiV-1 by Maximum Likelihood method based on Tamura 3 substitution model using a 266 bp sequence of the partial 3CD junction. 110

Figure 3.17: Molecular Phylogenetic analysis of AiV by Maximum Likelihood method based on Tamura 3 substitution model using a 472 bp sequence of the partial VP1..... 112

Chapter 4

Figure 4.1: Schematic representation of the HBoV VP1/VP2 region primer binding sites..... 120

Figure 4.2: 1% agarose gel electrophoresis of second round PCR products of the enteric HBoV VP1/VP2 coding region from swab samples..... 125

Figure 4.3: **A)** 1% agarose gel electrophoresis of plasmid DNA from swab sample 4 (S4). **B)** 1% agarose gel electrophoresis of restriction digest products of the plasmids..... 126

Figure 4.4: 1% agarose gel electrophoresis of second round PCR products of the enteric HBoV VP1/VP2 coding region from large mussel samples..... 128

Figure 4.5: **A)** 1% agarose gel electrophoresis of plasmid DNA from mussel sample 4 (ML4). **B)** 1% agarose gel electrophoresis of restriction digest products of the plasmids..... 129

Figure 4.6: Molecular Phylogenetic analysis of enteric HBoV by Maximum Likelihood method based on Hasegawa-Kishino-Yano substitution model using a 382 bp sequence of the partial VP1/VP2 gene..... 131

Chapter 5

Figure 5.1: Schematic representation of the HAdV hexon protein-coding region primer binding sites.. 138

Figure 5.2: **A)** Plasmid map of the HAdV hexon positive control. **B)** 2% agarose gel electrophoresis of uncut and cut adenovirus hexon positive control plasmid DNA..... 142

Figure 5.3: 2% agarose gel electrophoresis of second round PCR products of the enteric HAdV hexon coding region from swab samples 6 to 10..... 144

Figure 5.4: 2% agarose gel electrophoresis of plasmid DNA from swab sample 10 (S10)..... 145

Figure 5.5: Molecular Phylogenetic analysis of enteric HAdV by Maximum Likelihood method based on Tamura 3 substitution model using a 168 bp sequence of the partial hexon gene.. 148

List of Tables

Chapter 1

Table 1.1: Aetiological agents and their direct contribution to human mortality due to gastroenteritis for the year 2015	5
Table 1.2: Rotavirus vaccines	9
Table 1.3: Molecular methods for detection of HuNoVs in some studies around the world.....	12
Table 1.4: Molecular methods used for detection of AiV-1 in some studies.....	17
Table 1.5: Geographical regions and types of samples from which AiV-1 have been detected..	20
Table 1.6: Molecular methods for detection of enteric HBoVs in some studies worldwide	25
Table 1.7: Geographical regions and types of samples from which HBoVs were detected	26
Table 1.8: Molecular methods for detection of enteric HAdVs in some studies	30
Table 1.9: Some common HAdVs serotypes and their corresponding clinical manifestations	31
Table 1.10: Some examples of the geographical regions and types of samples from which enteric HAdVs were detected	33

Chapter 2

Table 2.1: Data pertaining to swab samples analysed.....	48
Table 2.2: Data pertaining to mussel samples analysed.....	50
Table 2.3: Forward and reverse degenerate oligonucleotides for HuNoV GII N/S domain	52
Table 2.4: Cycling parameters for thermal amplification of the capsid N/S domain of the HuNoV.....	54
Table 2.5: Serial dilutions of positive control HuNoV GII T7 synthesised RNA used to estimate the minimum concentration of RNA required to produce PCR products for a one-step RT-PCR assay versus a two-step RT-PCR assay.....	55
Table 2.6: RT-PCR results for swab samples	63
Table 2.7: RT-PCR results for mussel samples.....	67
Table 2.8: BLAST analysis results of PCR products of the HuNoV N/S domain of capsid VP1 coding region from swab (S) and large mussel (ML) samples	70

Chapter 3

Table 3.1: Forward and reverse oligonucleotides for AiV 5' UTR	76
Table 3.2: Forward and reverse oligonucleotides for AiV-1 3CD	77
Table 3.3: Forward and reverse oligonucleotides for PCR amplification AiV-1 VP1 region	79
Table 3.4: Cycling parameters for the first round PCR reaction to amplify a 1008 bp product of the AiV-1 5' UTR.	81
Table 3.5: Cycling parameters for the nested second round PCR reaction to amplify a 996 bp region of the AiV-1 5' UTR	82
Table 3.6: Cycling parameters to amplify a 266 bp partial 3CD coding region of AiV-1.....	83
Table 3.7: Data pertaining to swab samples analysed for AiV-1.....	84
Table 3.8: Data pertaining to mussel samples analysed for AiV-1	84
Table 3.9: Cycling parameters for the PCR amplification of AiV-1 partial VP1 region.....	88
Table 3.10: PCR results of the AiV-1 5' UTR assay for swab samples	95
Table 3.11: BLAST analysis results of AiV-1 5' UTR products from swab samples 3 and 9.....	98
Table 3.12: AiV-1 3CD RT-PCR results for swab samples.....	98
Table 3.13: BLAST analysis results of the AiV-1 partial 3CD products (266 bp) from swab samples	102
Table 3.14: PCR results of the AiV-1 partial VP1 assay for swab samples	103
Table 3.15: BLAST analysis results of the AiV-1 partial VP1 products from swab samples.....	105
Table 3.16: AiV-1 3CD RT-PCR results for mussel samples.....	106
Table 3.17: BLAST analysis results of the AiV-1 partial 3CD products (266 bp) from mussel samples.....	109

Chapter 4

Table 4.1: Forward and reverse oligonucleotides for HBoVs.....	119
Table 4.2: Data pertaining to swab samples analysed for enteric HBoVs	120
Table 4.3: Data pertaining to mussel samples analysed for enteric HBoVs	121

Table 4.4: Cycling parameters for the first and second round PCR reaction	122
Table 4.5: PCR results of the enteric HBoV VP1/VP2 assay for swab samples	124
Table 4.6: BLAST analysis results of PCR products of the enteric HBoV VP1/VP2 coding region from swab (S) samples.....	126
Table 4.7: PCR results of the enteric HBoV VP1/VP2 assay for mussel samples	127
Table 4.8: BLAST analysis results of PCR products of the enteric HBoV VP1/VP2 coding region from large mussel (ML) samples	129

Chapter 5

Table 5.1: Forward and reverse oligonucleotides for enteric HAdV.....	137
Table 5.2: Cycling parameters for the second round PCR reaction.....	139
Table 5.3: PCR results for swab samples.....	143
Table 5.4: BLAST analysis results of PCR products of the enteric HAdV hexon coding region from swab (S) samples.....	146

List of abbreviations

5' UTR	5' untranslated region
3' UTR	3' untranslated region
ADH	Adenovirus Hexon
AiV-1	Aichi virus 1
DNA	Deoxyribonucleic Acid
EIP	Expanded Immunisation Programme
ELISA	Ezyme Linked-Immunsorbent Serological Assay
HAdV	Human adenoviruses
HBoV	Human bocavirus
HuNoVs	Human noroviruses
IRES	Internal ribosome entry sites
HuNoV	Human norovirus

NP-1	Nuclear-phosphoprotein
PCR	Polymerase chain reaction
PEG	Polyethylene glycol
RdRp	RNA-dependent RNA polymerase
RNA	Ribonucleic Acid
rRNA	Ribosomal Ribonucleic acid
RT-PCR	Reverse transcriptase polymerase chain reaction
qRT-PCR	Real time reverse transcriptase polymerase chain reaction
TEM	Transmission electron microscopy

Units and symbols

%	Percentage
°C	Degrees Celcius
μl	Microlitres
μM	Micromolar
μg/mL	Microgram per millitre
bp	Base pairs
g	Gram
kb	Kilobase pairs
kHz	Kilohertz
mM	Millimolar
mg	Milligrams
mm	Millimetre
ml	Millilitre
min	Minute
M	Molar
ng/μL	Nanogram per microlitre

pH

Potential hydrogen

rpm

Revolutions per minute

x g

Times gravity

V

Volts

V/v

Volume per volume

W/v

Weight per volume

Acknowledgements

Funding for this work was provided by the Medical Research Council of South Africa, Rhodes University Research Council as well as the Department of Public Health, Ministry of Health and wellness, Botswana.

In addition, I would like to thank the Almighty God for giving me the strength to fulfil my dreams. Without Him this would have not been possible. Furthermore, I would like to extend my sincere gratitude to the following people for their support and assistance throughout my research project;

- My supervisor Professor Caroline Knox for her professional guidance, patience and undying motherly support.
- Dr Shelley Edwards and Caroline Ross for their assistance on construction of phylogenetic trees.
- Marvin Randal and Shirley Pinchuck for assistance with electron microscopy work
- Professor Brett Pletschke and family for their kindness and encouragement
- Brittany Jaquet, Claire Bramford, Laura Nisbert, Thobeka Mpanza, Tariro Sithole and Anjali Patel for their assistance in the Laboratory
- My laboratory colleagues for their input and making the laboratory a pleasant work space.
- My family, friends and most importantly my wife Ponatshego Onosi for their support, encouragement and prayers during the course of my study.

Chapter 1: Literature Review

1.1 Introduction

Gastroenteritis, also known as diarrhoeal disease, “stomach flu”, “Montezuma's revenge”, "Delhi belly", "la turista", and "back door sprint" among other names is a medical condition characterised by excretion of three or more loose and watery stools per day (Ingle and Hinge, 2012). Symptoms, which normally begin 12-72 hours post infection, include watery stools, vomiting, and nausea. In addition to that, the patient experiences fever, fatigue, head ache and muscle pains if the agent is viral in nature (Barrett and Brown, 2016; Desselberger, 2017; Ingle and Hinge, 2012). This disease mostly affects the young, the old and the immune-compromised. It deprives the body of water and necessary salts leading to dehydration and sometimes death (World Health Organisation, 2017).

Faecal contaminated water and poor sanitation are the leading risk factors for gastroenteritis. Faecal contamination of drinking water occurs as a result of many factors including distribution pipe bursts, sewer pipe bursts, seepage of untreated sewage into underground water sources and inadequately treated drinking water (Ingle and Hinge, 2012). Other risk factors include person-to-person contact as well as contact with animals some of which are known reservoirs such as primates. These animals naturally harbour microbes some of which are pathogenic to man. Asymptomatic adults may also act as reservoirs and transmit the pathogens to those with compromised immunity such as the young, the sick and the immuno-compromised when acting as care givers (Nix *et al.*, 2008).

1.2 Health and economic burden of gastroenteritis

Gastroenteritis leads to health (mortality and morbidity) as well as socio-economic burdens. Although present data shows that gastroenteritis is still a serious health problem, deaths from diarrhoea decreased by an average of 20.8% between 2005 and 2015 globally. However, the disease still remains one of the leading causes of death among all age brackets being responsible for approximately 1.4 million deaths annually (World Health Organization, 2017). Troeger *et al.* (2017) further reported that diarrhoeal disease is a common cause of infant mortality claiming up to 499 000 deaths annually. Moreover, it is the second cause of death in low income nations where it is believed to be responsible for approximately 57% of cases (World Health Organization, 2017). In Sub-

Saharan Africa alone, diarrhoeal disease is responsible for approximately 644 000 (6.7%) deaths annually (World Health Organization, 2014) and in South Africa it was responsible for 13 447 deaths in 2015, of which 3026 were infants less than 5 years of age (Troeger *et al.*, 2017). **Figures 1.1** and **1.2** below show the comparison between diarrhoea related mortality rates for 2005 and 2015. As shown on the figures there was a general reduction in mortality cases worldwide from 2005 to 2015. In 2015 no country had mortality rates above 200 per 100 000 persons as it was the case in 2005. Troeger *et al.* (2017) attributes this reduction in mortality cases to the positive impact of rotavirus vaccines used in many countries including South Africa.

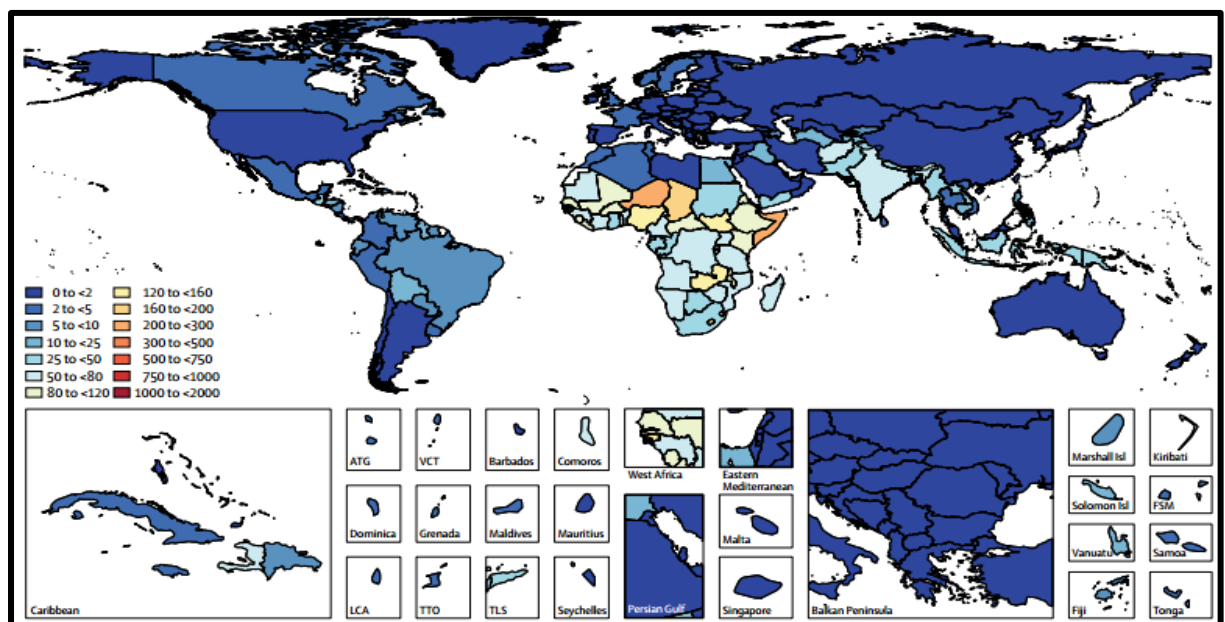


Figure 1. 1: Global mortality rates due to diarrhoea in 2005 (taken from Troeger *et al.*, 2017; [doi.org/10.1016/S1473-3099\(17\)30276-1](https://doi.org/10.1016/S1473-3099(17)30276-1)).

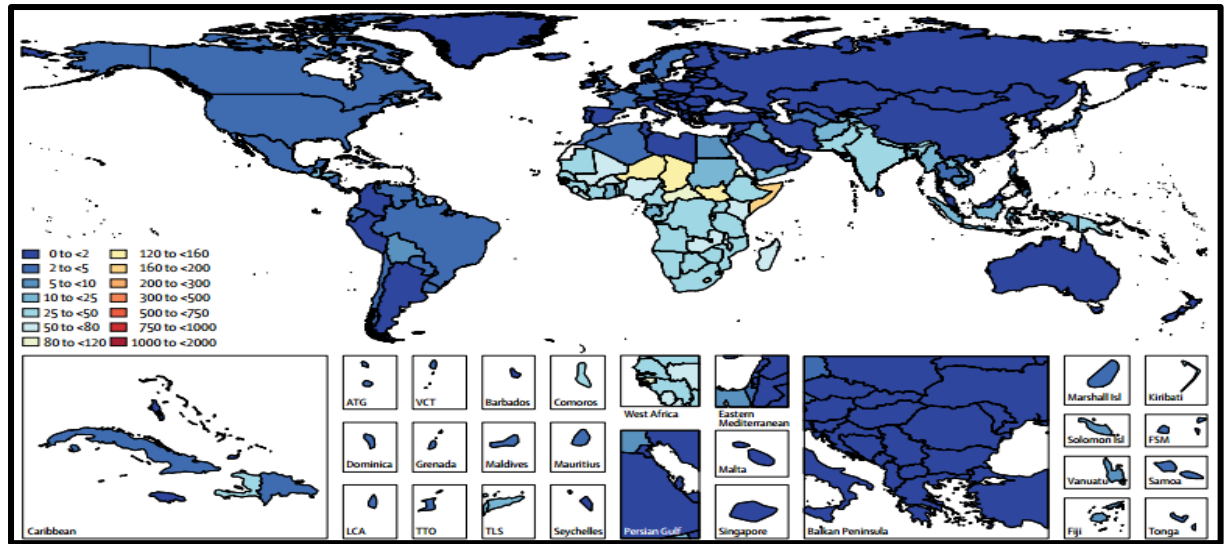


Figure 1. 2: Global mortality rates due to diarrhoea in 2015 (taken from Troeger *et al.*, 2017; [doi.org/10.1016/S1473-3099\(17\)30276-1](https://doi.org/10.1016/S1473-3099(17)30276-1)).

In addition to health associated burdens, there are severe economic losses to governments, companies and individuals due to gastroenteritis because of absenteeism from workplaces due to ill health, leading to shortages of staff and thus low productivity at work (Liu *et al.*, 2012). It was noted that in the United States alone, losses between US\$6.6 and US\$37.1 billion annually occurred as a result of gastroenteritis (Buzby and Roberts, 1997). There are also some instances where food items are recalled from suppliers because they had caused a food borne infection, at times leading to lawsuits, damaged reputation and distrust from customers and thus huge financial losses to the suppliers (Buzby and Frenzen, 1999).

Although there is limited data on the economic burden of gastroenteritis in Africa as a whole, data from individual countries show that hospitalisation due to gastroenteritis poses a significant economic burden to health systems and households. In Rwanda, for example, diarrhoeal diseases costed the health system and households averages of US\$1,607,294; US\$1,741,101; US\$1,656,135; US\$1,327,269 and US\$1,056,931 in 2008, 2009, 2010, 2011 and 2014 respectively (Ngabo *et al.*, 2016). The reductions in costs between 2008 and 2014 were partly attributed to the introduction of a rotavirus vaccine. In Ghana, treatment for diarrhoea was shown to cost the health system US\$2,873,548 and US\$6,023,450 annually for out-patients and in-patients respectively excluding household costs (Aikins *et al.*, 2010).

In South Africa, only two published reports on the economic burden of gastroenteritis to the general public and the government health system were found. A study by MacIntyre and De Villiers (2010) estimated that direct medical costs for diarrhoeal diseases ranged between US\$937 and US\$1140 annually per child under the age of five. Still in the same study, household costs were estimated to be around US\$16 per year for each child. Another study by Chola *et al.* (2015) estimated that the overall interventions to reduce childhood diarrhoeal deaths in South Africa will cost the health system approximately US\$2.6 billion by 2030. These two studies show that gastroenteritis is a serious problem in South Africa with significant negative impact on the country's economy.

1.3 Agents of gastroenteritis

Various organisms are recognised agents of human gastroenteritis. These include protozoal, bacterial as well as viral pathogens (Ingle and Hinge, 2012). For 2015 alone, the World Health Organization reported that 13 aetiological agents were the major cause of episodes of infant diarrhoea as well as deaths. The top three were rotaviruses (146 000 deaths), *Cryptosporidium* spp (60 400 deaths) and *Shigella* spp (54 900 deaths) (Troeger *et al.*, 2017). **Table 1.1** below summarises the 13 aetiological agents of gastroenteritis as well as the total number of people the world over who succumbed to death as a result of those given agents.

Table 1.1: Aetiological agents and their direct contribution to human mortality due to gastroenteritis for the year 2015 (extracted from Troeger *et al.*, 2017).

Aetiological agent of gastroenteritis	Global mortality in 2015
Human rotaviruses	146 000
<i>Cryptosporidium</i> spp	60 444
<i>Shigella</i> spp	54 905
Enteric adenovirus	46 041
<i>Salmonella</i> spp	38 526
<i>Campylobacter</i> spp	30 931
<i>Vibrio cholera</i>	28 835
Enterotoxigenic <i>Escherichia coli</i>	23 649
<i>Entamoeba histolytica</i>	15 471
Human norovirus	14 805
Enteropathogenic <i>Escherichia coli</i>	11 284
<i>Aeromonas</i> spp	7 293
<i>Clostridium difficile</i>	808

In addition to the above, *Giardia* spp, Citomegavirus, *Yersinia* spp, Blastocystishominis, *Aeromonas* spp, *Diantomoeba*, *Escherichia coli* (enteroinvasive), Helmintos (*Strongyloides*) and *Clostridium difficile* are said to be other major agents currently causing diarrhoea worldwide (Barrett and Brown, 2016; Fernández-Banares *et al.*, 2016). Although there are many aetiological agents of gastroenteritis, as described in **Table 1.1** above, the following review will focus on the primary viral agents of the disease.

1.4 Viral gastroenteritis

Viral gastroenteritis is the inflammation of the human gut, caused by several viral agents such as rotaviruses, caliciviruses, astroviruses, enteric adenoviruses and others leading to clinical symptoms ranging from mild diarrhoea to life-threatening dehydration. Incubation period for this syndrome is 1-2 days (Desselberger, 2017) and the infections normally last for less than a week (Fernández-Banares *et al.*, 2016; Ingle and Hinge, 2012). Viral gastroenteritis is believed to account for around 70% of diarrhoeal episodes in children (Webb and Starr, 2005). Although viruses have been suspected to play a role in gastroenteritis since the early 1940s, it was not until 1972 that this was fully confirmed when Norwalk virus (currently known as Norovirus) was directly linked to cases of diarrhoea in the USA. This was followed by human rotavirus in 1975 and, human adenovirus, astrovirus and Sapporo virus in 1980 (Desselberger, 2017; Oude Munnink and Van der Hoek, 2016; Wilhelmi *et al.*, 2003).

From the late 1980s, new and novel viruses associated with gastroenteritis were discovered around the world. These included Aichi virus 1, Saffold virus, cosavirus, polyomavirus, caliviruses, torovirus, bufavirus, tusavirus, recovirus and human bocavirus 2, 3 and 4 (for reviews see Desselberger, (2017); Knox *et al.*, 2012; Oude Munnink and Van der Hoek, 2016; Smits *et al.*, 2016). The clinical significance of some of these new viruses, for example Saffold virus and klassivirus remains unclear to this date due to limited epidemiological data.

Globally, human rotavirus and human norovirus are the major causes of viral gastroenteritis. In 2015 alone they were responsible for a combined 32.3% of all diarrhoea related mortality cases worldwide (Troeger *et al.*, 2017). This was stressed further in a review by Desselberger, (2017) who listed rotavirus and norovirus as the current top most aetiological agents of viral gastroenteritis worldwide, with global detection rates of up to 68% and 25% respectively. In Europe, a survey by Lopman *et al.* (2003) reported that between 1995 and 2000, most outbreaks of gastroenteritis were as a result of human norovirus and human rotavirus infections with norovirus being responsible for over 85% of the cases. In Asia a survey by Dey *et al.* (2014) reported that the most prevalent aetiological agents of gastroenteritis were rotavirus, norovirus, sapovirus, adenovirus, astrovirus and Aichi virus 1 in that order. In Africa, Fischer

Walker *et al.* (2013) stressed the importance of human rotaviruses as the top killer, being responsible for up to 26.8% of diarrhoeal deaths annually.

In South Africa, the role of human rotaviruses as major aetiological agents of gastroenteritis has been extensively reviewed by Steele and Glass (2011). On a more positive note is the observation that, since the introduction of a rotavirus vaccine, Rotarix® (Rixensart, Belgium), in the Expanded Immunisation Programme (EIP) in 2009, rotavirus related infant morbidity and mortality rates have generally declined (National Institute of Communicable Diseases, Annual review 2012/2013; Steele *et al.*, 2012). The National Institute of Communicable Diseases (NICD) recorded a reduction of 54-58% in rotavirus related diarrhoea cases between 2013 and 2015 (National Institute of Communicable Diseases, Rotavirus Surveillance Report, 2014/ 2015).

Although there are many viral agents responsible for gastroenteritis, this review will focus on Aichi virus 1, enteric human bocaviruses and enteric human adenoviruses. Aichi virus 1 is a known viral agent of gastroenteritis that is highly prevalent in Asia and has been detected worldwide from clinical samples of diarrhoeic patients, environmental and shellfish samples, although it has never been detected in South Africa. Enteric human bocaviruses are emerging viruses associated with diarrhoea and have also been detected worldwide from clinical samples of diarrhoeic patients and environmental samples. In South Africa there are published reports on detection of human bocavirus 1 which is not linked to gastroenteritis but respiratory infections (Smuts and Hardie, 2006; Smuts *et al.*, 2008). In relation to enteric human adenoviruses, there are published reports on their detection and role in enteric infections in South Africa although the data is limited (Adefisoye *et al.*, 2016; Chigor and Okoh, 2012; Osuolale and Okoh, 2015; Van Heerden *et al.*, 2005). This review will also highlight the importance of human rotavirus and human norovirus as major aetiological agents of gastroenteritis worldwide including in South Africa. The fact that there is a vaccine rolled out by the South African government to control rotavirus related diarrhoea and death will also be highlighted including the impact of the vaccine on cases of gastroenteritis nationally.

1.4.1 Rotaviruses as etiological agents of viral gastroenteritis

Rotaviruses, family *Reoviridae*, are characterised by their non-enveloped, round icosahedral structure (**Figure 1.3A**). They are about 70 nm in diameter (Wilhelmi *et al.*, 2003). As shown in **Figure 1.3B** below, the outer capsid consists of structural proteins

VP4, the protease cleaved protein (P protein) and VP7, the glycoprotein (G protein). These two outer proteins are the basis for typing of rotaviruses into P and G serotypes. The genes encoding for these outer proteins can segregate independently creating recombinant [P][G] serotypes (Wilhelmi *et al.*, 2003). Furthermore these outer proteins are targets for neutralising antibodies making them important for vaccine development (Harrison *et al.*, 2010). The inner capsid consists of the structural protein VP6, which holds the 11 segmented viral RNA genome. Each of the segments encodes various proteins including the toxin, NSP4, which is believed to cause diarrhoea (Wilhelmi *et al.*, 2003). There are over 100 serotypes classified into 8 species or groups, A-H. Group A rotaviruses are the major causes of gastroenteritis in humans with 6 serotypes namely; (G1P[8], G2P[4], G3P[8],G4P[8], G9P[8] and G12P[8]) being responsible for almost all cases of Rotavirus infections (Doro *et al.*, 2014).

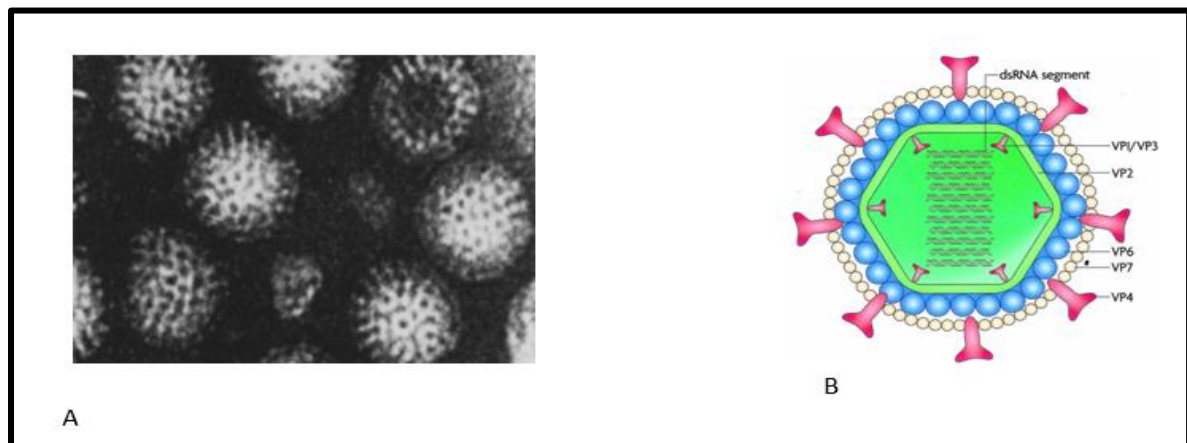


Figure 1.3: **A)** Transmission electron micrographs of rotavirus particles (Kogasaka *et al.*, 1979). **B)** Schematic representation of a rotavirus particle showing the major components of the virion (taken from Dennehy, 2008; doi.org/10.1016/j.vaccine.2007.01.102).

1.4.1.1 Rotavirus vaccines

Due to the tremendous burden of rotavirus infections worldwide, efforts were made since in the early 1980s to make vaccines some of which were withdrawn after clinical trials discovered that they had adverse health effects. For example RotaShield (by Wyeth) was withdrawn from the market in 1999 after discoveries that it compromised bowel movement in infants (Jiang *et al.*, 2010). First generation vaccines were replaced by second generation vaccines such as RotaTeq® (Merck, USA) in 2006 and RotaRix™ (GlaxoSmithKline, Belgium) in 2007. These are all live attenuated rotaviruses. **Table 1.2**

below shows all first generation and second generation rotavirus vaccines including the nature of their backbones. First generation vaccines had their backbones made from animal rotavirus while second generation vaccines had bovine-human rotavirus backbones e.g. RotaTeq® or human rotavirus backbones e.g. RotaRix™.

Table 1.2: Rotavirus vaccines (adapted from a review by Jiang *et al.* (2010)).

Vaccine	Type	Backbone	Valency	Antigens
RI T 4237	First generation	Bovine G6	Monovalent	G6, P6
RRV –MMU	First generation	Rhesus G3	Monovalent	G3, P3
WC3	First generation	Bovine G6	Monovalent	G6, P5
RRV-TV (Rotashield)	Second generation	Rhesus G3	Tetravalent	G1, G2, G4,
Reassortant WC3 (RotaTeq®)	Second generation	Bovine G6	Pentavalent	G1, G2, G3, G4, P8
RI X-4414 (RotaRix™)	Second generation	Human [P8]G1	Monovalent	[P8]G1

Although there are two second generation vaccines used worldwide to control rotavirus related morbidity and mortality namely; RotaTeq® and RotaRix™, this review will only focus on RotaRix™ which is used in South Africa.

1.4.1.1.1 RotaRix™

RotaRix™ is a live, attenuated monovalent human rotavirus G1 P1A[8] strain that is orally administered to infants at 2 and 4 months of age to induce immunity against serotype [P8]G1, which contains the most common VP7 and VP4 antigens and associated with gastroenteritis worldwide. In addition, the vaccine is known to induce immunity

against G3, G4 and G9 serotypes (Dennehy, 2007; Kocabas and Dayar, 2015). Furthermore Dennehy (2007) reported that the vaccine has efficacy of up to 92% against the predominant G1 serotype and up to 88% against G3, G4 and G9 serotypes. According to Kocabas and Dayar (2015) and Wang *et al.* (2015) the global overall general efficacy of RotaRix™ against rotavirus infections is 85%. In South Africa the vaccine efficacy is amongst the highest in Sub-Saharan Africa at 76.9% compared to that of Malawi at 49.4% (Bal and Kurugöl, 2016; Madhi *et al.*, 2010). This vaccine does not completely prevent infections but it prevents severe enteric infections (Wang *et al.*, 2015). The mechanism of protection by this vaccine is poorly understood (Bal and Kurugöl, 2016).

1.4.2 Human noroviruses as agents of gastroenteritis

1.4.2.1 Genome structure

Human noroviruses (HuNoVs) are positive sense, single stranded RNA viruses about 30 nm wide with a genome size of about 7.7 kb (Desselberger and Gray, 2013; Kapikian *et al.*, 1972). Initially they were known as Norwalk-like viruses, named after the city Norwalk in the state of Ohio in the United States of America, where they were first discovered after an outbreak in a school in 1968. As depicted in **Figure 1.4** below, the polyadenylated RNA genome of a HuNoV has three open reading frames, namely ORF 1, ORF 2 and ORF 3. ORF 1 encodes a polyprotein which undergoes enzymatic cleavage to produce several viral proteins including the helicase, protease and RNA-dependent RNA polymerase (RdRp) (Kobayashi *et al.*, 2000A). ORF 2 and ORF 3 encode major capsid protein, VP1 and minor capsid protein VP2 respectively. The VP1, which is relatively conserved, has several domains including two major ones being the protruding (P1 and P2) domain and the shell domain. The protruding domain, which is on the exterior of the capsid, is believed to possess attachment and antigenicity characteristics (Prasad *et al.*, 1999; Vinjé *et al.*, 2004). The shell domain plays a role in the icosahedral shell formation (Prasad *et al.*, 1999). The role of minor protein, VP2, remains unknown to this date.

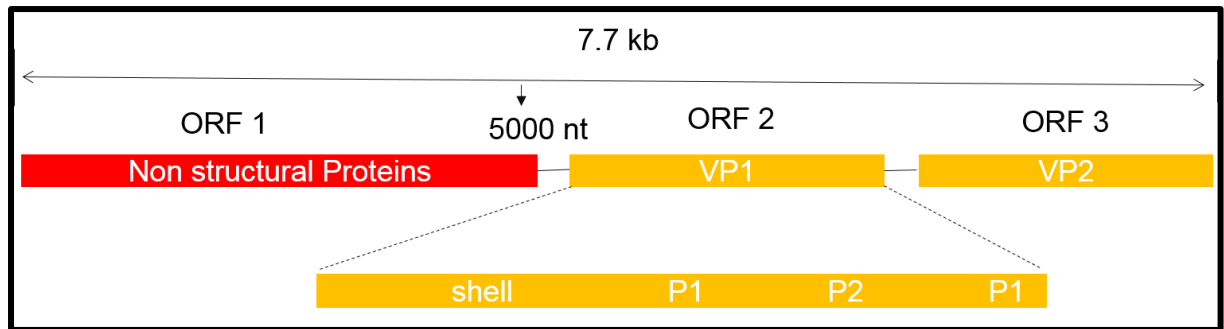


Figure 1. 4: Pictorial representation of a HuNoV genome (adapted from Debbink *et al.*, 2013). It has 3 open reading frames namely ORF1, ORF2 and ORF3 coding non-structural proteins, major capsid protein and minor capsid protein respectively.

1.4.2.2 Detection and genotyping of HuNoVs

Various methods and techniques have been used to isolate and detect HuNoVs from clinical, environmental and shellfish samples. These include transmission electron microscopy (TEM) and Enzyme-Linked Immunosorbent Assay (ELISA). These methods are time efficient and cheap but they are not as sensitive and reliable as modern techniques like reverse transcriptase polymerase chain reaction (RT-PCR) and real-time reverse transcriptase polymerase reaction polymerase chain reaction (qRT-PCR) which are used for detection of HuNoVs from clinical, environmental and shellfish samples in most current studies (see **Table 1.3**). Currently there is no reliable cell culture system to study the infectivity of HuNoVs. The recent model by Jones *et al.* (2014) is yet to be fully understood and validated. The same applies to another promising model by Ettayebi *et al.* (2016). In the absence of a well-established cell culture assay, molecular methods (RT-PCR and qRT-PCR) remain the only reliable ways of detecting HuNoVs.

Table 1.3: Molecular methods for detection of HuNoVs in some studies around the world.

Method	Sample types	Target region	Country of study	References
RT-PCR	human stools	Polymerase region	USA	Parra and Green, 2015
	human stools	N/S domain of capsid	Germany	Kojima <i>et al.</i> , 2002
	oysters	Capsid region	South Korea	Cho <i>et al.</i> , 2016
	water, stools, and environmental swabs	Polymerase region	China	Qin <i>et al.</i> , 2016
qRT-PCR	oysters	Polymerase region	Switzerland	Beuret, 2003
	human stools	Capsid N/S domain	Japan	Fukuda <i>et al.</i> , 2006

PCR amplification of conserved and variable regions of the genome is the cornerstone of molecular characterisation of HuNoVs. The amplification of the polymerase region has been used to detect HuNoVs in many studies (Ando *et al.*, 1995; Green *et al.*, 1968; Le Guyader *et al.*, 1996; Vinjé *et al.*, 1996). This region, which is found in ORF1, has a conserved sequence motif. A study by Katayama *et al.* (2002) reported that even though this region displayed a high average similarity score amongst the strains tested, the primers they designed could not amplify all the genotypes of HuNoVs. Kojima *et al.* (2002) asserted that this was due to high rate of amino acid substitution, especially in the third position of the codon, in this region. Prior to this, Kobayashi *et al.* (2000) had designed primers to amplify the conserved capsid N-terminal/shell domain region of VP1 which were able to amplify many strains of HuNoVs. A challenge arose that these primers had multiple mismatches at the 3' end so they gave false negatives (Kojima *et al.*, 2002). To solve this, Kojima *et al.* (2002), designed genogroup specific primers with

degenerate nucleotides to amplify as many strains as possible by amplification of the region encompassing the capsid N-terminal/shell domain. These primers by Kojima *et al.* (2002) have been used in many studies, including the recent ones for detection of HuNoVs from clinical, environmental and shellfish samples (Bruggink *et al.*, 2017; Fu *et al.*, 2015; Kazama *et al.*, 2016).

Currently there are seven known genogroups of HuNoVs namely; GI, GII, GIII, GIV, GV, GVI and the proposed GVII (Alam *et al.*, 2015). Amongst all these only GI, GII and GIV are recognised as agents of human viral gastroenteritis, especially GII genotype 4 (GII.4) (Aksu and Akçalı, 2016; Alam *et al.*, 2015; Chhabra and Chitambar, 2008; Mans *et al.*, 2013; Van Alphen *et al.*, 2014; Vinje, 2015).

1.4.2.3 Geographical distribution and prevalence of HuNoVs

There are many published reports on detection of HuNoV GI and GII from environmental and shellfish samples worldwide. Katayama *et al.* (2008), Nordgren *et al.* (2009) and Zhou *et al.*, 2017 detected HuNoV G1 and GII from raw sewage in Japan, Sweden and China respectively during surveillance studies. Furthermore, Le Guyader *et al.* (2006A) detected HuNoV GII from oysters implicated in a diarrhoea outbreak in France.

Globally HuNoVs are the second leading cause of viral gastroenteritis after rotaviruses with prevalence rates of up to 25% (Desselberger, 2017). A recent review by Mans *et al.* (2016) revealed that HuNoVs is a serious cause of morbidity and mortality to infants less than 5 years of age across Africa, with an overall prevalence of 13.5% with majority of cases being as a result of GII.4. In South Africa a survey conducted between 2009 and 2013 by Page *et al.* (2017) showed an average prevalence rate of 13.5% to infants less than 5 years old. GII.4 was found to be the most prevalent genotype. In addition to this survey by Page *et al.* (2017), there are many published reports describing the detection of HuNoV G1 and GII and their role as aetiological agents of enteric infections in South Africa (Kabue *et al.*, 2016; Kabue *et al.*, 2017; Mans *et al.*, 2010; Mans *et al.*, 2016; Mans *et al.*, 2014; Smit *et al.*, 1999; Smit *et al.*, 1997). In addition to the detection of HuNoVs in clinical samples, there are various reports describing the detection of HuNoVs, specifically genotypes GI and GII, from environmental samples such as raw sewage water and river water in South Africa during surveillance studies (Jaquet, 2017; Mabasa *et al.*, 2017; Mans *et al.*, 2013; Murray *et al.*, 2013).

1.4.3 Aichi virus 1 as an etiological agent of gastroenteritis

1.4.3.1 Genome structure

Aichi virus 1 (AiV-1), also known as human Aichi virus is a non-enveloped, single-stranded, positive-polarity RNA virus (**Figure 1.5B**) that was first described in Aichi Prefecture, Japan from an oyster-related outbreak of gastroenteritis (Yamashita *et al.*, 1991). This virus belongs to genus Kobuvirus in family *Picornaviridae* (Yamashita *et al.*, 1991; Yamashita *et al.*, 1998). The viral particle is approximately 27–30 nm in diameter and consists of 8,219–8,280 nucleotides, excluding a poly (A) tract (Chang *et al.*, 2013; Sasaki *et al.*, 2001).

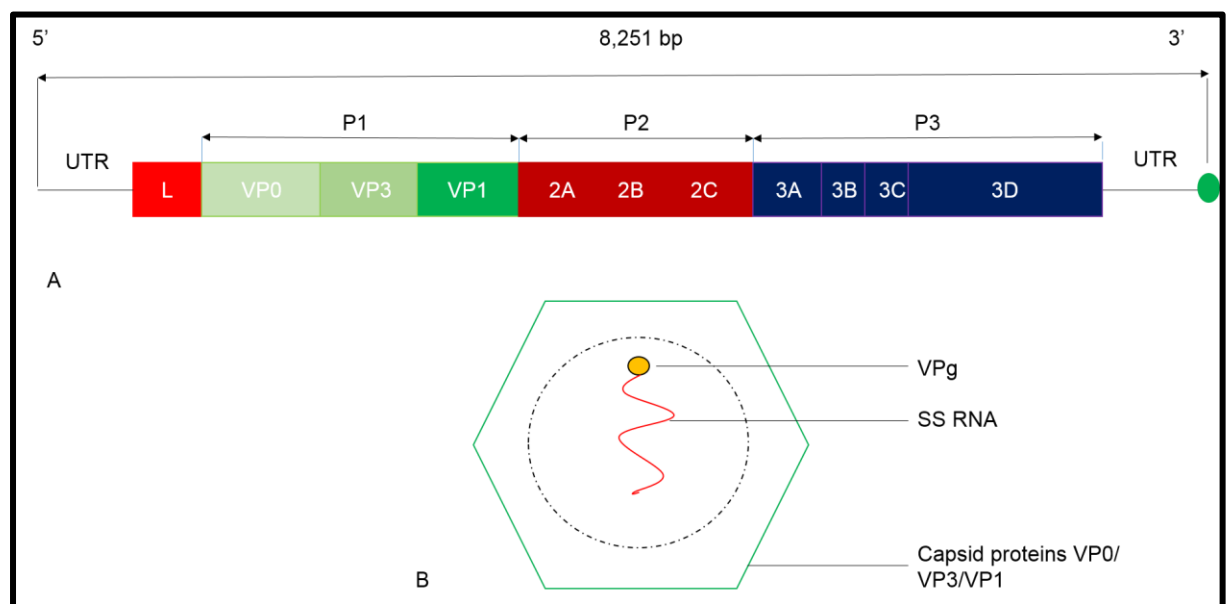


Figure 1. 5: **A)** Pictorial representation of AiV-1 genome showing. From left 5' untranslated region (5' UTR), leader protein (L), capsid proteins (VP0, VP3, VP1), non-structural proteins (2A, 2B, 2C, 3A, 3B, 3C 3D), 3' untranslated region (3' UTR) and poly (A) tail. The genome consist of a polyprotein which is enzymatically cleaved into precursor structural peptides (P1 and P2) and a non-structural one (adapted from Yamashita *et al.*, 1998) (P3) **B)** Schematic representation of an AiV-1 virion (adapted from Yamashita *et al.*, 1998).

The AiV-1 genome has a large open reading frame with approximately 7,302 nucleotides that encodes a potential polyprotein precursor of approximately 2,433 amino acids (aa), that is post translationally cleaved by the 3C^{protease} into mature structural proteins VP0, VP3, and VP1 (Yamashita *et al.*, 1998; Yang *et al.*, 2009). This is in contrast to other

Picornaviruses for which VP0 is further cleaved into VP2 and VP4 as shown below in **Figure 1.6**. In addition to the above structural proteins, the polyprotein is also cleaved into non-structural proteins 2A, 2B, 2C, 3A, 3B, 3C and 3D (**Figure 1.6**). The polyprotein is preceded by a leader protein (L) as well as a 5' UTR and followed by a 3' UTR of approximately 240 nucleotides and a poly (A) tail (**Figure 1.5A** above) (Chang *et al.*, 2013; Oh *et al.*, 2006; Sasaki *et al.*, 2001; Yamashita *et al.*, 1998; Yang *et al.*, 2009).

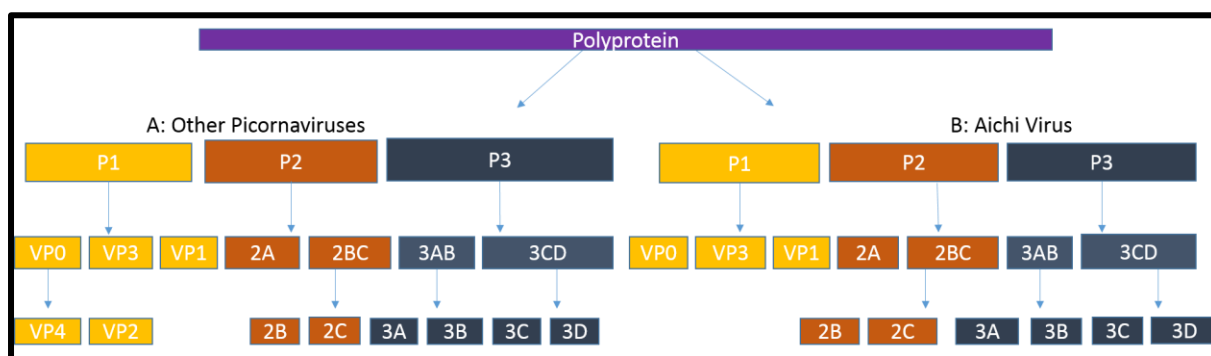


Figure 1.6: Schematic representation of post translational polyprotein processing of AiV-1 compared to other Picornaviruses. Unlike for other Picornaviruses, VP0 is not cleaved into VP4 and VP2 in AiV-1 (adapted from Yamashita *et al.*, 1998).

For the purpose of this study, only 3 regions of the genome namely the 5' UTR, the putative 3CD junction and the VP1 are important for molecular detection and genotyping of AiV-1 and will be discussed.

The UTR is approximately 712 nucleotides. It is preceded by the Leader protein (as shown in **Figure 1.5**) (Yamashita *et al.*, 1998). This region is believed to be involved in replication and encapsidation (Sasaki and Taniguchi, 2003). Stem-loops A to C (all at the 5' end of the 5' UTR), as found out by Nagashima *et al.* (2003) are responsible for replication. The internal ribosome entry sites (IRES) in this region interacts with ribosomes resulting in a ribonucleo-complex that leads to initiation of translation (Hellen and Sarnow, 2001). The 5' UTR is highly conserved in all picornaviruses so PCR amplification of this region aids in molecular detection of the virus (Drexler *et al.*, 2011). However, there is a problem as this region is more stable and resistant to external forces including thermal amplification. This is due to a high GC-content of approximately 60% compared to that of enteroviruses (e.g polio-virus 1) at 45%, rhinoviruses (e.g. human rhino virus 14) at 41%, hepatoviruses (e.g hepatovirus A) at 38%, cardioviruses (e.g. encephalomyocarditis virus) at 49% as well as high degree of secondary structure as a

result of the presence of stem loops in this region (Lukashev *et al.*, 2012; Yamashita *et al.*, 1998; Zhu *et al.*, 2016).

The leader protein (L), which lies upstream of the capsid region, is encoded by 170 amino acids. The leader protein for AiV-1 has a unique nucleotide and amino acid sequence compared to that of other Picornaviruses (Yamashita *et al.*, 1998). This property makes the region useful for molecular detection of AiV-1. The Leader protein is involved in replication and formation of the capsid (Sasaki *et al.*, 2003). The putative 3CD junction encompasses the C-terminus of the 3C and the N-terminus of the 3D (Yamashita *et al.*, 2000). This region is known to possess conserved as well as highly variable sequence motifs at some sites (Yamashita *et al.*, 1998). These characteristics make the 3CD junction less conserved compared to the 5' UTR and hence ideal for molecular identification and genotyping of the virus. The VP1 is the outer most region of the capsid. This makes it a target for AiV-1 antibodies (Chen *et al.*, 2013). Although this region possesses conserved sequence motifs at some sites, it is known to possess higher sequence variability among the AiV-1 genotypes compared to the 3CD region and, as a result of this, it is primarily used for typing this virus from clinical, environmental and shellfish samples (Drexler *et al.*, 2011; Oh *et al.*, 2006; Yamashita *et al.*, 2000).

1.4.3.2 Molecular detection and genotyping of AiV-1

Although various methods such as TEM, ELISA and cell culture (Goyer *et al.*, 2008; Sdiri-Loulizi *et al.*, 2010B; Yamashita *et al.*, 1991) have been used for detection of AiV-1, the most common method in the literature is RT-PCR targeting the conserved and variable regions including the highly conserved 5' UTR, the relatively conserved 3CD junction or the hypervariable capsid region, VP1 (Di Martino *et al.*, 2013; Drexler *et al.*, 2011; Han *et al.*, 2014; Jonsson *et al.*, 2012; Pham *et al.*, 2007; Yamashita *et al.*, 2000). **Table 1.4** below describes molecular methods used for detection of AiV-1 in some studies around the world.

Table 1.4: Molecular methods used for detection of AiV-1 in some studies.

Method	Sample types	Target region(s)	Country of study	References
RT-PCR	human stools	5' UTR	Denmark	Nielsen <i>et al.</i> , 2013
	paediatric stools	3D	Hungary	Reuter <i>et al.</i> , 2009
	oysters	3CD	France	Le Guyader <i>et al.</i> , 2008
	human stools	VP1 and VP3	Japan Bangladesh Thailand	Pham <i>et al.</i> , 2009
	human stools	5' UTR	Germany	Drexler <i>et al.</i> , 2011
qRT-PCR	oysters	3CD	France	Le Guyader <i>et al.</i> , 2008

Drexler *et al.* (2011) designed primers that successfully amplified the region encompassing the highly conserved 5' UTR and the leader protein of AiV-1. The RT-PCR assay using these primers have been described in only two published reports so far for molecular identification and typing of AiV-1 in clinical and environmental samples from Germany and South Korea respectively (Drexler *et al.*, 2011; Han *et al.*, 2014). In addition to these, Nielsen *et al.* (2013) designed and used another set of primers that target the 5' UTR and the leader protein for molecular detection of AiV-1 from clinical samples in Denmark. Furthermore Yip *et al.* (2014) designed and used degenerate primers that amplify a region between the 5' UTR and the leader protein for molecular detection of AiV-1 from clinical samples in Hong Kong. Even though the 5' UTR is highly conserved as reported by Drexler *et al.* (2011), there is limited sequence data available for the 5' UTR RT-PCR assay for AiV-1. Lukashev *et al.* (2012) attributes this to the region being stable as a result of high GC content and high degree of secondary structure rendering it resistant to PCR amplification and difficult to sequence. In addition to this,

the region is highly conserved making it ideal for molecular detection and unreliable for genotyping (Drexler *et al.*, 2011). In 2000 Yamashita *et al.* (2000) successfully designed primers that target the 3CD junction for molecular detection. Since then, these primers have been used worldwide for molecular detection and typing of AiV-1 from clinical, environmental and shellfish samples.

Concerning the VP1 region, there are no primers in the literature which can be regarded as being universal for this region as most studies seem to design and use different primers. For example, the first primers targeting the AiV-1 capsid region including VP1 were designed and used by Pham *et al.* (2008) for detection and molecular characterisation of AiV-1 in clinical samples from Japan, Thailand, Bangladesh and Thailand. Drexler *et al.* (2011) designed their own VP1 primers for typing of AiV-1 from clinical samples in Germany. Furthermore, Yip *et al.* (2014) designed and used their own primers for typing of AiV-1 from clinical samples in Hong Kong. In addition, Lodder *et al.* (2013) designed and used their own VP1 primers for molecular identification and typing of AiV-1 from raw sewage in the Netherlands. All these studies show that there are no universally trusted primers for the AiV-1 VP1 RT-PCR assay.

For genotyping purposes, the 3CD region is preferred in most studies. However, some authors including Yamashita *et al.* (2000), Pham *et al.* (2008) and Lukashev *et al.* (2012) argue that the sequence data for the 3CD is not sufficient for subtyping. Instead they prefer the use of the capsid region especially VP1 that codes for proteins that express the antigenicity of the virus and is more genetically diverse compared to the 3CD region. However Ambert-Balay *et al.* (2008), Saikruang *et al.* (2014B) and Yip *et al.* (2014) did not observe any changes in the clustering patterns when using both the 3CD and VP1 regions for genotyping and hence concluded that either of them can be used.

Based on the 3CD and VP1 DNA sequences, AiV-1 is classified into three genetically distinct lineages namely; A, B and C (Yamashita *et al.*, 2000; Ambert-Balay *et al.*, 2008). Although more than one genotype can co-exist in one geographical region, as revealed in some studies including Kitajima *et al.* (2011) and Lodder *et al.* (2013) data from the literature shows that genotypes A and B are more prevalent in Asian and European countries while genotype C was detected only in Africa (Burkina Faso and Mali) (Ambert-Balay *et al.*, 2008; Drexler *et al.*, 2011; Haramoto and Kitajima, 2017; Jonsson

et al., 2012; Kitajima *et al.*, 2011; Oh *et al.*, 2006; Ouédraogo *et al.*, 2016; Pham *et al.*, 2007; Verma *et al.*, 2011).

1.4.3.3 GenBank data on AiV-1

For comparison purposes, it is important to know how much data is available in GenBank. Currently (as of October 2017), there are only eleven complete genome sequences with accession numbers JX564249 (Taiwan), NC_001918, AB040749, (both Japanese), FJ890523 (Chinese), AY747174, GQ927711, GQ927712, GQ927704, GQ927706, GQ927705 (all German), DQ028632 (Brazilian) (Chang *et al.*, 2013; Drexler *et al.*, 2011; Oh *et al.*, 2006; Yamashita *et al.*, 1998; Yang *et al.*, 2009) deposited in GenBank which are used as reference sequences in many studies. In addition to that, there are many partial 3CD and VP1 sequences from all over the world available. However there are fewer 5' UTR sequences compared to the 3CD and VP1 sequences as only a few studies explored the 5' UTR assays

In relation to Africa, there are no complete genomes, 5' UTR and VP1 sequences available in GenBank for comparison purposes. However, there are a couple of partial 3CD sequences from Tunisia (Ibrahim *et al.*, 2017), Mali (Ambert-Balay *et al.*, 2008) Burkina Faso (Ouédraogo *et al.*, 2016) and Nigeria (Japhet *et al.*, 2016) available in GenBank which can be used.

1.4.3.4 Geographical distribution and prevalence of AiV-1

AiV-1 appears to be geographically widespread. **Table 1.5** below shows examples of geographical regions as well as types of samples from which AiV-1 was detected. As shown in **Table 1.5**, this virus has been detected from clinical, environmental as well as shellfish samples in many countries worldwide possibly because of human migration. In the Americas, it was detected in clinical and environmental samples from Brazil, Uruguay, Venezuela, USA and others (Alcala *et al.*, 2010; Burutarán *et al.*, 2015; Kitajima *et al.*, 2014; Oh *et al.*, 2006). In Asia it was detected in Thailand, Japan, Bangladesh, Vietnam, South Korea, China and many other Asian countries (Han *et al.*, 2014; Pham *et al.*, 2008; Yamashita *et al.*, 1991; Yip *et al.*, 2014). In fact, AiV-1 is predominantly found in Asia (Kitajima *et al.*, 2011). In Europe this virus was detected in Netherlands, Germany, France, and many other European countries (Drexler *et al.*, 2011; Goyer *et al.*, 2008; Lodder *et al.*, 2013). In Africa, the epidemiology of AiV-1 is poorly

understood because of limited data, hence there is need to do more research on this medically important virus. AiV-1 was detected from clinical and raw sewage samples in Tunisia (Ibrahim *et al.*, 2017; Sdiri-Loulizi *et al.*, 2008; Sdiri-Loulizi *et al.*, 2009). Ambert-Balay *et al.* (2008) and Ouédraogo *et al.* (2016) detected AiV-1 from clinical samples of diarrhoeic patients in Mali and Burkina Faso respectively. Recently AiV-1 was detected from clinical samples in Nigeria (Japhet *et al.*, 2016). To date, there have been no published reports of this virus and its role in gastroenteritis in South Africa.

Table 1.5: Geographical regions and types of samples from which AiV-1 have been detected.

Continent	Countries	Sample types	Genotypes	References
Africa	Mali	stool samples	C	Ambert-Balay <i>et al.</i> , 2008
	Burkina Faso	stool samples	A, B, C	Ouédraogo <i>et al.</i> , 2016
	Tunisia	stool samples	A	Sdiri-Loulizi <i>et al.</i> , 2009
		raw sewage	B	Ibrahim <i>et al.</i> , 2017
	Nigeria	stool samples	B	Japhet <i>et al.</i> , 2016
Asia	Thailand, Japan, Bangladesh	stool samples	A, B	Pham <i>et al.</i> , 2008
	Japan	stool samples	A	Yamashita <i>et al.</i> , 1991
	South Korea	stool samples	A, B	Han <i>et al.</i> , 2014
	Hong Kong	stool samples	A	Yip <i>et al.</i> , 2014
Americas	Brazil	stool samples	B	Oh <i>et al.</i> , 2006
	Uruguay	raw sewage	B	Burutaran' <i>et al.</i> , 2015
Europe	Netherlands	raw sewage	A, B	Lodder <i>et al.</i> , 2013
	France	stool samples	not stated	Goyer <i>et al.</i> , 2008

Although prevalence levels appear to be generally low, AiV-1 continues to play a significant role as an important viral pathogen. For example, prevalence levels as low as 0.1%, 0.5% and 0.9% were recorded in Japan, Finland and Thailand respectively (Kaikkonen *et al.*, 2009; Pham *et al.*, 2007). In Africa, Sdiri-Loulizi *et al.* (2009) recorded a higher prevalence level of 4.1% in Tunisia. In various serological studies, it was shown that at one point in life, people suffered from AiV-1 infection. This was evidenced by high prevalence of AiV-1 antibodies of between 70% and almost 100% in France, Spain, Japan and Tunisia (Goyer *et al.*, 2008; Ribes *et al.*, 2010; Sdiri-Loulizi *et al.*, 2010B; Yamashita *et al.*, 1993).

AiV-1 is amongst the most persistent viruses in the environment. This is shown by its high detection rates of between 45% and 100% in environmental samples from polluted rivers and sewage treatment plants in Venezuela, Uruguay, Japan, Nepal and the Netherlands (Alcala *et al.*, 2010; Burutan *et al.*, 2015; Haramoto and Kitajima, 2017; Kitajima *et al.*, 2011; Lodder *et al.*, 2013). This is partly due to its ability to withstand harsh conditions. It can survive at pH levels as low as pH 3.5 (Yamashita *et al.*, 1998). AiV-1 is not readily inactivated by widely used inactivation methods such as heat, chlorine, common detergents, alcohols, ether, chloroform as well as pressurised air (Yamashita *et al.*, 1998).

1.4.4 Enteric human bocaviruses as aetiological agents of gastroenteritis

1.4.4.1 Genome structure

Human bocavirus (HBoV), family *Parvoviridae*, genus *Parvovirus*, is a single stranded DNA virus with a naked icosahedral capsid about 18-26 nm in diameter with a genome size of approximately 5.2 kilo base pairs (Allander *et al.*, 2005; Lau *et al.*, 2007; Ong *et al.*, 2016; Yu *et al.*, 2008). This virus was first isolated from respiratory samples in Sweden in 2005 and was initially believed to be responsible for respiratory complications in paediatric patients (Allander *et al.*, 2005). However, this conclusion was short-lived as in 2007 HBoVs came to be associated with cases of acute gastroenteritis (Lau *et al.*, 2007). These viruses derived their name from their two initial hosts being ‘bovine’ and ‘canine’ hence ‘bocaviruses’ (Ong *et al.*, 2016).

The genome of HBoVs has two major open reading frames namely ORF1 and ORF3 and a minor one, ORF2 in the middle (**Figure 1.7A**). ORF1 encodes a non-structural protein (NS-1), ORF2 encodes a nuclear-phosphoprotein (NP-1) of unknown role whereas ORF 3

encodes capsid proteins VP1/VP2 (Allander *et al.*, 2005; Arthur *et al.*, 2009; Jartti *et al.*, 2012; Lau *et al.*, 2007)

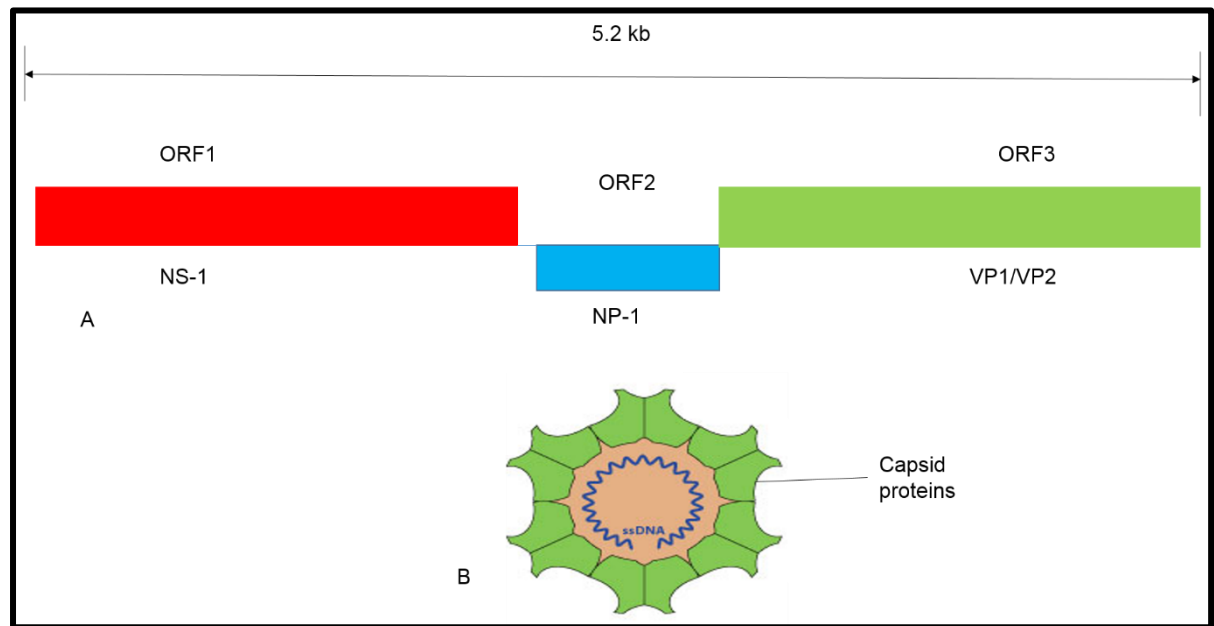


Figure 1.7: **A)** Schematic representation of an enteric HBoV genome (adapted from Allander *et al.*, 2005) **B)** An HBoV virion (www.viralzone.expasy.org/567?outline=all_by_species).

For the purpose of this study, the features and roles of the non-structural protein (NS-1), nuclear-phosphoprotein (NP-1) and the capsid VP1/VP2 proteins will be discussed. These regions are important for molecular identification as well as typing of enteric HBoVs. The NS-1 gene, encoded by ORF1 (**Figure 1.7A**), codes for approximately 781 amino acids. This region is the most conserved with minor single nucleotide polymorphisms (Jartti *et al.*, 2012; Lau *et al.*, 2007). In a recent review by Guido *et al.* (2016), the region was reported to play a role in DNA replication, apoptosis and cell cycle arrest. Furthermore Guido *et al.* (2016) mentioned that since the NS-1 is highly conserved, many studies use it only for molecular identification of the virus. The NP-1 gene, which is the smallest gene in the genome, codes for only 219 amino acids. It is located in ORF2 (**Figure 1.7A**). Like the NS-1, this region is also highly conserved and used only for molecular identification of the virus. However, its role remains unknown to this date (Guido *et al.*, 2016; Jartti *et al.*, 2012). Even though recent studies show that the NP-1 plays a role in expression of capsid proteins, this is not fully elucidated (Guido *et al.*, 2016).

The VP1/VP2 gene codes for structural proteins VP1 and VP2. It is found in the ORF3 (**Figure 1.7A**) (Jartti *et al.*, 2012). This region, which has the most hypervariable sites compared to others, is the gold standard for genotyping of human bocaviruses as it is a target for neutralising antibodies (Guido *et al.*, 2016; Lau *et al.*, 2007).

1.4.4.2 Molecular detection and typing of enteric HBoVs

Although the use of techniques such as TEM and ELISA have been reported in the literature such as in Kantola *et al.* (2007) and Santos *et al.* (2010), reliable isolation and detection of enteric human bocaviruses involves PCR amplification of the NS-1, NP-1 and the VP1/VP2 regions in ORF's 1, 2 and 3 respectively (Jartti *et al.*, 2012; Guido *et al.*, 2016). Although all these regions are known to possess conserved sequence motifs, this is more pronounced in the NS-1 region (Lau *et al.*, 2007). The VP1/VP2 region shows a higher level of variability amongst enteric HBoVs compared to other regions and therefore it is normally used for typing purposes (Allander *et al.*, 2005; Yu *et al.*, 2008).

Based on the DNA sequence of the VP1/VP2 gene, there are four genotypes, HBoV-1, HBoV-2, HBoV-3 and HBoV-4 (Guido *et al.*, 2016). HBoV-1 is mainly associated with severe and life threatening but self-limiting respiratory infections (Allander *et al.*, 2005; Kantola *et al.*, 2007; Uršic *et al.*, 2011). Although some studies reveal the presence of HBoV-1 in stool samples of diseased subjects, its role as an agent of gastroenteritis remains questionable. For example, Arthur *et al.* (2009) could not relate HBoV-1 to cases of gastroenteritis and argues that its presence in stool was because of patients swallowing respiratory fluids. Many studies associate HBoV-2 with gastroenteritis on several grounds, which include high ratios of mono-infections to co-infections as well as analysis of matched case control pairs (Arthur *et al.*, 2009; Campos *et al.*, 2016; Jin *et al.*, 2011; Zhang *et al.*, 2015). On the other hand some studies failed to relate HBoV-2 to gastroenteritis as the differences in prevalence rates between mono-infections and co-infections as well as between cases and healthy controls were statistically insignificant (Khamrin *et al.*, 2011; Tymentsev *et al.*, 2016; Kapoor *et al.*, 2010; Risku *et al.*, 2012; Lau *et al.*, 2007; Lee *et al.*, 2007). Even though the role of HBoV-2 as an aetiological agent of gastroenteritis remains disputed up to this date, high detection rates reported in the above studies suggest a potential role. However more epidemiological data is required to fully elucidate this as there are currently no cell culture or animal models for pathogenicity studies. In addition, HBoV-3 and HBoV-4 have also been linked to

diarrhoea cases but their roles as causative agents remain unknown (Guido *et al.*, 2016; Ong *et al.*, 2016).

In most published reports, molecular identification of HBoVs from clinical and environmental samples is carried out by PCR amplification of either the NS-1 gene or NP-1 gene, followed by typing the resultant viruses by use of the VP1/VP2 PCR assay. Examples of such studies include Cashman and O'Shea, (2012) in Ireland, La Rosa *et al.* (2016) in Albania and Yu *et al.* (2008) in China. In other studies, the VP1/VP2 assay has been successfully used for molecular identification as well as typing the virus from clinical and environmental samples such as raw sewage. These include studies by Blinkova *et al.* (2009) in the USA, Campos *et al.* (2016) in Brazil, Iaconelli *et al.* (2016) in Italy and Kapoor *et al.*, (2010) in Nigeria and Tunisia.

Primers designed by Kapoor *et al.* (2009) that target the VP1/VP2 region of HBoVs are considered universal for detection and genotyping of the virus from clinical and environmental samples. They have been used in most published reports such as by Campos *et al.* (2016), Kapoor *et al.* (2010), Khamrin *et al.* (2012), Tymentsev *et al.* (2016). However, these primers are species specific as they were designed based on VP1/VP2 DNA sequences of HBoV-1 and HBoV-2 so they do not bind to HBoV-3 and HBoV-4 sequences. Due to this La Rosa *et al.* (2016) designed broad range degenerate primers based on VP1/VP2 DNA sequences of all the 4 human bocavirus genotypes, HBoV-1, HBoV-2, HBoV-3 and HBoV-4. These later primers are useful for diagnostic and survey purposes in which no particular genotype is targeted. They were used to successfully detect all the 4 genotypes from raw sewage samples in Italy by Iaconelli *et al.* (2016). **Table 1.6** below shows molecular techniques normally used for detection of human bocaviruses from clinical as well as environmental samples including raw sewage.

Table 1.6: Molecular methods for detection of enteric HBoVs in some studies worldwide.

Method	Sample types	Target region	Country of study	References
PCR	human stools	NS-1, VP1/VP2	China	Yu <i>et al.</i> , 2008
	human stools	NS-1	Russia	Tymentsev <i>et al.</i> , 2016
	human stools	NP-1, VP1/VP2	Albania	La Rosa <i>et al.</i> , 2015
	human stools	NS-1 and VP1/2	Ireland	Cashman and Oshea, 2012
	raw sewage	VP1/VP2	Italy	Iaconelli <i>et al.</i> , 2016
	raw sewage	VP1/VP2	USA	Blinkova <i>et al.</i> , 2009

1.4.4.2 GenBank data on enteric HBoV

In GenBank there are many complete genomes for enteric HBoVs from all over the world. In addition to that there are many partial VP1/VP2 sequences for enteric HBoVs available. In relation to Africa, there are at least 50 partial VP1/VP2 sequences from Tunisia and Nigeria that can be used for comparison purposes (Kapoor *et al.*, 2010).

1.4.4.3 Geographical distribution and prevalence of enteric HBoVs

Enteric HBoVs viruses have been detected worldwide, as shown in **Table 1.7** below, showing that they are wide spread. They have been detected from clinical or environmental samples in the USA (Blinkova *et al.*, 2009), in Brazil (Campos *et al.*, 2016), in Italy (Iaconelli *et al.*, 2016), in Albania (La Rosa *et al.*, 2016), in China (Yu *et al.*, 2008) and many other European and Asian countries. In Africa, there is limited epidemiological data on these viruses. They were detected from stool samples of diarrhoeic patients in Tunisia and Nigeria (Kapoor *et al.*, 2010). In South Africa there are no published reports on detection as well as possible role of enteric HBoVs as aetiological agents of gastroenteritis. However, there are several reports describing the detection of HBoV-1 from respiratory fluids of patients with respiratory infections in South Africa (Madhi *et al.*, 2015; Nunes *et al.*, 2014; Smuts *et al.*, 2008; Smuts and Hardie, 2006).

There is no published literature directly linking HBoV-1 to gastroenteritis so far and as a result, it will not be the focus of the present study.

Currently, there is no published literature describing the detection of enteric HBoVs in shellfish worldwide. Since shellfish is a known reservoir of enteric viruses, it is possible that it harbors enteric HBoVs as well. The present study will be the first one to report on this and more research is required on this subject.

Table 1.7: Geographical regions and types of samples from which HBoVs were detected.

Continent	Countries	Sample types	Genotypes	References
Africa	Nigeria	human stools	2,3,4	Kapoor <i>et al.</i> , 2010
	Tunisia	human stools	2, 3, 4	Kapoor <i>et al.</i> , 2010
Asia	Thailand	human stools	2, 3, 4	Khamrin <i>et al.</i> , 2012
	China	human stools	2	Zhang <i>et al.</i> , 2015
	South Korea	human stools	2	Han <i>et al.</i> , 2009
America	Brazil	human stools	2	Campos <i>et al.</i> , 2016
	USA	raw sewage	2, 3	Blinkova <i>et al.</i> , 2009
Europe	Italy	raw sewage	2, 3	Iaconelli <i>et al.</i> , 2016
	Albania	human stools	2	La Rosa <i>et al.</i> , 2016
	Russia	human stools	2, 3, 4	Tymentsev <i>et al.</i> , 2016

Prevalence rates for enteric HBoVs (HBoV-2, HBoV-3 and HBoV-4) range from 0% to 41.9% (Ong *et al.*, 2016; Campos *et al.*, 2016). Detection rates as high as 79.1% and 81% were recorded for sewage water samples in Italy and the USA respectively depicting a general circulation of these viruses in the populations (Blinkova *et al.*, 2009; Iaconelli *et al.*, 2016). Although Iaconelli *et al.* (2016) did not observe any fluctuations in detection

rates throughout the year, other authors noted an increase in winter compared to other seasons (Lau *et al.*, 2007; Lee *et al.*, 2007; Tymmentsev *et al.*, 2016).

1.4.5 Enteric human adenoviruses as agents of gastroenteritis

1.4.5.1 Genome structure

Human adenoviruses (HAdV) are double stranded DNA viruses with a genome size measuring 30-36 kb with capsid of icosahedral symmetry belonging to family *Adenoviridae* and genus *Mastadenovirus* (Ghebremedhin, 2014). The HAdV virions, with their characteristic 'spike-like' appearance (**Figure 1.8A**) are between 65 and 100 nm in diameter (Arnold and MacMahon, 2017; Desselberger and Gray, 2013; Ghebremedhin, 2014). They were first isolated by Wallace Rowe in 1953 and were originally associated with infections of the adenoids (the basis of their name) causing respiratory infections (Heim *et al.*, 2003). In addition to this HAdVs have been linked to cases of gastroenteritis as well as other complications (Casas *et al.*, 2005; Flomenberg, 2014).

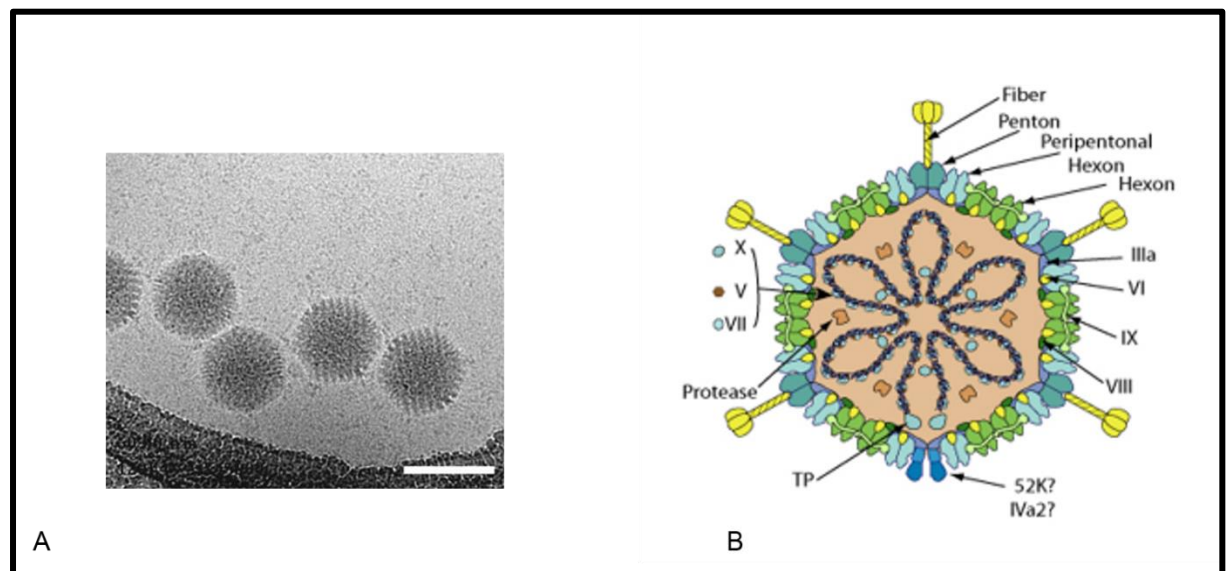


Figure 1.8: **A)** TEM images of HAdV virions (Stewart *et al.*, 1997) **B)** Schematic representation of an HAdV virion showing major components of the outer capsid, fibre, penton base and the hexon protein as well as minor protein (www.viralzone.expasy.org/183?outline=all_by_species).

Each virion capsid consists of 36 monomers of fibre protein, 60 monomers of penton base and 720 monomers of hexon protein (Khare *et al.*, 2011; Martin, 2012). In addition to these three major proteins, the capsid also has four minor proteins, namely IIIa, VI, VIII and IX which assist in capsid assembly (Khare *et al.*, 2011) (**Figure 1.8B**). For the

purpose of this study only three regions, namely the hexon protein, the penton base and the fibre protein, which are important for molecular detection and classification of these viruses, will be discussed in detail.

The hexon protein which is approximately 110 kDa, comprises of 919 to 968 amino acids making it the most abundant protein in the capsid. Out of all these amino acid residues, 765 of them are highly conserved with sequence divergence ranging from 0.7% to 25%. This property makes it suitable for molecular identification (Crawford-Miksza and Schnurr, 1996; Ebner *et al.*, 2005). Interestingly, the hexon protein also contains hypervariable sites on the protruding loops that code for serotype-specific epitopes for T-cell recognition and neutralising antibodies (**Figure 1.9**) (Harrison *et al.*, 2010; Leen *et al.*, 2004; Wohlfart *et al.*, 1988). These hypervariable sites are the basis for classification of HAdVs into various serotypes (Ebner *et al.*, 2005).

The penton base is approximately 63 kDa and forms part of the outer capsid. Its role is to bind to cellular integrins (Khare *et al.*, 2011). On the other hand, the fibre protein which is approximately 62 kDa is the outer most part of the capsid. It functions as a primary attachment protein to host cells (Khare *et al.*, 2011).

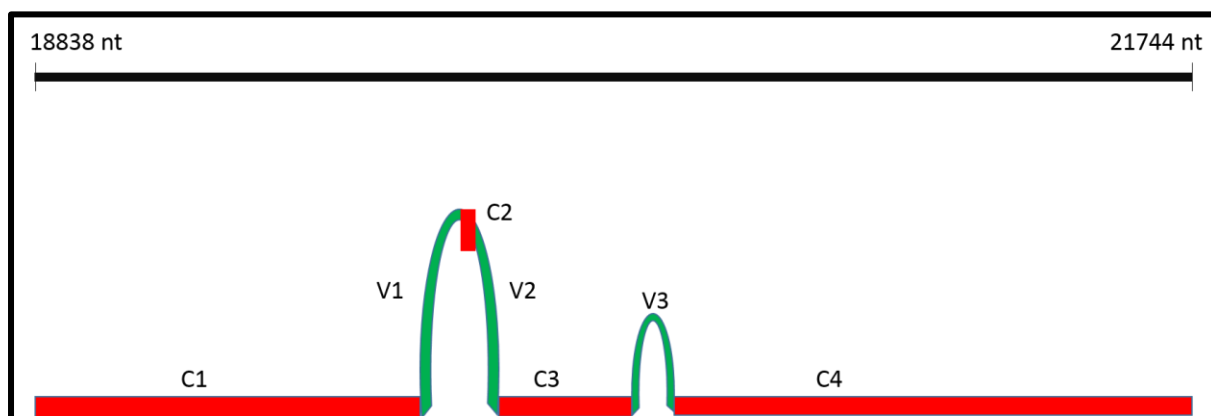


Figure 1. 9: Pictorial representation of HAdV hexon protein showing positions of conserved (red) and variable sites (green). C1 covers amino acid positions (aa) 1 to 137, C2 extends from aa 222 to 248, C3 from aa 317 to 419 and C4 from aa 461 to 961. The variable sites are concentrated on the protruding loops. V1 extends from aa 138 to 221, V2 from aa 249 to 316 and V3 from aa 420 to 460 (adapted from Ebner *et al.*, 2005).

1.4.5.2 Molecular detection and typing of enteric HAdVs

Various techniques including cell culture, ELISA, DNA restriction analysis, PCR and qPCR have been used successfully to isolate and detect enteric HAdV (Brown *et al.*, 1990; Casas *et al.*, 2005; Heim *et al.*, 2003; Le Guyader *et al.*, 2008; Wood *et al.*, 1989A, B). Amongst all these, Heim *et al.* (2003) argued that qPCR is the most suitable technique as it quantifies the viral load in a subject. They also argue that enteric HAdV (subtype F 40/41) require special cell lines and are fastidious. In spite of all this, data from literature shows that identification of human adenoviruses from clinical and environmental samples is mainly based on PCR amplification of the conserved and hypervariable hexon protein coding region. Many published primers are available for this purpose such as the ones used by Adefisoye *et al.* (2016), Osulale and Okoh (2015), Jiang *et al.* (2005) and Rezaei *et al.* (2012). However, most of these published primers are subtype specific, meaning that they can only be used if a particular subtype is of interest hence they are not appropriate in surveillance studies. Due to this, Avellon *et al.* (2001) designed broad range degenerate primers based on DNA sequence data of all known HAdV subtypes. These primers can bind to any adenovirus sequence in samples and hence they are very useful in surveillance studies. Furthermore, these primers by Avellon *et al.* (2001) have been used worldwide with great successes (Casas *et al.*, 2005; Magwalivha *et al.*, 2010; Van Heerden *et al.*, 2005; Van Heerden *et al.*, 2003). **Table 1.8** below describes molecular techniques used for detection of enteric HAdV from clinical and environmental samples.

Table 1.8: Molecular methods for detection of enteric HAdVs in some studies.

Method	Sample types	Target region	Country of study	References
PCR	human stools	hexon gene	Netherlands	Svraka <i>et al.</i> , 2007
	Stools	hexon gene	Thailand	Sriwana <i>et al.</i> , 2013
	Stools	hexon gene	Spain	Casas <i>et al.</i> , 2005
	river water	hexon gene	South Africa	Van Heerden <i>et al.</i> , 2005
qPCR	Stools	hexon gene	Germany	Heim <i>et al.</i> , 2003
	raw sewage	hexon gene	South Africa	Adefisoye <i>et al.</i> , 2016

Based on the DNA sequences of the hexon gene, over seventy HAdV serotypes categorised into seven species, A to G, have been identified up to this date (Arnold and MacMahon, 2017; Hage *et al.*, 2015). Amongst these, HAdV species A (Serotype 31), C, D, F and G are mainly recognised as etiological agents of acute gastroenteritis (Casas *et al.*, 2005; Heim *et al.*, 2003). **Table 1.9** below shows the various HAdV serotypes, subtypes as well as the types of infections they are associated with.

Table 1.9: Some common HAdVs serotypes and their corresponding clinical manifestations (from Arnold and MacMahon, 2017; Ghebremedhin, 2014).

Subtype	Serotypes	Type of infection
A	12, 18, 31	Gastroenteritis, respiratory, urinary
B	3, 7, 11, 14, 16, 21, 34, 35	Keratoconjunctivitis, gastroenteritis, respiratory, urinary
C	1,2,5,6	Gastroenteritis, respiratory, urinary
D	8–10,13,15,17,19,20,22–30,32,33,36–39,42–49	Keratoconjunctivitis, gastroenteritis
E	4	Keratoconjunctivitis, respiratory
F	40, 41	Gastroenteritis
G	52	Gastroenteritis

1.4.5.3 GenBank data on enteric HAdVs

Available in GenBank are many complete genomes as well as many complete hexon gene sequences of enteric HAdVs from all over the world including South Africa and many other African countries. In addition to that, there are many partial hexon gene and penton base sequences from around the world deposited in GenBank. This means that there is a large pool of sequences to choose from for comparison purposes.

1.4.5.4 Geographic distribution and prevalence of enteric HAdVs

Enteric HAdVs have been isolated from environmental as well as clinical samples of diarrhoeic people worldwide including in Bangladesh, Japan, China, India, Iran, Spain, Germany, Venezuela and many other countries (Banerjee *et al.*, 2017; Casas *et al.*, 2005; Dey *et al.*, 2009; Heim *et al.*, 2003; Liu *et al.*, 2014; Rodríguez-Díaz *et al.*, 2009; Shimizu *et al.*, 2007; Xu *et al.*, 2000). **Table 1.10** below shows the various geographical regions as well as the types of samples from which enteric HAdVs were detected as reported in

some studies worldwide. In Africa, there are many published reports on detection of enteric HAdVs from environmental as well as clinical samples of diarrhoeic patients. Enteric HAdVs were detected in the Republic of Congo (Mayindou *et al.*, 2016), Burkina Faso (Ouedraogo *et al.*, 2017), Nigeria (Aminu *et al.*, 2007), Gabon (Lekana-Douki *et al.*, 2015), Kenya (Magwalivha *et al.*, 2010), Democratic Republic of Congo, Central African Republic, Ivory Coast and Uganda (Pauly *et al.*, 2014).

Although the epidemiological status is unknown due to limited data, there are several publications on isolation of enteric HAdVs from clinical samples, drinking water as well as environmental samples in South Africa. Moore *et al.* (2000) detected enteric HAdV types F40 and F41 as well as unidentified serotypes from stool samples. To show that these viruses circulate around, Adefisoye *et al.* (2016) and Osulale and Okoh, (2015) detected enteric HAdV from final effluents of various wastewater treatment plants in the Eastern Cape Province of South Africa while Chigor and Okoh (2012) and Van Heerden *et al.* (2005) reported presence of enteric HAdVs in selected rivers in South Africa. Furthermore more Van Heerden *et al.* (2005) detected these viruses from drinking water samples in South Africa. In addition to these, Vos and Knox (2017) identified human HAdV subtype D in raw sewage and mussel samples in the Eastern Cape Province of South Africa.

Table 1.10: Some examples of the geographical regions and types of samples from which enteric HAdVs were detected.

Continent	Countries	Sample types	subtypes	References
Africa	Congo	human stools	F	Mayindou <i>et al.</i> , 2016
	Burkina Faso	human stools	A, B, C, D, F	Ouedraogo <i>et al.</i> , 2017
	Morocco	mussels	Not stated	Karamoko <i>et al.</i> , 2005
	South Africa	raw sewage	B, C, F	Adefisoye <i>et al.</i> , 2016
	South Africa	human stools	F	Moore <i>et al.</i> , 2000
Asia	India	human stools	F	Banerjee <i>et al.</i> , 2017
	China	human stools	A, B, C, E, F	Liu <i>et al.</i> , 2014
Americas	Venezuela	raw sewage	Not stated	Rodríguez-Díaz <i>et al.</i> , 2009
Europe	Spain	human stools	A, B, C, D, E, F	Casas <i>et al.</i> , 2005
	Spain	shellfish	Not stated	Rodriguez-Manzano <i>et al.</i> , 2014
Australia	Australia	raw sewage	Not stated	Sidhu <i>et al.</i> , 2013

Even though there are many published articles on the presence of enteric HAdVs in clinical environmental samples worldwide, there are very few published reports on the detection of these viruses from shellfish. Only five reports by Rigotto *et al.* (2005), Formiga-Cruz *et al.* (2005), Umesha *et al.* (2008), Karamoko *et al.* (2005) and Sdiri-

Loulizi *et al.* (2010A) on detection of enteric HAdVs in shellfish samples from Brazil, Spain, India, Morocco and Tunisia respectively were found. In South Africa, apart from a report by Vos and Knox (2017) no other published articles on presence of enteric HAdVs in shellfish were found.

1.5 Pathways of Transmission for agents of gastroenteritis

1.5.1 Faecal-oral as the major transmission mode

The faecal-oral route is the major mode of transmission of enteric pathogens including viral ones (Bosch, 1998). The transmission is made possible by various primary and secondary vehicles. Primary vehicles are those that directly expose people to enteric infections. These include sewage contaminated water and contaminated shellfish. Secondary vehicles include contact with infected persons or contaminated surfaces such as cups, diapers, food preparation surfaces. For the purpose of this study only the roles of the major primary vehicles namely; sewage water and shellfish will be discussed. **Figure 1.10** summarizes other possible pathways of transmission. As shown in the figure below, human enteric pathogens from infected persons get introduced into sewage treatment plants, surface water sources and underground water sources via the sewer system, surface run-off and seepage respectively (Bosch, 1998, Hata *et al.*, 2014). This ultimately leads to contamination of drinking water supplies, fresh produce as well as shellfish leading to gastroenteritis.

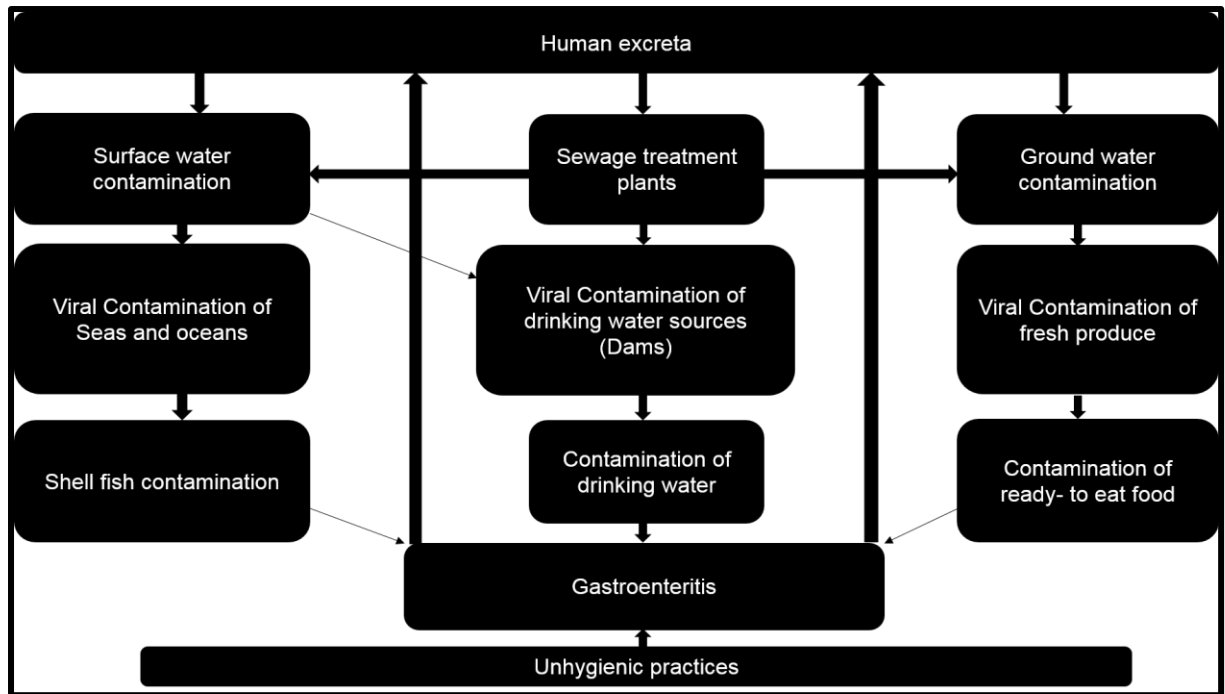


Figure 1.10: Pathways of transmission for agents of gastroenteritis. Arrows show directions of the aetiological agents of gastroenteritis (Adapted from Bosch, 1998; Gerba *et al.*, 1975).

1.5.2 Sewage polluted water as a primary vehicle of transmission of enteric viruses

Sewage polluted water has been shown to be the major source of gastroenteric viruses since the 1940s (Fong and Lipp, 2005). Its role as an important vehicle of enteric viruses is extensively reviewed in the literature and has been reported worldwide. For example, Bibby and Peccia (2013), Cantalupo *et al.* (2011) and Iaconelli *et al.* (2017) extensively reviewed the role played by sewage water in transmission of enteric viruses in the USA and Italy respectively. Treatment of sewage water does not completely eliminate enteric viruses (Fong and Lipp, 2005). For example, concentration of AiV-1 was noted to remain fairly high and constant in both influent and effluent water throughout the year in Japan, showing its resistance to water treatment processes and agents (Kitajima *et al.*, 2011; Kitajima *et al.*, 2014). Another study in Brazil by Da silva *et al.* (2007) reported that norovirus GI and GII genogroups were present in 24% and 14% of effluent water samples respectively. It is very unfortunate that in most poor countries of Africa and Asia much of the sewage water is not treated at all. For example, only about 3% of sewage water is treated in Jarkata, Indonesia. The rest is discharged into the environment as raw sewage.

This was in comparison to Sydney, Australia where almost 100% of the sewage water undergoes treatment before discharge (Corcoran *et al.*, 2010).

In South Africa, Okoh *et al.* (2010) have extensively reviewed the role of wastewater treatment plants as reservoirs for enteric viruses. Municipal wastewater treatment plants use sedimentation, activated sludge and trickling filters to decontaminate wastewater. Physical and chemical processes such as coagulation, flocculation, sedimentation, ultra-violet irradiation, chlorination and filtration aid in the removal of viruses. Furthermore, Okoh *et al.* (2010) stated that these processes are not 100% efficient. This was confirmed by Van Heerden *et al.* (2003), Van Heerden *et al.* (2005) and Ehlers *et al.* (2005) who reported presence of enteric viruses in drinking water supplies in South Africa. Since sewage water effluent is released unto the environment, it adversely affects the quality of surface water supplies such as rivers. This ultimately leads to contamination of shellfish which will be discussed below.

1.5.3 Shellfish (Oysters, mussels and others) as primary vehicles of transmission of enteric viruses

Human consumption of sewage contaminated shellfish is one of the leading causes of viral gastroenteritis. Presence of human enteric viruses in shellfish, especially from coastal areas has been extensively reviewed in the literature (Bellou *et al.*, 2012) and reported in many studies worldwide, for example in Japan, Spain and Morocco (Benabbes *et al.*, 2013; Formiga-Cruz *et al.*, 2005; Hansman *et al.*, 2008; Imamura *et al.*, 2016; Loutreul *et al.*, 2014; Rivadulla *et al.*, 2017). Shellfish concentrate bacterial as well as viral pathogens while feeding in sewage polluted waters (Bellou *et al.*, 2012). For example, noroviruses concentrate in the digestive track of shellfish where they bind to HBGA-like carbohydrates but do not appear to cause any infections to the host (Le Guyader *et al.*, 2006B).

Contaminated shellfish have been linked to cases of viral gastroenteritis in various studies around the world (Ambert-Balay *et al.*, 2008; Formiga-cruz *et al.*, 2005; Iritani *et al.*, 2014; Wang *et al.*, 2008). For example; AiV-1, an important viral pathogen was first isolated from clinical samples of a patient who had consumed raw oysters in Japan (Yamashita *et al.*, 1991). Consumption of raw shellfish is a common practice in some Asian countries like Japan and South Korea (Nishida *et al.*, 2003; Cho *et al.*, 2016). Coincidentally, it is in these Asian countries where outbreaks of shellfish-borne viral

gastroenteritis are common. Of all shellfish-borne cases recorded between 1980 and 2012, 63% were from Japan (Bellou *et al.*, 2012). In South Africa, except for a report by Vos and Knox (2017) no other published articles on the role of shellfish as a vehicle for enteric pathogens are available. Hence more research is needed in this field.

1.6 Motivation, aims and objectives

1.6.1 Motivation

Gastroenteritis is a serious problem in developing countries including South Africa where it is responsible for approximately 20% of infantile deaths annually. According to the NICD, Rotaviruses are responsible for most of the cases of viral gastroenteritis. The South African government introduced the vaccine RotaRix™ into the Expanded Programme on Immunisation beginning of 2009. In April of the same year, the NICD implemented a diarrhoea surveillance program to monitor Rotaviruses in diarrhoea cases as well as the vaccine efficacy. During this surveillance, the NICD noted a sharp decline in rotavirus related morbidity and mortality over the years. However, over 40% of diarrhoeal cases are still of unknown aetiology. This suggests that unknown, clinically significant viruses might be playing a role in that regard and may be circulating around and afflicting our communities.

AiV-1 has been extensively studied worldwide and is now recognised as one of the significant aetiological agents of gastroenteritis. To our knowledge, there are no reports describing the presence and involvement of AiV-1 in enteric infections in South Africa so there is need to develop techniques to isolate, detect and characterise this medically important viral pathogen. In addition there are currently no published reports on the presence of enteric human bocaviruses in clinical, environmental as well as shellfish samples in South Africa. Although several studies describe the presence of enteric human adenoviruses in clinical as well as environmental samples in South Africa, limited molecular data is available. Therefore, as a starting point to understand the epidemiology of these viruses, this study aimed to develop molecular tools to identify them in raw sewage and shellfish collected in the Eastern Cape Province of South Africa.

The specific objectives of this project were as follows;

- Development of sample preparation and concentration techniques for purification of AiV-1, enteric human bocaviruses and enteric human adenoviruses from raw sewage and mussel samples.
- Screening of the samples by transmission electron microscopy for the presence of viral particles.
- Extraction of viral RNA and DNA from selected samples for downstream applications.
- Development of conventional One-Step RT-PCR assays followed by nested PCR assays for the identification of AiV-1.
- Development of conventional PCR assays followed by nested PCR assays for the identification of enteric human bocaviruses and enteric human adenoviruses.
- Sequencing of PCR products and BLAST analysis
- Construction of phylogenetic trees to infer evolutionary relationships

1.6.2 Study Design

The study design is illustrated in **Figure 1.11** below. Chapter 1 covers the literature review, which includes a general overview of gastroenteritis, its health and economic burden (globally, in Africa and in South Africa), aetiological agents, transmission pathways of the agents, motivation, aims and objectives of the study. Chapter 2 describes development of sample preparation techniques. Chapter 3 describes isolation and detection of AiV-1 from mussel and swab samples. Chapter 4 describes isolation and detection of enteric HBoVs from mussel and swab samples. Chapter 5 describes isolation and typing of enteric HAdVs from mussel and swab samples. Lastly, Chapter 6 looks into general conclusions and future work.

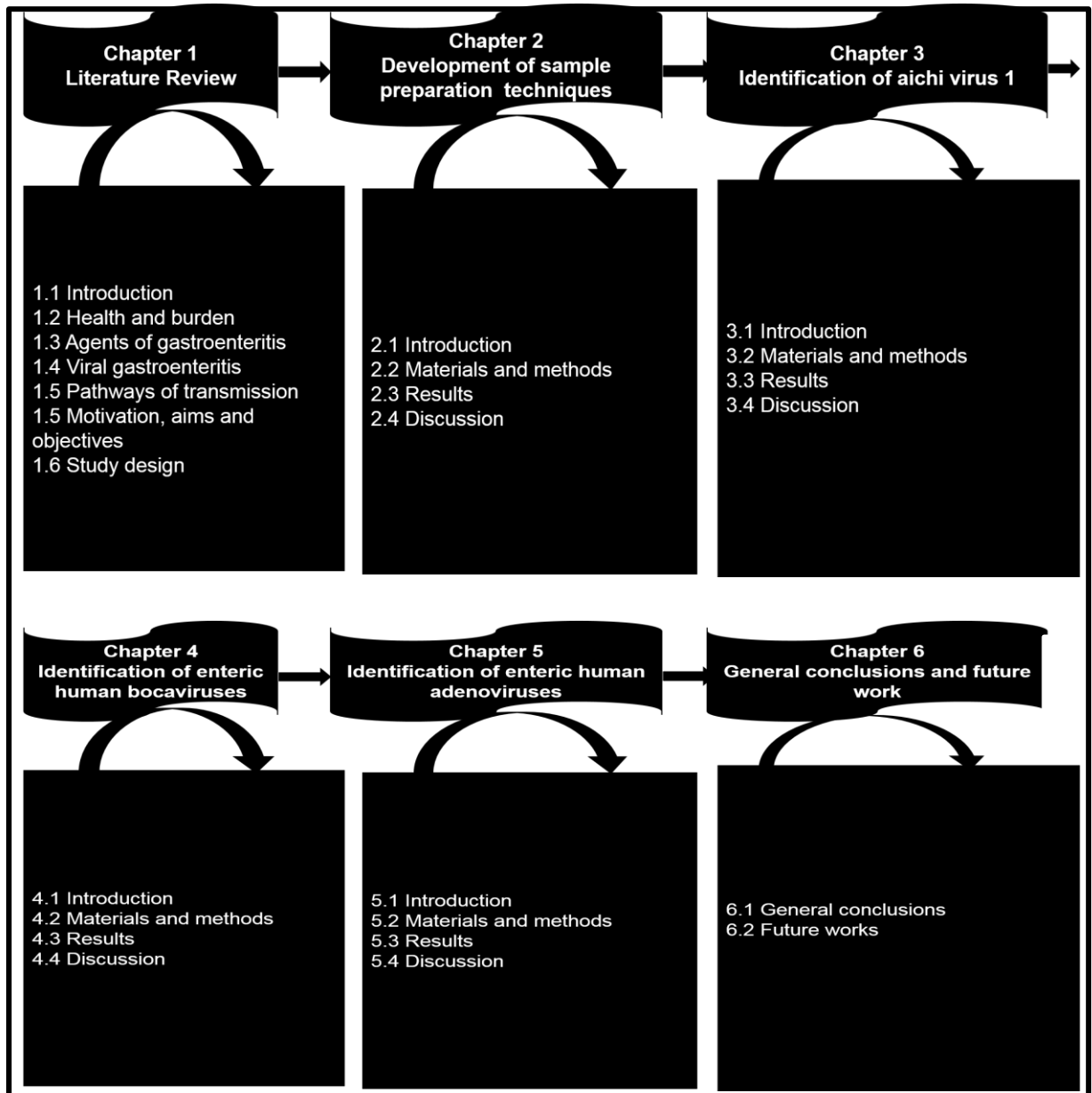


Figure 1.11: Flow diagram of the study design.

Chapter 2: Development of sample preparation techniques for PCR assays

2.1 Introduction

Human enteric viruses are known to be highly prevalent in environmental samples that include sewage water, river water as well as shellfish (Prevost *et al.*, 2015; Woods and Burkhardt, 2010). It is for this reason that samples used in this study were swab samples collected from a sewage treatment plant as well as mussel samples from a sewage polluted river. All the samples were collected in the Eastern Cape Province of South Africa.

Surveillance of enteric pathogens in environmental waters including sewage water has been going on since the 1940's (Fong and Lipp, 2005). The role of raw sewage water as an important transmission mode for enteric viruses worldwide is extensively reviewed in the literature including Eifan, (2013), Fong and Lipp, (2005) and O'Ryan *et al.*, (2012), and has been reported in many studies including Cantalupo *et al.* (2011) in Spain, Bibby and Peccia (2013) in the USA and Iaconelli *et al.* (2017) in Italy. In South Africa, sewage water and its role as a transmission vehicle of enteric viruses was reviewed by Okoh *et al.* (2010) who stated that sewage gives a broad idea of viruses and other pathogens that are being shed by a given community and circulating around.

Since viral particles are known to be of low concentrations in environmental sources, various treatment and concentration techniques for raw sewage water including use of cartridge filters (electropositive or electronegative), glass fibre filters, glass wool filters, vortex flow filtration, tangential flow filtration, and acid flocculation and polyethylene glycol (PEG) precipitation have been applied to concentrate the viruses to detectable levels (Fong and Lipp, 2005).

In the present study, swab samples were used instead of raw sewage water. The swabbing technique is not common as it was reported in only a handful of studies including by Di Martino *et al.* (2013) and more recently by Maunula *et al.* (2017), Park *et al.* (2017) and Oristo *et al.* (2017) for swabbing food preparation surfaces. For the present study, swab samples were collected from separation grids of a sewage treatment plant where all solid materials get trapped as the sewage water flows into the plant. The advantage of this technique is that it reduces the volume of sample to work with as swabs are suspended in small volumes of phosphate buffered saline (1 mL) making it fast and efficient. This is in

comparison to studies in which raw sewage waters, sometimes up to 10 L per sample, were collected and concentrated to small manageable volumes (Iaconelli *et al.*, 2017).

Mussels, like any other types of shellfish, are filter feeders so they concentrate viruses and other microbes when feeding in contaminated water. Their role as vehicles of transmission of enteric viruses is also well reviewed in the literature and reported worldwide (Bellou *et al.*, 2012; Benabbes *et al.*, 2013; Formiga-Cruz *et al.*, 2005; Hansman *et al.*, 2008; Imamura *et al.*, 2016; Loutreul *et al.*, 2014; Rivadulla *et al.*, 2017).

There are various ways by which enteric viral pathogens can be detected from samples. These include techniques like transmission electron microscopy (TEM), enzyme linked immune-assays (ELISA), cell culture and molecular techniques such as polymerase chain reaction (PCR) (Storch, 2000). All these techniques have their own advantages and setbacks.

TEM is one of the old techniques. It was first applied in the late 1930's for detection of the poxvirus (Storch, 2000). This technique is fast and saves resources including time and reagents as an initial screening method as only samples showing presence of viral particles are processed for downstream applications. One of the disadvantages of TEM is that it cannot always differentiate between some viruses. For example human norovirus and Aichi virus 1 are of similar size and morphology so it can't tell them apart. For reliable results, TEM is normally used in conjunction with other techniques such as cell culture and molecular techniques as in Yamashita *et al.* (2000) for identification of Aichi virus 1 from clinical samples of diarrhoeic patients in Japan.

Cell culture was first described in 1948 when mumps virus was cultured in cells (Storch, 2000). This technique is specific as some viruses are known to cause cytopathic effects in some specific cell lines. However cell culture technique is slow. Some pathogens, for example Enteric Human Adenovirus F40 and F41 require special cell lines and are fastidious (Heim *et al.*, 2003). The other disadvantage of cell culture is that some viruses, for example human norovirus, do not have a reliable cell culture system (Ettayebi *et al.*, 2016; Jones *et al.*, 2014).

Currently molecular detection by PCR is the corner stone of viral detection. Compared to other techniques it is fast, specific and efficient, making it reliable. This technique can be applied in various forms that include singleplex PCR when one virus is targeted or multiplex PCR for detection of more than one virus (Staggemeier *et al.*, 2012; Elnifro *et*

al., 2000). In order to increase sensitivity in samples with low concentrations of nucleic acids, nested or semi-nested PCR reactions are performed. These are PCR reactions in which first reaction products are used as templates in subsequent PCR reactions (Staggemeier *et al.*, 2012). In a nested PCR reaction, primers used for the second run reaction anneal within the first round product while in a semi-nested PCR reaction one of the second run primers anneal within the first run product while the other primer is one of those which was used in the first run (Staggemeier *et al.*, 2012).

For any PCR reaction, primers are very important. In a situation whereby a particular member in a given virus family is targeted, specific primers can be used. On the other hand broad based degenerate primers are very important when targeting a specific virus that may have different subtypes such as adenovirus as they are not specific for a particular genotype.

Molecular detection of viral pathogens of gastroenteritis by PCR depends on the type of viruses under study. Conventional PCR is used for DNA viruses like enteric human adenoviruses and enteric human bocaviruses. For detection of RNA viruses like human norovirus and Aichi virus 1, reverse transcriptase polymerase chain reaction (RT-PCR) is used (Ozoemena *et al.*, 2004). There are two forms of RT-PCR assays namely one-step RT-PCR and two-step RT-PCR. In a one-step RT-PCR assay, complementary DNA (cDNA) synthesis from the RNA template and PCR occurs in the same reaction tube. On the other hand, in a two-step RT-PCR cDNA synthesis and PCR take place in separate reaction tubes i.e. synthesised cDNA is subsequently used as a template in a PCR reaction (Garibyan and Avashia, 2013; Wacker and Godard, 2005). While each of the two forms of RT-PCR has their own advantages and disadvantages, there are contradicting findings in the literature as to which one is more sensitive than the other. In Wacker and Godard (2005), the sensitivities of the two reactions were similar for highly expressed genes but the one-step RT-PCR assay was found to be more sensitive than the two-step RT-PCR assay for less expressed genes. De Paula *et al.* (2004) also concluded that one-step RT-PCR systems were more sensitive than two-step RT-PCR ones. In the literature, the use of two-step RT-PCR assays to detect RNA viral pathogens of gastroenteritis is reported more frequently than the one-step RT-PCR assays.

This chapter describes the development of sample preparation and concentration techniques for downstream applications. Because human norovirus (HuNoV) GII has

been detected by RT-PCR in the same samples by Jaquet (2017), an RT-PCR reaction for human norovirus GII was applied to test the sample preparation techniques developed in the present study.

The specific objectives for this chapter were as follows;

- Collection and preparation of swab and mussel samples from the Belmont Valley Sewage Treatment Plant and the Swartkops River respectively
- Determination of morphological characteristics of the viral particles from the swab and mussel samples by use of TEM
- Comparison of sensitivity of the Verso 1-Step RT-PCR Hot-Start Kit (Thermo Scientific, USA), versus that of a 2-step RT-PCR system, the Maxima H Minus First Strand cDNA Synthesis Kit (Thermo Scientific, USA)
- Application of an RT-PCR assay to detect Norovirus GII from swab and mussel samples
- Cloning of appropriate PCR inserts, sequencing and BLAST analysis

2.2 Materials and methods

2.2.1 Sample collection- Swabs and mussels

In this study two sets of samples, swabs and mussels, were used. Two hundred swab samples were collected from separation grids at the Belmont Valley Sewage Treatment Plant (Makana Municipality, Grahamstown, Eastern Cape Province, South Africa) on two separate days. The first batch of one hundred swabs was collected on 10th May 2016 while the other batch was collected on the 20th March 2017. The Belmont Valley Sewage Treatment Plant is one of the two wastewater treatment plants that cater for about seventy thousand people living in Grahamstown. Different parts of the separation grids were swabbed using 15 cm long, sterile swabs wetted with sterile phosphate Buffered Saline buffer (10 mM Na₂HPO₄, 2.7 mM potassium chloride, 137 mM sodium chloride, and 1.76 mM potassium phosphate [pH 7.4]). The swabs were placed on ice in a cooler box and transported to the laboratory within 2 hours. The samples were stored at -20 °C awaiting preparation.

Mussel samples, two hundred in total, were collected from the Swartkops River (coordinates: 33°51'36.7"S 25°37'12.0"E), near Port Elizabeth, Eastern Cape, South Africa on the 2nd May 2016 during low tides under the licence of Professor C. McQuaid

(Department of Zoology and Entomology, Rhodes University), field permit RES2014/12, issued by the Department of Agriculture, Forestry and Fisheries of South Africa. The Swartkops River is reported to be polluted with industrial and domestic waste including sewage effluents (Odume *et al.*, 2012). Mussels, like any shellfish, are filter feeders and as a result concentrate microbes including enteric viruses in their digestive tract when feeding in polluted waters. Detection of human enteric viruses in shellfish from polluted river systems also gives a representation of circulating enteric viral pathogens as well as the quality of a given water body. The mussel samples were transported to the laboratory within 2 hours in an ice box. They were then sorted according to their sizes (diameter) being small (< 4 cm in diameter) and large (≥ 4 cm in diameter), and stored at -20 °C until use. **Figure 2.1** below shows the satellite image of Belmont Valley sewage treatment plant as well as the sampling point at the plant. **Figure 2.2** shows the satellite image of the sampling point in the Swartkops River as well as mussels clumped together attached to rocks.

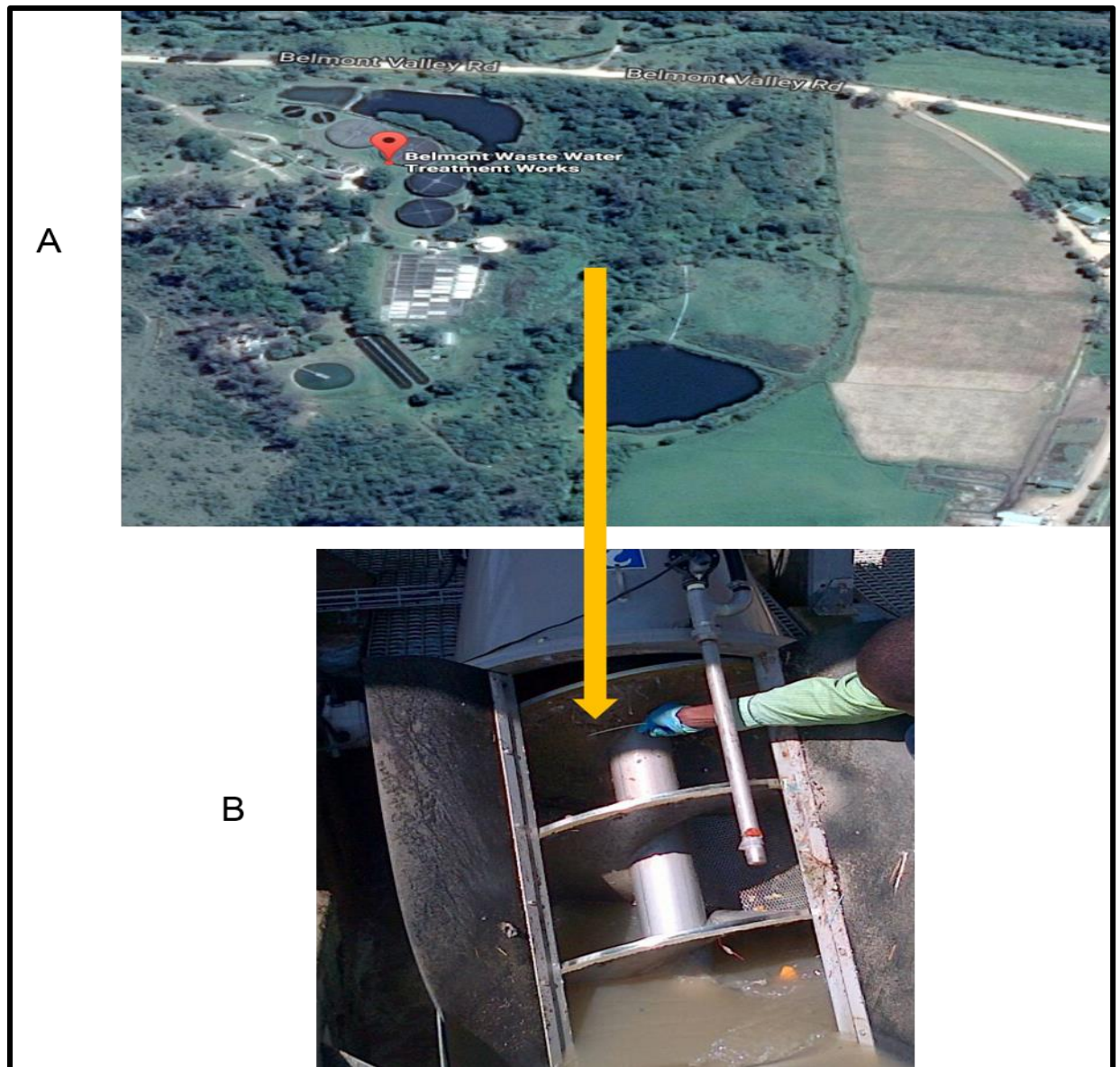


Figure 2.1: A) Satellite image of the Belmont Wastewater Treatment Plant, Grahamstown, South Africa. B) Separation grids at the plant where samples were collected.

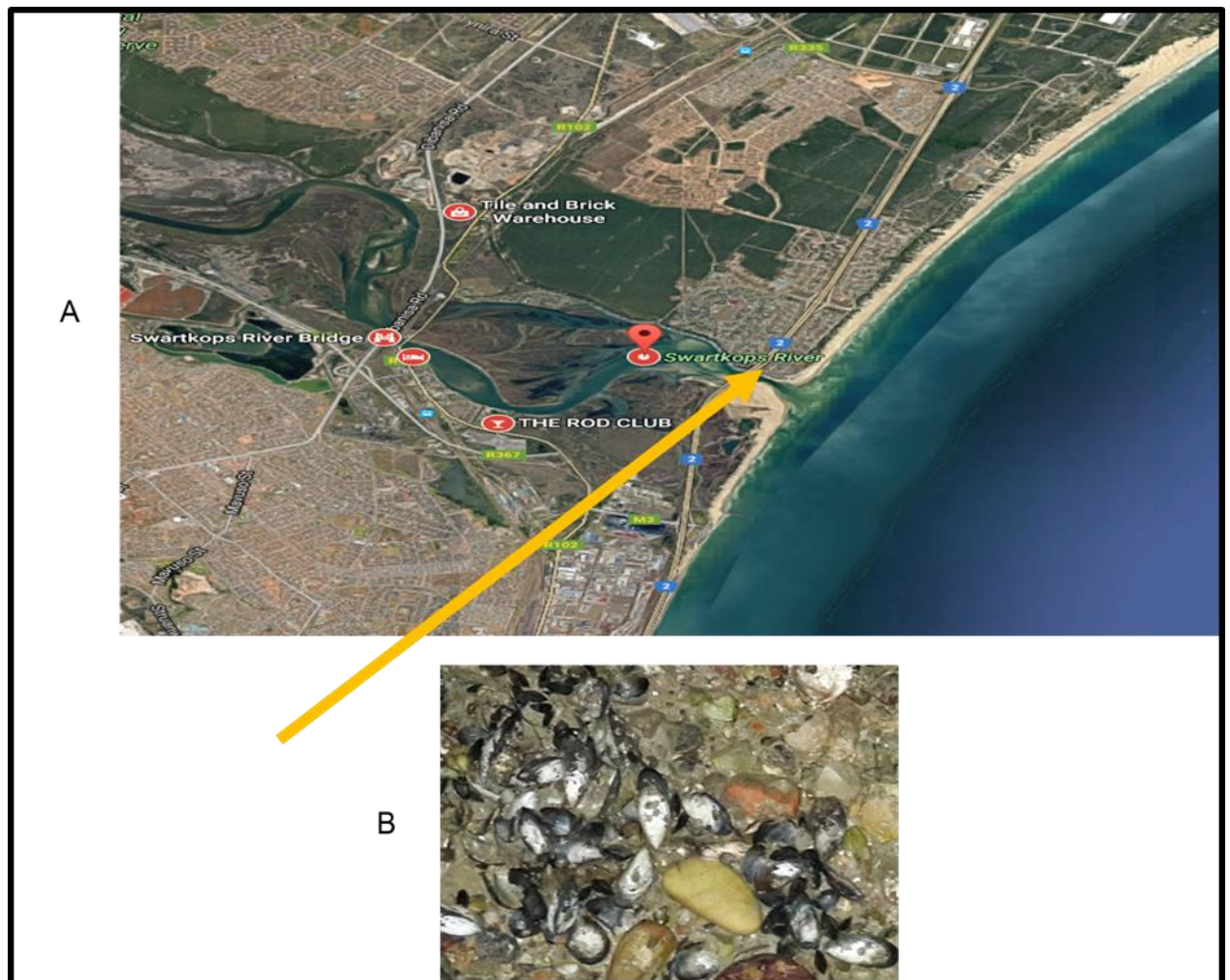


Figure 2.2: A) Satellite image of the Swartkops River. The river meanders through residential and industrial areas. The orange arrow points to the site where mussels were collected which was under the **bridge** B) Mussels clumped together attached to rocks (pictures courtesy of Hillary Vos, Rhodes University).

2.2.2 Preparation of swab samples for morphological characterisation and nucleic acid extraction

The preparation of swab samples, summarised in **Figure 2.3** below, was performed following a method by Di Martino *et al.* (2013) with some modifications. Briefly, ten swabs were pooled into each sterile eppendorf tube containing 1000 μL of 1x Phosphate Buffer containing NP-40 (Sigma-Aldrich, USA) to a final concentration of 1% on ice. The solutions were briefly vortexed and centrifuged at 9 000 x g for 3 minutes to pellet debris. The resulting supernatant was sonicated at 60 kHz for 5 seconds repeated 3 times to disrupt viral attachment to organic and inorganic materials before being filtered through a 0.20 μm membrane filter (GVS filter technology, USA) using a 2 mL sterile

hypodermic syringe. Prepared samples were stored at $-20\text{ }^{\circ}\text{C}$ in labelled 1.5 mL tubes (S1-20: swab1 to swab 20) as shown in **Table 2.1** below awaiting TEM analysis and nucleic acid extraction.

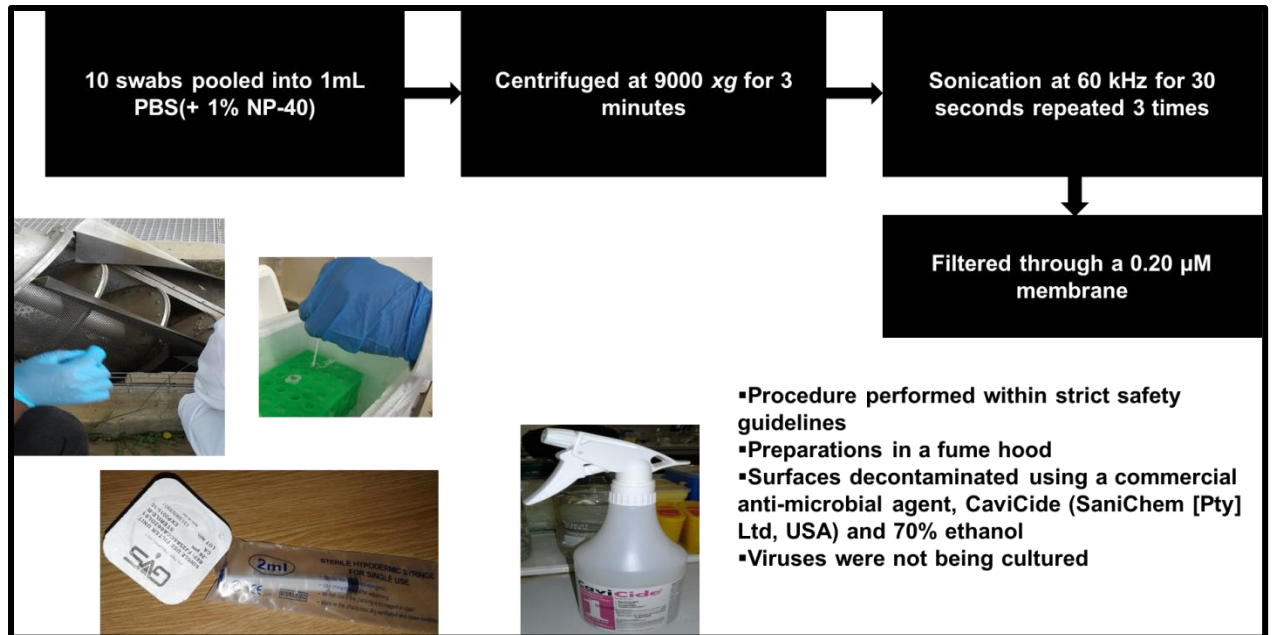


Figure 2.3: Swab samples (ten) were pooled to make a single sample, centrifuged at 9 000 x g for 3 minutes, sonicated at 60 kHz for 5 seconds repeated 3 times and then filtered through a 0.20 μM membrane filter before being subjected to TEM analysis followed by nucleic acid extraction.

Table 2.1: Data pertaining to swab samples analysed.

Sample	Sample ID	Date collected
Swab 1	S1	10-05-16
Swab 2	S2	10-05-16
Swab 3	S3	10-05-16
Swab 4	S4	10-05-16
Swab 5	S5	10-05-16
Swab 6	S6	10-05-16
Swab 7	S7	10-05-16
Swab 8	S8	10-05-16
Swab 9	S9	10-05-16
Swab 10	S10	10-05-16
Swab 11	S11	20-03-17
Swab 12	S12	20-03-17
Swab 13	S13	20-03-17
Swab 14	S14	20-03-17
Swab 15	S15	20-03-17
Swab 16	S16	20-03-17
Swab 17	S17	20-03-17
Swab 18	S18	20-03-17
Swab 19	S19	20-03-17
Swab 20	S20	20-03-17

2.2.3 Preparation of mussel samples for morphological characterisation of viral particles and nucleic acid extraction

Preparation of mussel samples, summarised in **Figure 2.4** below, was performed following a method by Pina *et al.* (1998) with some modifications. Briefly, on an RNase free surface, the gills and stomachs were cut off from the mussels using sterile scissors and forceps. Five mussels were pooled together to make a single sample. 10 g of tissue from each sample was mixed with 20 mL of glycine buffer (0.2N, [pH 10]) and gently homogenised using a mortar and pestle. NP-40 was added to the solution to a final concentration of 1%. The mixture was incubated at room temperature for 1 hour and 30

minutes with shaking at 150 rpm to extract as many virus particles as possible from the tissues. The solutions were briefly vortexed and centrifuged at 9 000 x g for 3 minutes. The resulting supernatant was sonicated at 60 kHz for 5 seconds repeated 3 times to disrupt viral attachment to organic and inorganic materials before being filtered through a 0.20 μ M membrane filter (GVS filter technology, USA) using a 2 mL sterile hypodermic syringe. Samples were stored in labelled 1.5 mL tubes (MS1-20 for small mussels and ML1-20 for large mussels) as shown in **Table 2.2** below at -20 °C for transmission electron microscopy analysis and nucleic acid extraction.

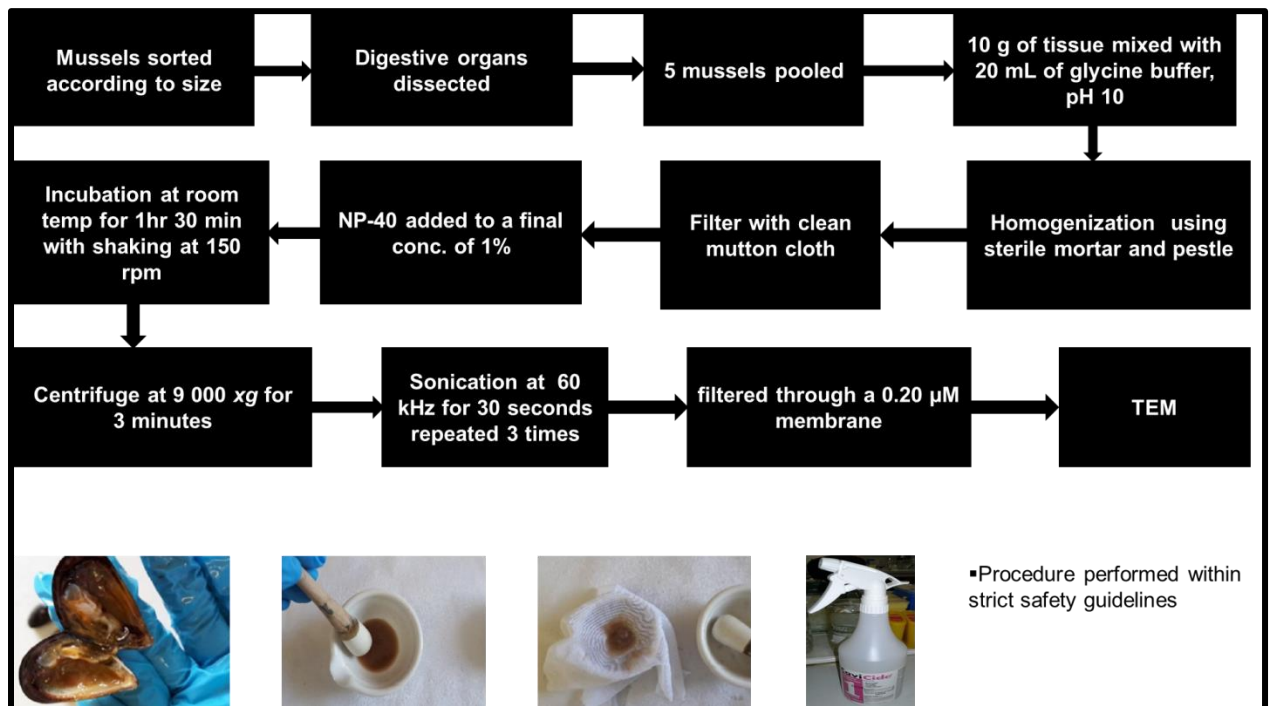


Figure 2.4: Mussel samples were sorted, dissected and homogenised in glycine buffer. To remove large debris, the samples were filtered with a clean mutton cloth. Incubation at room temperature with shaking ensured adequate extraction of viral particles from mussel tissues. Samples were then centrifuged briefly and the supernatant was filtered through 0.20 μ M membrane filter before being subjected to TEM and nucleic acid extraction.

Table 2.2: Data pertaining to mussel samples analysed.

Sample	Sample ID	Date collected
Large mussel 1	ML1	02-05-16
Large mussel 2	ML 2	02-05-16
Large mussel 3	ML 3	02-05-16
Large mussel 4	ML 4	02-05-16
Large mussel 5	ML 5	02-05-16
Large mussel 6	ML 6	02-05-16
Large mussel 7	ML 7	02-05-16
Large mussel 8	ML 8	02-05-16
Large mussel 9	ML 9	02-05-16
Large mussel 10	ML 10	02-05-16
Large mussel 11	ML 11	02-05-16
Large mussel 12	ML 12	02-05-16
Large mussel 13	ML 13	02-05-16
Large mussel 14	ML 14	02-05-16
Large mussel 15	ML 15	02-05-16
Large mussel 16	ML 16	02-05-16
Large mussel 17	ML 17	02-05-16
Large mussel 18	ML 18	02-05-16
Large mussel 19	ML 19	02-05-16
Large mussel 20	ML 20	02-05-16

2.2.4 Determination of morphological features of viral particles from swab and mussel samples by transmission electron microscopy

In order to analyse the swabs and mussels samples for presence and morphological characteristics of viral particles, a protocol described by Hayat (2000), with modifications, was used. Briefly, 1 μ L from each sample was placed on fovar carbon coated grid, left for 1 minute and dried with filter paper. A drop of uranyl acetate, which acts as a negative stain, was placed on top, left for 1 minute and dried with filter paper. The preparation was subjected to TEM analysis on a Zeiss Libra 120 transmission electron microscope, **Figure 2.5**, (Electron Microscopy Unit, Rhodes University). Images

were captured with the Mega View G2 camera (Olympus, Germany) and analysed with the i10 Soft Imaging System (Olympus, Germany).

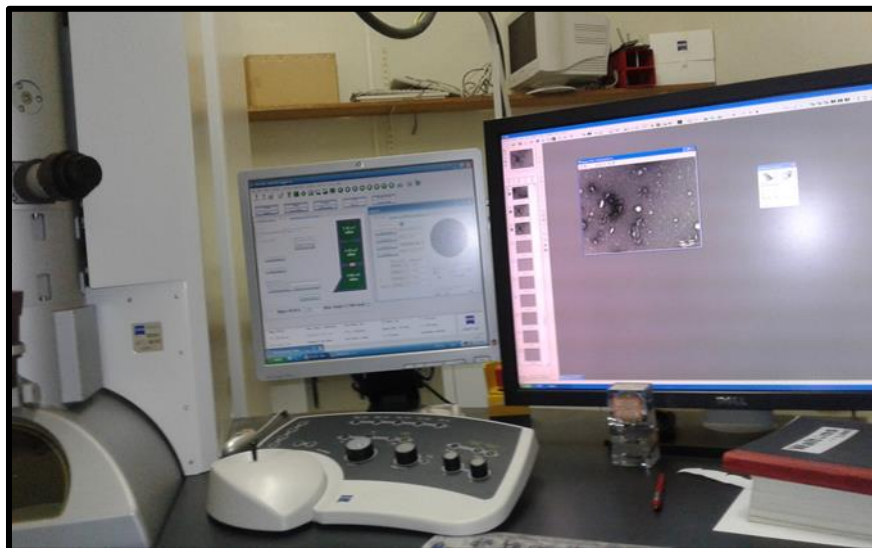


Figure 2.5: The Zeiss Libra 120 transmission electron microscope used to analyse the sizes and morphological characteristics of the viral particles from swab and mussel samples.

2.2.5 Nucleic acid extraction from swab and mussel samples

Viral nucleic acids were extracted from 140 μ L of the twenty swabs and twenty mussels samples (shown in **Tables 2.1** and **2.2**) using the QIAamp® Viral RNA Mini Kit, (Qiagen, USA), following manufacturer's instructions. The nucleic acids were then eluted into 50 μ L sterile deionised water, aliquoted and stored at -80 °C until use in subsequent RT-PCR and conventional PCR assays for molecular detection of RNA viruses (human norovirus and Aichi virus 1) and DNA viruses (enteric human bocaviruses and Enteric Adenoviruses) respectively.

2.2.6 Primers for RT-PCR of HuNoV GII N/S domain of capsid VP1 protein- 342 bp product

A set of degenerate genogroup specific primers designed by Kojima *et al.* (2002), that amplify a product of 342 bp of the conserved capsid N-terminal/shell domain of VP1 region (capsid N/S domain) of HuNoV GII, was used in this study. Group II HuNoV is a broad genogroup responsible for most of all norovirus related outbreaks of gastroenteritis. The details about these primers are shown in **Table 2.3** below.

Table 2.3: Forward and reverse degenerate oligonucleotides for HuNoV GII N/S domain as described by Kojima *et al.* (2002).

Primer ID No	Sequence, 5'→3'	Binding site	Genome location	Polarity	Amplicon size
G2SKF	CNTGGGAGGGC GATCGCAA	5046–5064 bp	Capsid	+	342 bp
G2SKR	CCRCCNGCATR HCCRTTRTACA T	5366–5388 bp	Capsid	-	

Shown below in **Figure 2.6** are primer binding sites on the HuNoV GII genome (Lordsdale virus, accession number: X86557). Both primers bind onto the shell domain of the capsid VP1 protein of the genome.

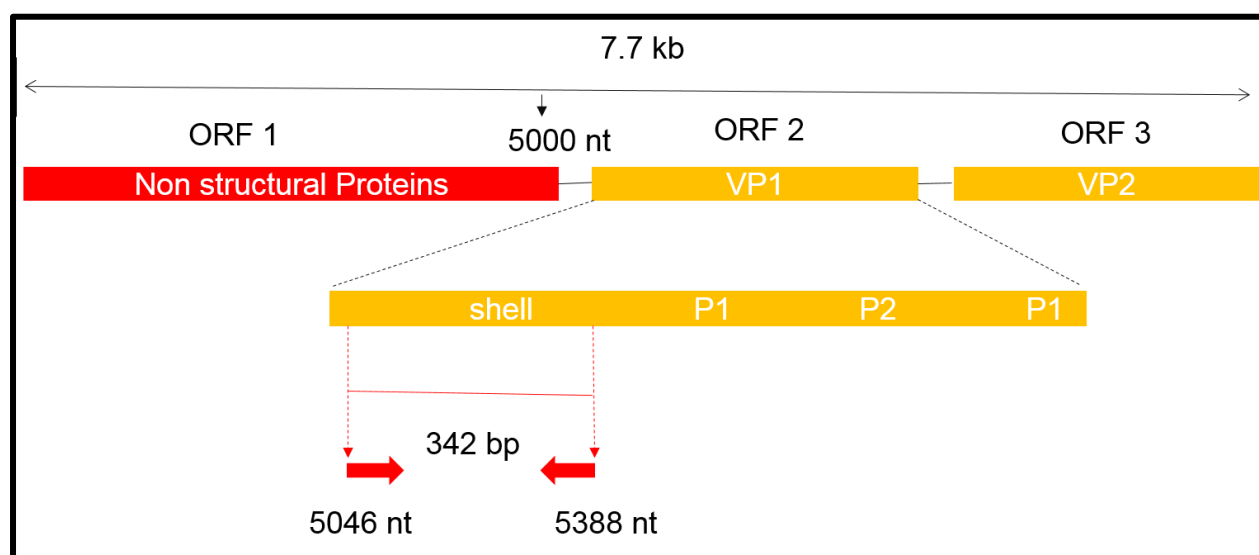


Figure 2.6: Schematic representation of the HuNoV N/S domain primer binding sites as on the complete genome of the Lordsdale virus. Forward primer G2SKF (→) and reverse primer G2SKR (←) amplify an approximately 342 bp product in the capsid VP1 region (adapted from Kojima *et al.*, 2002).

2.2.7 Preparation of positive control RNA and RT-PCR of HuNoV GII N/S domain of capsid VP1 protein- 342 bp product

A plasmid containing the 342 bp insert of the conserved capsid N-terminal/shell domain of VP1 region (capsid N/S domain) of HuNoV GII cloned into pGEM[®]-T Easy Vector (Promega, USA) was kindly provided by Brittany Jaquet, Rhodes University, South Africa (Jaquet, 2017). The plasmid was stored at -80 °C as glycerol stocks until use in the current study.

For the purpose of this study, cells from glycerol stocks above were thawed on ice and sterile wire loops were used to streak onto Luria agar (with ampicillin at a final concentration of 100 µg/mL) making discontinuous streaks. The plates were incubated at 37 °C overnight (15-18 hours). Isolated colonies (five) were each inoculated into 5 mL Luria broth (with ampicillin at a final concentration of 100 µg/mL) and incubated at 37 °C overnight (15-18hrs) with shaking at approximately 180 rpm. This was followed by extraction of the plasmid DNA by use of the GeneJET Plasmid Miniprep Kit (Thermo Scientific, USA) following manufacturer's instructions. The plasmid DNA was eluted into 40 µL of sterile, nuclease-free water and stored at -20 °C until use for *in vitro* transcription. To confirm the size of the insert, 2 µL of the plasmid DNA was subjected to a restriction digest using Fast Digest EcoRI (Thermo Scientific, USA) following manufacturer's instruction. The restriction digest product was analysed on a 1% agarose gel with ethidium bromide staining at 90 volts for 35 minutes.

2.2.7.1 In vitro transcription and RNA clean-up

In order to obtain RNA from plasmids, an *in vitro* transcription reaction was performed using the TranscriptAid T7 High Yield Transcription Kit (Thermo Scientific, USA) strictly following manufacturer's instructions. The T7 transcribed RNA was purified using the GeneJET RNA Purification Kit (Thermo Scientific, USA) following manufacturer's instructions. The purified RNA was aliquoted and stored at -80 °C until use.

2.2.7.2 Application of a one-step RT-PCR assay for amplification of the N/S domain of the capsid VP1 coding region for the HuNoV GII T7 transcribed Control RNA

The Verso 1-Step RT-PCR Hot-Start Kit (Thermo Scientific, USA) was used to PCR amplify a 342 bp product of the conserved capsid N-terminal/Shell domain of VP1 region

(capsid N/S domain) of HuNoV GII using degenerate genogroup specific primers described in Kojima *et al.* (2002) shown in **Table 2.3** above. The T7 synthesised HuNoV GII RNA was used as a template in the reaction. Briefly, 0.5 µL Verso enzyme mix, 12.5 µL of Verso 2x 1-step hot-start mix, 1.25 µL RT enhancer, 0.5 µL of 10 µM forward primer (G2SKF), 0.5 µL of 10 µM reverse primer (G2SKR), 1 µL of the positive control HuNoV GII T7 transcribed RNA and 8.75 µL nuclease-free, sterile water, all making up 25 µL, were mixed up in a sterile flat cap PCR tube and subjected to thermal amplification in a SimpliAmp Thermal cycler (Bio-Systems by Life Technologies) to amplify a 342 bp product of the capsid VP1 region. A no template control reaction (NTC), which consisted of 0.5 µL Verso enzyme mix, 12.5 µL of Verso 2x 1-step hot mix, 1.25 µL RT enhancer, 0.5 µL of 10 µM forward primer (G2SKF), 0.5 µL of 10 µM reverse primer (G2SKR), 9.75 µL nuclease-free, sterile water was also included.

The cycling parameters were as shown in **Table 2.4** below. The resultant PCR product was analysed by 1% agarose gel electrophoresis with ethidium bromide staining at 90 Volts for 35 minutes.

Table 2.4: Cycling parameters for PCR amplification of the capsid N/S domain of the HuNoV.

Step	Temperature	Duration	Cycles
cDNA synthesis	50 °C	15 minutes	1
Verso inactivation	95 °C	15 minutes	1
Denaturation	95 °C	20 seconds	
Annealing	55 °C	30 seconds	40
Extension	72 °C	1 minute	
Final extension	72 °C	5 minutes	1
Hold	4 °C	∞	1

2.2.7.3 Sensitivity of the Thermo Scientific Verso 1-Step RT-PCR Hot-Start Kit versus the Thermo Scientific Maxima H Minus First Strand cDNA Synthesis Kit

An experiment was carried out to compare the sensitivities of the Thermo Scientific Verso 1-Step RT-PCR Hot-Start Kit and the Maxima H Minus First Strand cDNA

Synthesis Kit (Thermo Scientific, USA) by determination of the minimum concentration of RNA required to produce a PCR product. This was done in order to determine the most suitable assay for detection of viral pathogens from the environmental samples under study for which low concentrations of the viruses were expected. The HuNoV GII T7 transcribed RNA was serially diluted with sterile nuclease free water as depicted in **Table 2.5** below. The RNA concentrations were measured using the NanoDrop 2000 (Thermo Scientific, USA). For each kit, the following concentrations of positive control HuNoV GII T7 transcribed RNA were used as templates; 4 ng/ μ L, 1.4 ng/ μ L, 0.7 ng/ μ L, 0.5 ng/ μ L, 0.3 ng/ μ L and 0.1 ng/ μ L (**Table 2.5** below). The kits were used following manufacturers' instructions to amplify a 342 bp product of the capsid VP1 region of HuNoV GII. The cycling parameters for the one-step RT-PCR assay were as described before in section 2.2.7.2. The cycling parameters for the two-step RT-PCR assay were as described in Kojima *et al.*, (2002) i.e. initial denaturation at 94 °C for 3 minutes, 40 cycles of denaturation at 94 °C for 30 seconds, annealing at 50 °C for 30 seconds, elongation at 72 °C for 1 minute, final extension at 72 °C for 7 minutes and an indefinite holding temperature of 4 °C. PCR products were analysed by 1% agarose gel electrophoresis with ethidium bromide staining.

Table 2.5: Serial dilutions of positive control HuNoV GII T7 synthesised RNA used to estimate the minimum concentration of RNA required to produce PCR products for a one-step RT-PCR assay versus a two-step RT-PCR assay.

Preparation	Dilution	RNA concentration
1	1: 1000	4.0 ng/ μ L
2	1: 5000	1.4 ng/ μ L
3	1: 10 000	0.7 ng/ μ L
4	1: 15 000	0.5 ng/ μ L
5	1: 20 000	0.3 ng/ μ L
6	1: 50 000	0.1 ng/ μ L

2.2.8 Development of a one-step RT-PCR assay for amplification of the N/S junction of the capsid VP1 coding region of HuNoV GII from mussel and swab samples

The Thermo Scientific Verso 1-Step RT-PCR Hot-Start Kit was used to PCR amplify a 342 bp product of the N-terminal domain and a part of the Shell domain of HuNoV GII capsid VP1 protein from eight swab (S1-S8) and eight large mussel (ML1-ML8) samples using primers (shown in **Table 2.3** above) described in Kojima *et al.* (2002). The reactions were set up as in section 2.2.7.2 except that 2 μ L RNA from mussel and swab samples was used. A positive control and an NTC, all set up as described before in section 2.2.7 were included. PCR amplification was carried out in a SimpliAmp Thermal cycler as described before in section 2.2.7.2. PCR products were analysed by 1% agarose gel electrophoresis with ethidium bromide staining at 90 Volts for 35 minutes.

The PCR products were gel purified by use of the GeneJET Gel Extraction Kit (Thermo Scientific, USA) following manufacturer's instructions. DNA was eluted into 40 μ L of sterile, nuclease-free water and stored at -20 °C until use. In order to confirm the success of the PCR clean-up stage, the purified PCR products were analysed by 1% agarose gel electrophoresis with ethidium bromide staining at 90 Volts for 35 minutes.

2.2.9 Cloning purified PCR products into pJET 1.2/blunt

In order to obtain complete sequence data of the PCR products, they were cloned into pJET 1.2/blunt vector (**Figure 2.7**), CloneJET™ PCR Cloning Kit (Thermo Scientific, USA) following the sticky-end protocol as the PCR products had 3'-dA overhangs generated by *Taq* DNA polymerase. The ligation mixture was incubated overnight at 4 °C.

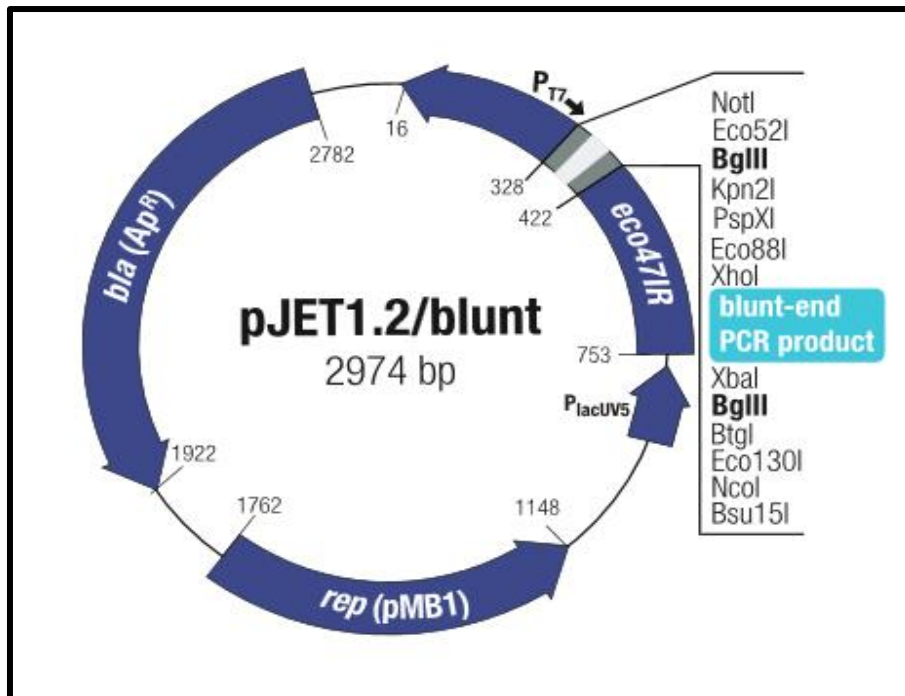


Figure 2.7: Pictorial representation of pJET1.2/blunt Cloning Vector. Important features for this vector include the T7 promoter, PlacUV5, Multiple cloning site, *eco47IR*, *bla* (*Ap^R*) and the insertion site for DNA fragments (Thermo Scientific, USA).

2.2.10 Transformation of competent cells

After overnight incubation at 4 °C, the ligation mixture (20 µL) was centrifuged briefly and transferred into 50 µL of competent *E.coli* cells (DH5α) on ice and incubated for 20 minutes. The mixture was then heat shocked for 45 seconds at 42 °C and incubated on ice for 2 minutes. 500 µL of Luria Broth (with no ampicillin) was added and the mixture was incubated at 37 °C with shaking at approximately 200 rpm for 45 minutes after which it was centrifuged at 6 000 x *g* for 2 minutes. The supernatant was decanted leaving approximately 100 µL which was then mixed gently by pipetting up and down, and then spread on Luria agar plate (with ampicillin at a final concentration of 100 µg/mL). The plates were incubated overnight at 37 °C.

After an overnight incubation at 37 °C, ten isolated colonies (labelled A-J) from each plate were inoculated into 5 mL Luria broth (with ampicillin at a final concentration of 1 µg/mL) and incubated at 37 °C overnight (15-18hrs) with shaking at approximately 200 rpm.

2.2.11 Plasmid extraction and restriction analysis

Plasmids were extracted from each Luria broth preparation from section 2.2.10 using the GeneJET Plasmid Miniprep Kit (Thermo Scientific, USA) following manufacturer's instructions. The plasmid DNA was eluted into 40 μ L of sterile, distilled, nuclease free water and stored at -20 °C in sterile Eppendorf tubes (labelled A-J for each sample). The presence and size of inserts was confirmed by double digest with Xho 1 (Promega, USA) and Xba 1 (Thermo Scientific, USA). Briefly, 13 μ L nuclease- free water, 4 μ L 10x Tango buffer, 2 μ L plasmid DNA and 1 μ L of Xho 1 were pipetted into a sterile 1.5 mL tube at room temperature and thoroughly mixed before being incubated in a water bath at 37 °C for 2 hours, after which Xho 1 was inactivated by heating at 80 °C on a heating block for 20 minutes. This was followed by addition of 1 μ L Xba 1 (FD) into the mixture, incubating at 37 °C in a water bath for 30 minutes. Inactivation of Xba 1 was carried out at 65 °C for 20 minutes. The digestion products were analysed by 1% agarose gel electrophoresis with ethidium bromide staining at 90 volts for 35 minutes.

2.2.12 Sequencing of plasmids and BLAST analysis of resultant sequences

Plasmids with inserts approximately 342 bp were Sanger sequenced at Inqaba Biotechnical Industries ([Pty] Ltd, Pretoria, South Africa). Sequencing was done in the forward direction only. Resultant sequences were viewed on SnapGene Viewer 3.2.1, manually edited and subjected to BLAST search for related sequences from GenBank by use of NCBI BLAST website (Blast.ncbi.nlm.nih.gov/Blast.cgi).

2.3 Results

2.3.1 Positive control

2.3.1.1 Confirmation of positive control plasmid DNA by restriction analysis

The plasmid map of the positive control used in the analysis is shown in **Figure 2.8A** below. Restriction analysis of this control plasmid using Fast Digest EcoRI confirmed that the insert was approximately 342 bp as expected. **Figure 2.8B** below shows an agarose gel of the uncut and cut plasmid DNA. Lane 1 shows the uncut plasmid DNA with its various conformations including supercoiled which is brighter compared to the other conformations. Lane 2 shows the cut plasmid DNA with the insert PCR product approximately 342 bp and the vector approximately 3015 bp. This shows that the insert PCR product cloned into the vector was of the correct size. As shown in **Figure 2.8B**, the insert PCR product was successfully cut from the plasmid.

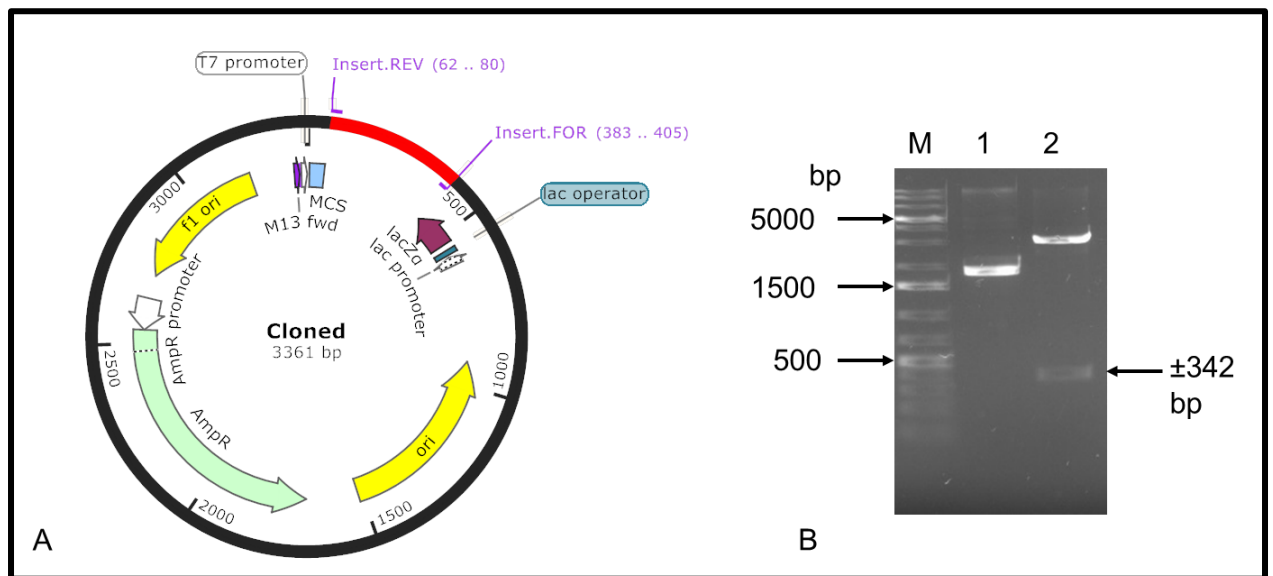


Figure 2.8: **A)** Plasmid map of the HuNoV GII insert (shown in red) cloned into pGEM[®]-T Easy. **B)** 1% agarose gel electrophoresis of uncut and cut Norovirus GII positive control plasmid DNA. M: GeneRuler™ 1 kb Plus DNA Ladder (Thermo Scientific, USA), lane 2: uncut control plasmid DNA, lane 3: Cut control plasmid DNA.

2.3.1.2 RNA synthesis by In vitro transcription and RT-PCR of positive control RNA

The *in vitro* transcription was successful as HuNoV GII RNA was obtained from the reactions. **Figure 2.9A**, below shows 1% agarose gel electrophoresis of the T7 synthesised RNA (lane 1) which presented as a smear running from 1600 bp down to 500 bp. The synthesised RNA was used as a template in a one-step RT-PCR assay described in section 2.2.7.2. **Figure 2.9B** below shows an RT-PCR product of the correct size (approximately 342 bp) obtained from the positive control RNA (lane 1). As expected no PCR product was visible in the NTC, shown in lane 2, as sterile nuclease-free water was used instead of an RNA template.

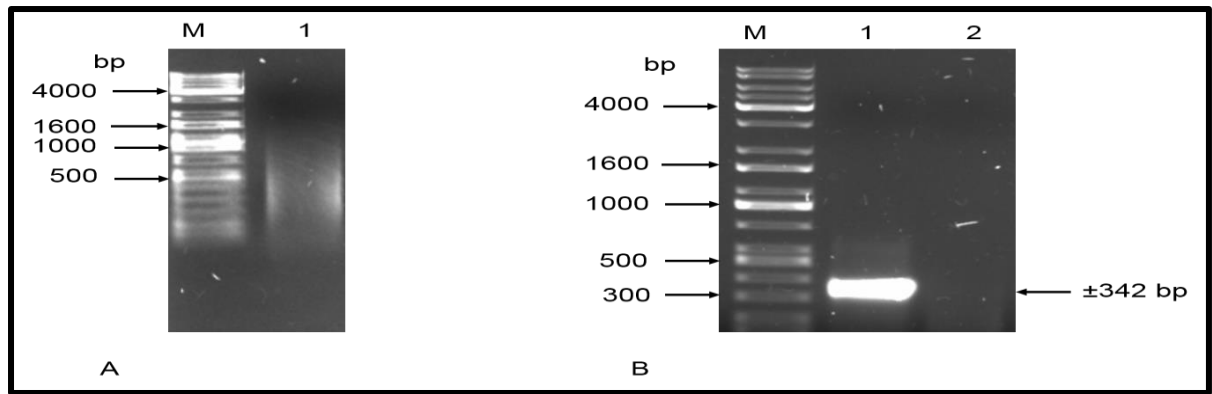


Figure 2.9: **A)** 1% agarose gel electrophoresis of positive control T7 synthesised RNA of the HuNoV GII N/S domain of the capsid VP1 protein. M: KAPA Universal Ladder, lane 1: Positive control T7 synthesised RNA. **B)** 1% agarose gel electrophoresis of the positive control RT-PCR product (342 bp) of the HuNoV N/S domain of the capsid VP1 protein, M: KAPA Universal Ladder, lane 1: Positive control RT-PCR product, lane 2: NTC.

2.3.1.3 Sensitivity of the Verso 1-Step RT-PCR Hot-Start Kit versus Maxima H Minus First Strand cDNA Synthesis system

The sensitivity of the Verso 1-Step RT-PCR Hot-Start Kit was shown to be more than that of the two-step RT-PCR system that uses the Maxima H Minus First Strand cDNA Kit. Shown below in **Figure 2.10A**, lanes 1-6 are bands of RT-PCR products generated from RNA concentrations of 4 ng/ μL , 1.4 ng/ μL , 0.7 ng/ μL , 0.5 ng/ μL , 0.3 ng/ μL and 0.1 ng/ μL respectively using the Maxima H Minus First Strand cDNA Kit. The bands decrease in intensity to an extent that that no band was visible at lane 5 (0.3 ng/ μL of RNA used) and lane 6 (0.1 ng/ μL of RNA used). On the other hand **Figure 2.10B**, lanes 1-6, are also bands of PCR products generated from RNA concentrations of 4ng/ μL , 1.4 ng/ μL , 0.7 ng/ μL , 0.5 ng/ μL , 0.3 ng/ μL and 0.1 ng/ μL respectively using the Verso 1-Step RT-PCR Hot-Start Kit. Although the bands also decreased in intensity to a decrease in RNA concentrations, PCR bands were still visible at lanes 5 (0.3 ng/ μL of RNA used) and 6 (0.1 ng/ μL of RNA used).

Figure 2.10B below shows that the Verso 1-Step RT-PCR Hot-Start Kit is more sensitive than the Maxima H Minus First Strand cDNA Synthesis Kit (**Figure 2.10A**) as it was able to detect lower RNA concentrations, down to 0.1 ng/ μL (**Figure 2.10B**, lane 6), compared to the two-step system which could not detect RNA concentrations of below 0.5 ng/ μL (**Figure 2.10A**, lane 5). Due to this, the Verso 1-step RT-PCR kit was

preferred for detection of the HuNoV GII and subsequently the AiV-1 in the present study.

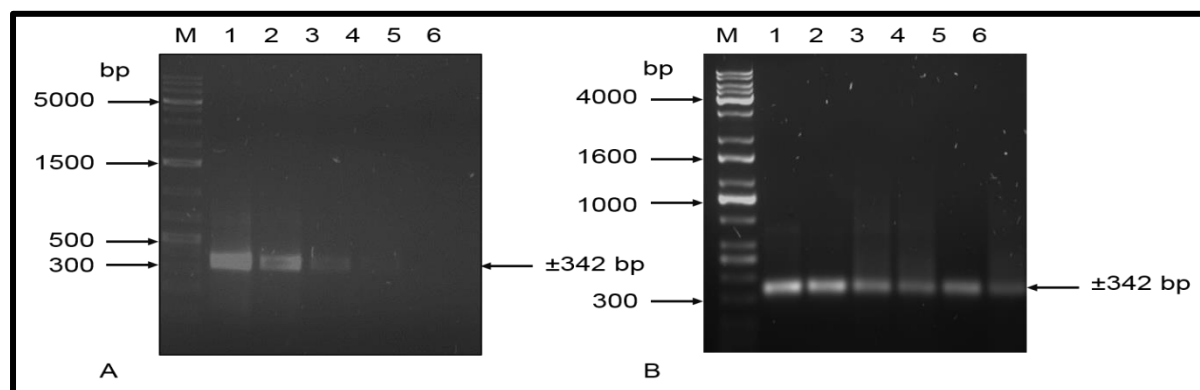


Figure 2.10: Sensitivities of the Maxima H Minus First Strand cDNA Synthesis Kit versus that of the Verso 1-Step RT-PCR Hot-Start Kit. **A)** 1% agarose gel electrophoresis of RT-PCR products of the NoV GII N/S domain of capsid VP1 protein produced using the Maxima H Minus First Strand cDNA Synthesis Kit. M: GeneRuler™ 1 kb Plus DNA Ladder, lanes 1-6: RT-PCR products from decreasing concentrations of the control T7 synthesised RNA (4 ng/ μ L, 1.4 ng/ μ L, 0.7 ng/ μ L, 0.5 ng/ μ L, 0.3 ng/ μ L and 0.1 ng/ μ L respectively). **B)** 1% agarose gel electrophoresis of RT-PCR products of the NoV GII N/S domain of capsid VP1 protein produced using the Verso 1-Step RT-PCR Hot-Start Kit. M: KAPA Universal Ladder, lanes 1-6: RT-PCR products from decreasing concentrations of the control T7 transcribed RNA (4 ng/ μ L, 1.4 ng/ μ L, 0.7 ng/ μ L, 0.5 ng/ μ L, 0.3 ng/ μ L and 0.1 ng/ μ L respectively).

2.3.2 Swab samples

2.3.2.1 Determination of morphological features of viral particles by TEM-Swab samples

Transmission electron microscopy revealed the presence of small round viral particles ranging between 20 nm and 40 nm in all samples. **Figure 2.11 (panels A-D)** below shows the representative results of the TEM for swab samples 1 to 4. Results from other swab samples were not included. In addition to the viral particles with diameters ranging from 20 nm and 40 nm, other viral particles with diameters up to 100 nm were also observed, some with spikes which are characteristic of human adenoviruses (**Figure 2.11, panel C**). However transmission electron microscopy is unreliable as there are many viruses that fall in the size range of human noroviruses. It is by use of molecular techniques such as

PCR that conclusive elucidations can be made. Samples positive with TEM were passed onto the next procedure, nucleic acid extraction, in preparation for RT-PCR and conventional PCR for DNA viruses under study.

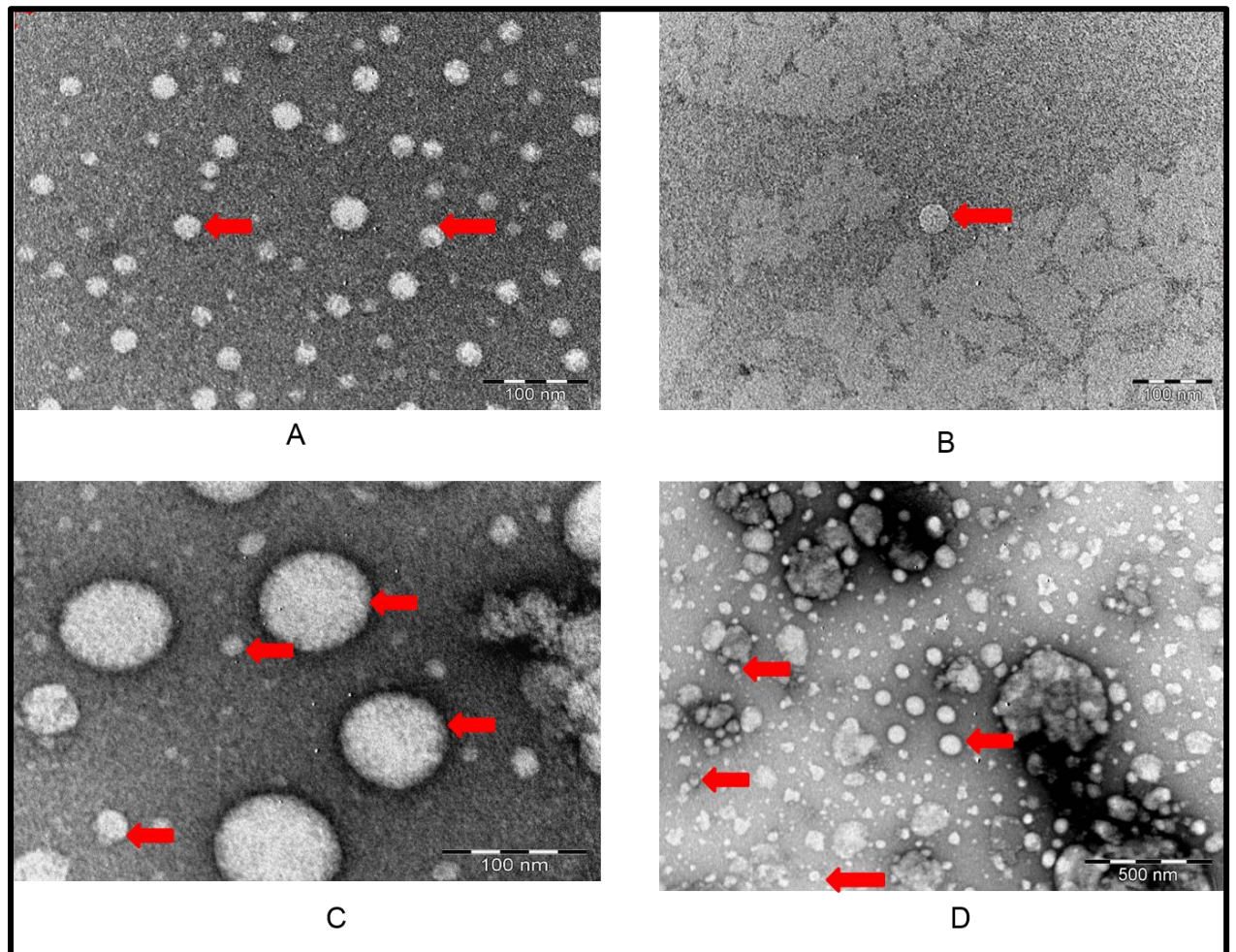


Figure 2.11: TEM images of viral particles from swab samples A: Swab 1(S1) B: Swab 2 (S2) C: Swab 3 (S3) D: Swab 4 (S4). Viral particles, ranging from less than 20 nm to more than 100 nm in diameter were visible on the grids.

2.3.2.2 RNA extraction from swab samples

All twenty swab samples showed the presence of viral particles with diameters ranging from around 20 nm to 100 nm and hence were subjected to nucleic acid extraction using the QIAamp® Viral RNA Mini Kit. **Figure 2.12**, lanes 1-6, shows a representative 1% agarose gel electrophoresis of nucleic acids extracted from swab samples 1-6 respectively. The extraction was also successful for the other fourteen swabs (S7 to S20)

for which results were not shown. The nucleic acids from all samples presented as smears ranging from above 10 kbp to below 500 bp.

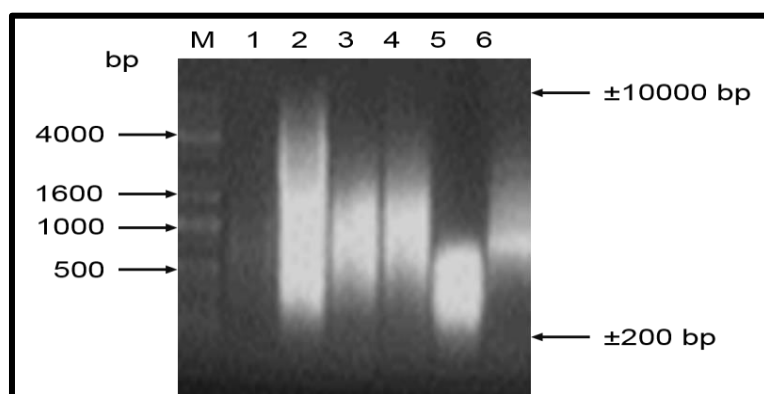


Figure 2.12: 1% agarose gel electrophoresis of nucleic acids extracted from swab samples. M: KAPA Universal Ladder, lanes 1-6 nucleic acids extracted from swab samples 1-6 respectively.

2.3.2.3 RT-PCR and gel purification of PCR products from swab samples

Amplicons of approximately 342 bp were obtained from four (S1, S2, S3 and S5) out of eight swab samples analysed as shown in **Table 2.6** below.

Table 2.6: RT-PCR results for swab samples

Sample ID	RT-PCR results
S1	PCR product obtained
S2	PCR product obtained
S3	PCR product obtained
S4	No PCR product obtained
S5	PCR product obtained
S6	No PCR product obtained
S7	No PCR product obtained
S8	No PCR product obtained

Figure 2.13 shows a representative 1% agarose gel of RT-PCR products from swab samples 1 and 2. Results from other swab samples were not shown. As expected the positive control (lane 1) produced a band of the right size which was much brighter compared to those obtained from environmental samples, swab 1 (lanes 3) and swab 2

(lane 4) as the T7 synthesised RNA used was purer and of high quality than the one from environmental samples. The NTC reaction (lane 2) did not produce any band as expected since sterile nuclease-free water was used instead of RNA template. The RT-PCR products from the swab samples were gel purified by use of the GeneJET Gel Extraction Kit.

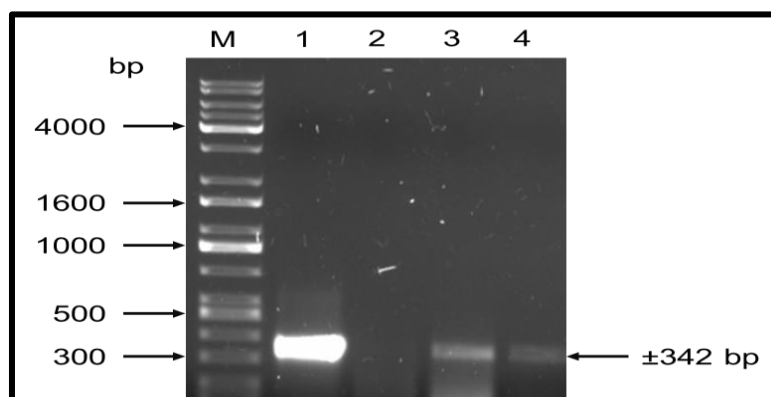


Figure 2.13: 1% agarose gel electrophoresis of RT-PCR products of the HuNoV N/S domain of the capsid VP1 coding region from swab samples. M: KAPA Universal Ladder, lane 1: Positive control PCR product (approximately 342 bp), lane 2: NTC, lane 3: RT-PCR product from swab sample 1, lane 4: RT-PCR products from swab sample 2.

2.3.2.4 Cloning of RT-PCR products from swab samples into pJET 1.2/blunt vector and restriction analysis of plasmid DNA

Gel purified RT-PCR products were cloned into pJET 1.2/blunt vector as described in section 2.2.9. Competent *E.coli* cells (DH5 α) were transformed as described in section 2.2.10. Ten colonies (A-J) from each sample were inoculated into Luria broth (with ampicillin) as described in section 2.2.10 and plasmids extracted from the samples.

Figure 2.14A below shows a representative gel of plasmid DNA extracted from the cells (five colonies from swab sample 2) by use of the GeneJET Plasmid Miniprep Kit as described in section 2.2.11 above. The results from other swab samples were not shown. Restriction analysis of plasmid DNA by use of digest Xho 1 and Xba 1 confirmed the presence and sizes of inserts which were approximately 342 bp. **Figure 2.14B** below shows representative results of the digests for the five plasmids from swab sample 2. Lanes 1, 3, 5, 7 and 9 show uncut plasmids. Lanes 2, 4, 6, 8 and 10 show cut plasmids for which linear vectors were approximately 2974 bp, the size of pJET 1.2/blunt vector, while inserts were approximately 342 bp as expected. Restriction results from other swab samples were not shown

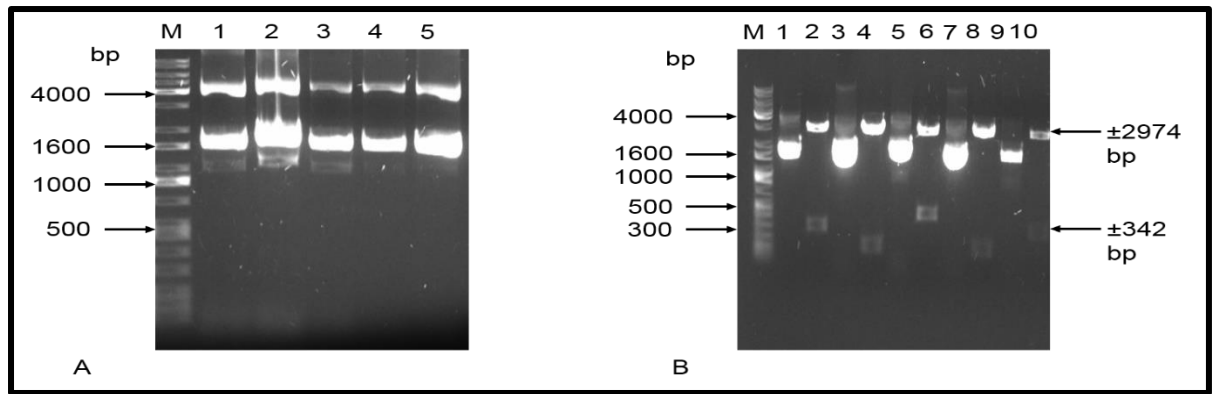


Figure 2.14: **A)** 1% agarose gel electrophoresis of plasmid DNA from swab sample 2 (S2). M: KAPA Universal Ladder, lane 1-6: Uncut plasmid DNA (S2A-E). **B)** 1% agarose gel electrophoresis of restriction digest products of the plasmids M: KAPA Universal Ladder, lane 1: Plasmid S2A uncut, lane 2: S2A cut, lane 3: Plasmid S2B uncut, lane 4: S2B cut, lane 5: Plasmid S2C uncut, lane 6: S2C cut, lane 7: plasmid S2D uncut, lane 8: S2D cut, lane 9: Plasmid S2E uncut lane 10: S2E cut.

2.3.3 Mussel samples

2.3.3.1 Determination of morphological features of viral particles by TEM-mussel samples

Transmission electron microscopy revealed the presence of small round viral particles ranging between 20 nm and 40 nm in the samples. **Figure 2.15, panels A-C** below shows representative results of the TEM from large mussel samples 1 to 3 with viral particles of different sizes. Results from other samples were not shown. There were few or no viral particles at all from those mussels classified as being small (< 4 cm in diameter), hence nucleic acids were only extracted from the twenty mussel samples which were classified as being large.

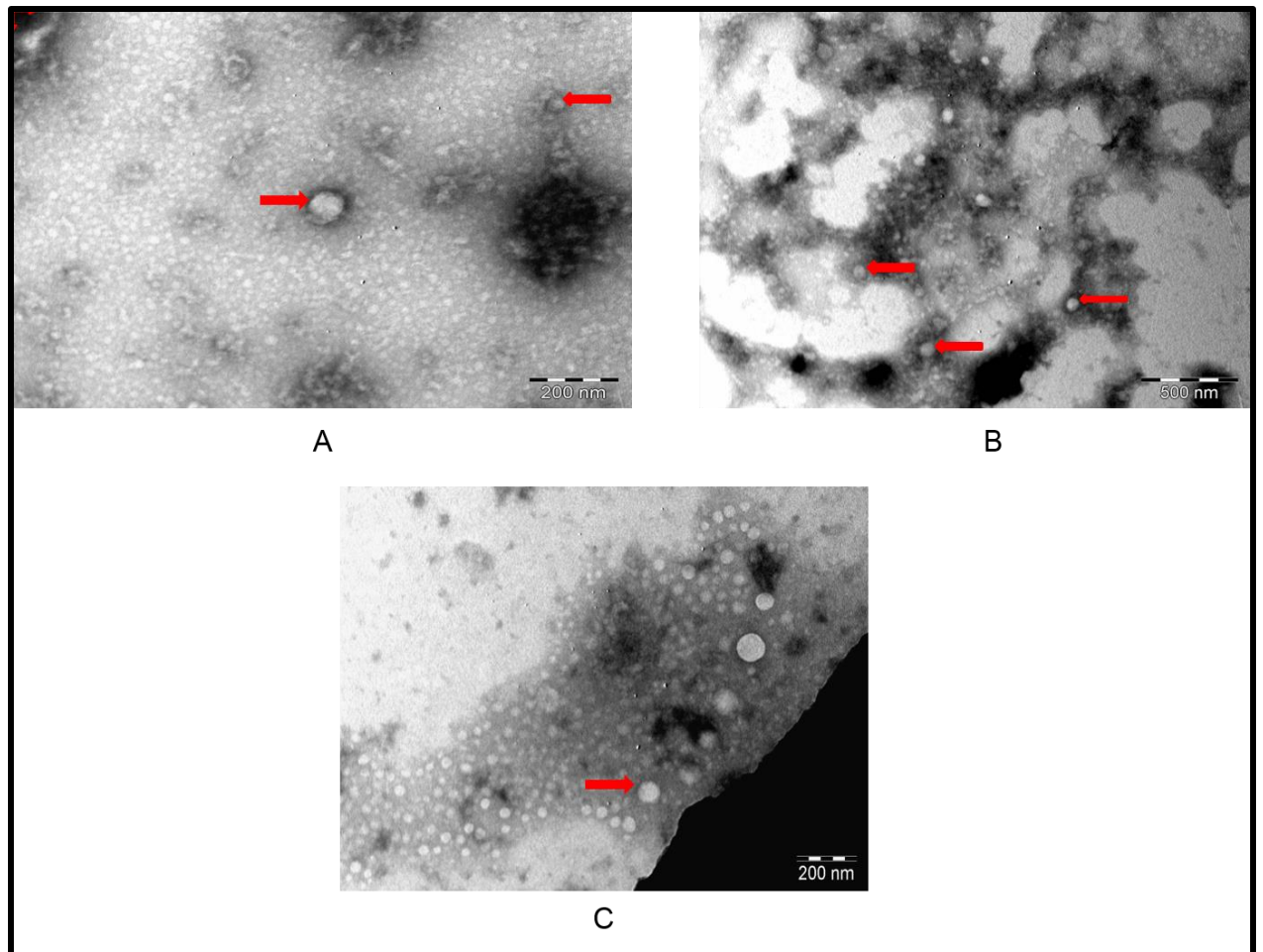


Figure 2.15: TEM images from mussel samples (large mussels) A: large mussel 1 (ML1) B: large mussel 2 (ML2) C: large mussel 3 (ML3). Viral particles, ranging from less than 20 nm to more than 100 nm in diameter were visible on the grids.

2.3.3.2 RNA extraction from mussel samples

Nucleic acids were extracted from the twenty large mussel samples (ML1 to ML20) as they showed the presence of viral particles with diameters ranging from less than 20 nm to 100 nm. **Figure 2.16** below shows a representative 1% agarose gel of nucleic acids extracted from large mussel samples, ML1 to ML8. The nucleic acids presented as smears running between 2500 kb and 100 bp in most samples. The extraction was also successful for other samples (ML9 to ML20) but the results were not shown.

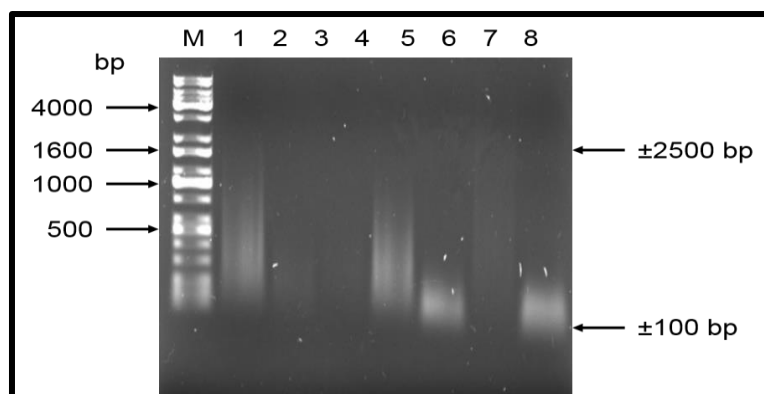


Figure 2.16: 1% agarose gel electrophoresis of nucleic acids. Lane 1 KAPA Universal Ladder, lanes 1-8: nucleic acids extracted from large mussel samples ML1 to ML8.

2.3.3.3 RT-PCR and gel purification of PCR products from mussel samples

Amplicons of approximately 342 bp were obtained from three out of eight mussel samples tested (**Table 2.7**).

Table 2.7: RT-PCR results for mussel samples

Sample ID	RT-PCR results
ML1	PCR product obtained
ML2	PCR product obtained
ML3	PCR product obtained
ML4	No PCR product obtained
ML5	No PCR product obtained
ML6	No PCR product obtained
ML7	No PCR product obtained
ML8	No PCR product obtained

Shown in **Figure 2.17A** below is a representative 1% agarose gel of PCR products of approximately 342 bp produced from mussel samples 1 to 3. The positive control sample (lane 1) produced a bright band while NTC reaction (lane 2) produced no band as expected. Lanes 3 to 5 show PCR products which were obtained from the mussel samples ML1 to ML3 respectively. The PCR products were gel purified by use of the GeneJET Gel Extraction Kit as described before in section 2.2.8.

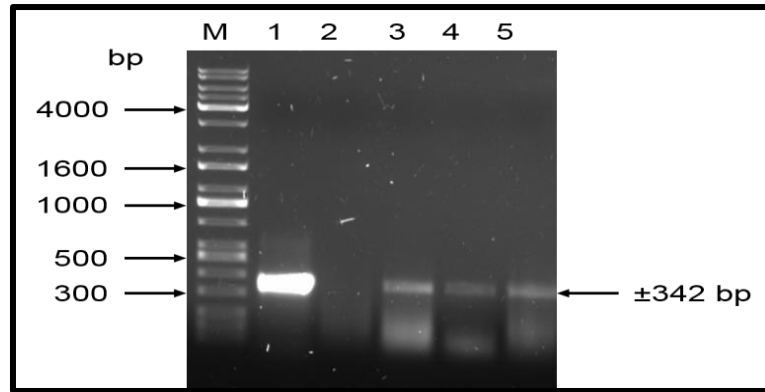


Figure 2.17: 1% agarose gel electrophoresis of RT-PCR products of the HuNoV N/S domain of the capsid VP1 coding region from mussel samples. M: KAPA Universal Ladder, lane 1: Positive control PCR product (approximately 342 bp), lane 2: NTC, lanes 3 to 5: PCR products from large mussel samples, ML1, ML2 and ML3 respectively

2.3.3.4 Cloning of RT-PCR products from mussel samples into pJET 1.2/blunt vector and restriction analysis of plasmid DNA

The gel purified PCR products were cloned into pJET 1.2/blunt vector as described in section 2.2.9. Competent *E.coli* cells (DH5 α) were transformed as described in section 2.2.10. Ten colonies (A-J) from each sample were inoculated into Luria broth (with ampicillin) as described in section 2.2.10 and plasmids extracted from the samples.

Figure 2.18A below shows a representative 1% agarose gel of plasmid DNA extracted from the cells (five colonies from ML1) by use of the GeneJET Plasmid Miniprep Kit as described in section 2.2.11 above. The results from other mussel samples were not shown. Restriction analysis of plasmids by use of Xho 1 and fast digest Xba 1 confirmed the presence and sizes of inserts which were approximately 342 bp. **Figure 2.18B** below shows a representative 1% agarose gel of the restriction digest results of five plasmids from sample ML1. Lane 1 shows the positive control PCR product (approximately 342 bp) which was included on the gel to estimate the sizes of the inserts. Lanes 2, 4, 6, 8 and 10 show uncut plasmids. Lanes 3, 5, 9 and 11 show cut plasmids for which linear vectors were approximately 2974 bp, the size of pJET 1.2/blunt vector, while inserts were approximately 342 bp as expected.

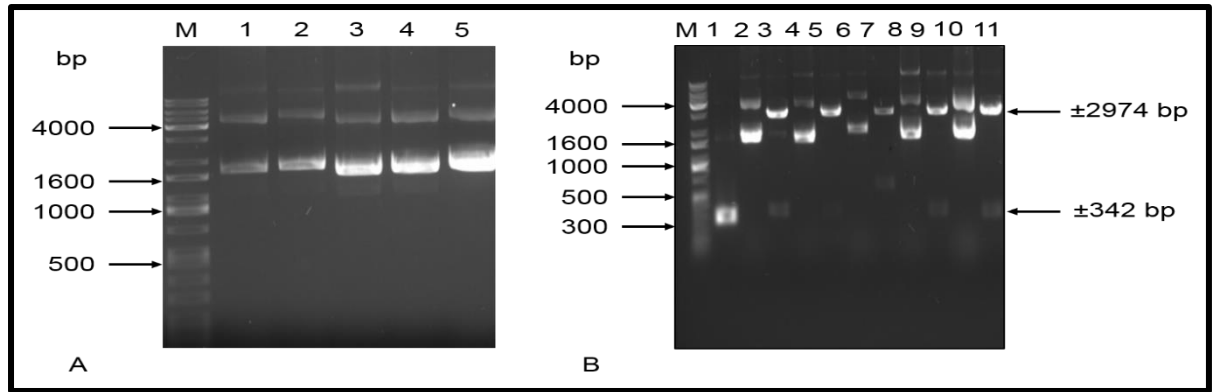


Figure 2.18: **A)** 1% agarose gel electrophoresis of plasmid DNA from large mussel sample 1 (ML1). M: KAPA Universal Ladder, lane 1-6: Uncut plasmid DNA (ML1A, ML1B, ML1C, ML1D and ML1E respectively). **B)** 1% agarose gel electrophoresis of cut and uncut plasmids M: KAPA Universal Ladder, lane 1: Positive control PCR product (approximately 342 bp), lane 2: Plasmid ML1A uncut, lane 3: ML1A cut, lane 4: Plasmid ML1B uncut, lane 5: ML1B cut, lane 6: Plasmid ML1C uncut, lane 7: ML1C cut, lane 8: plasmid ML1D uncut, lane 9: ML1D cut, lane 10: Plasmid ML1E uncut lane 11: ML1E cut.

2.3.3.5 BLAST analysis of HuNoV GII PCR products from swab and mussel samples

Some plasmids from both swab (five plasmids) and mussel (three plasmids) samples with inserts approximately 342 bp were Sanger sequenced at Inqaba Biotechnical Industries ([Pty] Ltd, Pretoria, South Africa). The resultant DNA sequences were highly identical to various GII HuNoV strains in GenBank. As shown in **Table 2.8** below, all samples had percentage identities of between 99% and 100% to known GII.4 HuNoV strains with E-values ranging from $8e-171$ to $2e-167$.

Table 2.8: BLAST analysis results of PCR products of the HuNoV N/S domain of capsid VP1 coding region from swab (S) and large mussel (ML) samples.

Sample ID	Description	Accession number	E-value	% Identity
S1D	HuNoV GII/ NP-598	KX685491.1	4e-169	99%
S2A	HuNoV GII/1733/2006	HM590545.2	2e-167	99%
S2B	HuNoV GII/ NPC-405_2	KX685499.1	8e-171	99%
S2C	HuNoV GII/NPC-405_2	KX685499.1	2e-172	99%
S3D	HuNoV GII/NP-544_3	KX685486.1	6e-172	99%
ML1A	HuNoV GII/1733/2006	HM590545.2	4e-169	100%
ML2D	HuNoV GII/NP-544_3	KX685486.1	6e-174	99%
ML3C	HuNoV GII/NP-544_3	KX685486.1	5e-174	99%

2.4 Discussion

The main objective of this chapter was to develop sample preparation and concentration techniques for mussel samples collected from the Swartkops River as well as swab samples collected from the separation grids of the Belmont Valley sewage treatment plant. In addition an RT-PCR assay was developed for the detection of HuNoV GII from the samples in order to determine the suitability of the sample preparation method, the nucleic acid extraction method as well as the RT-PCR kit used, for subsequent use in the present study. HuNoV GII was detected by Jaquet (2017) from raw sewage collected from the same wastewater treatment plant and oysters collected from Port Elizabeth. This virus has also been detected before from clinical and environmental samples in other regions of South Africa and linked to cases of gastroenteritis (Mans *et al.*, 2010; Mans *et al.*, 2013).

Viral particles are generally in low concentration in environmental samples making it hard to detect them. There are various techniques used to concentrate these viruses to detectable levels as discussed above. In the present study, samples were pooled into a small volume (1 mL) of phosphate buffer and centrifuged at 9 000 x g for 3 minutes before they were filtered through 0.20 µM membrane filters. Although this sample preparation technique is not widely reported in the literature, it proved successful as

electron micrographs revealed the presence of viral particles ranging from less than 20 nm in diameter to around 90 nm. Even though it is a fast technique which is normally used as an initial technique to check for the presence of viral particles before attempting to do any PCR, TEM cannot differentiate between morphologically similar viruses such as HuNoV and AiV-1. Therefore, a one-step RT-PCR, which is more reliable than TEM, was developed to detect HuNoV from the mussel and swab samples.

An experiment to determine the sensitivities of a one-step versus a two-step RT-PCR assay showed that a one-step RT-PCR was more sensitive as it was able to produce PCR products from low concentrations of RNA template. This emphasises the suitability of one-step RT-PCR assays over two-step RT-PCR assays for detection of enteric RNA viruses like HuNoV GII as similar results were obtained elsewhere in the literature (De Paula *et al.*, 2004; Wacker and Godard, 2005). For this reason, the one-step RT-PCR using the Verso 1-Step RT-PCR kit was preferred in the present study.

Extraction of good quality nucleic acids is a critical step of any PCR assay. In the present study, the QIAamp Viral RNA Mini Kit was used to extract nucleic acids from the swabs and mussel samples. This kit has been used in similar studies before for extraction of viral DNA and RNA for surveillance as well as diagnostic purposes (Khamrin *et al.*, 2012; Longtin *et al.*, 2008; Neske *et al.*, 2007; Rohayem *et al.*, 2004). In fact it is one of the widely used nucleic acid extraction kits in the literature. Using the nucleic acids extracted by this kit in a one-step RT-PCR assay for detection of HuNoV GII, PCR products of the expected size were obtained. This showed that the extraction of RNA using this kit was successful confirming the reliability of the kit as described in other studies.

Cloning of PCR products helps in two major ways, one of which is that the sequence data at the extreme ends of the sequence is not lost. The other importance of cloning PCR products, more specially from environmental samples, is that several genetically distinct strains can be obtained per clone whereas in direct sequencing only the dominant strain is detected per sample (Kitajima *et al.*, 2011). In the present study, PCR products were cloned into pJET 1.2/blunt vector and genetically distinct strains were obtained from some individual samples similar to what Kitajima *et al.* (2011) reported. The HuNoV GII strain isolated from swab sample 1 was 99% identical to a HuNoV GII strain isolated from stool samples of a diarrhoeic patient in Cambodia. Swab 2 sample had 2 strains which were 99% identical to the GII strains from Russia and Cambodia respectively. This

same scenario was observed with mussel samples. Mussel sample 1 had a strain which was 100% identical to the Russian isolate while mussel samples 2 and 3 had strains 99% identical to the Cambodian strain. These results were expected for environmental samples such as raw sewage which can have multiple strains. Also to note in the present study were the E-values which ranged from $8e-171$ to $2e-167$. These values were expected as the DNA fragments obtained were small (approximately 342 bp). All these results are consistent with findings from other studies worldwide.

In conclusion, sample preparation techniques were successfully developed using HuNoV GII as a model virus. Electron micrographs showed the presence of viral particles with morphological characteristics of HuNoV and other viruses. Using RNA extracted from swab and mussel samples prepared by applying the developed sample preparation techniques in a one-step RT-PCR assay, specific PCR products were amplified and the resultant sequences were positive for HuNoV GII as expected. This confirmed the suitability of the developed sample preparation techniques for detection of other enteric viruses from the same samples. These techniques will be applied for detection of AiV-1, enteric HBoV as well as enteric HAdV from swabs and mussel samples. Chapter 3 will describe the application of a one-step RT-PCR assay to detect AiV-1 from swab and mussel samples prepared using the techniques described in this chapter.

Chapter 3: Development of RT-PCR assays for molecular identification of Aichi virus 1 from swab and mussel samples

3.1 Introduction

Aichi virus 1 (AiV-1) is a single stranded, positive sense RNA virus with an icosahedral capsid that belongs to the genus Kobuvirus, family *Picornaviridae*. This virus is around 30 nm in diameter and has a genome of approximately 8250 bp in size (Yamashita *et al.*, 1998). There are 3 genetically distinct genotypes, namely A, B and C (Ambert-Balay *et al.*, 2008; Yamashita *et al.*, 2000). Genotype A is predominantly found in Japan while genotype B is mostly found in many Asian countries other than Japan (Pham *et al.*, 2007). On the other hand, genotype C has only been detected in Africa (Ambert-Balay *et al.*, 2008; Ouédraogo *et al.*, 2016).

AiV-1 was initially isolated in 1989 during an oyster-related gastroenteritis outbreak in Aichi prefecture, Japan, the basis of its name (Yamashita *et al.*, 1991). It is widely recognised as an important aetiological agent of gastroenteritis. This virus, like other enteric pathogens is transmitted via the oral-faecal route, as shown by its detection in stool samples of diarrhoeic patients in many studies around the world in all continents (Ambert-Balay *et al.*, 2008; Burutaran *et al.*, 2016; Drexler *et al.*, 2011; Iritani *et al.*, 2014; Jonsson *et al.*, 2012; Kaikkonen *et al.*, 2010; Oh *et al.*, 2008; Ouédraogo *et al.*, 2016; Pham *et al.*, 2008; Sdiri-Loulizi *et al.*, 2009; Verma *et al.*, 2011; Yip *et al.*, 2014).

In addition to its detection in clinical samples, AiV-1 has been detected from environmental sources during surveillance studies. These sources include polluted river water, for example, in Venezuela (Alcala *et al.*, 2010), the Netherlands (Lodder *et al.*, 2013), Japan (Kitajima *et al.*, 2011), France (Prevost *et al.*, 2015) and the USA (Kitajima *et al.*, 2014) as well as raw sewage, for example, in Italy (Di Martino *et al.*, 2013) and Japan (Kitajima *et al.*, 2011). Furthermore, this virus has been detected from shellfish in some surveillance studies such as by Ambert-Balay *et al.* (2008) in France, Iritani *et al.* (2014) in Japan and Le Guyader *et al.* (2008) in France. These studies emphasise the roles played by shellfish as major transmission vehicles of enteric viruses including AiV-1, as discussed in chapter 1 especially when they are collected from sewage polluted water sources.

In Africa, there is limited epidemiological data on this medically important virus. It was detected from stool samples of diarrhoeic patients in Mali (Ambert-Balay *et al.*, 2008),

Burkina Faso (Ouédraogo *et al.*, 2016), Nigeria (Japhet *et al.*, 2016) and Tunisia (Sdiri-Loulizi *et al.*, 2009). In addition to that, AiV-1 was detected from raw sewage in Tunisia during a surveillance study to determine the efficiency of some sewage treatment plants (Ibrahim *et al.*, 2017). In South Africa there are currently no reports describing the detection and prevalence of this virus.

In the literature, the most common method for detection of AiV-1 is RT-PCR using oligonucleotides targeting various regions of the genome (see for example, Drexler *et al.*, 2011; Yamashita *et al.*, 2000; Lodder *et al.*, 2013; Pham *et al.*, 2008). Currently detection of AiV-1 from clinical, environmental and shellfish samples mostly relies on the PCR amplification of the highly conserved 5' untranslated region (5' UTR) stretching into the leader protein, the 3CD junction as well as the viral peptide 1 (VP1) regions of AiV-1. The nucleotide as well as an amino acid sequence of the leader protein is unique to AiV-1, hence making the 5' UTR assay specific for its detection (Yamashita *et al.*, 1998). In 2011, Drexler *et al.* (2011) designed 2 sets of primers that amplify a region between the 5' UTR and the leader protein, specifically for AiV-1. By using these primers, which are applied in a nested set up to increase sensitivity, Drexler *et al.* (2011) successfully detected AiV-1 from stool samples of diarrhoeic patients. Han *et al.* (2014) also used these 5' UTR primers to successfully detect AiV-1 from raw sewage in South Korea during a surveillance study. On the other hand, Nielsen *et al.* (2013) as well as Yip *et al.* (2014) designed and used their own degenerate 5' UTR primers to successfully detect AiV-1 from stool samples of diarrhoeic patients in Denmark and Hong Kong respectively. In the literature, there are fewer studies that used the 5' UTR RT-PCR assay compared to the 3CD and VP1 RT-PCR assays. This is attributed to the region being difficult to amplify due to its high degree of secondary structure as well as high GC content (Lukashev *et al.*, 2012). In Africa there is no published study in which the 5' UTR RT-PCR assay was used for molecular detection of AiV-1 from stool, environmental and shellfish samples.

The AiV-1 3CD junction is known to be relatively conserved with many hypervariable sites compared to the 5' UTR region and as a result is used for genotyping the virus (Oh *et al.*, 2006; Pham *et al.*, 2007; Yamashita *et al.*, 2000). Yamashita *et al.* (2000) first designed 2 sets of primers that amplify the partial 3CD region. These primers, which are used in a nested set up to increase sensitivity, have been used in many studies worldwide for molecular detection of AiV-1 from stool samples of diarrhoeic patients (Jonsson *et al.*,

2012; Kaikkonen *et al.*, 2010; Le Guyader *et al.*, 2008, Pham *et al.*, 2007), environmental samples including raw sewage (Burutarán *et al.*, 2016; Di Martino *et al.*, 2013; Haramoto and Kitajima, 2017) and shellfish samples (Iritani *et al.*, 2014; Ambert-Balay *et al.*, 2008). In Africa, Ambert-Balay *et al.* (2008), Ouédraogo *et al.* (2016), Japhet *et al.* (2016) and Sdiri-Loulizi *et al.* (2009) successfully used the 3CD RT-PCR assay to detect AiV-1 from stool samples of diarrhoeic patients in Mali, Burkina Faso, Nigeria and Tunisia respectively. Ibrahim *et al.* (2017) also used the 3CD RT-PCR to successfully detect AiV-1 from raw sewage in Tunisia during a surveillance study.

On the other hand the VP1 region, which forms the outer part of the capsid, is the least conserved compared to the other two regions and as a result it is believed to be more reliable for genotyping than the 3CD junction (Yamashita *et al.*, 2000, Pham *et al.*, 2008; Lukashev *et al.*, 2012). However, in the literature, there are no universally used primers for the VP1 assay as all studies designed and used their own primers. Pham *et al.* (2008) was the first to design and use the VP1 primers by which AiV-1 was detected in stool samples from Japan, Thailand, Vietnam and Bangladesh. Since then many other studies worldwide used the VP1 assay to successfully detect this virus from clinical and environmental samples including raw sewage water. These include studies by Han *et al.* (2014) and Lodder *et al.* (2013) who detected AiV-1 from raw sewage during surveillance studies in South Korea and the Netherlands respectively. Drexler *et al.* (2011), Yip *et al.* (2014) and Verma *et al.* (2011) are some of the studies in which the VP1 RT-PCR assay was used to detect AiV-1 from stool samples of diarrhoeic patients in Germany, Hong Kong and India respectively. However in Africa, including South Africa, there is no published report in which the VP1 RT-PCR was used for molecular detection of this virus.

AiV-1 has received much attention in recent years and there is extensive genome data in GenBank for comparison with novel isolates. Currently there are about twelve complete genomes, many complete as well as partial 3CD and VP1 sequences and few 5' UTR sequences available in GenBank for comparison purposes. This chapter describes the development of RT-PCR assays targeting the 5' UTR, the 3CD junction and the VP1 for identification of AiV-1 from raw sewage and mussel samples collected in the Eastern Cape Province of South Africa.

The specific objectives for this chapter were as follows;

- Development of RT-PCR assays to detect AiV-1 from swab and mussel samples by amplification of the 5' UTR, the 3CD junction and the VP1 region.
- Cloning of appropriate PCR inserts into a vector
- Sequencing of plasmids and BLAST analysis of resultant sequences
- Construction of phylogenetic trees

3.2 Materials and methods

3.2.1 Primers for RT-PCR of AiV-1 5' UTR, 3CD coding region and VP1

Two sets of primers, published by Drexler *et al.* (2011) that amplify a region encompassing the AiV-1 highly conserved 5' UTR and the leader protein were used in this study. The details about these primers are shown in **Table 3.1** below.

Table 3.1: Forward and reverse oligonucleotides for AiV 5' UTR as described by Drexler *et al.* (2011).

Primer No	ID	Sequence, 5'→3'	Binding site	Genome location	Polarity	Amplicon size
AiV-F65		CACCGTTACTCCA TTCAGCTTCTTC	65-89	5' UTR	+	1008 bp
AiV-R1049		GGATAGAACCAG GATTGGACATCAG	1049-1073	Leader	-	
AiV-F69		GTTACTCCATTCA GCTTCTTCGGAAC	69-94	5' UTR	+	996 bp
AiV-R1039		CAGGATTGGACAT CAGAATCATAGAG	1039-1064	Leader	-	

Shown in **Figure 3.1** below are the primer binding sites on the AiV-1 genome (accession number: AB010145). All the forward primers bind to the 5' UTR while the reverse primers bind to the leader protein.

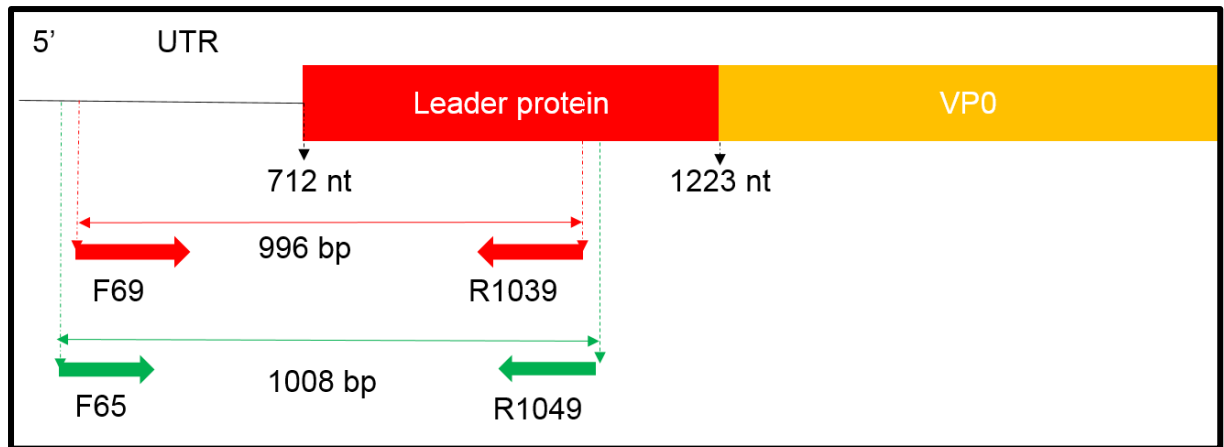


Figure 3. 1: Schematic representation of the AiV-1 5' UTR primer binding sites on the AiV-1 genome. Outer primers AiV-F65 (→) and AiV-R1049 (←) amplify an approximately 1008 bp region while inner primers AiV-F69 (→) and AiV-R1039 (←) amplify a region approximately 996 bp (adapted from Drexler *et al.*, 2011).

For PCR amplification of the relatively conserved AiV-1 partial 3CD coding region, a set of primers published by Yamashita *et al.* (2000) that amplify a PCR product of approximately 266 bp were used. Details about these primers including their binding sites is shown in **Table 3.2** and **Figure 3.2** below

Table 3. 2: Forward and reverse oligonucleotides for AiV-1 3CD as described by Yamashita *et al.* (2000).

Primer No	ID	Sequence, 5'→ 3'	Binding site	Genome location	Polarity	Amplicon size
AiV-C94b		GACTTCCCCGGAGT CGTCGTCT	6398-6419	3CD	+	266 bp
AiV-246K		GACATCCGGTTGAC GTTGAC	6663-6644	3CD	-	

Figure 3.2 below shows the binding sites of the 3CD primers on an AiV-1 genome (accession number: AB010145). The forward primer binds to the 3C region while the reverse primer binds to the 3D region of the genome.

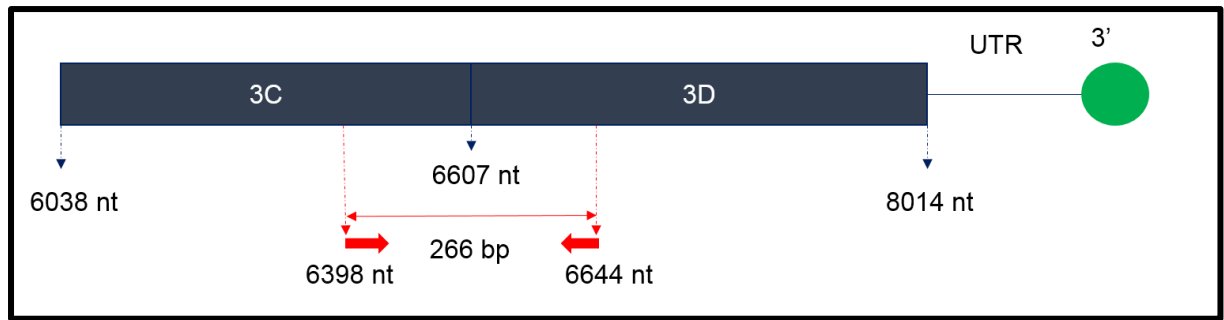


Figure 3.2: Schematic representation of the AiV-1 3CD primer binding sites. The primers AiV-C94B (→) and AiV-246K (←) amplify a product approximately 266 bp in the 3CD junction (adapted from Pham *et al.*, 2007).

For PCR amplification of AiV-1 partial VP1 region, published primers as well as primers designed in this study were used in a semi-nested PCR reaction to produce a 472 bp product of the VP1 region. Primers designed in the present study were based on multiple sequence alignment of 10 full VP1 sequences of AiV-1 randomly selected from GenBank and using Primer3 Plus software. AiV-1 sequences used for the alignment were accession numbers DQ028632.1 (Brazil), FJ890523.1 (China), GQ927711.2, GQ927712.2, GQ927704.2, GQ927705.2, GQ927706.2 (all Germany), HM363007.1 (India), KC196315.1, KC196317.1 (all South Korea). Shown in **Figure 3.1S (Supplementary 1)** is the multiple sequence alignment used to generate the VP1 primers designed in this study. The details about all the VP1 primers including their binding sites on the AiV-1 genome are given in **Table 3.3** and **Figure 3.3** below.

Table 3.3: Forward and reverse oligonucleotides for amplification of AiV-1 VP1 region.

Primer ID No	Sequence, 5'→3'	Binding site	Genome location	Polarity	References	Amplicon size
Cap E	CTA GTC GGA CCC CAC ACC GC	2897- 2915	VP1	+	Pham <i>et al.</i> (2008)	598 bp
AiV- VP1 IR	GGGATGGAA AAGGAGACC AT	3494- 3475	VP1	-	This study	
AiV- VP1-F2	CTCGATGCRC CMCAAGACA CCGG	3023- 3045	VP1	+	Lodder <i>et al.</i> (2013)	472 bp
AiV- VP1-IR	GGGATGGAA AAGGAGACC AT	3494- 3475	VP1	-	This study	

Shown below are the binding sites for the VP1 primers as on an AiV-1 genome, accession number DQ028632.1. The outer forward primer binds to the VP3 while the outer reverse and all the inner primers bind to the VP1.

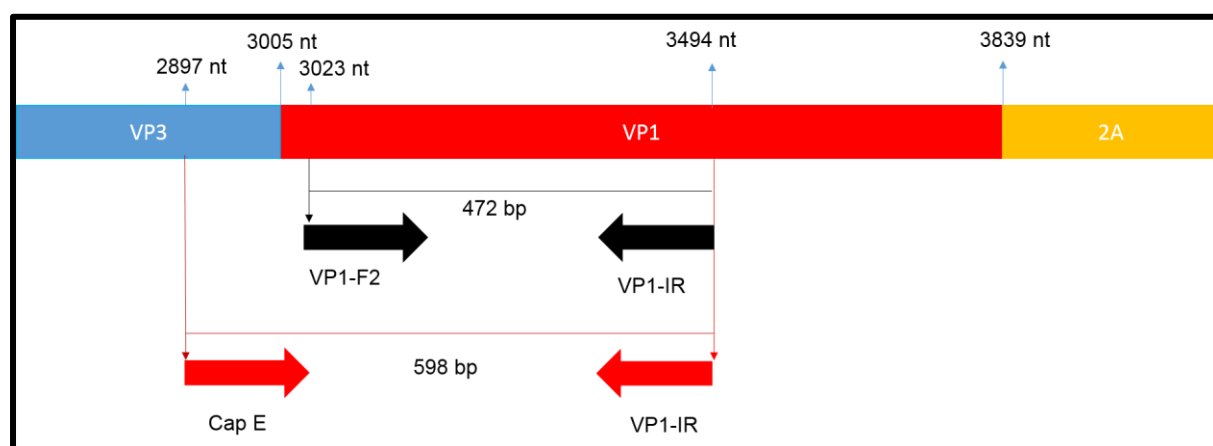


Figure 3.3: Schematic representation of the AiV-1 VP1 primer binding sites. Primers, Cap E (→) and VP1-IR (←) produce a PCR product approximately 598 bp while primers VP1-F2 (→) and VP1-IR (←) produce a PCR product approximately 472 bp.

3.2.2 Preparation of positive control RNA and RT-PCR of AiV-1 5' UTR and 3CD junction

A plasmid containing some part of the AiV-1 between the 5' UTR and the leader protein was kindly provided by Jaquet (2017) to use as positive control in the present study. This plasmid consisted of an insert approximately 1008 bp cloned into pGEM[®]-T Easy Vector (Promega, USA). Jaquet (2017) furthermore provided another plasmid of the AiV-1 3CD region containing an insert approximately 266 bp cloned into pGEM[®]-T Easy Vector. The plasmids were stored at -80 °C as glycerol stocks until use in the current study.

For the purpose of this study, cells from glycerol stocks above were thawed on ice and sterile wire loops were used to streak onto Luria agar (with ampicillin at a final concentration of 100 µg/mL) making discontinuous streaks. The plates were incubated at 37 °C overnight (15-18 hours). Isolated colonies (five) were each inoculated into 5 mL Luria broth (with ampicillin at a final concentration of 100 µg/mL) and incubated at 37 °C overnight (15-18hrs) with shaking at approximately 180 rpm. This was followed by extraction of the positive control plasmid DNA by use of the GeneJET Plasmid Miniprep Kit (Thermo Scientific, USA) following manufacturer's instructions. The plasmid DNA was eluted into 40 µL of sterile, nuclease free water and stored at -20 °C until use for *in vitro* transcription. To confirm the sizes of the inserts, 2 µL of the plasmid DNA was subjected to restriction analysis using Fast Digest EcoRI (Thermo Scientific, USA) following manufacturer's instruction. The restriction digest products were analysed by 1% agarose gel electrophoresis with ethidium bromide staining at 90 volts for 35 minutes.

3.2.2.1 *In vitro* transcription and RNA clean-up

In order to obtain RNA from plasmids, an *in vitro* transcription reaction was performed using the TranscriptAid T7 High Yield Transcription Kit (Thermo Scientific, USA) strictly following manufacturer's instructions. The T7 synthesised RNA was purified using the GeneJET RNA Purification Kit (Thermo Scientific, USA) following manufacturer's instructions. The purified RNA was aliquoted and stored at -80 °C until use.

3.2.2.2 Application of a one-step RT-PCR assay for amplification of the 5' UTR region of AiV-1 Control T7 transcribed RNA

The Verso 1-Step RT-PCR Hot-Start Kit (Thermo Scientific, USA) was used to PCR amplify an approximately 1008 bp product of the highly conserved region encompassing the 5' UTR and the leader protein of AiV-1 using primers described in Drexler *et al.* (2011) shown in **Table 3.1**. The T7 synthesised AiV-1 5' UTR RNA was used as a template in the reaction. Briefly, 0.5 μ L Verso enzyme mix, 12.5 μ L of Verso 2x 1-step hot-start mix, 1.25 μ L RT enhancer, 0.5 μ L of 10 μ M forward primer (AiV-F65), 0.5 μ L of 10 μ M reverse primer (AiV-R1049), 1 μ L of the positive control 5' UTR T7 synthesised RNA, 2.5 μ L of dimethyl sulfoxide (DMSO) and 6.25 μ L of sterile, nuclease-free water, all making up 25 μ L, were mixed up in a sterile flat cap PCR tube and subjected to thermal amplification in a SimpliAmp Thermal cycler (Bio-Systems by Life Technologies) to amplify a 1008 bp product between the 5' UTR and leader protein. A no template control reaction (NTC) was included.

The cycling parameters were as shown in **Table 3.4** below. 3 μ L of the resultant PCR product was analysed by 1% agarose gel electrophoresis with ethidium bromide staining at 90 Volts for 35 minutes.

Table 3.4: Cycling parameters for the first round PCR reaction to amplify a 1008 bp product of the AiV-1 5' UTR.

Step	Temperature	Duration	Cycles
cDNA synthesis	50 °C	15 minutes	1
Verso inactivation	95 °C	15 minutes	1
Denaturation	95 °C	20 seconds	
Annealing	55 °C	30 seconds	40
Extension	72 °C	1 minutes	
Final extension	72 °C	5 minutes	1
Hold	4 °C	∞	1

In order to increase sensitivity, a nested PCR was developed using the KAPA Taq-Readymix PCR kit (KAPA Biosystems, USA). A set of inner primers described by Drexler *et al.* (2011) were used to amplify an approximately 996 bp product of the 5'

UTR in a nested PCR reaction. These primers are shown in **Table 3.1**. Briefly, 12.5 μL 2x KAPA TaqReadyMix, (1.5 mM MgCl_2 at 1X), 1 μL of 10 μM forward primer (AiV-F69), 1 μL of 10 μM Reverse Primer (AiV-F1039), 2.5 μL of DMSO, 1 μL of first round PCR product and 7 μL of sterile, nuclease-free water were mixed thoroughly in a PCR tube and loaded into a SimpliAmp Thermal cycler, and the cycling parameters were set up as shown in **Table 3.5** below. The second round PCR products were analysed by 1% agarose gel electrophoresis with ethidium bromide staining at 90V for 35 minutes.

Table 3.5: Cycling parameters for the nested second round PCR reaction to amplify a 996 bp region of the AiV-1 5' UTR.

Step	Temperature	Duration	Cycles
Initial denaturation	95 °C	3 minutes	1
Denaturation	95 °C	30 seconds	
Annealing	55 °C	30 seconds	35
Extension	72 °C	1 minute	
Final extension	72 °C	5 minutes	1
Hold	4 °C	∞	1

3.2.2.3 Application of a one-step RT-PCR assay for amplification of the AiV-1 partial 3CD Control T7 transcribed RNA

An RT-PCR reaction was developed using the Thermo Scientific Verso 1-Step RT-PCR Hot-Start Kit to amplify an approximately 266 bp product of the relatively conserved 3CD region of AiV-1, using a set of primers (shown in **Table 3.2**) described in Yamashita *et al.* (2000), following manufactures instructions.

In this reaction, 12.5 μL of Verso 2x 1-Step Hot-Start mix, 1.25 μL RT enhancer, 0.5 μL of 10 μM forward primer (AiV-C94B), 0.5 μL of 10 μM reverse primer (AiV-246K), 1 μL AiV 3CD cleaned up T7 transcribed RNA, 0.5 μL Verso enzyme mix and 7.5 μL of sterile, nuclease-free water, all making up 25 μL were mixed up in a sterile PCR tube and subjected to PCR amplification in a SimpliAmp Thermal cycler to amplify a 266 bp product. A no template control reaction (NTC) was also included.

The cycling parameters were as described in **Table 3.6** below. The PCR products were analysed by 1% agarose gel electrophoresis with ethidium bromide staining at 90V for 35 minutes.

Table 3.6: Cycling parameters to amplify a 266 bp partial 3CD coding region of AiV-1.

Step	Temperature	Duration	Cycles
cDNA synthesis	50 °C	15 minutes	1
Verso inactivation	95 °C	15 minutes	1
Denaturation	95 °C	20 seconds	
Annealing	55 °C	30 second	40
Extension	72 °C	1 minutes	
Final extension	72 °C	5 minutes	1
Hold	4 °C	∞	1

3.2.3 Development of one-step RT-PCR Assays for swab and mussel samples

3.2.3.1 Samples

Swabs and mussel samples were collected and prepared as described in Chapter 2 (sections 2.2.1-2.2.3). For the detection of AiV-1, not all the twenty swabs and twenty mussel samples were analysed due to time constraints. Shown in **Tables 3.7** and **3.8** is data on swabs and mussel samples respectively, that were analysed.

Table 3.7: Data pertaining to swab samples analysed for AiV-1.

Sample	Sample ID	Date collected
Swab 1	S1	10-05-16
Swab 2	S2	10-05-16
Swab 3	S3	10-05-16
Swab 4	S4	10-05-16
Swab 5	S5	10-05-16
Swab 6	S6	10-05-16
Swab 7	S7	10-05-16
Swab 8	S8	10-05-16
Swab 9	S9	10-05-16
Swab 10	S10	10-05-16
Swab 11	S11	20-03-17
Swab 12	S12	20-03-17

Table 3.8: Data pertaining to mussel samples analysed for AiV-1.

Sample	Sample ID	Date collected
Large mussel 1	ML1	02-05-16
Large mussel 2	ML 2	02-05-16
Large mussel 3	ML 3	02-05-16
Large mussel 4	ML 4	02-05-16
Large mussel 5	ML 5	02-05-16
Large mussel 6	ML 6	02-05-16
Large mussel 7	ML 7	02-05-16
Large mussel 8	ML 8	02-05-16
Large mussel 9	ML 9	02-05-16
Large mussel 10	ML 10	02-05-16
Large mussel 11	ML 11	02-05-16
Large mussel 12	ML 12	02-05-16

3.2.3.2 RNA extraction

RNA was extracted from swab and mussel samples using the QIAamp® Viral RNA Mini Kit, (Qiagen, USA), following manufacturer's instructions as described in section 2.2.5 (Chapter 2). The nucleic acids were then eluted into 50 µL sterile deionised water, aliquoted and stored at -80 °C until use.

3.2.3.3 Amplification of the 5' UTR of AiV-1 from mussel and swab samples

For the amplification of the 5' UTR, two RT-PCR assays were developed. The first one was a one-step RT-PCR in which the Thermo Scientific Verso 1-Step RT-PCR Hot-Start Kit was used to PCR amplify an approximately 1008 bp product of AiV-1 5' UTR using outer primers (shown in **Table 3.1**) described in Drexler *et al.* (2011). The reactions were set up as described in section 3.2.2.2 above except that 2 µL of RNA from swab and mussel samples (described in section 3.2.3.2) was used in these reactions.

Reaction in a total of 25 µL included; 12.5 µL of Verso 2x 1-step Hot-Start mix, 1.25 µL RT enhancer, 0.5 µL of 10 µM forward primer (AiV-F65), 0.5 µL of 10 µM reverse primer (AiV-R1049), 0.5 µL Verso enzyme mix, 2 µL RNA from mussel and swab samples, 2.5 µL DMSO and 5.25 µL of sterile, nuclease-free water were mixed up in a sterile PCR tube and subjected to thermal amplification in a SimpliAmp Thermal cycler to amplify a 1008 bp product. A positive control and an NTC were as described in section 3.2.2.2 above. The cycling parameters were as described in **Table 3.4**. First round PCR products were analysed by 1% agarose gel electrophoresis with ethidium bromide staining at 90 Volts for 35 minutes.

To increase sensitivity, a nested PCR assay was used to amplify a 996 bp product in the AiV-1 5' UTR using second round primers, shown in **Table 3.1**. The reactions were carried out as in section 3.2.2.2 above. These second round reactions which were made up of 12.5 µL 2X KAPA TaqReadyMix, (1.5 mM MgCl₂ at 1X), 1 µL of 10 µM forward primer (AiV-F69), 1 µL of 10 µM reverse primer (AiV-F1039), 1 µL of first round PCR product, 2.5 µL DMSO and 7 µL sterile, nuclease-free water were mixed thoroughly in PCR tubes and loaded into a SimpliAmp Thermal cycler. The cycling parameters were as shown in **Table 3.5**. A positive control and an NTC reaction were also included. Second

round PCR products were analysed by 1% agarose gel electrophoresis with ethidium bromide staining at 90V for 35 minutes.

Despite repeated attempts to amplify the 5' UTR, only one sample was positive for this assay. As discussed before in section 3.1, the 5' end of AiV-1 is difficult to amplify due to the high GC content as well as high degree of secondary structure due to the presence of hair-pins. It is then that a two-step RT-PCR assay was developed using cycling parameters described in Drexler *et al.* (2011). For this reaction the Maxima H Minus First Strand cDNA Synthesis Kit (Thermo Scientific, USA), which has a reverse transcriptase that can withstand temperatures up to 65 °C was used following manufacturers' instructions. For cDNA synthesis, the reactions were prepared as follows for each sample; 10 µL (approximately 1 µg) of total RNA from swabs and mussel samples, 1 µL of the outer reverse primer (AiV-R1049), 1 µL 10 mM dNTP Mix and 3 µL of sterile, nuclease-free water, all making up 15 µL were mixed thoroughly and incubated at 65 °C for 5 minutes. This was followed by addition of 4 µL of 5X RT Buffer and 1 µL of Maxima H Minus Enzyme Mix. The reactions were incubated at 65 °C for 30 minutes after which the cDNA was used in a PCR reaction set up as follows; 12.5 µL of Ampliqon Taq 2x Master Mix Red (1.5 mM MgCl₂ at 1X), 1 µL of 10 µM forward primer (AiV-F65), 1 µL of 10 µM reverse primer (AiV-F1049), 1 µL cDNA, 2.5 µL DMSO and 7 µL of sterile nuclease-free water. The cycling parameters were as described in Drexler *et al.* (2011) i.e. 15 min at 95 °C; 10 cycles of 20 seconds at 94 °C, 30 seconds starting at 60 °C with a decrease of 1 °C per cycle, and 50 seconds at 72 °C; and 40 cycles of 20 seconds at 95 °C, 30 seconds at 54 °C, and 50 seconds at 72 °C; and a final elongation step of 5 minutes at 72 °C. A positive control and an NTC reaction were also included. The PCR products were analysed by 1% agarose gel electrophoresis with ethidium bromide staining at 90V for 35 minutes.

3.2.3.4 Amplification of AiV-1 partial 3CD coding region from swab and mussel samples

The Thermo Scientific Verso 1-Step RT-PCR Hot-Start Kit was used to PCR amplify an approximately 266 bp product of AiV-1 partial 3CD coding region using primers (shown in **Table 3.2**) described in Yamashita *et al.* (2000). The reactions were set up as in section 3.2.2.3 above except that 2 µL of RNA extracted from swab and mussel samples was used. Each reaction consisted of 12.5 µL of Verso 2x 1-step hot mix, 1.25 µL RT

enhancer, 0.5 µL of 10 µM forward primer (AiV-C94B), 0.5 µL of 10 µM reverse primer (AiV-246K), 2 µL sample RNA, 0.5 µL Verso enzyme mix and 7.75 µL of sterile, nuclease-free water, all making up 25 µL mixed in a sterile PCR tube and subjected to PCR amplification in a SimpliAmp Thermal cycler to amplify a 266 bp product. A positive control and an NTC reaction were included. The PCR products were analysed by 1% agarose gel electrophoresis with ethidium bromide staining at 90 Volts for 35 minutes.

3.2.3.5 Amplification of AiV-1 partial VP1 from swab and mussel samples

For PCR amplification of the partial viral peptide 1 of AiV-1, one-step RT-PCR assay was developed using the Thermo Scientific Verso 1-Step RT-PCR Hot-Start Kit. The reactions were set up as follows; 12.5 µL of Verso 2x 1-step hot mix, 1.25 µL RT enhancer, 0.5 µL of 10 µM forward primer (CapE) designed by Pham *et al.* (2008), 0.5 µL of 10 µM reverse primer (AiV-VP1 IR) designed in this study by multiple sequence alignment of AiV-1 VP1 sequences followed by using Primer3Plus software to design the primer, 2 µL RNA from swab and mussel samples (only those which were positive with the 3CD assay- S1, S2, S3, S5, S6, S7, S9, S11, S12, ML2, ML3, ML4, ML5, ML6), 0.5 µL Verso enzyme mix and 7.75 µL of sterile, nuclease-free water, all making up 25 µL mixed in a sterile PCR tube and subjected to PCR amplification in a SimpliAmp Thermal cycler to amplify a 598 bp product of the AiV-1 partial VP1 coding region. Although S10 was positive for the AiV-1 partial 3CD RT-PCR assay, it was not included as the RNA had run out. The primer details and binding sites on the AiV-1 genome (accession number DQ028632.1) are shown in **Table 3.3** and **Figure 3.3**. While there was no positive control for this assay, an NTC was included. The cycling parameters were as shown in **Table 3.9** below.

Table 3.9: Cycling parameters for the PCR amplification of AiV-1 partial VP1 region.

Step	Temperature	Duration	Cycles
Initial denaturation	95 °C	3 minutes	1
Denaturation	95 °C	30 seconds	
Annealing	55 °C	30 seconds	35
Extension	72 °C	1 minute	
Final extension	72 °C	5 minutes	1
Hold	4 °C	∞	1

In order to increase sensitivity, a semi-nested PCR reaction was set up as follows; 12.5 µL 2X KAPA TaqReadyMix, (1.5 mM MgCl₂ at 1X), 1 µL of 10 µM forward primer (AiV-F2) designed by Lodder *et al.* (2013) , 1 µL of 10 µM reverse primer (AiV-VP1 IR) designed in this study by multiple sequence alignment of AiV-1 full VP1 sequences followed by using Primer3Plus software to design the primer, and 7 µL of sterile, nuclease-free water were mixed thoroughly in PCR tubes and subjected to thermal amplification in a SimpliAmp Thermal cycler to amplify a PCR product of approximately 472 bp. Primer details and binding sites on the AiV-1 full genome (accession number DQ028632.1) are depicted in **Table 3.3** and **Figure 3.3**. While there was no positive control for this assay, an NTC reaction was included. The cycling parameters were as shown in **Table 3.9** above.

3.2.4. PCR clean-up and cloning PCR products into pJET 1.2/blunt vector

PCR products from these 3 assays (5' UTR, 3CD junction and VP1) were gel purified by use of the GeneJET Gel Extraction Kit (Thermo Scientific, USA) following manufacturer's instructions. DNA was eluted into 40 µL of sterile, nuclease-free water and stored at -20 °C until use. The purified PCR products were cloned into pJET 1.2/blunt vector CloneJET™ PCR Cloning Kit (Thermo Scientific, USA) as described before in section 2.2.9 (Chapter 2).

3.2.5 Transformation of competent cells

Competent *E.coli* cells (DH5 α) were transformed as in section 2.2.10 (Chapter 2). After an overnight incubation at 37 °C, 10 isolated colonies (labelled A-J) from each plate were inoculated into 5 mL Luria broth (with ampicillin at a final concentration of 100 μ g/mL) and incubated at 37 °C overnight (15-18hrs) with shaking at approximately 200 rpm.

3.2.6 Plasmid extraction and restriction enzyme analysis

Plasmids were extracted using the GeneJET Plasmid Miniprep Kit (Thermo Scientific, USA) as described before in section 2.2.11 (Chapter 2). Presence and sizes of the various inserts were confirmed by restriction analysis with normal digest Xho 1 (Promega, USA) and fast digest Xba 1 (Thermo Scientific, USA) as described before in section 2.2.11 (Chapter 2).

3.2.7 Sequencing and BLAST analysis

Plasmids with correct inserts (i.e. 1008 for the AiV-1 5' UTR, 266 bp for AiV-1 3CD junction and 472 bp for AiV-1 partial VP1 coding region) were Sanger sequenced at Inqaba Biotechnical Industries ([Pty] Ltd, Pretoria, South Africa). Sequencing was done in both forward and reverse directions. Resultant forward and reverse sequences were manually edited and aligned in MEGA 6 software to obtain consensus sequences which were then subjected to BLAST search from GenBank.

3.2.8 Multiple sequence analysis and phylogeny

AiV-1 5' UTR sequences from various regions of the world from GenBank were randomly selected to use in multiple sequence analysis of nucleotides to compare them to the ones isolated in the present study. Information concerning the various reference isolates used for the alignments is given in **Table 3.1S (Supplementary 2)**. Multiple sequence alignments of nucleotides were performed using MEGA 6 followed by uploading the alignment into Geneious version 9.1.8 in order to obtain the image of the alignment.

For AiV-1 partial 3CD coding region, reference sequences from various regions of the world from GenBank were selected based on a publication by Jonsson *et al.* (2012) to use in multiple sequence analysis of nucleotides in order to infer how they diverge from the ones isolated in the present study. In addition to that African isolates from Tunisia, Mali,

Burkina Faso and Nigeria in GenBank were also included. Information about the various reference isolates used for the alignments is given in **Table 3.2S (Supplementary 3)**. Multiple sequence alignments of nucleotides, computation (including model tests) and construction of a phylogenetic tree were performed using Molecular Evolutionary Genetics Analysis 6 software (MEGA 6) followed by uploading the alignment into Geneious version 9.1.8 in order to obtain the image of the alignment. The phylogenetic tree was constructed using the Maximum Likelihood method by nonparametric bootstrap analysis with 1,000 pseudo-replicates based on the Tamura 3 substitution model as described in Jonsson *et al.* (2012). Bovine Kobuvirus and Porcine Kobuvirus were used as out-groups.

In addition, AiV-1 partial VP1 coding sequences from various regions of the world in GenBank were selected based on a publication by Jonsson *et al.* (2012) to use in multiple sequence analysis of nucleotides and construction of a phylogenetic tree in order to infer how they differ from the ones isolated in the present study. Unfortunately there are no African VP1 sequences in GenBank for comparison purposes. Information concerning the various reference isolates used for the alignments is given in **Table 3.3S (Supplementary 4)**. Multiple sequence alignments of nucleotides, computation (including model tests) and construction of phylogenetic trees were performed using Molecular Evolutionary Genetics Analysis 6 software (MEGA 6) followed by uploading the alignment into Geneious version 9.1.8 in order to obtain the image of the alignment. The phylogenetic tree was constructed using the Maximum Likelihood by nonparametric bootstrap analysis with 1,000 pseudo-replicates as described in Jonsson *et al.* (2012). Bovine Kobuvirus was used as an out-group.

3.3 Results

3.3.1 Positive controls

3.3.1.1 AiV-1 5' UTR

3.3.1.1.1 Confirmation of positive control plasmid DNA by restriction Analysis

The plasmid map is of a positive control plasmid which was used in the analysis is shown in **Figure 3.4A** below. Restriction analysis of this control plasmid using Fast Digest EcoRI confirmed the presence of an insert approximately 1008 bp as expected. **Figure**

3.4B below shows 1% agarose gel electrophoresis of the uncut and cut plasmid DNA. Lane 1 shows the uncut plasmid DNA. Lane 2 shows the cut plasmid DNA with the insert PCR product approximately 1008 bp and the vector approximately 3016 bp. This shows that the insert PCR product cloned into the vector was of the right size. As shown in **Figure 3.4B**, the insert PCR product was successfully cut from the plasmid.

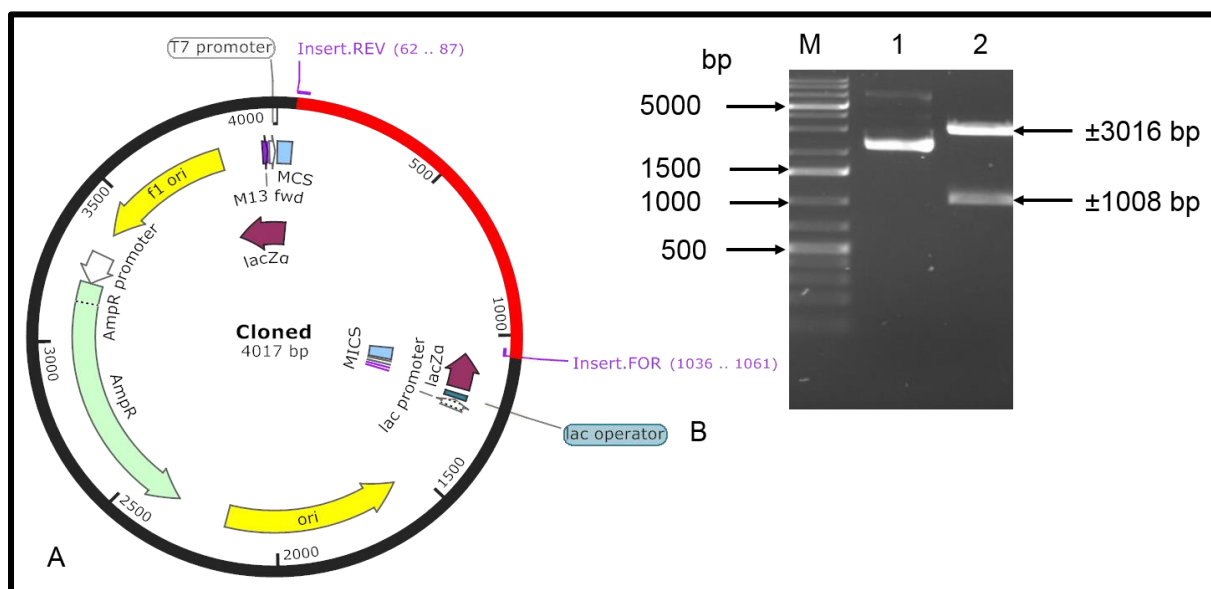


Figure 3. 4: **A)** Plasmid map of the AiV-1 5' UTR positive control plasmid DNA consisting of an insert approximately 1008 bp (shown in red) cloned into pGEM[®]-T Vector. **B)** 1% agarose gel electrophoresis of uncut and cut AiV-1 5' UTR positive control plasmid DNA. M: GeneRuler[™] 1 kb Plus DNA Ladder (Thermo Scientific, USA), lane 2: uncut control plasmid DNA, lane 3: Cut control plasmid DNA.

3.3.1.1.2 RNA synthesis by *In vitro* transcription and RT-PCR of positive control RNA (AiV-1 5' UTR)

In vitro transcription was successful as AiV-1 5' UTR RNA was obtained from plasmid DNA. This resultant RNA was used as a positive control in RT-PCR assays. **Figure 3.5A**, below shows 1% agarose gel electrophoresis of the T7 synthesised RNA (lane 1) which presented as a smear running from above 10000 bp down to below 100 bp. **Figure 3.5B**, lane 1 below shows an RT-PCR product of the correct size (approximately 1008 bp) obtained from the positive control RNA. As expected no PCR product was visible in the NTC reaction (lane 2) as sterile, nuclease-free water was used instead of an RNA template.

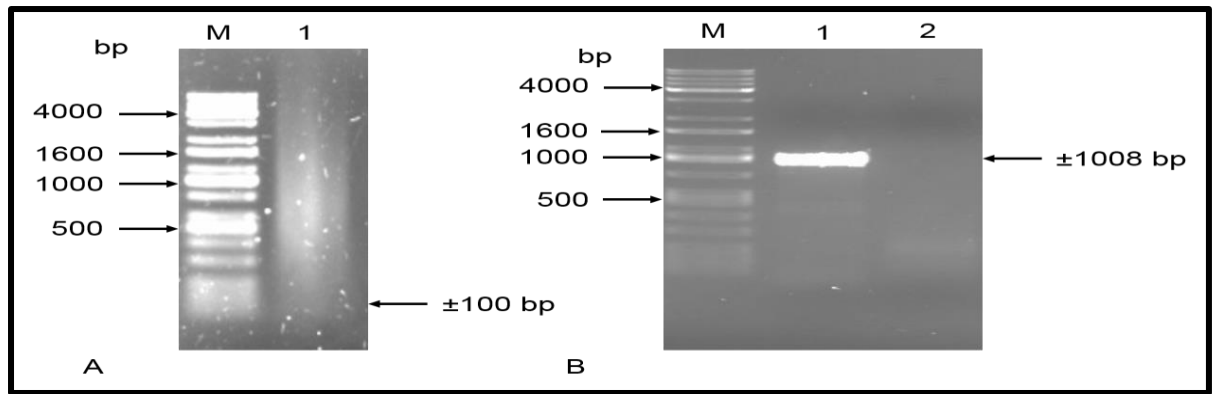


Figure 3.5: **A)** 1% Agarose gel electrophoresis of positive control T7 synthesised RNA of the AiV-1 5' UTR. M: KAPA Universal Ladder, lane 1: Positive control T7 synthesised RNA. **B)** 1% agarose gel electrophoresis of the positive control PCR product (approximately 1008 bp) of the AiV-1 5' UTR, M: KAPA Universal Ladder, lane 1: Positive control PCR product, lane 2: NTC reaction.

3.3.1.2 AiV-1 partial 3CD coding region

3.3.1.2.1 Confirmation of positive control Plasmid DNA by restriction analysis

The plasmid map of a positive control plasmid which was used in the analysis is shown in **Figure 3.6A** below. Restriction analysis of this control plasmid DNA using Fast Digest EcoRI was successful as an insert of approximately 266 bp was obtained. **Figure 3.6B** below shows 1% agarose gel electrophoresis of the uncut and cut plasmid DNA. Lane 1 shows the uncut plasmid DNA. Lane 2 shows the cut plasmid DNA with the insert PCR product approximately 266 bp and the vector approximately 3016 bp. This shows that the insert PCR product cloned into the vector was of the correct size. As shown in **Figure 3.6B**, the insert PCR product was successfully cut from the plasmid.

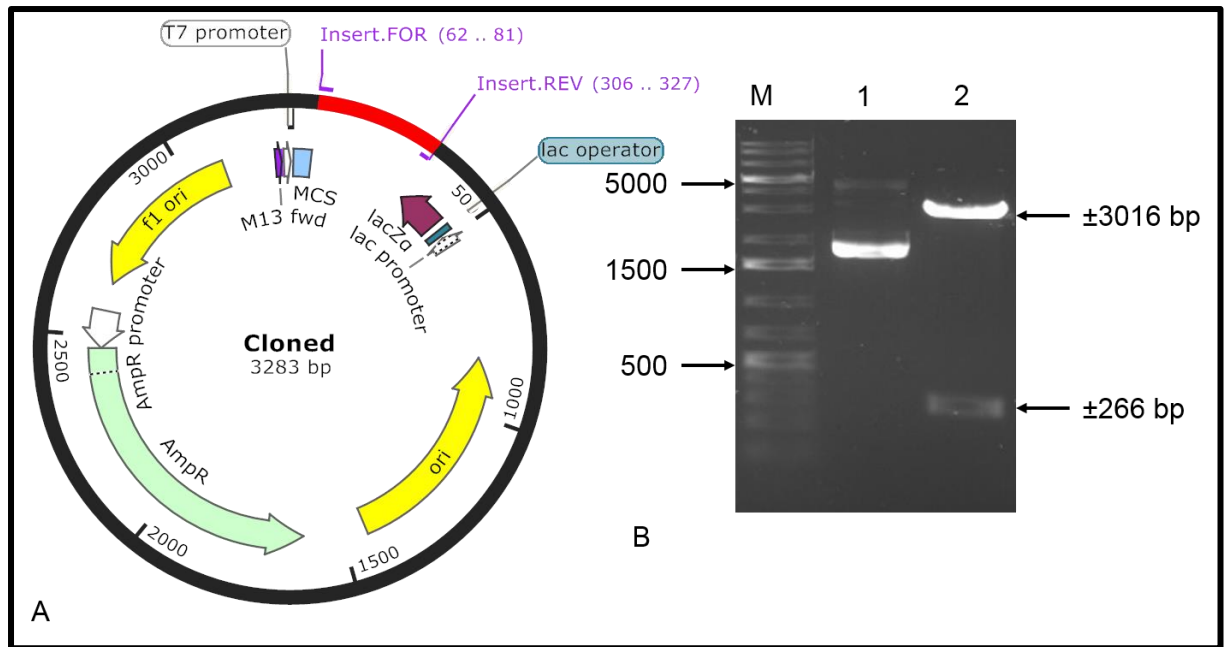


Figure 3.6: **A)** 1% agarose gel electrophoresis of positive control plasmid DNA consisting of an insert approximately 266 bp of the AiV-1 partial 3CD junction cloned into pGEM[®]-T Vector. **B)** 1% agarose gel electrophoresis of uncut and cut AiV-1 3CD positive control plasmid DNA. M: GeneRuler™ 1 kb Plus DNA Ladder (Thermo Scientific, USA), lane 2: uncut control plasmid DNA, lane 3: Cut control plasmid DNA.

3.4.1.2.2 RNA synthesis by *In vitro* transcription and RT-PCR of positive control RNA (AiV-1 partial 3CD)

An *In vitro* transcription reaction was successfully carried out using the TranscriptAid T7 High Yield Transcription Kit. The T7 synthesised AiV-1 3CD RNA obtained was used as a positive control in the 3CD RT-PCR assays. **Figure 3.7A**, below shows 1% agarose gel electrophoresis of the T7 synthesised RNA (lane 1) which presented as a smear running from above 1600 bp down to below 100 bp. **Figure 3.7B**, lane 1 below shows an RT-PCR product of the correct size (approximately 266 bp) obtained from the positive control RNA. As expected no PCR product was visible in the NTC reaction (lane 2) as sterile, nuclease-free water was used instead of an RNA template.

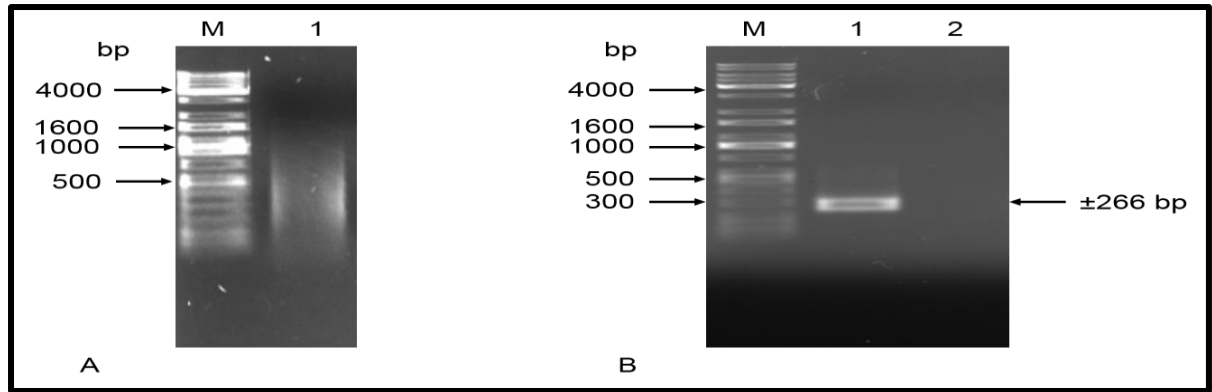


Figure 3.7: **A)** 1% agarose gel electrophoresis of positive control T7 synthesised RNA of the AiV-1 partial 3CD coding region. M: KAPA Universal Ladder, lane 1: Positive control T7 synthesised RNA. **B)** 1% agarose gel electrophoresis of the positive control PCR product (approximately 266 bp) of the AiV-1 partial 3CD coding region, M: KAPA Universal Ladder, lane 1: Positive control PCR product, lane 2: NTC reaction.

3.3.2 Swab samples

3.3.2.1 AiV-1 5' UTR RT-PCR and gel purification

For the detection of AiV-1 from swab samples two nested RT-PCR assays were developed. The first one was a one-step RT-PCR assay, using the Verso 1-Step RT-PCR Kit with addition of DMSO to a final concentration of 10% for which an amplicon of the expected size (approximately 1008 bp), was produced from one sample (S3) out of the twelve swab samples analysed as shown in **Table 3.10** below. The second assay was a two-step RT-PCR reaction using the Maxima H Minus First Strand cDNA Synthesis Kit for which an amplicon of approximately 1008 bp was obtained for S9.

Table 3.10: PCR results of the AiV-1 5' UTR assay for swab samples.

Swab sample	AiV-1 5' UTR PCR results
S1	No visible PCR products
S2	No visible PCR products
S3	PCR product produced
S4	No visible PCR products
S5	No visible PCR products
S6	No visible PCR products
S7	No visible PCR products
S8	No visible PCR products
S9	PCR product produced
S10	No visible PCR products
S11	No visible PCR products
S12	No visible PCR products

Figure 3.8A below shows a 1% agarose gel of the AiV-1 5' UTR RT-PCR products from swab 3 (S3). In lane 1 was the RT-PCR product from the positive control T7 synthesised RNA which was of the correct size (approximately 1008 bp) as expected showing that the assay was successful. The NTC reaction (lane 2) produced no PCR product as expected because no RNA template was added but sterile, nuclease-free water. An RT-PCR product of approximately 1008 bp was observed on lane 3. There was another bright band of approximately 500 bp visible on the gel which was most probably the result of non-specific binding.

In addition, by using the second protocol, a faint band of approximately 1008 bp was visible for swab sample 9. **Figure 3.8B** below shows a 1% agarose gel of the RT-PCR product from swab sample 9 (S9). Lane 1 was the RT-PCR product from the positive control T7 synthesised RNA which was approximately 1008 bp as expected showing that the assay was successful. Lane 2 was the NTC which produced no band showing that there was no contamination. An RT-PCR product of approximately 1008 bp was produced in swab 9 (lane 3). This product was not as bright as the one from swab sample 3 (**Figure 3.8A**, lane 3), nevertheless the reaction was successful. As in **Figure 3.8A**, another band of approximately 500 bp was visible on lane 3 as well as lane 1 (positive

control). This could be the result of non-specific binding. The RT-PCR products from swabs 3 and 9 were gel purified by use of the GeneJET Gel Extraction Kit as described before in section 3.2.4.

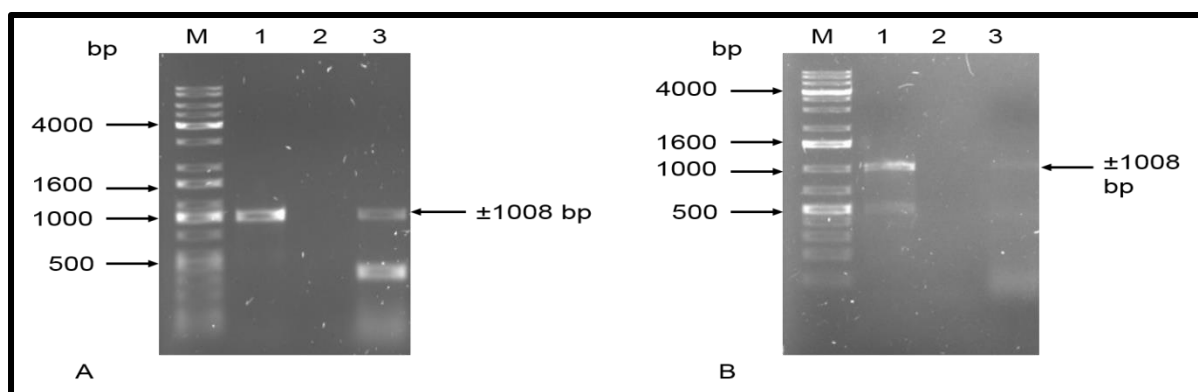


Figure 3.8: **A)** 1% agarose gel electrophoresis of RT-PCR products of the AiV-1 5' UTR from swab sample 3. M: KAPA Universal Ladder, lane 1: Positive control RT-PCR product (approximately 1008 bp), lane 2: NTC, lane 3: PCR product from swab 3. **B)** 1% agarose gel electrophoresis of RT-PCR product of the AiV-1 5' UTR from swab 9. M: KAPA Universal Ladder, lane 1: Positive control RT-PCR product (approximately 1008 bp), lane 2: NTC, lane 3: RT-PCR product from swab 9.

3. 3.2.2 Cloning of AiV-1 5' UTR RT-PCR products from swab samples into pJET 1.2/blunt vector and restriction analysis of plasmid DNA

The gel purified 5' UTR PCR products were cloned into pJET 1.2/blunt vector as described in section 3.2.4. Competent *E.coli* cells (DH5 α) were transformed as described in section 3.2.5. Ten colonies (A-J) from each sample were inoculated into Luria broth (with ampicillin) as described in section 3.2.5 and plasmids extracted from the samples as described in section 3.2.6. **Figure 3.9A** below shows a representative 1% agarose gel of plasmid DNA extracted from the cells (five colonies from swab sample 3) by use of the GeneJET Plasmid Miniprep Kit as described before. The results from swab sample 9 were not shown. Restriction analysis of plasmid DNA by use of Xho I and Xba I confirmed the presence and sizes of inserts which were approximately 1008 bp. **Figure 3.9B** below shows the results of the restriction analysis for the five plasmids from swab sample 3. Lanes 1, 3, 5, 7 and 9 show uncut plasmids. Lanes 2, 4, 6, 8 and 10 show cut plasmids for which linearised vectors were approximately 2974 bp, the size of pJET 1.2/blunt vector, while majority of inserts were approximately 1008 bp as expected. Inserts in lanes 6 and

10 appear to be larger than expected but it is possible that they are the right size but running skewed on the gel.

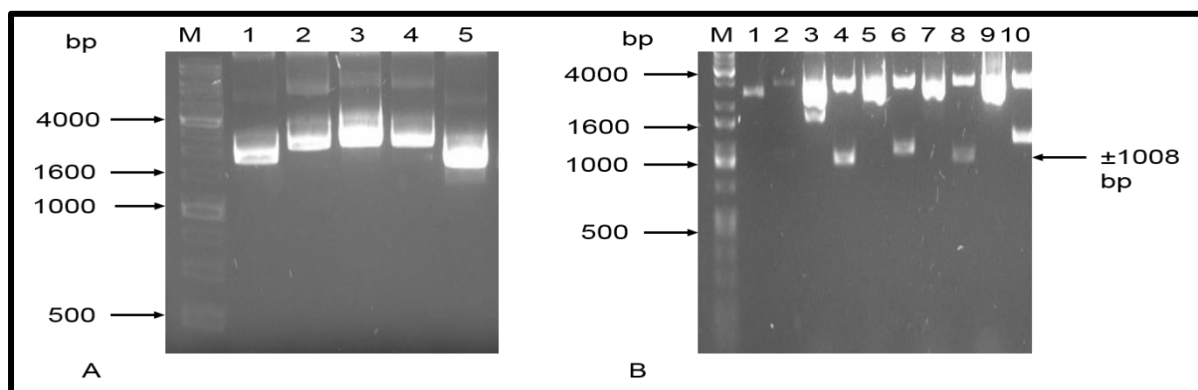


Figure 3.9: **A)** 1% agarose gel electrophoresis of plasmid DNA from swab sample 3. M: KAPA Universal Ladder, lanes 1-5: Uncut plasmid DNA (S3A, S3B, S3C, S3D and S3E respectively). **B)** 1% agarose gel electrophoresis of cut and uncut plasmids M: KAPA Universal Ladder, lane 1: Plasmid S3A uncut, lane 2: S3A cut, lane 3: Plasmid S3B uncut, lane 4: S3B cut, lane 5: Plasmid S3C uncut, lane 6: S3C cut, lane 7: plasmid S3D uncut, lane 8: S3D cut, lane 9: Plasmid S3E uncut lane 10: S3E cut.

3.3.2.3 BLAST analysis and multiple sequence alignment of AiV-1 5' UTR PCR products from swab samples

Two plasmids (S3G and S9A) for swab samples 3 and 9 respectively, with inserts approximately 1008 bp were Sanger sequenced at Inqaba Biotechnical Industries ([Pty] Ltd, Pretoria, South Africa) and resultant sequences were highly identical to an isolate in GenBank when subjected to blast analysis by use of NCBI BLAST website (Blast.ncbi.nlm.nih.gov/Blast.cgi). **Table 3.11** below shows top BLAST hits of the AiV-1 5' UTR products from GenBank for swab samples 3 and 9. All the two samples had percentage identities of 98% to an AiV-1 strain in GenBank (accession number: JX564249.1) with E-values of 0.0. This isolate was detected by Chang *et al.* (2013) from a rectal swab of a diarrhoeic patient in Taiwan.

Table 3.11: BLAST analysis results of AiV-1 5' UTR products from swab samples 3 and 9.

Sample ID	Description	Accession number	E-value	% Identity
S3G	kvgh99012632/2010 polyprotein gene	JX564249.1	0.0	99%
S9A	kvgh99012632/2010 polyprotein gene	JX564249.1	0.0	99%

The 5' UTR sequences from swab samples as well as those from GenBank were aligned on MEGA 6 using Clustal W algorithm as described in section 3.2.8. The results of the alignment are shown in **Figure 3.2S (Supplementary 5)**.

3.3.2.4 AiV-1 3CD RT-PCR and gel purification

Amplicons of approximately 266 bp were obtained from PCR amplification of AiV-1 3CD region from nine out of the twelve swab samples tested. These positive samples were S1, S2, S3, S5, S6 S7, S9, S10, and S12. **Table 3.12** shows the results from all the 12 samples analysed by the 3CD RT-PCR assay.

Table 3.12: AiV-1 3CD RT-PCR results for swab samples.

Swab sample ID	3CD RT-PCR results
S1	PCR product obtained
S2	PCR product obtained
S3	PCR product obtained
S4	PCR product obtained
S5	No visible PCR product obtained
S6	PCR product obtained
S7	PCR product obtained
S8	No visible PCR product obtained
S9	PCR product obtained
S10	PCR product obtained
S11	PCR product obtained
S12	PCR product obtained

Shown below in **Figure 3.10** and **3.11** are representative 1% agarose gels of the 3CD RT-PCR results from swab samples. **Figure 3.10A** below shows a 1% agarose gel of 3CD RT-PCR products from swab 1 to swab 5. Lane 1 is the positive control RT-PCR product from the T7 synthesised RNA which was of the correct size (approximately 266 bp). Lane 2 was the NTC reaction which as expected produced no PCR product because sterile, nuclease-free water was used instead of RNA template. Lanes 3 to 5 were RT-PCR product from swabs 1 to 3 respectively. No product was obtained from swab 4 (lane 6). In lane 7 was the RT-PCR product from swab 5, which like those from swab 1 to 3 were of the correct size (approximately 266 bp). **Figure 3.10B** shows a 1% agarose gel of RT-PCR products from swabs 6 to 10. Lane 1 contained the positive control RT-PCR product which was approximately 266 bp as expected while the NTC reaction (lane 2) produced

no PCR products as sterile, nuclease-free water was used instead of an RNA template. Lanes 3 and 4 show RT-PCR products approximately 266 bp from swabs 6 and 7 respectively. No product was obtained from swab 8 (lane 5). Lanes 6 and 7 show RT-PCR products of approximately 266 bp from swabs 9 and 10 respectively. Results from swabs 11 and 12 were not shown.

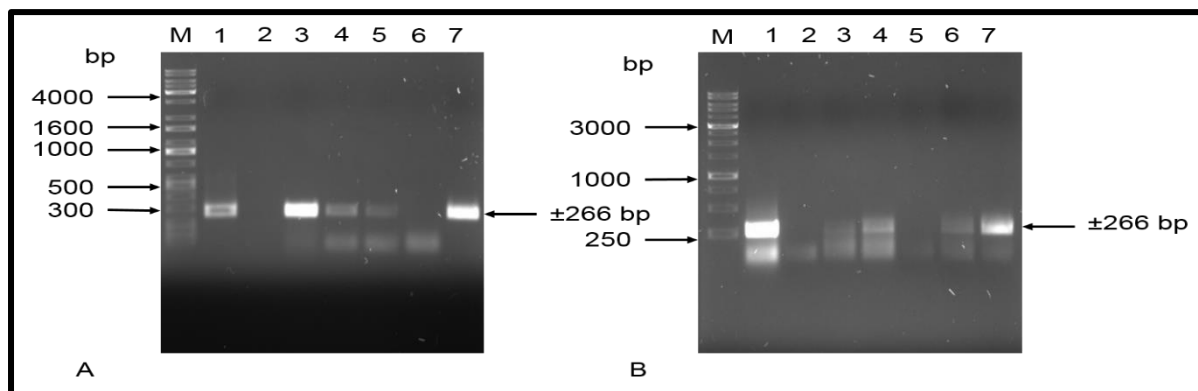


Figure 3.10: **A)** 1% agarose gel electrophoresis of RT-PCR products of the AiV-1 partial 3CD coding region from swab samples 1 to 5. M: KAPA Universal Ladder, lane 1: Positive control PCR product (approximately 266 bp), lane 2: NTC, lane 3-7: RT-PCR products from swab samples 1 to 5 respectively. **B)** 1% agarose gel electrophoresis of RT-PCR products of the AiV-1 partial 3CD coding region from swab samples 6 to 10. M: KAPA Universal Ladder, lane 1: Positive control PCR product (approximately 266 bp), lane 2: NTC, lanes 3-7: RT-PCR products from swab samples 6 to 10 respectively.

3.3.2.5 AiV-1 partial 3CD coding region (266 bp) - Cloning into pJET 1.2/blunt vector and restriction analysis of plasmid DNA

The cleaned up 3CD PCR products from swab samples were ligated into pJET 1.2/blunt vector in order to obtain the full sequence data for the insert as described before in section 3.2.4. Competent *E.coli* cells (DH5 α) were transformed as described in section 3.2.5. Ten colonies (A-J) from each sample were inoculated into Luria broth (with ampicillin) as described in section 3.2.5 and plasmids extracted from the samples as described in section 3.2.6. **Figure 3.11A** below shows a representative 1% agarose gel of plasmid DNA extracted from the cells (5 colonies from swab sample 1) by use of the GeneJET Plasmid Miniprep Kit as described before. The results from other swab samples were not shown. Restriction analysis of plasmid DNA by use of Xho 1 and fast digest Xba 1 confirmed the presence and sizes of inserts which were approximately 266 bp. **Figure 3.11B** below

shows the results of the digest for the 5 plasmids from swab sample 1. Lane 1 shows the positive control RT-PCR product which was used to estimate the sizes of inserts. Lanes 2, 4, 6, 8 and 10 show uncut plasmids. Lanes 3, 5, 7, 9 and 11 show cut plasmids for which empty vectors were approximately 2974 bp, the size of pJET 1.2/blunt vector. Apart from an insert in lane 3 which was approximately 266 bp as expected, no other inserts were visible from the majority of plasmids showing that they were re-ligated pJET 1.2/blunt vectors. Nevertheless, the cloning was successful as one plasmid had an insert of the expected size.

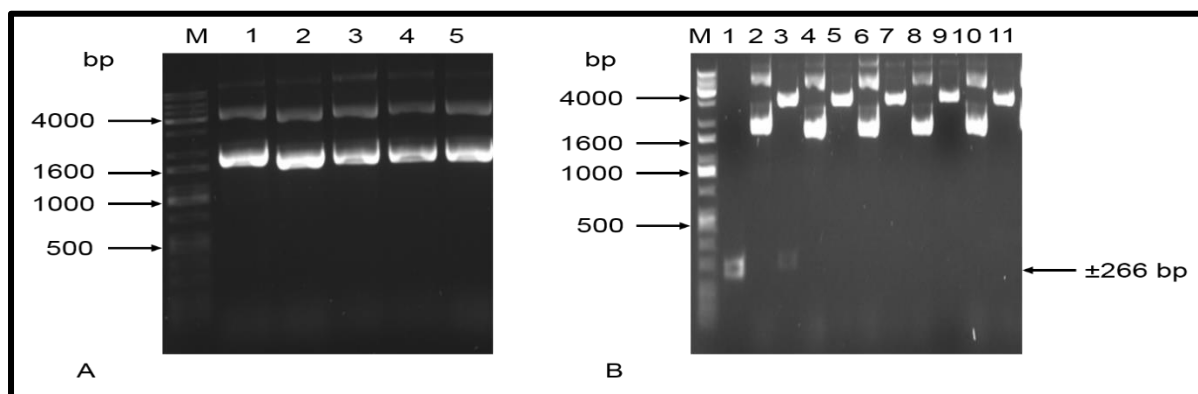


Figure 3.11: A) 1% agarose gel electrophoresis of plasmid DNA from swab sample 1. M: KAPA Universal Ladder, lanes 1-5: Uncut plasmid DNA (S1A, S1B, S1C, S1D and S1E respectively). **B)** 1% agarose gel electrophoresis of cut and uncut plasmids M: KAPA Universal Ladder, lane 1: Positive control PCR product (approximately 266 bp), lane 2: Plasmid S1A uncut, lane 3: S1A cut, lane 4: Plasmid S1B uncut, lane 5: S1B cut, lane 6: Plasmid S1C uncut, lane 7: S1C cut, lane 8: plasmid S1D uncut, lane 9: S1D cut, lane 10: Plasmid S1E uncut lane 11: S1E cut.

3.3.2.6 AiV-1 partial 3CD coding region- BLAST results

Plasmids with inserts approximately 266 bp from 4 swab samples (at least 1 plasmid from S1, S3, S9 and S11) were Sanger sequenced at Inqaba Biotechnical Industries ([Pty] Ltd, Pretoria, South Africa) and resultant sequences were highly identical to various isolates in GenBank when subjected to BLAST analysis by use of NCBI BLAST website (Blast.ncbi.nlm.nih.gov/Blast.cgi). **Table 3.13** below shows top BLAST hits of AiV-1 3CD sequences from GenBank. All samples were identical to AiV-1 isolates in GenBank with E-values ranging from $1e-136$ to $8e-130$. Samples S3B and S3G from the present study had percentage identities of 99% to AiV-1 isolates from the People's Republic of

China, Accession numbers FJ890520.1 and FJ890521.1 which were isolated from faecal samples of diarrhoeic patients. Samples S1A and S11A were 99% identical to an AiV-1 isolate (Accession number JQ792245.1) which was detected by Northill *et al.* (2012) from Australia. There is no further information about this isolate as it was from an unpublished source.

Table 3.13: BLAST analysis results of the AiV-1 partial 3CD products (266 bp) from swab samples.

Sample ID	Descriptions	Accession number	E-value	% Identity
S1A	AiV-1 isolate Qld/2008/268	JQ792245.1	5e-132	99%
S3B	AiV-1 Chshc2 polyprotein	FJ890520.1	8e-130	99%
S3G	AiV-1 isolate Chshc3 polyprotein	FJ890521.1	1e-136	99%
S11A	AiV-1 isolate Qld/2008/268	FJ890521.1	1e-136	99%

3.3.2.7 AiV-1 partial VP1 RT-PCR and gel purification

Amplicons of the expected size (approximately 472 bp), were produced from two (S9 and S11) of the nine swab samples analysed using the AiV-1 partial VP1 RT-PCR assay. There were no visible PCR products from first round PCR reactions. **Table 3.14** below shows second round PCR results for all the nine swab samples analysed using the VP1 RT-PCR assay.

Table 3.14: PCR results of the AiV-1 partial VP1 assay for swab samples.

Swab sample	Aiv-1 VP1 PCR results
S1	No visible PCR products
S2	No visible PCR products
S3	No visible PCR products
S5	No visible PCR products
S6	No visible PCR products
S7	No visible PCR products
S9	PCR product obtained
S11	PCR product obtained
S12	No visible PCR products

Shown below in **Figure 3.12** is a 1% agarose gel of the AiV-1 second round VP1 PCR results from swab samples. Lane 1 is the NTC reaction for which no PCR product was visible as expected because sterile, nuclease-free water was used instead of a DNA template. Lanes 2 to 6 are PCR products for swabs 6, 7, 9, 11 and 12 in that order. In lane 2 (for swab 6) a PCR product of approximately 300 bp was visible. This could be the result of non-specific binding because the expected product should be approximately 472 bp. In lane 3 (swab 7) no visible PCR product was produced. In lanes 3 and 4 for swabs 9 and 11 respectively, PCR products of the expected size were produced. In lane 5 (swab 12) a faint product of approximately 1500 bp was visible but this could be the result of non-specific binding as this product was much bigger than the expected product. Swabs 1, 2, 3 and 5 were all negative for the VP1 assay and their results are not shown. The PCR products for swabs 9 and 11 were gel purified by use of the GeneJET Gel Extraction Kit as described before in section 3.2.4.

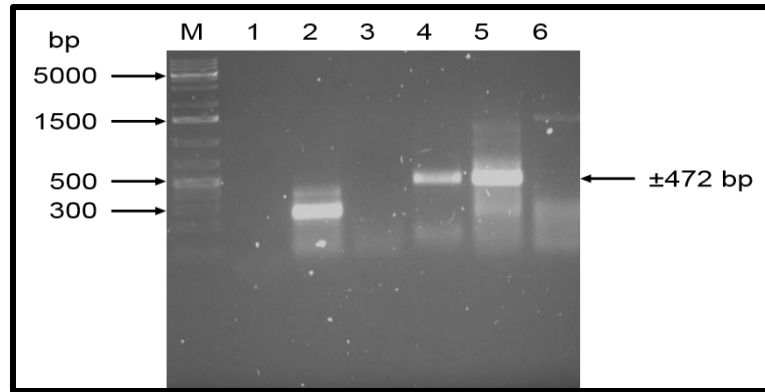


Figure 3.12: 1% Agarose gel electrophoresis of second round PCR products of the AiV-1 partial VP1 coding region from swab samples 6, 7, 9, 11 and 12. M: GeneRuler™ 1 kb Plus DNA Ladder (Thermo Scientific, USA), lane 1: NTC, lane 2-6: PCR products from swab samples 6, 7, 9, 11 and 12 respectively.

3.3.2.8 AiV-1 partial VP1 coding region- Cloning into pJET 1.2/blunt vector and restriction analysis of plasmid DNA

The cleaned up PCR products were ligated into pJET 1.2/blunt vector in order to obtain the full sequence data for the insert as described before. Competent *E.coli* cells (DH5 α) were transformed as described in section 3.2.5. Ten colonies (A-J) from each sample were inoculated into Luria broth (with ampicillin) as described in section 3.2.5 and plasmids extracted from the samples as described in section 3.2.6. **Figure 3.13A** below shows a representative 1% agarose gel of plasmid DNA extracted from the cells (five colonies from swab sample 9) by use of the GeneJET Plasmid Miniprep Kit as described before. The results from swab 11 were not shown. Restriction analysis of plasmids by use of Xho 1 and fast digest Xba 1 confirmed the presence and sizes of inserts which were approximately 472 bp. **Figure 3.13B** below shows the results of the digest for the 5 plasmids from swab sample 9. Lanes 1, 3, 5, 7 and 9 show uncut plasmids. Lanes 2, 4, 6, 8 and 10 show cut plasmids for which linearised vectors were approximately 2974 bp, the size of pJET 1.2/blunt vector and inserts approximately 472 bp as expected showing that the PCR products were successfully cloned in the vector.

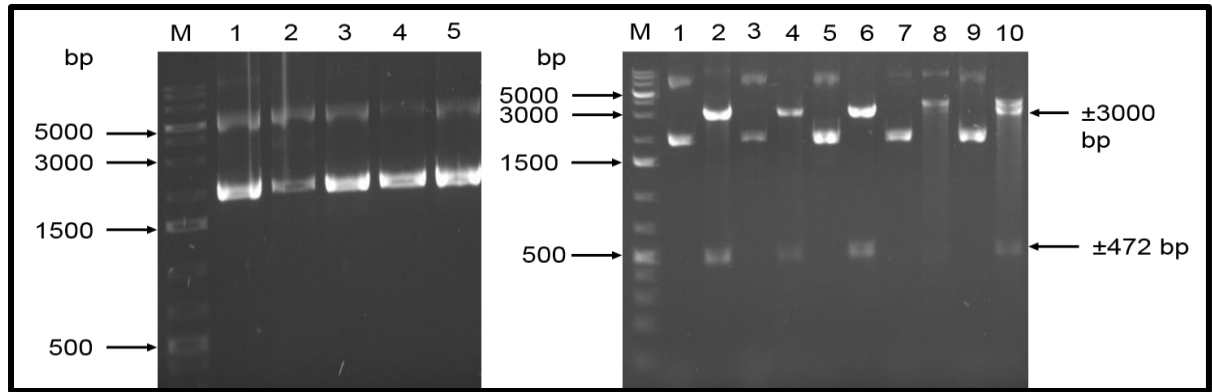


Figure 3.13: A) 1% agarose gel electrophoresis of plasmid DNA from swab sample 9. M: GeneRuler™ 1 kb Plus DNA Ladder, lanes 1-5: Uncut plasmid DNA (S9A, S9B, S9C, S9D and S9E respectively). **B)** 1% agarose gel electrophoresis of cut and uncut plasmids M: GeneRuler™ 1 kb Plus DNA Ladder, lane 1: Plasmid S9A uncut, lane 2: S9A cut, lane 3: Plasmid S9B uncut, lane 4: S9B cut, lane 5: Plasmid S9C uncut, lane 6: S9C cut, lane 7: plasmid S9D uncut, lane 8: S9D cut, lane 9: Plasmid S9E uncut lane 10: S9E cut.

3.3.2.9 AiV-1 partial VP1 coding region- BLAST results

Two plasmids with inserts approximately 472 bp from swab samples 9 and 11 were Sanger sequenced at Inqaba Biotechnical Industries ([Pty] Ltd, Pretoria, South Africa) and resultant sequences were highly identical to an isolate in GenBank when subjected to BLAST analysis by use of NCBI BLAST website (Blast.ncbi.nlm.nih.gov/Blast.cgi). **Table 3.15** below shows top BLAST hits of AiV-1 VP1 sequences from GenBank. Both samples were 98% identical to AiV-1 isolates from South Korea (accession number: KC167094.1) with E-values of 0.0. This South Korean isolate was isolated by Han *et al.* (2014) from stool sample of a diarrhoeic patient using primers different from the ones used in the present study.

Table 3.15: BLAST analysis results of the AiV-1 partial VP1 products from swab samples.

Sample ID	Descriptions	Accession number	E-value	% Identity
S9A	C2_Junggu_0102 VP1 gene, partial cds	KC167094.1	0.0	98%
S11A	C2_Junggu_0102 VP1 gene, partial cds	KC167094.1	0.0	98%

3.3.3 Mussel samples

3.3.3.1 AiV-1 5' UTR RT-PCR and gel purification

Molecular detection of AiV-1 from mussel samples using the Verso 1-Step RT-PCR Kit with addition of DMSO to a final concentration of 10% was not successful after several attempts as no PCR products were obtained from the first and second round reactions and no data is available.

3.3.3.2 AiV-1 partial 3CD coding region- RT-PCR and gel purification

When the one-step RT-PCR assay targeting the AiV-1 3CD region was applied to mussel samples 1 to 12, amplicons of approximately 266 bp were obtained from eight of the twelve samples analysed. **Table 3.16** below shows RT-PCR PCR results for all the 12 mussel samples analysed.

Table 3.16: AiV-1 3CD RT-PCR results for mussel samples.

Swab sample ID	3CD RT-PCR results
ML1	No visible PCR products
ML2	PCR product obtained
ML3	PCR product obtained
ML4	PCR product obtained
ML 5	PCR product obtained
ML 6	PCR product obtained
ML 7	No visible PCR products
ML 8	No PCR product obtained
ML 9	PCR product obtained
ML 10	PCR product obtained
ML 11	No PCR product obtained
ML 12	PCR product obtained

Shown in **Figure 3.14** below are representative 1% agarose gels of RT-PCR products from large mussel samples. **Figure 3.14A** shows results for samples ML1 to ML4. Lane 1 is the positive control RT-PCR product from the T7 synthesised RNA which was of the correct size (approximately 266 bp) as expected. Lane 2 was the NTC reaction which as expected produced no PCR product because sterile, nuclease-free water was used instead

of RNA template. Lanes 3 to 6 were RT-PCR product from ML1 to ML4 respectively. No product was obtained from ML1 (lane 3). Lanes 4 to 6 were RT-PCR product from ML2 to ML4 which were of the correct size (approximately 266 bp) showing that the reaction was successful. **Figure 3.14B** shows results for samples ML5 to ML7. Lane 1 is the positive control RT-PCR product from the T7 synthesised RNA which was of the correct size (approximately 266 bp) as expected. Lane 2 was the NTC reaction which as expected produced no PCR product because sterile, nuclease-free water was used instead of RNA template. Lanes 3 to 5 were RT-PCR product from ML5 to ML7 respectively. No product was obtained from ML7 (lane 5). Lanes 3 and 4 were RT-PCR product from ML5 and ML6 which were of the correct size (approximately 266 bp) showing that products were successfully amplified from these samples. Results from other mussel samples were not shown. The PCR products for ML2, ML3, ML4 and ML5 were gel purified by use of the GeneJET Gel Extraction Kit as described before in section 3.2.4.

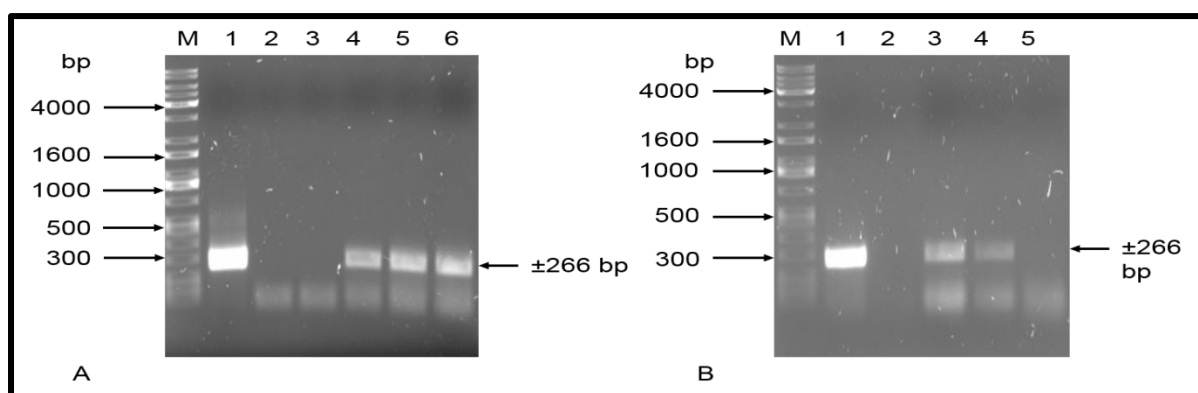


Figure 3.14: **A)** 1% agarose gel electrophoresis of PCR products of the AiV-1 partial 3CD coding region from mussel samples ML1 to ML4. M: KAPA Universal Ladder, lane 1: Positive control PCR product (approximately 266 bp), lane 2: NTC, lanes 3-6: PCR products from mussel samples ML1 to ML4. **B)** 1% agarose gel electrophoresis of PCR products of the AiV-1 partial 3CD coding region from mussel samples ML5 to ML7. M: KAPA Universal Ladder, lane 1: Positive control PCR product (approximately 266 bp), lane 2: NTC, lanes 3-5: PCR products from mussel samples ML5 to ML7.

3.3.3.3 AiV-1 partial 3CD coding region- Cloning into pJET 1.2/ blunt vector and restriction analysis of plasmid DNA

The gel purified 3CD PCR products from the mussel samples were ligated into pJET 1.2/blunt vector in order to obtain the full sequence data for the insert as described before in section 3.2.4. Competent *E.coli* cells (DH5 α) were transformed as described in section

3.2.5. Ten colonies (A-J) from each sample were inoculated into Luria broth (with ampicillin) as described in section 3.2.5 and plasmids extracted from the samples. **Figure 3.15A** below shows a representative 1% agarose gel of plasmids extracted from mussel sample 2 (ML2A-D) by use of the GeneJET Plasmid Miniprep Kit as described before. Other results were not shown. Restriction analysis of plasmid DNA by use of Xho 1 and Xba 1 confirmed the presence and sizes of inserts which were approximately 266 bp. **Figure 3.15B** below shows the results of the restriction analysis. Lane 1 shows the positive control RT-PCR product which was used to estimate the sizes of inserts. Lanes 2, 4, 6 and 8 show uncut plasmids. Lanes 3, 5, 7 and 9 show cut plasmids for which empty vectors were approximately 2974 bp, the size of pJET 1.2/blunt vector and all inserts were approximately 266 bp showing that the assay was successful.

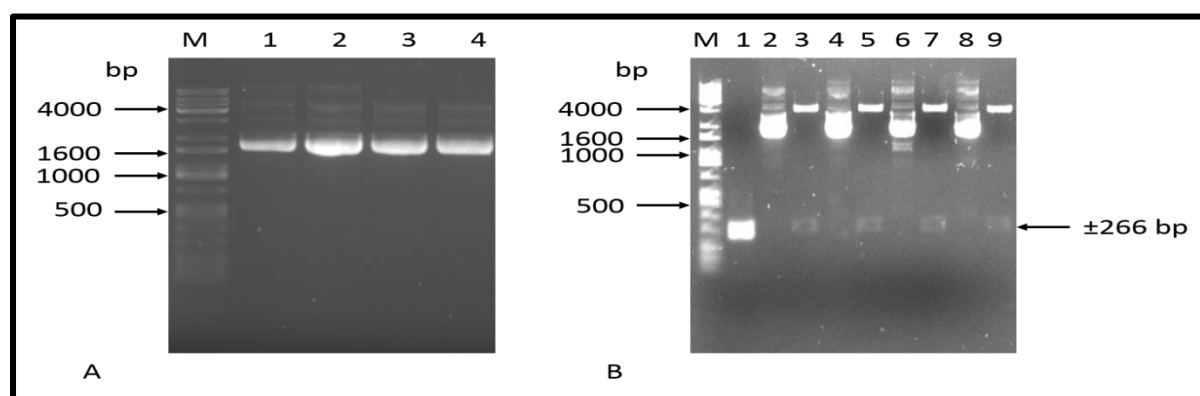


Figure 3.15: **A)** 1% agarose gel electrophoresis of plasmid DNA from mussel sample 2 (ML2). M: KAPA Universal Ladder, lane 1-4: Uncut plasmid DNA (ML2A, ML2B, ML2C and ML2D respectively). **B)** 1% agarose gel electrophoresis of cut and uncut plasmids M: KAPA Universal Ladder, lane 1: Positive control PCR product, lane 2: Plasmid ML2A uncut, lane 3: ML2A cut, lane 4: Plasmid ML2B uncut, lane 5: ML2B cut, lane 6: Plasmid ML2C uncut, lane 7: ML2C cut, lane 8: plasmid ML2D uncut, lane 9: ML2D cut.

3.3.3.4 AiV-1 partial 3CD coding region- BLAST results

Four plasmids with inserts approximately 266 bp from mussel samples 2, 3, 5 and 9 were Sanger sequenced and subjected to BLAST search for related sequences from GenBank by use of NCBI BLAST website. Shown in **Table 3.17** below are BLAST results of the AiV-1 partial 3CD products from mussel samples. All the samples had percentage identities of 99% to an AiV-1 strain from Australia by Northill *et al.* (2012), isolate

Qld/2008/268 polyprotein gene (Accession number: JQ792245.1) with E-values ranging from 6e-131 to 2e-131. Since this Australian isolate is from an unpublished source, there is limited information about it.

Table 3. 17: BLAST analysis results of the AiV-1 partial 3CD products (266 bp) from mussel samples.

Sample ID	Descriptions	Accession number	E-value	% Identity
ML2A	AiV-1 isolate Qld/2008/268	JQ792245.1	2e-131	99%
ML3H	AiV-1 isolate Qld/2008/268	JQ792245.1	6e-131	99%
ML4B	AiV-1 isolate Qld/2008/268	JQ792245.1	5e-132	99%
ML5J	AiV-1 1 isolate Qld/2008/268	JQ792245.1	5e-132	99%

3.3.3.5 AiV-1 partial VP1 coding region- RT-PCR and gel purification

Molecular detection of AiV-1 from mussel samples using the Verso 1-Step RT-PCR Kit to amplify the AiV-1 partial VP1 coding region from mussel samples was not successful after several attempts as no PCR products were visible on agarose gels and no data is available.

3.3.4 AiV-1 multiple sequence analysis and phylogeny- 3CD region

Based on the 3CD and VP1 sequences, AiV-1 is classified into three genetically distinct genotypes namely A, B and C. Alignment of the 3CD sequences from mussels, swab samples as well as those from GenBank was carried out on MEGA 6 using Clustal W and the results of the alignment are shown in **Figure 3.3S (Supplementary 6)**. A phylogenetic tree constructed from the alignment using the Maximum-Likelihood method is shown in **Figure 3.16**. This Maximum-Likelihood tree was constructed from 1,000 pseudo-replicates based on Tamura 3 substitution model (Tamura, 1992). The results show that strains isolated in the present study belong to AiV-1 Genotype B as they clustered with genotype B isolates from several countries including an isolate from Burkina Faso (accession number: LN62595.1).

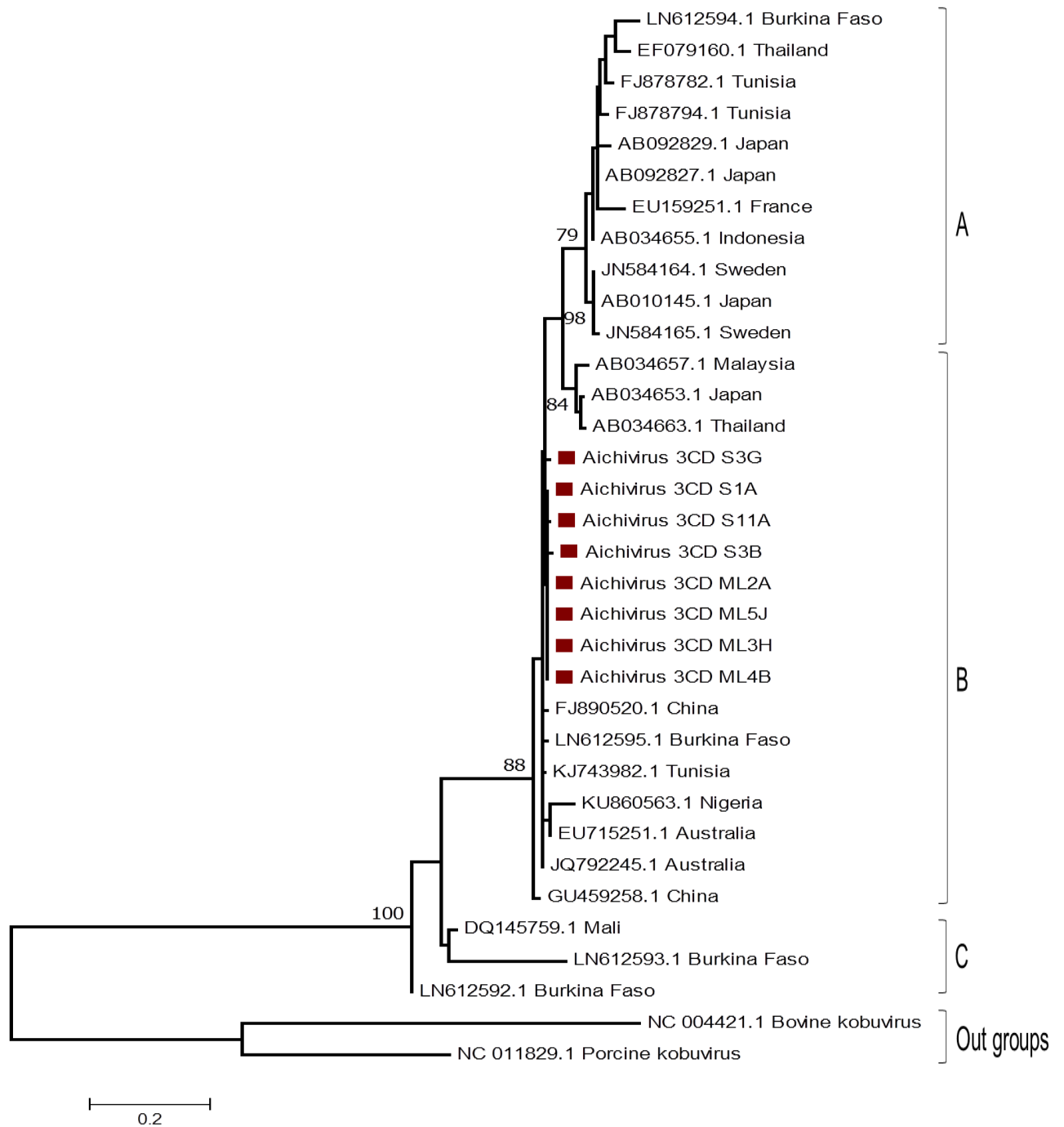


Figure 3.16: Molecular phylogenetic analysis of AiV-1 by Maximum Likelihood method based on Tamura 3 substitution model using a 266 bp sequence of the partial 3CD junction. Isolates from the present study are indicated by maroon boxes. The tree was evaluated by nonparametric bootstrap analysis with 1,000 pseudo-replicates. Only bootstrap values $\geq 70\%$ are shown. Scale bars represent the genetic distance (nucleotide substitutions per site). Bovine Kobuvirus and Porcine Kobuvirus were used as out-groups.

Furthermore, the partial VP1 sequences from the two swab samples (S9 and S11) and those from GenBank were aligned on MEGA 6 using Clustal W algorithm and the results of the alignment are shown in **Figure 3.4S (Supplementary 7)**. A phylogenetic tree constructed from the alignment using the Maximum-Likelihood method is shown in **Figure 3.17** below. This Maximum-Likelihood tree was constructed from 1,000 pseudo-replicates based on Tamura 3 substitution model (Tamura, 1992). The results show that strains isolated in the current study belongs to AiV-1 Genotype B where they cluster with various strains which were isolated from stool samples of diarrhoeic children and environmental samples such as raw sewage and surface water from South Korea and the Netherlands respectively during surveillance studies on AiV-1.

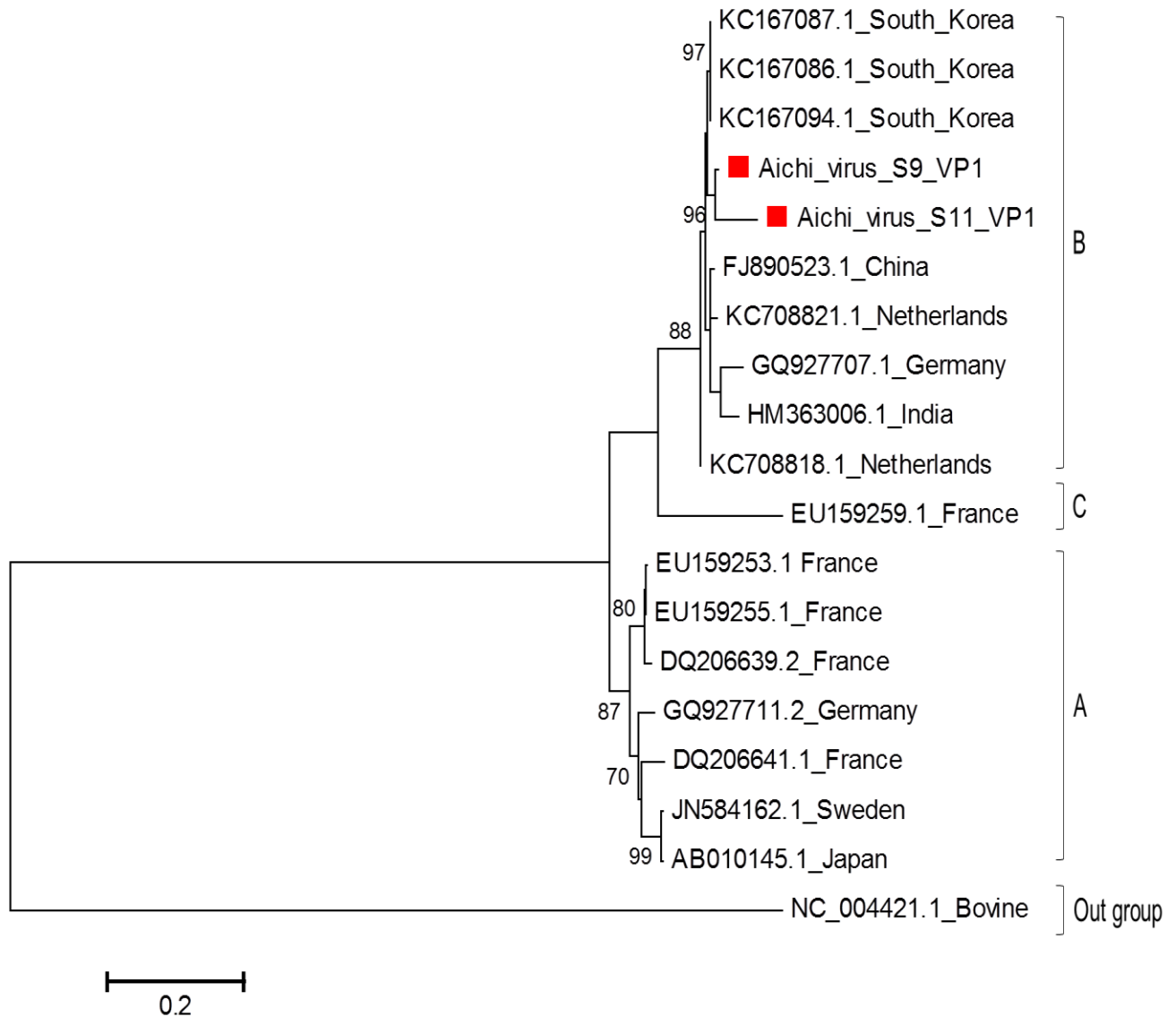


Figure 3. 17: Molecular phylogenetic analysis of AiV by Maximum Likelihood method based on Tamura 3 substitution model using a 472 bp sequence of the partial VP1. Isolates from the present study are indicated by red boxes. The tree was evaluated by nonparametric bootstrap analysis with 1,000 pseudo-replicates. Only bootstrap values $\geq 70\%$ are shown. Scale bar represents the genetic distance (nucleotide substitutions per site). Bovine Kobuvirus was used as an out-group.

3.4 Discussion

The main objective of this chapter was to develop RT-PCR assays to detect AiV-1 5' UTR, 3CD and VP1 sequences in swab samples collected from the Belmont Valley Sewage Treatment Plant, Grahamstown, as well as from mussel samples collected from the Swartkops River, Port Elizabeth. In order to develop the assays, samples were prepared and viral RNA extracted as described in chapter 2 (section 2.2.5). The RT-PCR assays were developed using gene-specific primers described in the literature as well as the ones designed in this study. The 5' UTR primers used were described in Drexler *et al.* (2011) which have been used successfully in only a handful of studies such as one by Han *et al.* (2014) who used them on clinical samples of diarrhoeic patients.

A 1008 bp product encompassing some area between the AiV-1 5' UTR and the leader protein was amplified from two swab samples, S3 and S9 showing that the RT-PCR assays developed in this study were successful. The 5' UTR is the most conserved region in Picornaviruses including AiV-1 (Drexler *et al.*, 2011). On the other hand, AiV-1 leader protein has a unique nucleotide as well as amino acid sequence to that of other Picornaviruses (Yamashita *et al.*, 1998). Amplification of the region encompassing the two regions introduces an element of specificity in molecular detection. However, the 5' UTR is highly stable as a result of the high GC content (approximately 60%) and a high degree of secondary structure making amplification difficult. It is most probably due to this reason that positive results were obtained from only 2 swab samples and not from all mussel samples tested.

There are various ways by which difficult to amplify regions are managed in PCR reactions. Addition of low molecular weight sulfoxides including Dimethyl sulfoxide (DMSO) to PCR reactions is one of the techniques used for that purpose (Kitade *et al.*, 2003). In the literature final DMSO concentrations of between 0.5% and 20% have been reported. In the present study, DMSO was added to final concentrations of between 5% and 15%. However PCR products were only obtained in reactions with 10% final DMSO concentration. Similar results were obtained by Kitade *et al.* (2003) although their optimal DMSO concentration was at 5%. Other techniques used to amplify highly stable regions include touch-down PCR, slow down PCR and addition of betaine (Frey *et al.*, 2008; Henke *et al.*, 1997). In the present study, two RT-PCR assays were developed for PCR amplification of the AiV-1 5' UTR. In the first assay DMSO (to a final concentration of

10%) was added to the reactions. For this assay one sample out of twelve was positive. In the second RT-PCR assay DMSO (to a final concentration of 10%) was used in combination with touch-down PCR, for which another sample became positive for AiV-1. This was consistent with some studies in which two or more techniques were applied to manage difficult to amplify regions. One example is a study by Sahdev *et al.* (2007) who used a combination of DMSO, betaine, primer modifications and increased denaturing temperature. This multi-prong strategy is believed to be more effective than using one technique.

The AiV-1 5' UTR sequences are not used for genotyping because of the highly conserved nature of the region. The region is only suitable for molecular detection of the virus from sample. Even though only two positives for the 5' UTR RT-PCR assay in the present study, it shows that AiV-1 is present in the Eastern Cape Province of South Africa.

On the other hand, the 3CD primers, initially designed by Yamashita *et al.* (2000), used in the present study have been used worldwide for detection of AiV-1 from shellfish and raw sewage as reviewed by Kitajima *et al.* (2015). PCR amplification using inner partial 3CD primers designed by Yamashita *et al.* (2000) appears to be more efficient than other PCR assays used in the present study as it readily gave PCR products from swab and mussel samples. This can be useful in routine diagnostic procedures. Yamashita *et al.* (2000) also found this assay to be more reliable compared to other assays they used for detection of AiV-1.

In regard to the VP1 assay, no visible PCR products were obtained when using published primers. Therefore, new primers were designed using Primer3 Plus software based on multiple sequence alignment of complete AiV-1 VP1 sequences randomly selected from GenBank and aligned in MEGA 6. A semi-nested PCR assay was developed to detect AiV-1 sequences from swab and mussel samples as described. In the first run reactions, the forward primer designed by Pham *et al.* (2008) and a reverse primer designed in this study were used in PCR reactions. The PCR products from these first run reactions did not produce any visible band on the agarose gel from swab and mussel samples. This was consistent with most semi-nested PCR assays in the literature for which no visible product is obtained from the first round PCR reaction. In the second round reactions a forward primer designed by Lodder *et al.* (2013) was used in combination with a reverse

primer designed in the present study. It was from this second run reaction that visible PCR products were obtained from two samples, S9 and S11. Unfortunately no VP1 products were visible from all the mussel samples tested. This could possibly be the result of PCR inhibitors in the samples as all the samples used in the VP1 RT-PCR assay were those positive for the 3CD assay and hence were expected to be positive for the VP1 assay as well. To improve this assay, samples should be spiked with an internal control such as bacteriophage PP7 as in Burutaran *et al.* (2016). This will help to analyse the impact of the PCR inhibitors in the reactions.

Based on analysis of the partial 3CD and VP1 sequences, isolates from the present study clustered with the genotype B's in GenBank. Although genotype B is found predominantly in South East Asian countries other than Japan, it has been detected from environmental and clinical samples worldwide such as in France, Brazil, Netherlands and Germany (Drexler *et al.*, 2011; Goyer *et al.*, 2008; Lodder *et al.*, 2013; Oh *et al.*, 2006). In Africa, genotype B was detected from raw sewage samples in Tunisia (Ibrahim *et al.*, 2017) as well as clinical samples in Burkina Faso (Ouédraogo *et al.*, 2016) and Nigeria (Japhet *et al.*, 2016). It is for this reason that its detection in South Africa is not surprising.

In this study, AiV-1 was successfully isolated from raw sewage as well as mussel samples. Based on the multiple sequence analysis and the phylogeny tree constructed it appears there are various strains circulating. It is not uncommon to isolate various strains from one source especially a sewage treatment plant as it caters for the whole community. Similar results were obtained by Alcalá *et al.* (2010), Kitajima *et al.* (2011) and Lodder *et al.* (2013) from raw sewage samples during surveillance studies on AiV-1.

Although this is the first time AiV-1 is reported in South Africa, this virus has been isolated from environmental samples and shellfish including mussels before in Tunisia (Ibrahim *et al.*, 2017; Sdiri-Loulizi *et al.*, 2010B) and many other countries worldwide (Alcalá *et al.*, 2010; Burutan *et al.*, 2015; Fusco *et al.*, 2017; Haramoto and Kitajima, 2017; Kitajima *et al.*, 2011; Le Guyader *et al.*, 2008; Lodder *et al.*, 2013). It is now considered as an important aetiological agent of gastroenteritis transmitted by sewage polluted water, hence its presence in shellfish and subsequently in stool samples of diarrhoeic patients after consumption of sewage contaminated shellfish.

Aichi virus 1 is linked to many cases of sewage and shellfish related gastroenteritis in East and South East Asian countries especially in Japan, China, Bangladesh, Thailand, Vietnam and South Korea (Han *et al.*, 2014; Hansma *et al.*, 2008; Iritani *et al.*, 2014; Kitajima *et al.*, 2011; Kitajima *et al.*, 2013; Li *et al.*, 2017; Ng *et al.*, 2012; Pham *et al.*, 2007). These are mostly developing countries in which most inhabitants do not have access to clean potable water, raw sewage is not adequately treated before disposal into river systems and hygiene levels are low (Corcoran *et al.*, 2010). The same applies to South Africa as reviewed by Okoh *et al.* (2010), who stated that municipal wastewater treatment processes in South Africa are not 100% efficient leading to disposal of raw or partially treated sewage into the environment which then flows into river systems. This was further complemented by Van Heerden *et al.* (2003), Van Heerden *et al.* (2005) and Ehlers *et al.* (2005) who reported presence of enteric viruses in river waters as well as drinking water supplies in South Africa. Although Aichi virus 1 was not amongst the viruses tested for in these studies, it is possible that it was present. Further research and epidemiological studies on this medically important virus are needed in order to elucidate its role in enteric infections in South Africa. The next chapter (Chapter 4) describes development of a nested PCR assay for molecular identification of enteric human bocaviruses from swab and mussel samples prepared in chapter 2. Enteric human bocaviruses are emerging agents of gastroenteritis which are yet to be detected in South Africa.

CHAPTER 4: Development of a nested PCR assay for molecular identification of enteric human bocaviruses from swabs and mussel samples

4.1 Introduction

Human bocaviruses (HBoVs) are single stranded DNA viruses belonging to the genus Parvovirus in family *Parvoviridae*. These viruses are about 18-26 nm in diameter with a genome size of approximately 5.2 kb (Allander *et al.*, 2005; Lau *et al.*, 2007; Ong *et al.*, 2016). The genome has got 3 open reading frames, namely ORF1 (coding for non-structural protein), ORF2 (coding for nucleo-phosphoprotein of unknown role) and ORF3 (coding for capsid proteins, VP1/VP2). Although HBoVs were initially associated with respiratory complications, they became to be linked to gastroenteritis in 2007 (Lau *et al.*, 2007).

Currently 4 viral species namely HBoV-1, HBoV-2, HBoV-3 and HBoV-4 have been identified (Guido *et al.*, 2016). Amongst these, HBoV-2 and HBoV-3 are directly linked to gastroenteritis by analysis of matched case control pairs (Arthur *et al.*, 2009; Campos *et al.*, 2016; Jin *et al.*, 2011; Zhang *et al.*, 2015). HBoV-1 is believed to play a role in respiratory infections (Allander *et al.*, 2005; Kantola *et al.*, 2008; Uršic *et al.*, 2011; Zhao *et al.*, 2013). On the other hand, there is limited molecular and epidemiological data on HBoV-4 as it is a rare species, but it has been isolated from stool samples of diarrhoeic patients and it is believed to play a role in causing gastroenteritis (Guido *et al.*, 2016).

For detection of enteric HBoVs, transmission electron microscopy, ELISA and PCR are the only techniques used so far (Guido *et al.*, 2016; Ong *et al.*, 2016). Currently, molecular detection (PCR) of enteric HBoVs is the only reliable method which is reported in almost all studies about detection of these viruses. This technique relies on PCR amplification of the highly conserved non-structural protein (NS-1), the relatively conserved nuclear-phosphoprotein (NP-1) and the hypervariable VP1/VP2 region. The NS-1 is most suitable for molecular identification and not for genotyping as it is highly conserved (Guido *et al.*, 2016). The NP-1 is less conserved than the NS-1, but it is still not the preferred region for genotyping. It is normally used for molecular identification of these viruses (Guido *et al.*, 2016; Jartti *et al.*, 2012). The VP1/VP2 region which forms the capsid, has many hypervariable sites and is used for genotyping purposes (Guido *et al.*, 2016; Lau *et al.*, 2007). There are many primers in the literature that are used for PCR

amplification of the VP1/VP2 region of HBoVs. However, almost all the VP1/VP2 primers in the literature are species specific such as the ones designed by Kapoor *et al.* (2010) which are specific for detection of HBoV-1 and HBoV-2. La Rosa *et al.* (2016) designed broad range degenerate primers using VP1/VP2 sequence data from all the 4 species of human bocaviruses, namely HBoV-1, HBoV-2, HBoV-3 and HBoV-4. These primers can detect all the HBoV species making them useful for surveillance studies. They have been used by several researchers including Iaconelli *et al.* (2016) who did surveillance study on human bocaviruses in raw sewage in Italy.

Enteric human bocaviruses, HBoV-2, HBoV-3 and HBoV-4, are those that are associated with human gastroenteritis. They have been detected worldwide mostly from stool samples of diarrhoeic patients in China (Yu *et al.*, 2008), Russia (Tymantsev *et al.*, 2016), Albania (La Rosa *et al.*, 2016), Brazil (Santos *et al.*, 2010), South Korea (Han *et al.*, 2009), Thailand (Khamrin *et al.*, 2012). In Africa there is limited epidemiological data available concerning these viruses. They were detected in stool samples of patients from only two African countries namely Nigeria and Tunisia (Kapoor *et al.*, 2010).

Detection of enteric HBoVs from environmental samples including raw sewage water is reported in fewer studies worldwide compared to the detection in clinical (stool) samples. Enteric HBoVs were detected from raw sewage samples during surveillance studies in Italy by PCR of the VP1/VP2 region (Iaconelli *et al.*, 2016), in USA by PCR amplification of the VP1 region (Blinkova *et al.*, 2008) and in Thailand by metagenomic analysis (Ng *et al.*, 2012). In Africa, these viruses were detected from raw sewage samples during surveillance studies in Nigeria by metagenomic analysis (Ng *et al.*, 2012). In the literature, no report on the detection of enteric HBoVs from shellfish was found. In South Africa, there is no published literature on the detection as well as possible role of these viruses as agents of gastroenteritis.

This chapter describes the application of a PCR assay that targets the VP1/VP2 region for detection of enteric HBoV from swab samples collected from the Belmont Valley Sewage Treatment Plant, Grahamstown, South Africa as well as mussel samples collected from the Swartkops River, Port Elizabeth, South Africa.

The specific objectives for this chapter are as follows;

- Development of a nested PCR assay to detect enteric HBoVs from the mussel and swab samples prepared in chapter 2.

- Cloning of appropriate PCR inserts
- Sequencing of plasmids and BLAST analysis of resultant sequences
- Construction of phylogenetic trees

4.2 Materials and methods

4.2.1 Primers for PCR amplification of the VP1/VP2 region of the HBoV genome

Two sets of degenerate primers, published by La Rosa *et al.* (2016) that amplify a final product of approximately 382 bp in the VP1/VP2 region (ORF3) of the HBoV genome were used in this study. The details about these primers are shown in **Table 4.1** below.

Table 4.1: Forward and reverse oligonucleotides for HBoVs as described by La Rosa *et al.* (2016).

Primer ID	Sequence, 5'→ 3'	Binding site	Genome location	Polarity	Amplicon size
HBoV-VP-F1	GAAATGCTTTCTG CTGYTGAAAG	3022-3044	VP1/VP2	+	543 bp
HBoV-VP-R1	GTGGATATACCCA CAYCAGAA	3545-3565	VP1/VP2	-	
HBoV-VP-F2	GGTGGGTGCTTCC TGGTTA	3084-3102	VP1/VP2	+	382 bp
HBoV-VP-R2	TCTTGRATTCATT TTCAGACAT	3444-3466	VP1/VP2	-	

The primer binding sites on the HBoV genome are shown in **Figure 4.1** below. All the primers bind to the VP1/VP2 coding region of the genome.

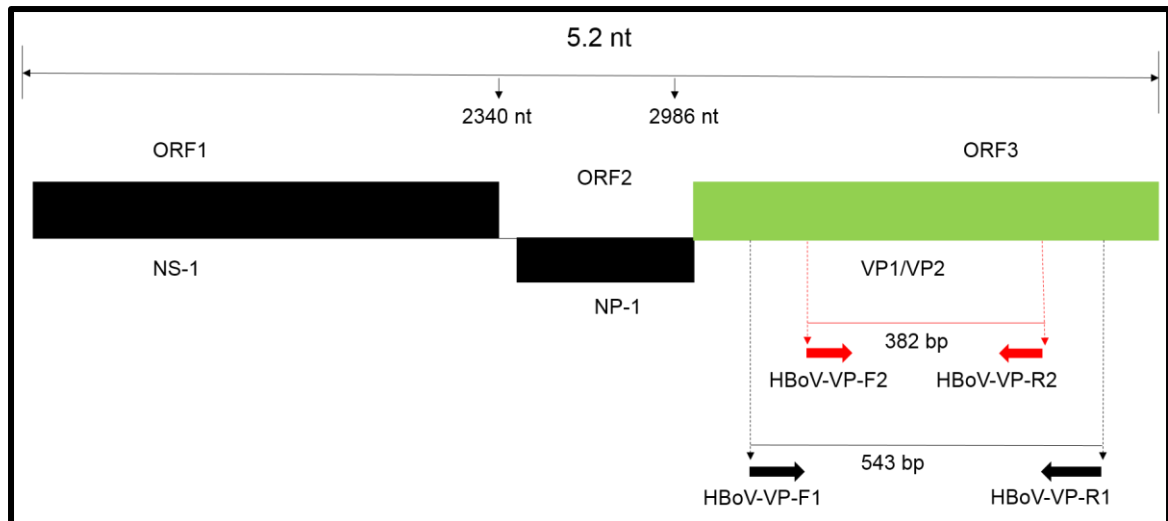


Figure 4. 1: Schematic representation of the human bocavirus VP1/VP2 region primer binding sites. Outer primers HBoV-VP-F1 (➡) and HBoV-VP-R1 (⬅) amplify an approximately 543 bp product while inner primers HBoV-VP-F2 (➡) and HBoV-VP-R2 (⬅) amplify a PCR product approximately 382 bp (adapted from La Rosa *et al.*, 2016).

4.2.2 Development of a nested PCR assay for amplification of the VP1/VP2 region of enteric HBoVs

4.2.2.1 Samples

Swab and mussel samples were collected and prepared as described in Chapter 2. For the detection of enteric HBoVs, not all the twenty swabs and twenty mussel samples were analysed due to time constraints. Only six swabs and six mussel samples were analysed. Shown in **Tables 4.2** and **4.3** is data on swabs and mussel samples respectively, that were analysed.

Table 4.2: Data pertaining to swab samples analysed for enteric HBoVs

Sample	Sample ID	Date collected
Swab 1	S1	10-05-16
Swab 2	S2	10-05-16
Swab 3	S3	10-05-16
Swab 4	S4	10-05-16
Swab 5	S5	10-05-16
Swab 6	S6	10-05-16

Table 4.3: Data pertaining to mussel samples analysed for enteric HBoVs

Sample	Sample ID	Date collected
Large mussel 1	ML1	02-05-16
Large mussel 2	ML 2	02-05-16
Large mussel 3	ML 3	02-05-16
Large mussel 4	ML 4	02-05-16
Large mussel 5	ML 5	02-05-16
Large mussel 6	ML 6	02-05-16

The swab and mussel samples were prepared as described in chapter 2 (section 2.2.2) and stored in aliquots at -20 °C awaiting downstream applications such as TEM and nucleic acid extraction.

4.2.2.2 Nucleic acid extraction

Nucleic acids were extracted from 140 µL of prepared swab and mussel samples using the QIAamp® Viral RNA Mini Kit, (Qiagen, USA) as described before in chapter 2 (section 2.2.5). The extracted nucleic acids were used for both RT-PCR and conventional PCR assays.

4.2.2.3 Amplification of the VP1/VP2 region of enteric HBoVs

The Ampliqon Taq PCR kit (Ampliqon Bio Reagents and Molecular Diagnostics, Denmark) was used to PCR amplify a part of the VP1/VP2 region using 2 sets of degenerate primers described in La Rosa *et al.* (2016). First round PCR reactions were set up as follows for each reaction; 12.5 µL of Ampliqon Taq 2x Master Mix Red, 1 µL of 10 µM forward primer (HBoV-VP-F1), 1 µL of 10 µM reverse primer (HBoV-VP-R1), 2 µL DNA from mussel and swab samples and 8.5 µL nuclease-free, sterile deionised water, all making up 25 µL were mixed up in a sterile PCR tube and subjected to thermal amplification in a SimpliAmp Thermal cycler to amplify a 543 bp product. A no template control reaction (NTC) consisting of 12.5 µL of Ampliqon Taq 2x Master Mix Red, 1 µL of 10 µM forward primer (HBoV-VP-F1), 1 µL of 10 µM reverse primer (HBoV-VP-R1), 10.5 µL nuclease-free, sterile deionised water was also included. The cycling parameters were as described in La Rosa *et al.* (2016) shown in **Table 4.4** below. The first round PCR products were analysed by 1% agarose gel electrophoresis with ethidium bromide staining at 90 Volts (V) for 35 minutes.

Table 4.4: Cycling parameters for the first and second round PCR reaction as described in La Rosa *et al.*, (2016).

Step	Temperature	Duration	Number of cycles
Initial Denaturation	94 °C	10 minutes	1
Denaturation	94 °C	30 seconds	
Annealing	55 °C	30 seconds	40
Extension	72 °C	1 minute	
Final extension	72 °C	5 minutes	1
Hold	4 °C	∞	1

To increase sensitivity, a nested PCR assay was developed to amplify a 382 bp PCR product in the VP1/VP2 region using second round primers, shown in **Table 4.1**. For each reaction, 12.5 µL of Ampliqon Taq 2x Master Mix Red, 1 µL of 10 µM forward primer (HBoV-VP-F2), 1 µL of 10 µM reverse primer (HBoV-VP-R2), 2 µL first round PCR product and 8.5 µL nuclease-free, sterile deionised water, all making up 25 µL were mixed up in a sterile PCR tube and subjected to thermal amplification in a SimpliAmp Thermal cycler. An NTC consisting of 12.5 µL of Ampliqon Taq 2x Master Mix Red, 1 µL of 10 µM forward primer (HBoV-VP-F2), 1 µL of 10 µM reverse primer (HBoV-VP-R2), 10.5 µL nuclease-free, sterile deionised water was also included. The cycling parameters are also as described in **Table 4.4** above. The second round PCR products were analysed by 1% agarose gel electrophoresis with ethidium bromide staining at 90 Volts for 35 minutes.

The second round PCR products were gel purified by use of the GeneJET Gel Extraction Kit (Thermo Scientific, USA) as described before in chapter 2 (section 2.2.8) and analysed by 1% agarose gel electrophoresis with ethidium bromide staining at 90V for 35 minutes.

4.2.2.4 Cloning PCR products into pJET 1.2/blunt vector

The purified second round PCR products (2 µL) from the mussel and swab samples were cloned into pJET 1.2/blunt vector, CloneJET™ PCR Cloning Kit (Thermo Scientific, USA) following the sticky-end protocol as described in chapter 2 (section 2.2.9). The PCR products were cloned so as not to lose any sequence data from the small DNA fragments (of approximately 382 bp).

4.2.2.5 Transformation of competent cells

Competent *E.coli* cells (DH5 α) were transformed as described in chapter 2 (section 2.2.10). Approximately 100 μ L of transformation mixture was then mixed gently by pipetting up and down, and then spread on Luria agar plate (with ampicillin at a final concentration of 100 μ g/mL). The plates were incubated overnight at 37 °C after which isolated colonies were inoculated into Luria broth (with ampicillin at a final concentration of 100 μ g/mL) and incubated at 37 °C overnight (15-18hrs) with shaking at approximately 200 rpm.

4.2.2.6 Plasmid extraction and restriction enzyme analysis

Plasmids were extracted from the cells using the GeneJET Plasmid Miniprep Kit (Thermo Scientific, USA) following manufacturer's instructions as described in chapter 2 (section 2.2.11). Presence and size of inserts was confirmed by double digestion of 2 μ L with Xho 1 (Promega, USA) and Xba 1 (Thermo Scientific, USA) as described before. The digestion products were analysed by 1% agarose gel electrophoresis with ethidium bromide staining at 90V for 35 minutes.

4.2.2.7 Sequencing of plasmids and BLAST analysis of resultant sequences

Plasmids with inserts approximately 382 bp were Sanger sequenced at Inqaba Biotechnical Industries ([Pty] Ltd, Pretoria, South Africa). Sequencing was done in the forward direction only. Resultant sequences were viewed on SnapGene Viewer 3.2.1, manually edited and subjected to BLAST search for related sequences from GenBank by use of NCBI BLAST website (Blast.ncbi.nlm.nih.gov/Blast.cgi).

4.2.2.8 Multiple sequence analysis and phylogeny

Enteric HBoV sequences from various regions of the world including African isolates from GenBank were selected based on a publication by La Rosa *et al.* (2016) to use in multiple sequence analysis of nucleotides in order to infer how they diverge from the ones isolated in the present study. Information concerning the various reference isolates used for the alignments is given in **Table 4.1S (Supplementary 8)**. Multiple sequence alignments of nucleotides, computation (including model tests) and construction of phylogeny trees were performed on Molecular Evolutionary Genetics Analysis 6 software (MEGA 6) followed by uploading the alignments into Geneious version 9.1.8 in order to obtain images of the alignments. The phylogenetic tree was constructed using the

Maximum Likelihood method by nonparametric bootstrap analysis with 1,000 pseudo-replicates based on Hasegawa-Kishino-Yano substitution model as described in La Rosa *et al.* (2016).

4.3 Results

4.3.1 Swab samples

4.3.1.1 Enteric HBoV VP1/VP2 PCR and gel purification

Amplicons of approximately 382 bp were obtained from all the six swab samples analysed as shown in **Table 4.5** below. This shows that the assay was successful.

Table 4.5: PCR results of the enteric HBoV VP1/VP2 assay for swab samples

Swab sample	VP1/VP2 PCR results
S1	PCR product produced
S2	PCR product produced
S3	PCR product produced
S4	PCR product produced
S5	PCR product produced
S6	PCR product produced

Figure 4.2 shows a representative 1% agarose gel electrophoresis of PCR products of HBoV VP1/VP2 coding region from swab samples 1 to 5. The reaction was also successful for swab sample 6 as a PCR product of the correct size was obtained but the results are not shown. In lane 1 no PCR product was obtained as expected because this was the NTC reaction in which sterile nuclease-free water was used in place of template DNA. Lanes 2 to 6 show bright PCR products approximately 382 bp obtained from swabs 1 to 5. The second round PCR products from swabs 4 and 6 were gel purified by use of the GeneJET Gel Extraction Kit as described in section 4.2.2.3.

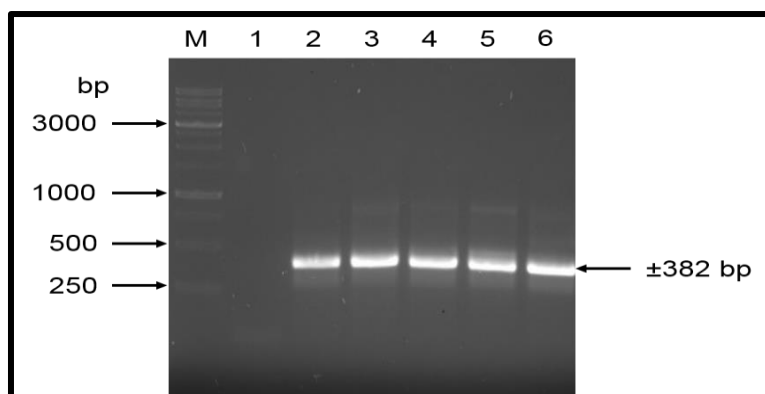


Figure 4. 2: 1% agarose gel electrophoresis of PCR products of the enteric HBoV VP1/VP2 coding region from swab samples. M: PCR Bio Ladder II (PCR Biosystems Ltd, United Kingdom), lane 1: NTC reaction, lanes 2-6: Second round PCR products from swab samples 1 to 5

4.3.1.2 Cloning of PCR products into pJET 1.2/blunt vector and restriction analysis of plasmid DNA

Gel purified second round PCR products (2 μ L) from swab samples 4 and 6 were cloned into pJET 1.2/blunt vector as described before in section 4.2.2.4 in order to get the full sequence data of the inserts. Only two swab samples were cloned due to time constraints. **Figure 4.3A** shows a representative 1% agarose gel electrophoresis of plasmid DNA extracted from cells (three colonies, A-C, from swab 4). Plasmid extraction was also successful for swab 6 although the results are not shown here. Restriction analysis of 2 μ L of plasmid DNA with Xho 1 and Xba 1 confirmed presence and sizes of inserts which were approximately 382 bp. **Figure 4.3B** shows 1% agarose gel of the restriction digest products from swab 4. Lanes 1, 3 and 5 show uncut plasmids (S4A-C). Lanes 2, 4 and 6 show cut plasmids for which linearised vectors were approximately 2974 bp, the size of pJET 1.2/blunt vector, while inserts were approximately 382 bp as expected. Restriction analysis was also successful for plasmids from swab 6 although the results are not shown.

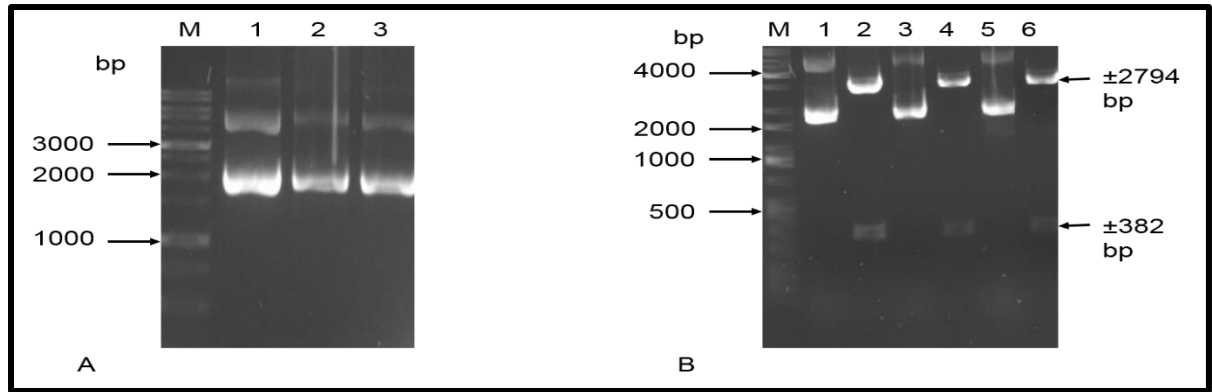


Figure 4.3: **A)** 1% agarose gel electrophoresis of plasmid DNA from swab sample 4 (S4). M: PCR Bio Ladder II, lane 1-3: Uncut plasmid DNA (S4A-C). **B)** 1% agarose gel electrophoresis of restriction digest products of the plasmids M: KAPA Ladder, lane 1: Plasmid S4A uncut, lane 2: S4A cut, lane 3: Plasmid S4B uncut, lane 4: S4B cut, lane 5: Plasmid S4C uncut, lane 6: S4C cut.

4.3.1.3 BLAST analysis of enteric HBoV VP1/VP2 PCR products from swab samples

Four plasmids (S4A, S4C, S6A and S6B) from swab samples with inserts approximately 382 bp were Sanger sequenced at Inqaba Biotechnical Industries ([Pty] Ltd, Pretoria, South Africa) and the resultant DNA sequences were highly identical to HBoV-3 strains in GenBank. As shown in **Table 4.6** below, all swab samples analysed had percentage identities ranging between 98% and 99% to an enteric HBoV-3 strain from China (Accession number: HM132056.1) with E-values of 0.0.

Table 4.6: BLAST analysis results of PCR products of the enteric HBoV VP1/VP2 coding region from swab (S) samples

Sample ID	Description	Accession number	E-value	% Identity
S4A	HBoV-3 isolate 46-BJ07	HM132056.1	0.0	99%
S4C	HBoV-3 isolate 46-BJ07	HM132056.1	0.0	99%
S6A	HBoV-3 isolate 46-BJ07	HM132056.1	0.0	98%
S6B	HBoV-3 isolate 46-BJ07	HM132056.1	0.0	99%

4.3.2 Mussel samples

4.3.2.1 Enteric HBoV VP1/VP2 RT-PCR and gel purification

Amplicons of approximately 382 bp were obtained from five out of six mussel samples analysed as shown in **Table 4.7** below.

Table 4.7: PCR results of the enteric HBoV VP1/VP2 assay for mussel samples

Swab sample	VP1/VP2 PCR results
ML1	No visible PCR product
ML2	PCR product produced
ML3	PCR product produced
ML4	PCR product produced
ML5	PCR product produced
ML6	PCR product produced

Figure 4.4 shows 1% agarose gel electrophoresis of PCR products of HBoV VP1/VP2 coding region from mussel samples 1 to 6. As shown below in **Figure 4.4** the second round PCR reactions were successful as PCR bands approximately 382 bp were obtained from five out of 6 samples. In lane 1 no PCR product was obtained as expected because this was the NTC reaction in which sterile nuclease-free water was used in place of template DNA. No PCR product was also obtained from large mussel sample 1 (ML1) as shown on lane 2. Lanes 3 to 7 show PCR products approximately 382 bp obtained from large mussel samples 2 to 6 (ML2 to ML6). PCR products from samples 3 (lane 4), sample 5 (lane 6) and sample 6 (lane 7) were brighter compared to those from samples 2 (lane 3) and sample 4 (lane 5). The second round PCR products from samples 4 and 6, which were amongst the brightest ones compared to others, were gel purified by use of the GeneJET Gel Extraction Kit as described before in section 4.2.2.3.

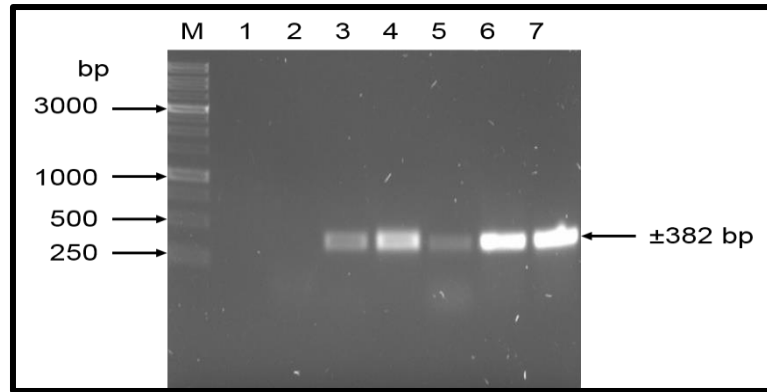


Figure 4. 4: 1% agarose gel electrophoresis of PCR products of the enteric HBov VP1/VP2 coding region from large mussel samples. M: PCR Bio Ladder II (PCR Biosystems Ltd, United Kingdom), lane 1: NTC reaction, lanes 2-7: Second round PCR products from samples 1 to 6

4.3.2.2 Cloning of PCR products into pJET 1.2/blunt vector and restriction analysis of plasmid DNA

Gel purified second round PCR products from mussel samples 4 (ML4) and mussel sample 6 (ML6) were cloned into pJET 1.2/blunt vector as described before in order to get the full sequence data of the inserts. **Figure 4.5A** below shows a representative 1% agarose gel electrophoresis of plasmid DNA extracted from cells (3 colonies, A-C, from ML4). Plasmid extraction was also successful for sample ML6 although results are not shown. Restriction analysis of 2 μ L of plasmid DNA with Xho 1 and Xba 1 confirmed presence and sizes of inserts which were approximately 382 bp. **Figure 4.5B** shows 1% agarose gel of the restriction digest products of plasmid DNA from mussel sample ML4. Lanes 1, 3 and 5 show uncut plasmids (ML4A-C). Lanes 2, 4 and 6 show cut plasmids for which linearised vectors were approximately 2974 bp, the size of pJET 1.2/blunt vector, while inserts were approximately 382 bp as expected. Restriction digestion was also successful for mussel sample 6 although results are not shown.

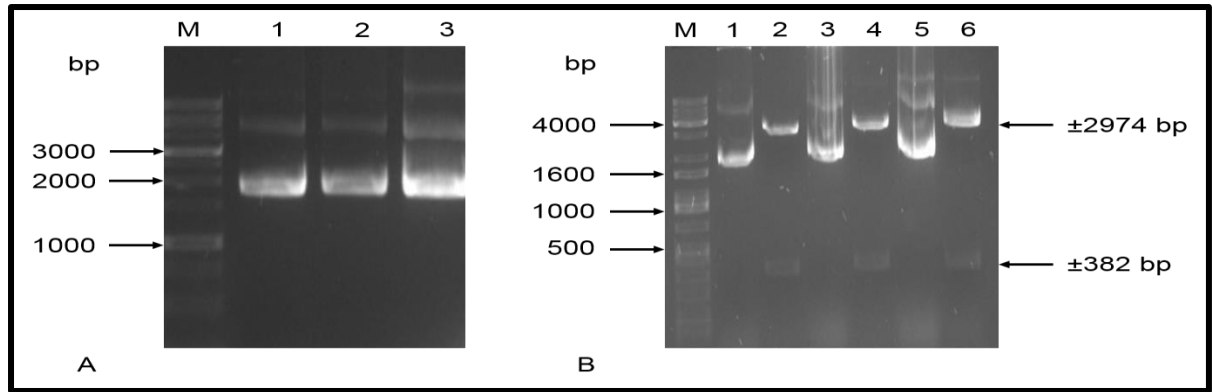


Figure 4.5: **A)** 1% agarose gel electrophoresis of plasmid DNA from mussel sample 4 (ML4). M: PCR Bio Ladder II, lane 1-3: Uncut plasmid DNA (ML4A-C). **B)** 1% agarose gel electrophoresis of restriction digest products of the plasmids M: KAPA Ladder, lane 1: Plasmid ML4A uncut, lane 2: ML4A cut, lane 3: Plasmid ML4B uncut, lane 4: ML4B cut, lane 5: Plasmid ML4C uncut, lane 6: ML4C cut

4.3.3 BLAST analysis of enteric HBoV VP1/VP2 PCR products from mussel samples

Two plasmids (ML4A and ML6C) from mussel samples with inserts approximately 382 bp were Sanger sequenced at Inqaba Biotechnical Industries ([Pty] Ltd, Pretoria, South Africa) and resultant DNA sequences were highly identical to HBoV-2 strains in GenBank. As shown in **Table 4.8** below, both mussel samples had percentage identities of 99% to an enteric HBoV-2 strain from Australia (Accession number: FJ948860.1) with E-values of 0.0.

Table 4.8: BLAST analysis results of PCR products of the enteric HBoV VP1/VP2 coding region from large mussel (ML) samples

Sample ID	Description	Accession number	E-value	% Identity
ML4A	HBoV-2 strain W298	FJ948860.1	0.0	99%
ML6C	HBoV-2 strain W298	FJ948860.1	0.0	99%

4.3.4 Multiple sequence analysis and phylogeny

The alignment of VP1/VP2 sequences from mussels, swab samples as well as those from GenBank was carried out on MEGA 6 using Clustal W algorithm. The results of the alignment are shown in **Figure 4.1S (Supplementary 9)**. A phylogenetic tree constructed

from the alignment using the Maximum-Likelihood method is shown in **Figure 4.6** below. This Maximum-Likelihood tree was constructed from 1,000 pseudo-replicates based on Hasegawa-Kishino-Yano substitution model. The results show that isolates from swab samples belong to HBoV-3 whereas isolates from mussel samples belong to HBoV-2.

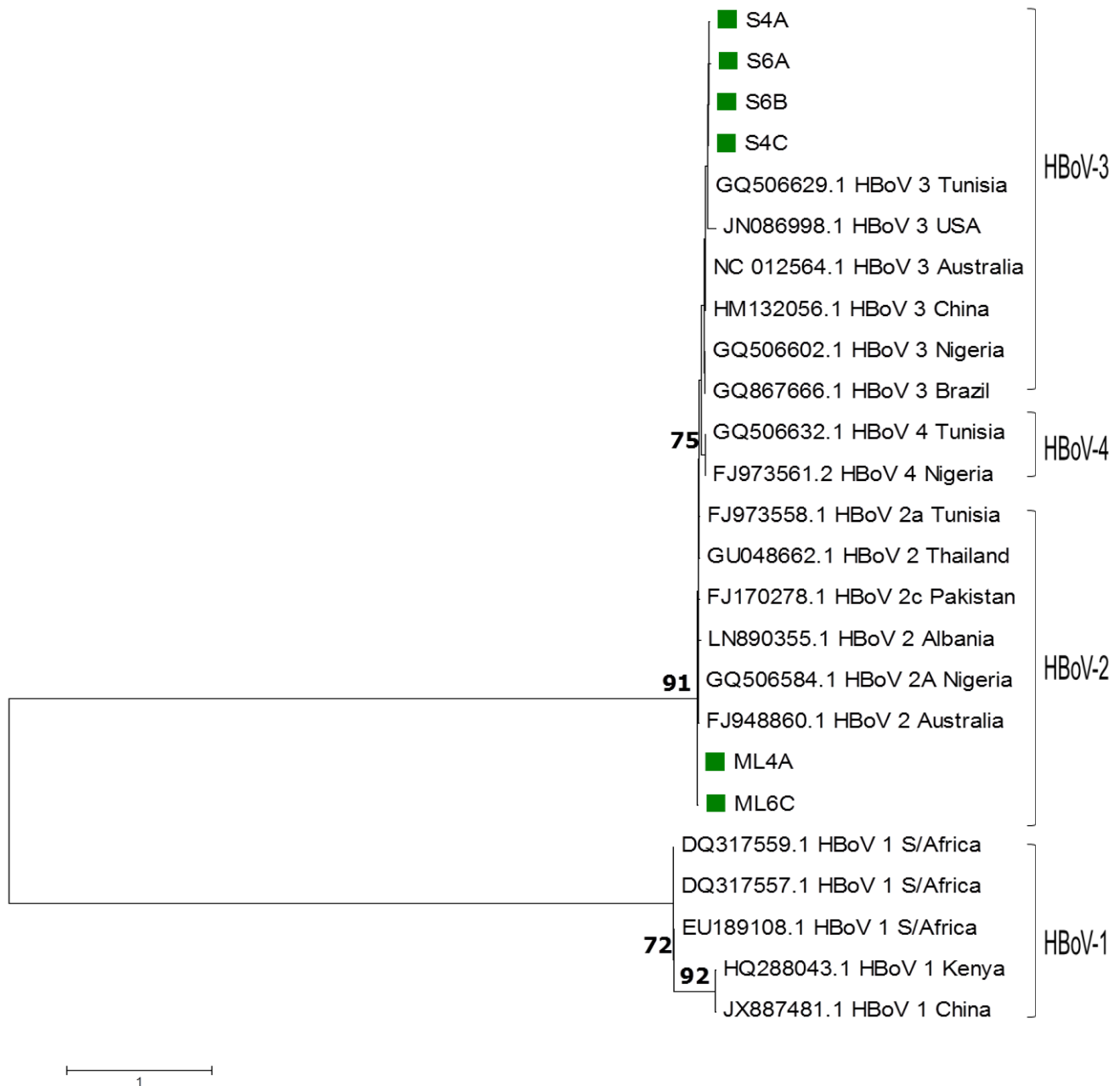


Figure 4. 6: Molecular phylogenetic analysis of enteric HBov by Maximum Likelihood method based on Hasegawa-Kishino-Yano substitution model using a 382 bp sequence of the partial VP1/VP2 gene. Isolates from the present study are indicated by green boxes. The tree was evaluated by nonparametric bootstrap analysis with 1,000 pseudo-replicates. Only bootstrap values $\geq 60\%$ are shown. Scale bar represents the genetic distance (nucleotide substitutions per site).

4.4 Discussion

The main objective of this chapter was to perform PCR amplification of the VP1/VP2 region for detection and typing of enteric HBoVs using DNA extracted from mussel samples collected from the Swartkops River as well as swab samples from the Belmont Valley Sewage Treatment Plant.

The DNA used in this study was extracted using the QIAamp® Viral RNA Mini Kit, (Qiagen, USA). This kit has been used before for extraction of DNA from environmental and clinical specimen for detection of human bocaviruses (Kapoor *et al.*, 2010; Longtin *et al.*, 2008; Neske *et al.*, 2007; Pham *et al.*, 2011). By application of a nested PCR reaction, PCR products of the expected size (382 bp) were obtained from the mussel and swab samples in the second round PCR reactions. This was consistent with all studies in which this nested PCR assay was used, including La Rosa *et al.* (2016) who did not report obtaining PCR products from the first round PCR reactions. The results obtained in this study shows that the assay was successful and confirms the suitability of the QIAamp® Viral RNA Mini Kit for extraction of DNA from environmental and clinical samples as described in other studies (Kapoor *et al.*, 2010; Longtin *et al.*, 2008; Neske *et al.*, 2007; Pham *et al.*, 2011).

The PCR products obtained were gel purified and successfully cloned into pJET 1.2/blunt vector as depicted by presence of inserts of the right size (approximately 382 bp) after digestion of the plasmids with Xho 1 and Xba 1. Cloning of PCR products into pJET 1.2/blunt vector served its intended purpose as the full sequence data, approximately 382 bp, was obtained from all samples sequenced. This means that the full sequence data was available for analysis and thus accuracy of the results was ensured.

Even though not all plasmids from mussel and swab samples were sequenced due to time constraints, the BLAST results showed that all those sequenced were highly identical to known enteric HBoVs in GenBank. The swab samples had percentage identities of between 98% and 99% to HBoV-3 (accession number: HM132056.1), which was detected from stool specimen of a diarrhoeic child in a study by Wang *et al.* (2011). The mussel samples were 99% identical to HBoV-2 from Australia (accession number: FJ948860.1), which was detected from stool samples of a diarrhoeic child in a study by Arthur *et al.* (2009). HBoV-2 and HBoV-3 are known aetiological agents of gastroenteritis. They have been detected from clinical samples of diarrhoeic patients

worldwide, for example in China (Jin *et al.*, 2011), in Brazil (Campos *et al.*, 2016), in Ireland (Cashman and O'Shea, 2012), in Russia (Tymmentsev *et al.*, 2016), in Thailand (Khamrin *et al.*, 2012), in Tunisia and Nigeria (Kapoor *et al.*, 2010). Currently there are only a handful of published reports on the presence of HBoV-3 in sewage treatment plants worldwide i.e. in Italy, the USA, Thailand, Nepal and Nigeria (Iaconelli *et al.*, 2016; Blinkova *et al.*, 2009; Ng *et al.*, 2012). To our knowledge, apart from findings in this study, there are no published reports on the detection of enteric HBoV from shellfish including mussels worldwide.

In the present study, because of time constraints, only a few swabs and mussel samples were analysed for HBoV. This could possibly be the reason why only two species of HBoV, namely HBoV-2 and HBoV-3 were detected. In future, the number of samples should be increased so that chances of detecting HBoV-4 are increased. According to Guido *et al.* (2016), HBoV-4 is rarely detected. It has been detected before from stool specimen of diarrhoeic children in Tunisia and Nigeria (Kapoor *et al.*, 2010).

In conclusion, nested PCR assays developed in this study were successful as enteric HBoV genotypes 2 and 3 were detected from mussel and swab samples respectively. These viruses might be playing a role as aetiological agents of enteric infections in South Africa. However more clinical and epidemiological data is required for elucidation. Chapter 5 will describe the development of a nested PCR assay to detect and type enteric human adenoviruses from swab and mussel samples prepared using the techniques described in chapter 2.

CHAPTER 5: Development of a nested PCR for molecular identification of enteric human adenoviruses from swab and mussel samples

5.1 Introduction

Human adenoviruses (HAdV) are double stranded DNA viruses belonging to the genus Mastadenovirus in family *Adenoviridae*. These viruses are about 70-100 nm in diameter with a genome size of approximately 30 kb (Ghebremedhin, 2014). The adenovirus virion consists of 3 major proteins, namely the fibre protein, the penton base and the hexon protein. The fibre protein, being the outer-most part of the capsid plays a role in attachment to host cells. The penton base is believed to bind to cellular integrins (Khare *et al.*, 2011). The hexon protein, which is the most abundant protein in the capsid has antigenic properties. This protein is the most conserved but with hypervariable sites (Crawford-Miksza and Schnurr, 1996). It is used for molecular detection and classification of human adenoviruses (Harrison *et al.*, 2010; Ebner *et al.*, 2005). In addition to the 3 major proteins mentioned above, the capsid also consists of at least 4 minor proteins, IIIa, VI, VIII and IX, which are believed to play a role in capsid assembly (Khare *et al.*, 2011).

Currently there are over 70 HAdV serotypes classified into 7 subtypes, A-G, known to cause various complications including keratoconjunctivitis, respiratory infections, urinary infections and gastroenteritis (Arnold and MacMahon, 2017). While some serotypes in subtypes A, C and D are believed to play a role in enteric infection, all serotypes in subtype F and G are directly linked to enteric infections (Arnold and MacMahon, 2017; Ghebremedhin, 2014).

For detection of enteric HAdV, techniques such as transmission electron microscopy, ELISA, cell culture, PCR and qPCR are used (Ghebremedhin, 2014). PCR and qPCR are currently the gold standard techniques especially for detection of these viruses from environmental sources such as wastewater where viral concentrations are low (Arnold and MacMahon, 2017; Sidhu *et al.*, 2013). Molecular detection of HAdV is mostly based on PCR amplification of the conserved hexon gene (Casas *et al.*, 2005). In the literature there are many primers that are used for molecular detection of HAdV. However, most of these published primers are subtype specific or for a few subtypes such as those used in Jiang *et al.* (2005) and Rezaei *et al.* (2012) for detection of subtype F from environmental

samples in the USA and stool specimen of diarrhoeic patients in Iran respectively. Subtype specific primers were also used by Adefisoye *et al.* (2016) and Osuolale and Okoh (2015) for detection of subtypes B, C, E and F in wastewater treatment plants in South Africa. These subtype specific primers are not suitable for detection of enteric human adenoviruses for surveillance purposes in which several serotypes are involved and the status is unknown. It is for this reason that Avellon *et al.* (2001) designed broad range degenerate primers targeting the hexon gene, that were able to detect all subtypes of human adenoviruses. Compared to the previously designed broad range primers by Hierholzer *et al.* (1993), Kidd *et al.* (1996) and Puig *et al.* (1994), primers described by Avellon *et al.* (2011) are more sensitive and hence suitable for rapid diagnosis of any adenovirus serotype even at extremely low concentrations such as in environmental samples. These primers have been used in many studies worldwide for molecular detection of enteric human adenoviruses from stool specimens of diarrhoeic patients (Casas *et al.*, 2005; Magwalivha *et al.*, 2010; Van Heerden *et al.*, 2005; Van Heerden *et al.*, 2003).

In the literature, various commercial nucleic acid extraction kits have been used for purification of DNA for molecular detection of enteric HAdV. These DNA kits include the Quick-gDNATM MiniPrep (Zymo Research, USA) (Adefisoye *et al.*, 2016; Chigor and Okoh, 2012), the High Pure Nucleic Acid Kit (Roche Diagnostics, Mannheim, Germany) (Van Heerden *et al.*, 2005). In addition, the use of the QIAamp[®] Viral RNA Mini Kit for DNA purification was reported in some studies including one by Jiang *et al.* (2005) for purification of DNA from environmental samples for molecular detection of human adenoviruses during a surveillance study.

Different HAdV subtypes and species have been detected worldwide from clinical, environmental and shellfish samples and linked to cases of gastroenteritis. For example, studies have reported them in stool samples in Spain (Casas *et al.*, 2005), Thailand (Sriwanna *et al.*, 2013), Iran (Dashti *et al.*, 2016), Australia (Fletcher *et al.*, 2013), Brazil (Reis *et al.*, 2016) and USA (Jiang *et al.*, 2005). In Africa, enteric human adenoviruses were detected from stool samples in many countries including Republic of Congo (Mayindou *et al.*, 2016), Burkina Faso (Ouedraogo *et al.*, 2017), Nigeria (Aminu *et al.*, 2007), Gabon (Lekana-Douki *et al.*, 2015), Kenya (Magwalivha *et al.*, 2010), Democratic Republic of Congo, Central African Republic, Ivory Coast and Uganda (Pauly *et al.*, 2014).

These viruses have also been detected from water samples including raw sewage, river water and drinking water during surveillance studies in Australia (Sidhu *et al.*, 2013), USA (Bambic *et al.*, 2015), Norway (Grøndahl-Rosado *et al.*, 2014), Venezuela (Rodríguez-Díaz *et al.*, 2009) and Ghana (Silverman *et al.*, 2013). Several studies also reported the presence of enteric HAdV in shellfish such as mussels and oysters collected in polluted water in Brazil, Spain, India, Morocco and Tunisia (Rigotto *et al.*, 2005; Formiga-Cruz *et al.*, 2005; Umesha *et al.*, 2008; Karamoko *et al.*, 2005; Sdiri-Loulizi *et al.*, 2010A).

Studies describing the epidemiology and prevalence of HAdV subtypes in South Africa are limited. However subtype F (serotypes 40 and 41) were reported in stool specimen of diarrhoeic patients in Gauteng Province by Moore *et al.* (2000). Adefisoye *et al.* (2016) and Osulale and Okoh, (2015) described the presence of subtypes B, C and F in final effluents of selected wastewater treatment plants in the Eastern Cape Province. Other studies have reported the detection of HAdV subtypes B, C, D and F in rivers and drinking water supplies in South Africa (Chigor and Okoh, 2012; Van Heerden *et al.* 2005). Apart from a study by Vos and Knox (2017), there is no other published report on presence of enteric human adenoviruses in shellfish collected from polluted river water.

This chapter describes the application of a nested PCR using broad range degenerate primers designed by Avellon *et al.* (2001) to amplify a region of the hexon for molecular detection of enteric HAdV from swab samples collected from the Belmont Valley Sewage Treatment Plant, Grahamstown, South Africa as well as mussel samples collected from the Swartkops River, Port Elizabeth, South Africa. Furthermore, the sequences obtained were used to infer phylogenetic relationships by comparison with hexon sequences retrieved from GenBank database.

The specific objectives for this chapter are as follows;

- Development of a nested PCR assay to detect enteric human adenoviruses from the mussel and swab samples prepared in chapter 2.
- Cloning of selected PCR inserts
- Sequencing of plasmids and BLAST analysis of resultant sequences
- Construction of phylogenetic trees

5.2 Materials and methods

5.2.1 Primers for PCR amplification of the hexon gene

Two sets of published degenerate primers designed by Avellon *et al.* (2001) were used for thermal amplification of the adenovirus hexon gene. These primers are designed such that they bind to any of the seventy adenovirus serotypes. The primers and their binding sites are shown in **Table 5.1** below. They amplify a final product of 168 bp in the hexon coding region.

Table 5. 1: Forward and reverse oligonucleotides for enteric HAdV as described by Avellon *et al.* (2001).

Primer No	ID	Sequence, 5'→ 3'	Binding site	Genome location	Polarity	Amplicon size
	ADHEX1F	CAACACCTAYG ASTACATGAA	20380–20400 nt	Hexon	+	473 bp
	ADHEX1R	KATGGGGTARA GCATGTT	20836–20854 nt	Hexon	-	
	ADHEX2F	CCCITTYAACCA CCACCG	20485–20505 nt	Hexon	+	168 bp
	ADHEX2R	TCTTGRATTTCA TTTTTCAGACAT	20632–20652 nt	Hexon	-	

Shown in **Figure 5.1** below are the primers binding sites on the HAdV 2 genome. All the primers bind to the hexon coding region of the genome.

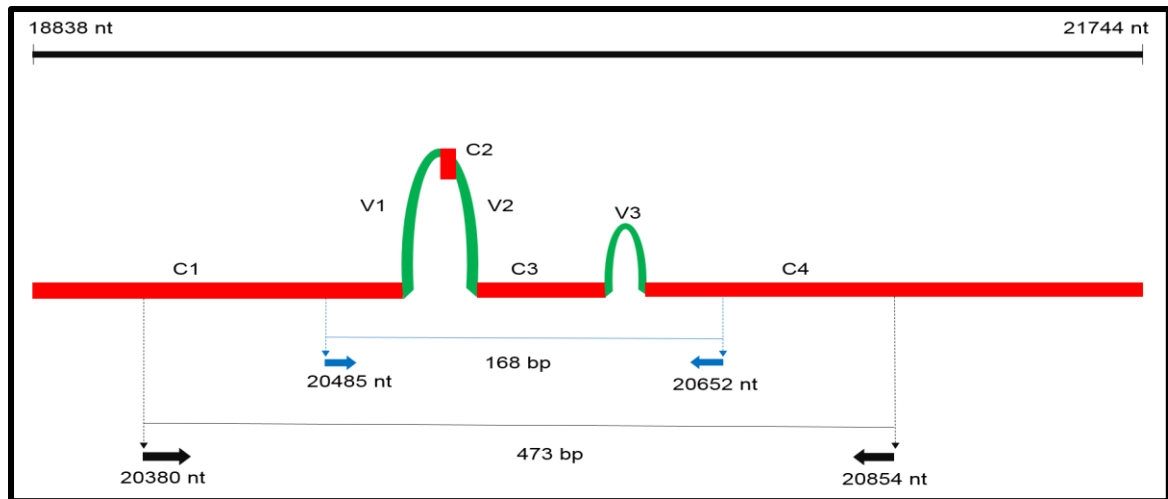


Figure 5. 1: Schematic representation of the HAdV hexon protein-coding region primer binding sites. Outer primers ADHEX1F (➡) and ADHEX1R (⬅) amplify an approximately 473 bp product while inner primers ADHEX2F (➡) and ADHEX2R (⬅) amplify a product of 168 bp. C1-C4 (red) are conserved sites while V1- V3 (green) are hypervariable sites of the hexon gene.

5.2.2 Positive control

A plasmid containing the 168 bp region of the hexon region of HAdV subtype D cloned into pJET1.2/blunt vector was described by Vos and Knox (2017) and was used in all PCR assays. In order to confirm the presence and size of the insert, this plasmid was digested with Xho 1 (Promega, USA) and Xba 1 (Thermo Scientific, USA) as described in chapter 2 (section 2.2.11). The plasmid was then diluted 1:1000 with sterile distilled water and used as a positive control template in the PCR reactions.

5.2.3 Samples

Swabs and mussel samples were collected and prepared as described in Chapter 2 (sections 2.2.1-2.2.3). For the detection of enteric HAdV, all the twenty swabs and twenty mussel samples were analysed to increase chances of identifying different subtypes associated with gastroenteritis. Details about all the samples analysed are shown in **Tables 2.1** and **2.2** (Chapter 2).

5.2.4 Nucleic acid extraction

Nucleic acids were extracted from 140 µL of prepared swabs and mussel samples using the QIAamp® Viral RNA Mini Kit, (Qiagen, USA) as described before in section 2.2.5

(Chapter 2). The extracted nucleic acids were used for both RT-PCR and conventional PCR assays.

5.2.5 Nested PCR assay for amplification of the hexon gene

The Ampliqon Taq PCR kit (Ampliqon Bio Reagents and Molecular Diagnostics, Denmark) was used to PCR amplify a region of the conserved and hypervariable hexon gene using 2 sets of degenerate primers described by Avellon *et al.* (2001). First round PCR reactions were set up as follows for each reaction: 12.5 μ L of Ampliqon Taq 2x Master Mix Red, 1 μ L forward primer (ADH1F, 10 μ M), 1 μ L reverse primer (ADH1R, 10 μ M), 2 μ L of sample DNA and 8.5 μ L nuclease-free, sterile deionised water, all making up 25 μ L were mixed up in a sterile PCR tube and subjected to thermal amplification in a SimpliAmp Thermal cycler (Bio-Systems by Life Technologies) to amplify a 473 bp product. A no template control reaction (NTC) consisting of 12.5 μ L of Ampliqon Taq 2x Master Mix Red, 1 μ L of 10 μ M forward primer (ADH1F), 1 μ L of 10 μ M reverse primer (ADH1R), 10.5 μ L nuclease-free, sterile deionised water was also included. The cycling parameters were as described in Van Heerden *et al.* (2003) and shown in **Table 5.2** below. The PCR products were analysed by 2% agarose gel electrophoresis with ethidium bromide staining at 90 Volts for 35 minutes.

Table 5.2: Cycling parameters for the second round PCR reaction as described in Van Heerden *et al.*, (2003).

Step	Temperature	Duration	Number of cycles
Initial denaturation	94 °C	2 minutes	1
Denaturation	93 °C	1 minutes	
Annealing	50 °C	1 minute	30
Extension	72 °C	1 minutes	
Final extension	72 °C	6 minutes	1
Hold	4 °C	∞	1

To increase sensitivity, a nested PCR assay was developed to amplify a 168 bp product in the hexon region using second round primers, shown in **Table 5.1**. For each reaction, 12.5 μ L of Ampliqon Taq 2x Master Mix Red, 1 μ L forward primer (ADH2F, 10 μ M), 1 μ L reverse primer (ADH2R, 10 μ M), 2 μ L of first round PCR product and 8.5 μ L nuclease-free, sterile deionised water, all making up 25 μ L were mixed up in a sterile PCR tube and

subjected to thermal amplification in a SimpliAmp Thermal cycler. A no template control reaction (NTC) consisting of 12.5 μL of Ampliqon Taq 2x Master Mix Red, 1 μL forward primer (ADH2F, 10 μM), 1 μL reverse primer (ADH2R, 10 μM), 10.5 μL nuclease-free, sterile deionised water was also included. The cycling parameters were as shown in **Table 5.2** below except that the annealing temperature was increased to 55 $^{\circ}\text{C}$. The second round PCR products were analysed by 2% agarose gel electrophoresis with ethidium bromide staining at 90 Volts for 35 minutes.

The second round PCR products from the samples were gel purified by use of the GeneJET Gel Extraction Kit (Thermo Scientific, USA) as described before in section 2.2.8 (Chapter 2) and analysed by 2% agarose gel electrophoresis with ethidium bromide staining at 90 Volts for 35 minutes.

5.2.6 Cloning of purified PCR products into pJET 1.2/ blunt vector

The purified second round PCR products (2 μL) from the samples were cloned into pJET 1.2/blunt vector, CloneJET™ PCR Cloning Kit (Thermo Scientific, USA) following the sticky-end protocol as described in section 2.2.9 (Chapter 2). The PCR products were cloned so as not to lose any sequence data from the small DNA fragments (168 bp).

5.2.7 Transformation of competent cells

Competent *E.coli* cells (DH5 α) were transformed as described in section 2.2.10 (Chapter 2). Approximately 100 μL of transformation mixture was then mixed gently by pipetting up and down, and then spread on Luria agar plate (with ampicillin at a final concentration of 100 $\mu\text{g}/\text{mL}$). The plates were incubated overnight at 37 $^{\circ}\text{C}$ after which isolated colonies were inoculated into Luria broth (with ampicillin at a final concentration of 100 $\mu\text{g}/\text{mL}$) and incubated at 37 $^{\circ}\text{C}$ overnight (15- 18hrs) with shaking at approximately 200 rpm.

5.2.8 Plasmid extraction and restriction enzyme analysis

Plasmids were extracted from the cells using the GeneJET Plasmid Miniprep Kit (Thermo Scientific, USA) following manufacturer's instructions as described in section 2.2.11 (Chapter 2). Presence and size of inserts was confirmed by double digestion of 2 μL of plasmid DNA with Xho 1 (Promega, USA) and Xba 1 (Thermo Scientific, USA) as described before in section 2.2.11 (chapter 2). The digestion products were analysed by 2% agarose gel electrophoresis with ethidium bromide staining at 90V for 35 minutes.

5.2.9 Sequencing of plasmids and BLAST analysis

Plasmids with inserts of 168 bp were Sanger sequenced at Inqaba Biotechnical Industries ([Pty] Ltd, Pretoria, South Africa). Sequencing was done in the forward direction only. Resultant sequences were viewed on SnapGene Viewer 3.2.1, manually edited and subjected to BLAST search for related sequences from GenBank by use of NCBI BLAST website (Blast.ncbi.nlm.nih.gov/Blast.cgi).

5.2.10 Multiple sequence analysis and phylogeny

Enteric human adenovirus sequences from various regions of the world including African isolates from GenBank were selected to use in multiple sequence analysis of nucleotides in order to infer how they diverge from the ones isolated in the present study. Information about the various reference isolates used for the alignments is given in **Table 5.1S (Supplementary 10)**. Multiple sequence alignments of nucleotides, computation (including model tests) and construction of phylogeny trees were performed using Molecular Evolutionary Genetics Analysis 6 software (MEGA 6) followed by uploading the alignments into Geneious version 9.1.8 in order to obtain images of the alignments. The phylogenetic tree was constructed using the Maximum Likelihood method by nonparametric bootstrap analysis with 1,000 pseudo-replicates based on Tamura 3 substitution model (Tamura, 1992).

5.3 Results

5.3.1 Positive control

5.3.1.1 Confirmation of insert by restriction analysis with Xho 1 and Xba1

The plasmid map of positive control plasmid is shown in **Figure 5.2A** below. Restriction analysis using normal digest Xho 1 and fast digest Xba 1 confirmed the presence of the insert which was approximately 168 bp as expected. **Figure 5.2B** below shows 2% agarose gel electrophoresis of the uncut and cut plasmid DNA. Lane 1 shows the uncut plasmid DNA. Lane 2 shows the cut plasmid DNA with the insert PCR product approximately 168 bp and the vector backbone of approximately 2974 bp. This shows that the insert PCR product cloned into the vector was of the correct size and can be used as a positive control.

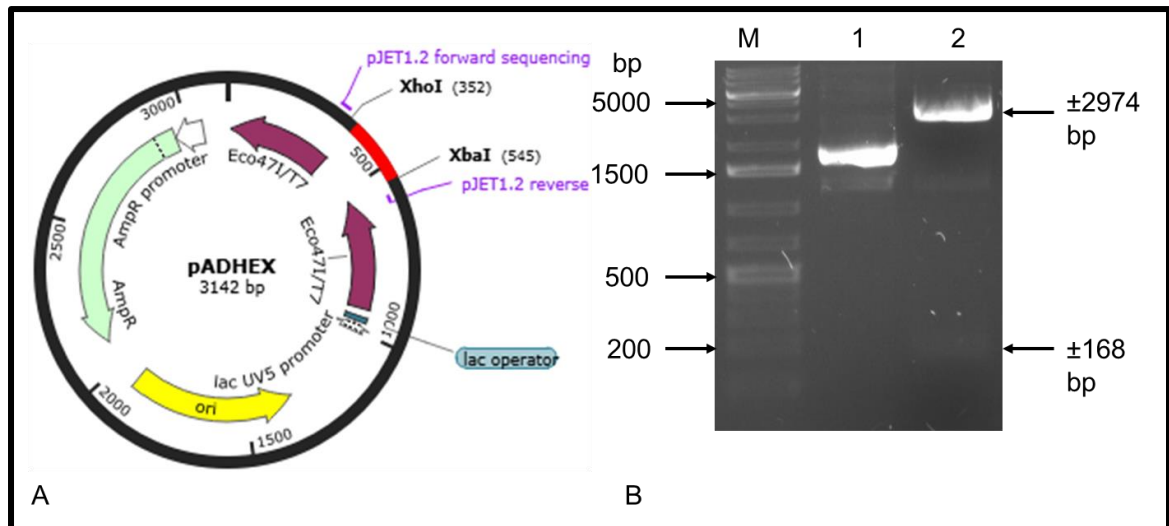


Figure 5.2: A) Plasmid map of the HAdV hexon positive control (Vos and Knox, 2017) consisting of an insert approximately 168 bp (shown in red) cloned into pJET 1.2/blunt vector. B) 2% agarose gel electrophoresis of uncut and cut adenovirus hexon positive control plasmid DNA. M: GeneRuler™ 1 kb Plus DNA Ladder (Thermo Scientific, USA), lane 2: uncut control plasmid DNA, lane 3: Cut control plasmid DNA.

5.3.2 Swab samples

5.3.2.1 Enteric HAdV hexon gene PCR and gel purification

A nested PCR reaction which was carried out using the Ampliqon Taq 2x Master Mix did not yield any visible PCR products in first round reactions. However, when 2 μ L from first round reactions was used as template in second round reactions, amplicons of approximately 168 bp were produced. As shown below in **Figure 5.3** the second round PCR assay was successful as PCR bands of 168 bp were obtained from ten out of twenty swab samples analysed as shown in **Table 5.3**.

Table 5.3: PCR results for swab samples.

Sample ID	RT-PCR results
S1	No visible PCR product obtained
S2	No visible PCR product obtained
S3	No visible PCR product obtained
S4	PCR product obtained
S5	No visible PCR product obtained
S6	PCR product obtained
S7	No visible PCR product obtained
S8	No visible PCR product obtained
S9	PCR product obtained
S10	PCR product obtained
S11	PCR product obtained
S12	PCR product obtained
S13	PCR product obtained
S14	No visible PCR product obtained
S15	PCR product obtained
S16	PCR product obtained
S17	PCR product obtained
S18	No visible PCR product obtained
S19	No visible PCR product obtained
S20	No visible PCR product obtained

Shown below in **Figure 5.3** is a representative 2% agarose gel electrophoresis of PCR products obtained from swabs 6 to 10. A PCR product of the correct size, approximately 168 bp, was obtained in lane 1 (positive control) and no product was obtained in lane 2 (NTC) as expected. A bright PCR product approximately 168 bp was obtained from swab 6 (lane 3). Another PCR product approximately 800 bp is visible in lane 3. This could possibly be the result of non-specific binding by the primers. No visible PCR products were obtained for swabs 7 and 8 (lanes 4 and 5 respectively). Faint products of approximately 168 bp were obtained for swabs 9 and 10 (lanes 6 and 7 respectively). Only results for swabs 6 to 10 are shown. The PCR products from swabs 4, 6, 10, 11, 12, 13, 15, 16 and 17 were gel purified by use of the GeneJET Gel Extraction Kit as

described before in section 5.2.5. The band from swab 9 (lane 6) was not gel purified as the DNA concentration was too low for gel purification as shown by a faint band on the gel.

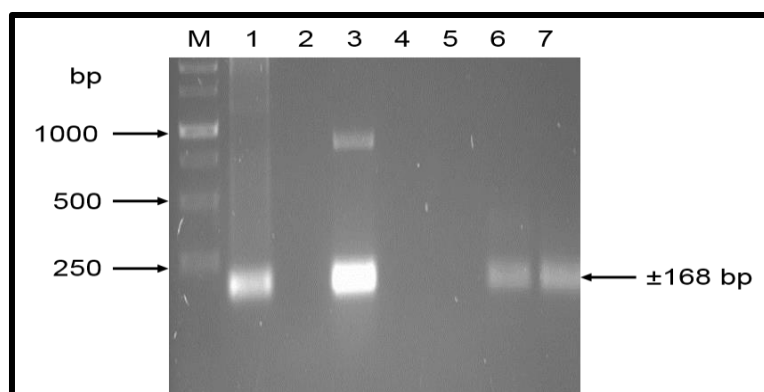


Figure 5.3: 2% agarose gel electrophoresis of second round PCR products of the enteric HAAdV hexon coding region from swab samples 6 to 10. M: PCR Bio Ladder II (PCR Biosystems Ltd, United Kingdom), lane 1: positive control PCR product, lane 2: NTC, lanes 3-7: Second round PCR products from swab samples 6 to 10.

5.3.2.2 Cloning of PCR products into pJET 1.2/blunt vector and restriction analysis of plasmid DNA

Gel purified second round PCR products (2 μ L) from swab samples (4, 6, 10, 11, 12, 13, 15, 16 and 17) were cloned into pJET 1.2/blunt vector as described before in order to get the full sequence data of the inserts. **Figure 5.4A** shows a representative 2% agarose gel electrophoresis of plasmid DNA extracted from cells (three colonies, A-C, from swab 10). The extraction was also successful for other swab samples although the results are not shown. Restriction analysis of 2 μ L of plasmid DNA with Xho I and Xba I confirmed the presence and sizes of inserts which were approximately 168 bp. **Figure 5.4B** shows a representative 2% agarose gel electrophoresis of the restriction digest products. Lane 1 contains the positive control PCR product of approximately 168 bp for estimation of sizes of inserts from samples. Lanes 2, 4 and 6 show uncut plasmids (S10A-C). Lanes 3, 5 and 7 show cut plasmids for which linearised vectors were approximately 2974 bp, the size of pJET 1.2/blunt vector, while inserts were approximately 168 bp as expected.

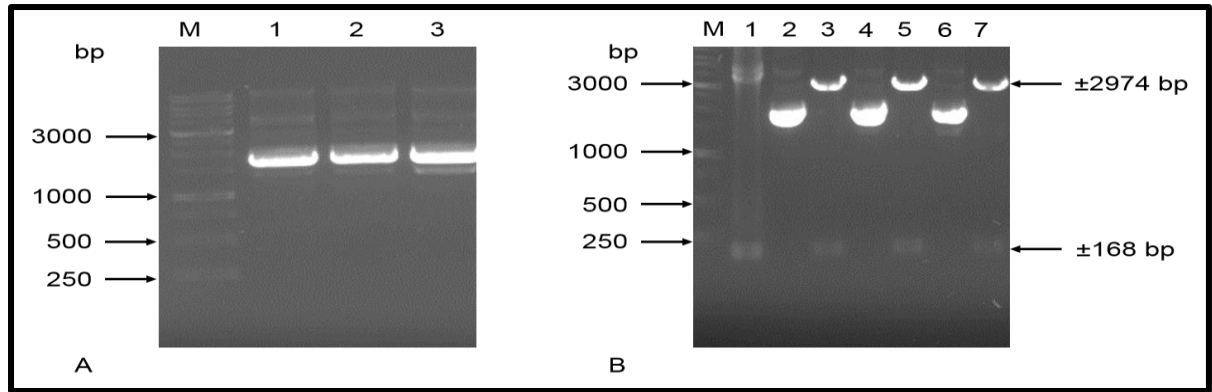


Figure 5.4: **A)** 2% agarose gel electrophoresis of plasmid DNA from swab sample 10 (S10). M: PCR Bio Ladder II, lane 1-3: Uncut plasmid DNA (S10A-C). **B)** 2% agarose gel electrophoresis of restriction digest products of the plasmids M: PCR Bio Ladder II, lane 1 positive control PCR product, lane 2: Plasmid S10A uncut, lane 3: S10A cut, lane 4: Plasmid S10B uncut, lane 5: S10B cut, lane 6: Plasmid S10C uncut, lane 7: S10C cut.

5.3.2.3 BLAST analysis of enteric HAdV hexon gene PCR products from swab samples

Plasmids from swab samples S4, S6, S10, S11, S12, S13, S15, S16 and S17 with inserts approximately 168 bp were Sanger sequenced at Inqaba Biotechnical Industries ([Pty] Ltd, Pretoria, South Africa). Resultant DNA sequences were highly identical to various HAdV strains in GenBank and the results are shown in **Table 5.4** below.

Table 5.4: BLAST analysis results of PCR products of the enteric HAdV hexon coding region from swab (S) samples.

Sample ID	Description	Accession number	E-value	% Identity
S4A	Human adenovirus C strain T215/Ft, USA/2002	KX384959.1	2e-74	99%
S4C	Human adenovirus C strain T215/Ft, USA/2002	KX384959.1	3e-78	99%
S6D	Human adenovirus D isolate hu4751_IC	KF976527.1	4e-71	96%
S10C	Human adenovirus D isolate hu4751_IC	KF976527.1	4e-71	96%
S11D	Human adenovirus F41 isolate DA75/Mor/09	HM641819.2	4e-76	98%
S12D	Human adenovirus F40 strain HoviX	KU162869.1	2e-73	99%
S13A	Human adenovirus D isolate	JN226756.1	8e-68	99%
S15C	Human adenovirus D isolate hu4882_IC	KF976531.1	1e-70	98%
S16A	Human adenovirus D strain human/DEU/HEIM	KF268327.1	7e-69	97%
S17A	Human adenovirus D isolate hu4882_IC	KF976531.1	9e-73	97%

As shown in **Table 5.4** above all sequences submitted to BLAST had percentage identities ranging between 96% and 99% to various HAdV isolates in GenBank. S6D, S10C, S13A, S15C, S16A and S17A had percentage identities ranging from 96% to 99% to HAdV subtype D isolates from Ivory Coast and Germany. S4A and S4C had 99% identity to an adenovirus subtype C (serotype 2) isolate from the USA. S11D was 98% identical to a subtype F (serotype 41) isolate from Morocco while S12 was 99% identical to a subtype F (serotype 40) isolate from Finland.

5.3.3 Mussel samples

Despite several PCR amplification attempts no visible PCR products were obtained from all mussel samples tested and the data is not included.

5.4 Multiple sequence analysis and phylogeny

Based on the sequence data of the hexon region, HAdV are classified into seven subtypes (A-G). The alignment of hexon sequences from swab samples as well as reference sequences was carried out on MEGA 6 using Clustal W algorithm. The results of the alignment are shown in **Figure 5.1S (Supplementary 11)**. A phylogenetic tree constructed from the alignment using the Maximum-Likelihood method is shown in **Figure 5.5**. This Maximum-Likelihood tree was constructed from 1,000 pseudo-replicates based on Tamura 3 substitution model (Tamura, 1992). The results show that strains isolated from swab samples in the current study belong to subtypes C, D and F.

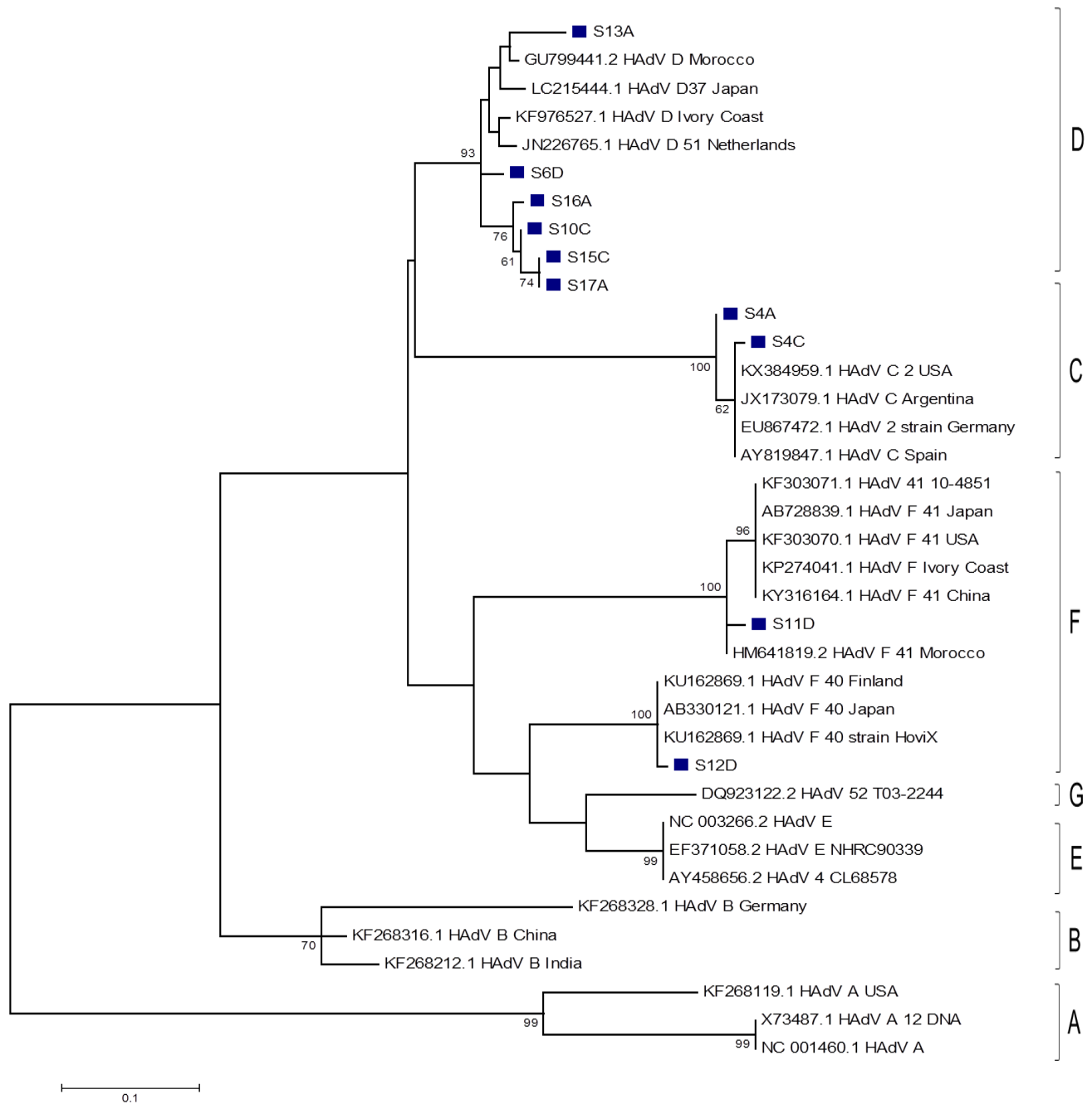


Figure 5.5: Molecular phylogenetic analysis of enteric HAAdV by Maximum Likelihood method based on Tamura 3 substitution model using a 168 bp sequence of the partial hexon gene. Isolates from the present study are indicated by dark blue boxes. The tree was evaluated by nonparametric bootstrap analysis with 1,000 pseudo-replicates. Only bootstrap values $\geq 60\%$ are shown. Scale bar represents the genetic distance (nucleotide substitutions per site).

5.5 Discussion

The main objective of this chapter was to perform a nested PCR for detection of enteric HAdV from swab and mussel samples by PCR amplification of a region of the adenovirus hexon gene. A total of twenty swab samples collected from separation grids at the Belmont Valley Sewage Treatment Plant (Makana Municipality) were analysed and ten samples gave positive results. In addition twenty mussel samples collected from the Swartkops River were analysed and no positive results were obtained.

A plasmid containing an insert, approximately 168 bp, of HAdV subtype D (Vos and Knox, 2017) was used as a positive control. The plasmid was initially digested with appropriate restriction enzymes to confirm its integrity. This positive control sample was used in all PCR reactions with swab and mussel samples as an indication of what size amplicon should be expected. The positive control is also useful in order to ensure that the PCR reaction was successful.

For extraction of DNA used in the PCR amplification of the hexon gene, the QIAamp® Viral RNA Mini Kit, (Qiagen, USA) was used as described. According to the manufacturer this kit can be used for DNA extraction as well. In the literature this kit was used in several studies including by Rohayem *et al.* (2004) and Jiang *et al.* (2005) to extract DNA from clinical sample for molecular detection of DNA viruses including enteric HAdV. In fact Rohayem *et al.* (2004) found the DNA recovery for this kit to be similar to a DNA extraction kit, the QIAamp DNA stool kit (Qiagen, Germany) while Jiang *et al.* (2005) found it to be more efficient than a DNA kit they used. The present study further confirms the suitability of this RNA extraction kit for DNA extraction as it was successfully used to purify DNA for PCR assays.

Published broad range degenerate primers designed by Avellon *et al.* (2001) were used in a nested set up to amplify the hexon gene of enteric HAdV. These primers, which are not subtype specific like most published adenovirus primers, were designed such that they bind to any adenovirus sequence from all the 7 subtypes (A-G). Avellon *et al.* (2001) found these primers to be more sensitive than those designed previously by Hierholzer *et al.* (1993), Kidd *et al.* (1996) and Puig *et al.* (1994). PCR products of the expected size (168 bp) were obtained from swab samples in the second round PCR reactions. This was similar to what is reported in the literature. For all studies in which this same PCR assay was used, there is no report of visible product for the first round reaction (Casas *et al.*,

2005; Magwalivha *et al.*, 2010; Van Heerden *et al.*, 2005; Van Heerden *et al.*, 2003). No PCR products were obtained from mussel samples after the second round PCR reactions. This could be as a result of PCR inhibitors in samples or low concentration of viral particles as seen on the electron micrographs for mussel samples (on chapter 2). Inclusion of an internal control system is necessary to investigate the effects of inhibitors in the PCR reactions.

The PCR products were gel purified and successfully cloned into pJET 1.2/blunt vector. For all swab samples, no DNA sequence data was lost. This further stresses the importance of cloning PCR amplicons compared to direct sequencing of the PCR products. All the swab samples sequenced had percentage identities of 96% to 99% to enteric HAdV subtypes C, D and F sequences in the GenBank. S4 was 99% identical to a subtype C isolate from the USA (accession number: KX384959.1) which was detected from respiratory fluids of army trainees by Hang *et al.* (2017) during an outbreak of a respiratory infection that affected army trainees.

S6 and S10 were all 96% identical to a subtype D isolate from Ivory Coast (accession number: KF976527.1) which was detected from stool specimen of a diarrhoeic patient by Pauly *et al.* (2014). S13 was 99% identical to a subtype D isolate (accession number: JN226756.1) from the USA which was detected from stool specimen of diarrhoeic patients by Singh *et al.* (2013). S15 and S17 were 98% and 97% identical to a subtype D isolate (accession number: KF976531.1) which was detected by Pauly *et al.* (2014) from stool specimen of diarrhoeic patients in Ivory Coast. S16 was 97% identical to a subtype D isolate (accession number: KF268327.1) which was detected from stool specimen of diarrhoeic patients in Germany by Heim *et al.* (2003).

Out of the ten swab samples that tested positive for HAdV in the present study, six (60%) of them were subtype D. This was consistent with results of Van Heerden *et al.* (2005) who detected subtype D in the majority of drinking water samples collected from various points in South Africa. Vos and Knox (2017) also detected only subtype D from raw sewage as well as mussel samples collected in the Eastern Cape Province of South Africa. This shows a possible high prevalence of subtype D in South Africa. In fact, Ghebremedhin *et al.* (2014) stated that subtype D is the most abundant of all HAdV subtypes worldwide. This can be attributed to its resistance to treatment and disinfection processes (Sauerbrei *et al.*, 2004). Although HAdV subtype D is associated with

gastroenteritis as reviewed by Arnold and MacMahon (2017) and Ghebremedhin (2014), it is also believed to cause respiratory as well as urinary infections. Its presence in sewage water may be as a result of respiratory fluids which were swallowed by some members of the community with respiratory infections.

S11 was 98% identical to a subtype F isolate from Morocco (accession number: HM641819.2) which was detected by Nourlil *et al.* (2012) from stool specimen of a diarrhoeic patient. S12 was 99% identical to a subtype F isolate (accession number: KU162869.1) which was detected in Finland by Pacesa *et al.* (2016). No additional information about this isolate is available as it is from an unpublished source. Subtype F, which is highly pathogenic, is one of the major agents of viral gastroenteritis worldwide (Ghebremedhin *et al.*, 2014). Its detection in sewage water samples from the present study is worrisome. It can be catastrophic if it finds its way into drinking water supplies. In fact Van Heerden *et al.* (2005) detected it in drinking water samples collected in South Africa. Based on this, it is possible that subtype F is one of the major candidates responsible for enteric infections in South Africa.

The results from the present study were expected as raw sewage is known to contain many species of the same virus. These results are consistent with other studies done in South Africa. It is a common phenomenon to isolate different strains or even different subtypes from environmental sources such as raw sewage. Osulale and Okoh, (2015) and Adefisoye *et al.* (2016) detected HAdV subtypes B, C and F from sewage effluents in the Eastern Cape Province. Chigor and Okoh (2012) detected HAdV subtypes B and F from the Buffalo River in the Eastern Cape Province while Van Heerden *et al.* (2005) detected subtypes C, D and F from selected rivers and drinking water supplies. On the other hand, Moore *et al.* (2000) detected subtype F and other unspecified subtypes from stool samples of diarrhoeic patients. All these results, including the ones from the present study show that enteric HAdV are circulating and they might be playing a role in high rates of enteric infections in South Africa. More clinical and epidemiological data is required for elucidation. In conclusion, a nested PCR developed in the present study led to the detection of enteric HAdV subtypes C, D and F from raw sewage in the Eastern Cape Province of South Africa. Chapter 6 will focus on general conclusions from the findings of this study as well as recommendations for future studies on the present subject.

Chapter 6: General conclusions and future work

6.1 Introduction

Viral gastroenteritis is a serious problem that leads to substantial morbidity and mortality worldwide including in South Africa. It is caused by many viral agents such as rotaviruses, human noroviruses and others such as Aichi virus 1, enteric human bocaviruses and enteric human adenoviruses. In South Africa most of the cases were as a result of rotavirus infection before the introduction of a monovalent rotavirus vaccine, Rotarix®, in 2009, which led to over 50% reduction in rotavirus related morbidity and mortality cases. However, about 40% of the diarrhoea cases remain of unknown aetiology up to this date. Various viral agents such as Aichi virus 1, enteric human bocaviruses and enteric human adenoviruses might be playing a role. However, the prevalence of these viruses and their effects on human health are poorly understood in South Africa and Africa in general.

The main objective of the present study was to develop and apply molecular techniques to detect and identify Aichi virus 1, enteric human bocaviruses and enteric human adenoviruses from swabs and mussel samples collected from the Eastern Cape Province of South Africa. This was done as a preliminary study to investigate their presence in environmental samples in the province. This objective was met as Aichi virus 1 and enteric human bocavirus were detected in raw sewage as well in the mussel samples by PCR assays developed in this study. Furthermore, this is the first study to report the presence of these particular viruses in the Eastern Cape Province and South Africa as a whole. Although research on enteric adenoviruses is being carried in South Africa, this study has highlighted the diversity of subtypes that can be found in a particular sample.

6.2 Distribution and prevalence of Aichi virus 1, human bocaviruses and human adenoviruses

Aichi virus 1 (AiV-1) was initially identified from stool specimen of a diarrhoeic patient during an oyster-related outbreak in Aichi Prefecture, Japan in 1989 (Yamashita *et al.*, 1991). Since then this virus has been detected from clinical and environmental samples including raw sewage, river water as well as shellfish throughout the world with prevalence rates of up to 100% in raw sewage, and it is now considered an important aetiological agent of gastroenteritis (Kitajima *et al.*, 2015). However, in Africa the

epidemiology of AiV-1 is poorly understood due to limited molecular data. It was detected from clinical samples of diarrhoeic patients in only four African countries namely; Mali, Burkina Faso, Tunisia and Nigeria (Ambert-Balay *et al.*, 2008; Japhet *et al.*, 2016; Ouédraogo *et al.*, 2016; Sdiri-Loulizi *et al.*, 2009). In addition to that, AiV-1 was detected from raw sewage samples in Tunisia during surveillance studies (Ibrahim *et al.*, 2017). In the present study different strains of AiV-1, all genotype B were detected from raw sewage and mussel samples in the Eastern Province of South Africa. However, our knowledge about the various strains and their contribution to enteric infections is limited. Although AiV-1 has been detected worldwide and considered as a serious enteric viral pathogen, this is the first study on this medically important virus in the country. Diarrhoeal disease is a cause of significant morbidity and mortality in South Africa so it is possible that AiV-1 is one of the viral agents involved in this regard. The present study has contributed to our knowledge about this virus and will further contribute to our understanding of the distribution of AiV-1 in South Africa.

Human bocaviruses (HBoVs) were initially detected from respiratory aspirates of patients with respiratory infections in Sweden (Allander *et al.*, 2005). In 2007, these viruses were directly linked to gastroenteritis by Lau *et al.* (2007). Since then four viral species have been identified, namely HBoV-1, HBoV-2, HBoV-3 and HBoV-4 (Guido *et al.*, 2016). HBoV-1 is the one associated with respiratory infections while HBoV-2, HBoV-3 and HBoV-4 are linked to enteric infections (Guido *et al.*, 2016; Ong *et al.*, 2016). Enteric HBoVs have been detected worldwide mainly from stool specimens of diarrhoeic patients with prevalence rates ranging from 1.3% to 63% (Guido *et al.*, 2016). There is limited information in relation to detection of enteric human bocaviruses in environmental sources such as raw sewage worldwide. In addition, as of December 2017, no published reports on presence of enteric HBoVs from shellfish were available. In Africa, enteric HBoVs were detected from stool specimens of diarrhoeic patients in Nigeria and Tunisia (Kapoor *et al.*, 2010), as well as from raw sewage in Nigeria during a surveillance study by Ng *et al.* (2012). In the present study enteric HBoV-3 and HBoV-2 were detected in raw sewage and mussel samples respectively in the Eastern Cape of South Africa. Although these viruses have been detected worldwide and linked to gastroenteritis, this is the first report in South Africa. The findings from this study have improved our knowledge about these viruses and will be crucial in understanding the epidemiology, distribution and their possible role in high rates of enteric infections in the country.

Furthermore, apart from findings of the present study, there are no published reports on presence of enteric HBoVs in shellfish including mussels. This is the first report in South Africa and the world over; hence it provides a platform for further epidemiological and prevalence studies.

Human adenoviruses (HAdVs) were first detected from human adenoids in 1953 (Ghebremedhin, 2014). Since then these viruses have been detected from various bodily specimens such as respiratory fluids, urine and stools, and are directly associated with various ailments including gastroenteritis (Arnold and MacMahon, 2017; Ghebremedhin, 2014). There are over seventy serotypes classified into seven subtypes, A-G. Members in subtypes C, D and F are directly linked to enteric infections and have been detected from clinical and environmental specimens worldwide including in many African countries such as Morocco, Tunisia and Ivory Coast (Ghebremedhin, 2014; Nourlil *et al.*, 2012; Sdiri-Loulizi *et al.*, 2010A). In South Africa, several published articles describe the presence of enteric HAdVs from stool specimens of diarrhoeic patients (Moore *et al.*, 2000) as well as raw sewage samples in the Eastern Cape Province from surveillance studies similar to the present study (Adefisoye *et al.*, 2016; Osulale and Okoh, 2015).

In the present study, HAdV subtypes C, D and F were detected in raw sewage from the Eastern Cape province of South Africa. These findings show that enteric HAdV are circulating in the populations and possibly play a role in high rates of enteric infections in South Africa. The findings from this study will add to our limited knowledge about the prevalence and distribution of the various subtypes, and will be instrumental in epidemiological studies in South Africa as a whole.

6.3 Sample preparation, virus purification and virus detection

Various techniques are used to prepare environmental samples such as raw sewage and shellfish for extraction of AiV-1, enteric HBoVs and enteric HAdVs because viral particles are generally present in low concentrations in such samples. In relation to raw sewage techniques such as adsorption-elution, use of beef extract and $AlCl_3$, use of cation-coated filter and ultracentrifugation are some of the common sample preparation methods (Alcala *et al.*, 2010; Ibrahim *et al.*, 2017; Kitajima *et al.*, 2011; Rodríguez-Díaz *et al.*, 2008; Sdiri-Loulizi *et al.*, 2010B). In relation to extraction of viral particles from shellfish, the most common method is the one developed by Pina *et al.* (1998) in which digestive diverticula from five to ten samples are pooled and viral particles extracted in

glycine buffer. This technique has been used in many studies including by Formiga-Cruz *et al.* (2003), Karamoko *et al.* (2005) and Muniain-Mujika *et al.* (2003). Other techniques such as extraction with chloroform–butanol and treatment with Cat-floc have also been used to extract viral particles from shellfish (Benabbes *et al.*, 2013).

In the present study, a swab sample preparation technique developed by Di Martino *et al.* (2013) and a mussel preparation technique developed by Pina *et al.* (1998) with some modifications were adopted. Using these techniques viral particles, with characteristic features of the viruses under study, were observed using TEM. Compared to other methods, the swab method was found to be more efficient and less time consuming as samples were pooled into small volumes which are easier to work with. However, the sample preparation techniques used in the present study had shortfalls, the main one being the clogging of filter membrane pores by debris leading to lower viral recoveries, as shown on TEM images, most probably because the viral particles were trapped in the debris. To improve on this, there should be more optimisation of the sample preparation method such as by application of two consecutive centrifugation steps at 9 000 x g for 3 minutes to get rid of much of the large debris that has the potential to clog membrane pores.

For extraction of nucleic acids from samples, there are various commercial kits available in the market depending on whether the virus of interest is an RNA or DNA virus. In relation to extraction of RNA viruses such as AiV-1 from raw sewage and shellfish, the most common kit used is the QIAamp viral RNA Mini kit (Irritani *et al.*, 2014; Sdiri-Loulizi *et al.*, 2010A; Kitajima *et al.*, 2011). For extraction of DNA viruses such as enteric HBoVs and enteric HAdVs the Qiagen DNeasy Blood and Tissue kit (BT) and the QIAamp DNA Stool Mini kit (ST) are commonly used extraction kits (Rohayem *et al.*, 2004; Sidhu *et al.*, 2013;). In the present study, nucleic acids (both RNA and DNA) were extracted using the QIAamp viral RNA Mini kit.

This kit has been used before for extraction of RNA and DNA from clinical and environmental samples including raw sewage water and shellfish (Kapoor *et al.*, 2010; Longtin *et al.*, 2008; Neske *et al.*, 2007; Pham *et al.*, 2011). This kit is useful when both RNA and DNA viruses are under study as it can be used for simultaneous extraction of RNA and DNA. However, only one study by Rohayem *et al.* (2004) compared the efficiency of the QIAamp viral RNA Mini kit versus that of QIAamp DNA stool kit for

recovery of DNA and concluded that the QIAamp viral RNA Mini kit was more efficient than the QIAamp DNA stool kit. In the present study nucleic acids were sufficiently recovered from both raw sewage and mussel samples as observed on 1% agarose gels and the protocol was successful in amplifying sequences from both RNA and DNA viruses. Precautionary measures were put in place to prevent contamination and deterioration of the nucleic acids extracted in the present study. These measures included decontamination of working benches and pipettes by RNase-away (Thermo Scientific, USA), storing positive control and sample nucleic acids in separate storage boxes, use of filter tips as well as double autoclaving of pipette tips and glassware.

Another objective of the study was to develop nested RT-PCR assays targeting the 5' untranslated region, the partial 3CD and VP1 coding regions for detection and identification of AiV-1 from the prepared swabs and mussel samples. Initial attempts to PCR amplify the 5' UTR coding region using primers developed by Drexler *et al.* (2011) in a nested RT-PCR assay were not successful most probably due to the high GC-content nature as well as high degree of secondary structure in this region. Therefore, two nested RT-PCR assays were developed using the same primers. In the first assay 10% DMSO was added to the PCR reaction. This assay was successful as one of the swab samples gave a positive result. However, this assay worked only once making it unreliable. Due to this setback, another RT-PCR that targets the 5' UTR of AiV-1 was developed. In this assay, 10% DMSO was used in combination with touch-down PCR. For this reaction, the annealing temperature was set higher than the optimal melting temperature of the primers with a 1 °C decrease per cycle as in Drexler *et al.* (2011). This assay also was also successful as another swab sample gave positive result. However, the later RT-PCR assay was only applied once due to limited time and hence its efficiency was not fully established and needs to be optimised further in future studies.

In relation to the PCR amplification of the partial 3CD coding region, inner primers designed by Yamashita *et al.* (2000) were used in an RT-PCR assay. This was successful as a couple of swab and mussel samples gave positive results. In addition to that, a combination of primers developed by Pham *et al.* (2008), Lodder *et al.* (2013) as well as primers designed in the present study for the partial VP1 coding region produced positive results from some swab samples. Based on 3CD and VP1 sequence data, isolates in the present study were shown to be genotype B. All these positive results from the three assays show that the objective was achieved. However, there was a challenge of false

negative results as some samples were positive for the 3CD assay and on the other hand the same samples were negative for either the 5' UTR assay or the VP1 assay. To resolve the problem of false negative results, samples for each assay could be spiked with an internal process control such as PP7 bacteriophage as in Burutarán *et al.* (2016) to determine if inhibitors had an impact on the RT-PCR assay or not. In this regard, Burutarán *et al.* (2016) spiked raw sewage samples with a known concentration of PP7 bacteriophage and every sample that gave positive results for this bacteriophage was considered free of PCR inhibitors and processed. In most studies in the literature, detection of AiV-1 is based on a nested two-step RT-PCR assay that targets the partial 3CD coding region developed by Yamashita *et al.* (2000). Several studies used a nested two step RT-PCR assay that targets the hypervariable VP1 coding region first described by Pham *et al.* (2008). Very few studies applied the 5' UTR assay first described by Drexler *et al.* (2011) most probably because of the difficulty of the 5' UTR end to PCR amplification due to high G-C content and high degree of secondary structure as experienced in the present study.

The next objective was to develop a nested PCR assay that targets the VP1/VP2 region to detect and identify enteric HBoVs from the prepared swabs and mussel samples. By using primers described in La Rosa *et al.* (2016), enteric HBoV-2 and HBoV-3 were detected from raw sewage and mussel samples respectively, hence the objective was achieved. To our knowledge, this is the first report on detection of enteric HBoVs from environmental and shellfish samples in South Africa and the first report on detection of enteric HBoVs from mussel samples worldwide. In the literature, the VP1/VP2 assay is the most common one compared to both the NS-1 and the NP-1 assays. In addition to molecular detection of HBoVs from samples, the VP1/VP2 assay is also important for typing purposes, and that explains why it is so common (Guido *et al.*, 2016; Lau *et al.*, 2007).

The last objective was to develop a nested PCR assay to detect and identify enteric HAdVs from the prepared swabs and mussel samples. This objective was also achieved as HAdVs subtypes C, D and F, which are associated with gastroenteritis, were detected from swab samples by using primers described in Avellon *et al.* (2001). These findings are consistent with similar studies carried out in the Eastern Cape province of South Africa even though they used quantitative PCR, using different primers from the ones used in the present study (Adefisoye *et al.*, 2016; Osuolale and Okoh, 2015). In these studies, quantification of HAdVs in the samples was of major interest to the authors while

the present study was interested in determination of presence or absence of the viruses. The present study was also consistent with findings of Vos and Knox (2017) in which HAdV subtype D was identified from swab and mussel samples. However, in the present study, no positive results were obtained from mussel samples. It is possible that PCR inhibitors played a role in this regard or the PCR conditions were not optimal. The use of real time PCR, which is more sensitive than conventional PCR used in the present study, might alleviate the problem.

6.4 Implications for effluent treatment and river water quality

River pollution, especially from inadequately treated effluents is a serious problem in South Africa. This discharge of improperly treated sewage water is the source of viral enteric pathogens in the rivers and ultimately into drinking water sources (Okoh *et al.*, 2010). The Swartkops River is no exception to this. This river system flows through a heavily industrialised area and hence suffers human induced impacts such as industrial and domestic effluents (Odume *et al.*, 2012). The results from the present study show that the efficiency of wastewater treatment in the country is low. As stated in Okoh *et al.* (2010), current wastewater treatment processes in South Africa are not 100% efficient so presence of viral agents of gastroenteritis such as AiV-1, enteric HBoV and enteric HAdV calls for concern as these pathogens can have catastrophic effects should they find their way into drinking water sources. These viral pathogens are known to be resistant to chemicals used in routine treatment of water and as a result of this they can cause diarrhoea outbreaks to communities as only a few viral particles, as low as nine particles can cause diarrhoea (Desselberger *et al.*, 2017). This calls for municipalities to improve the efficiency of wastewater treatment processes such that it is thoroughly disinfected before being released to the environment.

The fact that AiV-1 and enteric HAdVs were detected from mussel samples collected from the Swartkops River is evident enough that wastewater in the Eastern Cape is not properly treated. This is consistent with findings of Odume *et al.* (2012) who stated that the Swartkops River is heavily contaminated with effluents from nearby wastewater treatment plants. This has negative health implications to communities in coastal areas that use shellfish such as mussels as sources of proteins. Consumption of virus contaminated shellfish is a worldwide health hazard that leads to enteric infections to communities especially the young, the old and the immuno-compromised. Although there

are no studies done on this subject in South Africa, it is possible that some of the diarrhoea cases in the country are as a result of consumption shellfish contaminated with enteric viruses. However, more research is needed to confirm this.

6.5 Conclusion and future perspectives

In conclusion, this preliminary study has contributed to an understanding of the presence of AiV-1, enteric HBoVs and enteric HAdVs in raw sewage as well as shellfish in the Eastern Cape Province of South Africa. Furthermore, the findings provide a platform for further investigations into prevalence and epidemiological studies.

For future work, the first objective will be to expand the scope of the project to include swab and mussel samples collected from different regions of the Eastern Cape Province as well as samples from all other provinces of South Africa so as to generate more data for epidemiological studies in South Africa as a whole. The other objective for the future will be the use of the techniques developed in the present study to investigate the presence of the enteric viruses in clinical samples to investigate their direct roles in enteric infections in South Africa. This can be expanded to include clinical samples such as stools from all South African provinces as well. In the present study clinical samples were not analysed due to unavailability of Biosafety facilities for handling of such samples.

In addition future work will include the use of the multi-prong strategy developed in this study for PCR amplification of highly stable region. Reactions will be repeated several times with freshly prepared RNA to increase chances of getting more positive results. Due to limited time, this was only done once for amplification of the 5' UTR region of Aiv-1. Furthermore, sulfolane will be used instead of DMSO as it is believed to be more efficient in high GC template amplification than DMSO (Chakrabarti and Schutt, 2000). In addition, a combination of 1M betaine and 5% DMSO will be used in the RT-PCR assays as it was shown to produce better results in Bhagya *et al.* (2013) for amplification of a gene with a much higher GC-content than the 5' UTR region of Aiv-1.

Furthermore, for the future, real time PCR will be used in cases where no positive results were obtained using conventional PCR as it is believed to be more sensitive and can tolerate the effects of PCR inhibitors in environmental samples better than conventional PCR (Adefisoye *et al.*, 2016).

Although other studies on AiV-1, HBoV and HAdV use qRT-PCR and qPCR assays, the present study describes molecular detection and not quantification of these viruses. Once stool samples are sourced it will be necessary to study prevalence in future studies, and hence quantification of the viruses will be required. In addition to that, future studies will include other new and emerging viruses associated with gastroenteritis such as klassivirus, sappovirus and coronavirus which have not been described in South Africa. This may lead to more understanding about why 40% of diarrhoeal cases are of unknown aetiology.

References

- Adefisoye, M.A., Nwodo, U.U., Green, E. and Okoh, A.I., 2016. Quantitative PCR detection and characterisation of human adenovirus, rotavirus and hepatitis A virus in discharged effluents of two wastewater treatment facilities in the Eastern Cape, South Africa. *Food and Environmental Virology*, **8** (4), pp. 262–274.
- Aikins, M., Armah, G., Akazili, J. and Hodgson, A., 2010. Hospital health care cost of diarrhoeal disease in northern Ghana. *Journal of Infectious Diseases*, **202** (1), pp. S126-S130.
- Alam, M.M., Khurshid, A., Shaukat, S., Sharif, S., Suleman, R.M., Angez, M., Nisar, N., Aamir, U.B., Naeem, M. and Zaidi, S.S.Z., 2015. Human bocavirus in Pakistani children with gastroenteritis. *Journal of Medical Virology*, **87** (4), pp. 656-663.
- Alcalá, A., Vizzi, E., Rodríguez-Díaz, J., Zambrano, J.L., Betancourt, W. and Liprandi, F., 2010. Molecular detection and characterisation of Aichi viruses in sewage-polluted waters of Venezuela. *Applied and Environmental Microbiology*, **76** (12), pp. 4113-4115.
- Allander, T., Tammi, M.T., Eriksson, M., Bjerkner, A., Tiveljung-Lindell, A. and Andersson, B., 2005. Cloning of a human parvovirus by molecular screening of respiratory tract samples. *Proceedings of the National Academy of Sciences of the United States of America*, **102** (36), pp. 12891-12896.
- Ambert-Balay, K., Lorrot, M., Bon, F., Giraudon, H., Kaplon, J., Wolfer, M., Lebon, P., Gendrel, D. and Pothier, P., 2008. Prevalence and genetic diversity of Aichi virus strains in stool samples from community and hospitalised patients. *Journal of Clinical Microbiology*, **46** (4), pp. 1252-1258.
- Amdiouni, H., Faouzi, A., Fariat, N., Hassar, M., Soukri, A. and Nourlil, J., 2012. Detection and molecular identification of human adenoviruses and enteroviruses in wastewater from Morocco. *Letters in Applied Microbiology*, **54** (4), pp. 359–366.
- Aminu, M., Ahmad, A.A., Umoh, J.U., de Beer, M.C., Esona, M.D. and Steele, A.D., 2007. Adenovirus infection in children with diarrhoea disease in northwestern Nigeria. *Annals of African Medicine*, **6** (4), pp. 168-173.

- Arnold, A. and MacMahon, E., 2017. Adenovirus infections. *Medicine (United Kingdom)*, **45** (12), pp. 777-780.
- Arthur, J.L., Higgins, G.D., Davidson, G.P., Givney, R.C. and Ratcliff, R.M., 2009. A novel bocavirus associated with acute gastroenteritis in Australian children. *PLoS Pathogens*, **5** (4), pp. 1-9.
- Avellón, A., Pérez, P., Aguilar, J.C., Lejarazu, R.O.D. and Echevarría, J.E., 2001. Rapid and sensitive diagnosis of human adenovirus infections by a generic polymerase chain reaction. *Journal of Virological Methods*, **92** (2), pp. 113-120.
- Bal, Z.S. and Kurugöl, Z., 2016. New generation rotavirus vaccines. *Cocuk Enfeksiyon Dergisi*, **10** (1), pp. 22-27.
- Bambic, G.D., Kildare-Hann, B.J., Rajal, V.B., Sturm, B.S.M., Minton, C.B., Schriewer, A. and Wuertz, S., 2015. Spatial and hydrologic variation of bacteroidales, adenovirus and enterovirus in a semi-arid, wastewater effluent-impacted watershed. *Water Research Journal*, **7** (5), pp. 83-94.
- Banerjee, A., De, P., Manna, B. and Chawla-Sarkar, M., 2017. Molecular characterisation of enteric adenovirus genotypes 40 and 41 identified in children with acute gastroenteritis in Kolkata, India during 2013–2014. *Journal of Medical Virology*, **89** (4), pp. 606-614.
- Barrett, J. and Brown, M., 2016. Travellers' diarrhoea. *BMJ (Online)*, **353**.
- Bellou, M., Kokkinos, P. and Vantarakis, A., 2013. Shellfish-borne viral outbreaks: A Systematic Review. *Food and Environmental Virology*, **5** (1), pp. 13-23.
- Benabbes, L., Ollivier, J., Schaeffer, J., Parnaudeau, S., Rhaissi, H., Nourlil, J. and Le Guyader, F.S., 2013. Norovirus and other human enteric viruses in Moroccan shellfish. *Food and Environmental Virology*, **5** (1), pp. 35-40.
- Bibby, K. and Peccia, J., 2013. Prevalence of respiratory adenovirus species B and C in sewage sludge. *Environmental Sciences: Processes and Impacts*, **15** (2), pp.336-338.
- Blinkova, O., Rosario, K., Li, L., Kapoor, A., Slikas, S., Bernardin, F., Breitbart, M. and Delwart, E., 2008. Frequent detection of highly diverse variants of cardiovirus, cosavirus, bocavirus and circovirus in sewage samples collected in the United States. *Journal of Clinical Microbiology*, **47** (11), pp. 3507-3513.

- Bon, F., Lorrot, M. and Pothier, P., 2005. Unpublished.
- Bosch, A., 1998. Human enteric viruses in the water environment: A minireview. *International Microbiology*, **1** (3), pp. 191-196.
- Brown, M., 1990. Laboratory identification of adenoviruses associated with gastroenteritis in Canada from 1983 to 1986. *Journal of Clinical Microbiology*, **28** (7), pp. 1525-1529.
- Bruggink, L.D., Moselen, J.M. and Marshall, J.A., 2017. The molecular epidemiology of norovirus outbreaks in Victoria, 2014 to 2015. *Communicable Diseases Intelligence Quarterly Report*, **41** (1), pp. E21-E32.
- Bull, R.A., Tu, E.T.V., McIver, C.J., Rawlinson, W.D. and White, P.A., 2006. Emergence of a new norovirus genotype II.4 variant associated with global outbreaks of gastroenteritis. *Journal of Clinical Microbiology*, **44** (2), pp. 327-333.
- Burutarán, L., Lizasoain, A., García, M., Tort, L.F.L., Colina, R. and Victoria, M., 2016. Detection and molecular characterisation of Aichi virus 1 in wastewater samples from Uruguay. *Food and Environmental Virology*, **8** (1), pp. 13-17.
- Buzby, J.C. and Frenzen, P.D., 1999. Food safety and product liability. *Food Policy*, **24** (6), pp. 637-651.
- Buzby, J.C. and Roberts, T., 1997. Economic costs and trade impacts of microbial foodborne illness. *World Health Statistics Quarterly*, **50** (1-2), pp. 57-66.
- Campos, G.S., Silva Sampaio, M.L., Menezes, A.D.L., Tigre, D.M., Moura Costa, L.F., Chinalia, F.A. and Sardi, S.I., 2016. Human bocavirus in acute gastroenteritis in children in Brazil. *Journal of Medical Virology*, **88** (1), pp. 166-170.
- Cantalupo, P.G., Calgua, B., Zhao, G., Hundesa, A., Wier, A.D., Katz, J.P., Grabe, M., Hendrix, R.W., Girones, R., Wang, D. and Pipasa, J.M., 2011. Raw sewage harbors diverse viral populations. *Medical Biology Journals*, **2** (5), pp. 180-183.
- Casas, I., Avelon, A., Mosquera, M., Jabado, O., Echevarria, E., Campos, R.H., Rewers, M., Perez-Brena, P., Lipkin, W.I. and Palacios, G., 2005. Molecular identification of adenoviruses in clinical samples by analyzing a partial hexon genomic region. *Journal of Clinical Microbiology*, **43** (12), pp. 6176–6182.

- Cashman, O. and O'Shea, H., 2012. Detection of human bocaviruses 1, 2 and 3 in Irish children presenting with gastroenteritis. *Archives of Virology*, **157** (9), pp. 1767-1773.
- Chang, J., Chen, Y., Chen, B., Chao, D. and Chang, T., 2013. Complete genome sequence of the first Aichi virus isolated in Taiwan. *Genome Announcements*, **1** (1), pp. 107-112.
- Chen, Y., Chen, B., Lin, Y., Chang, J., Huang, T., Chen, J. and Chang, T., 2013. Detection of Aichi virus with antibody targeting of conserved viral protein 1 epitope. *Applied Microbiology and Biotechnology*, **97** (19), pp. 8529-8536.
- Chhabra, P. and Chitambar, S.D., 2008. Norovirus genotype IIb associated acute gastroenteritis in India. *Journal of Clinical Virology*, **42** (4), pp. 429-432.
- Chieochansin, T., Simmonds, P. and Poovorawan, Y., 2010. Determination and analysis of complete coding sequence regions of new discovered human bocavirus types 2 and 3. *Archives of Virology*, **155** (12), pp. 2023-2028.
- Chigor, V.N. and Okoh, I.A., 2012. Quantitative detection and characterisation of human adenoviruses in the Buffalo River in the Eastern Cape Province of South Africa. *Food Environmental Virology*, **4**, pp. 198–208.
- Cho, H.G., Lee, S.G., Lee, M.Y., Hur, E.S., Lee, J.S., Park, P.H., Park, Y.B., Yoon, M.H. and Paik, S.Y., 2016. An outbreak of norovirus infection associated with fermented oyster consumption in South Korea, 2013. *Epidemiology and Infection*, **144** (13), pp. 2759-2764.
- Chola, L., Michalow, J., Tugendhaft, A. and Hofman, K., 2015. Reducing diarrhoea deaths in South Africa: costs and effects of scaling up essential interventions to prevent and treat diarrhoea in under-five children. *BMC Public Health*, **15**, pp. 394.
- Chourouk, I., Abdennaceur, H. and Pierre, P., 2014. First molecular detection of a new Aichi virus genotype B after two wastewater treatment procedures in the Tunis region of Tunisia, unpublished.
- Chuchaona, W., Khamrin, P., Yodmeeklin, A., Kumthip, K., Saikruang, W., Thongprachum, A., Okitsu, S., Ushijima, H. and Maneekarn, N., 2017. Detection and characterisation of Aichi virus 1 in pediatric patients with diarrhoea in Thailand. *Journal of Medical Virology*, **89** (2), pp. 234-238.

Corcoran, E., Nellesmann, C., Baker, E., Bos, R., Osborn, D. and Savelli, H. (eds). (2010). The central role of wastewater management in sustainable development- A rapid response assessment. UNEP (United Nations Environment Programme), UN-HABITAT, Nairobi, Kenya.

Crawford-Miksza, L. and Schnurr, D.P., 1996. Analysis of 15 adenovirus hexon proteins reveals the location and structure of seven hypervariable regions containing serotype-specific residues. *Journal of Virology*, **70** (3), pp. 1836-1844.

Da Silva, A.K., Le Saux, J., Parnaudeau, S., Pommepey, M., Elimelech, M. and Le Guyader, F.S., 2007. Evaluation of removal of noroviruses during wastewater treatment, using real-time reverse transcription-PCR: Different behaviors of genogroups I and II. *Applied and Environmental Microbiology*, **73** (24), pp. 7891-7897.

Dashti, A.S., Ghahremani, P., Hashempoor, T. and Karimi, A., 2016. Molecular epidemiology of enteric adenovirus gastroenteritis in under-five-year-old children in Iran. *Gastroenterology Research and Practice*, **2016** (1), pp. 1-5.

Debbink, K., Lindesmith, L.C., Donaldson, E.F., Costantini, V., Beltramello, M., Corti, D., Swanstrom, J., Lanzavecchia, A., Vinjé, J. and Baric, R.S., 2013. Emergence of new pandemic gII.4 Sydney norovirus strain correlates with escape from herd immunity. *Journal of Infectious Diseases*, **208** (11), pp. 1877-1887.

Dennehy, P.H., 2008. Rotavirus vaccines: An overview. *Clinical Microbiology Reviews*, **21** (1), pp. 198-208.

Dennehy, P.H., 2007. Rotavirus vaccines- An update. *Vaccine*, **25** (16), pp. 3137-3141.

De Paula, S.O., de Melo Lima, C., Torres, M.P., Pereira, M.R.G. and Lopes da Fonseca, B.A., 2004. One-Step RT-PCR protocols improve the rate of dengue diagnosis compared to Two-Step RT-PCR approaches. *Journal of Clinical Virology*, **30** (4), pp. 297–301.

Desselberger, U., 2017. Viral gastroenteritis. *Medicine (United Kingdom)*, **45** (11), pp. 690-694.

Desselberger, U. and Gray, J., 2013. Viral gastroenteritis. *Medicine (United Kingdom)*, **41** (12), pp. 700-704.

Dey, S.K., Nahar, S., Akter, T., Sultana, H., Akter, A., Sarkar, O.S., Ahmed, M.F., Talukder, A.A. and Ahmed, F., 2014. A retrospective analysis of viral gastroenteritis in Asia. *Journal of Pediatric Infectious Diseases*, **9** (2), pp. 53-65.

Dey, S.K., Shimizu, H., Phan, T.G., Hayakawa, Y., Islam, A., Salim, A.F.M., Khan, A.R., Mizuguchi, M., Okitsu, S. and Ushijima, H., 2009. Molecular epidemiology of adenovirus infection among infants and children with acute gastroenteritis in Dhaka City, Bangladesh. *Infection, Genetics and Evolution*, **9** (4), pp. 518-522.

Di Martino, B., Di Profio, F., Ceci, C., Di Felice, E. and Marsilio, F., 2013. Molecular detection of Aichi virus in raw sewage in Italy. *Archives of Virology*, **158** (9), pp. 2001-2005.

Drexler, J.F., Baumgarte, S., Luna, L.K.S., Eschbach-Bludau, M., Lukashev, A.N. and Drosten, C., 2011. Aichi virus shedding in high concentrations in patients with acute diarrhoea. *Emerging Infectious Diseases*, **17** (8), pp. 1544-1547.

Ebner, K., Pinsker, W. and Lion, T., 2005. Comparative sequence analysis of the hexon gene in the entire spectrum of human adenovirus serotypes: Phylogenetic, taxonomic, and clinical implications. *Journal of Virology*, **79** (20), pp. 12635-12642.

Ehlers, M.M., Grabow, W.O.K. and Pavlov, D.N., 2005. Detection of enteroviruses in untreated and treated drinking water supplies in South Africa. *Water Research*, **39** (11), pp. 2253-2258.

Eifan, S.A., 2013. Enteric viruses and aquatic environment. *Internet Journal of Microbiology*, **12** (1).

Elnifro, E.M., Ashshi, A.M., Cooper, R.J. and Klapper, P.E., 2000. Multiplex PCR: Optimisation and application in diagnostic virology. *Clinical Microbiology Reviews*, **13** (4), pp. 559-570.

Ettayebi, K., Crawford, S.E., Murakami, K., Broughman, J.R., Karandikar, U., Tenge, V.R., Neill, F.H., Blutt, S.E., Zeng, X., Qu, L., Kou, B., Opekun, A.R., Burrin, D., Graham, D.Y., Ramani, S., Atmar, R.L. and Estes, M.K., 2016. Replication of human noroviruses in stem cell-derived human enteroids. *Science*, **353** (6306), pp. 1387-1393.

- Fernández-Bañares, F., Accarino, A., Balboa, A., Domènech, E., Esteve, M., Garcia-Planella, E., Guardiola, J., Molero, X., Rodríguez-Luna, A., Ruiz-Cerulla, A., Santos, J. and Vaquero, E., 2016. Chronic diarrhoea: Definition, classification and diagnosis. *Gastroenterologia Hepatologia*, **39** (8), pp. 535-559.
- Fletcher, S., Van Hal, S., Andresen, D., McLaws, M., Stark, D., Harkness, J. and Ellis, J., 2013. Gastrointestinal pathogen distribution in symptomatic children in Sydney, Australia. *Journal of Epidemiology and Global Health*, **3** (1), pp. 11-21.
- Flomenberg, P., 2014. Adenovirus infections. *Medicine (United Kingdom)*, **42** (1), pp. 42-44.
- Fong, T. and Lipp, E.K., 2005. Enteric viruses of humans and animals in aquatic environments: Health risks, detection, and potential water quality assessment tools. *Microbiology and Molecular Biology Reviews*, **69** (2), pp. 357-371.
- Formiga-Cruz, M., Hundesa, A., Clemente-Casares, P., Albiñana-Gimenez, N., Allard, A. and Girones, R., 2005. Nested multiplex PCR assay for detection of human enteric viruses in shellfish and sewage. *Journal of Virological Methods*, **125** (2), pp. 111-118.
- Frey, U.H., Bachmann, H.S., Peters, J. and Siffert, W., 2008. PCR-amplification of GC-rich regions: 'Slowdown PCR'. *Nature Protocols*, **3** (8), pp. 1312-1317.
- Fu, J., Ai, J., Jin, M., Jiang, C., Zhang, J., Shi, C., Lin, Q., Yuan, Z., Qi, X., Bao, C., Tang, F. and Zhu, Y., 2015. Emergence of a new GII.17 norovirus variant in patients with acute gastroenteritis in Jiangsu, China, September 2014 to March 2015. *Eurosurveillance*, **20** (24), pp. 1-7.
- Fukuda, S., Takao, S., Kuwayama, M., Shimazu, Y. and Miyazaki, K., 2006. Rapid detection of norovirus from faecal specimens by real-time reverse transcription-loop-mediated isothermal amplification assay. *Journal of Clinical Microbiology*, **44** (4), pp. 1376-1381.
- Fusco, G., Di Bartolo, I., Cioffi, B., Ianiro, G., Palermo, P., Monini, M. and Amoroso, M.G., 2017. Prevalence of foodborne viruses in mussels in Southern Italy. *Food Environmental Virology*, **9** (2), pp. 187-194.

Garibyan, L. and Avashia, N., 2013. Polymerase Chain Reaction. *Journal of Investigative Dermatology*, **133** (3), pp. 1-4.

Gentsch, J.R., Laird, A.R., Bielfelt, B., Griffin, D.D., Bányai, K., Ramachandran, M., Jain, V., Cunliffe, N.A., Nakagomi, O., Kirkwood, C.D., Fischer, T.K., Parashar, U.D., Bresee, J.S., Jiang, B. and Glass, R.I., 2005. Serotype diversity and reassortment between human and animal rotavirus strains: Implications for rotavirus vaccine programs. *Journal of Infectious Diseases*, **192** (1), pp. S146-S159.

Gerba, C.P., Wallis, C. and Melnick, J.L., 1975. Viruses in water: the problem, some solutions. *Environmental Science and Technology*, **9** (13), pp. 1122-1125.

Ghebremedhin, B, 2014. Human adenovirus: viral pathogen with increasing importance. *European Journal of Microbiology and Immunology*, **4** (1), pp. 26–33.

Goyer, M., Aho, L., Bour, J., Ambert-Balay, K. and Pothier, P., 2008. Seroprevalence distribution of Aichi virus among a French population in 2006-2007. *Archives of Virology*, **153** (6), pp. 1171-1174.

Green, D.M., Scott, S.S., Mowat, D.A., Shearer, E.J. and Thomson, J.M., 1968. Water-borne outbreak of viral gastroenteritis and Sonne dysentery. *Journal of Hygiene*, **66** (3), pp. 383-392.

Grøndahl-Rosado, R.C., Yarovitsyna, E., Trettenes, E., Myrmel, M. and Robertson, L.J., 2014. A one year study on the concentrations of norovirus and enteric adenoviruses in wastewater and a surface drinking water source in Norway. *Food and Environmental Virology*, **6** (4), pp. 232-245.

Guido, M., Tumolo, M.R., Verri, T., Romano, A., Serio, F., De Giorgi, M., De Donno, A., Bagordo, F. and Zizza, A., 2016. Human bocavirus: Current knowledge and future challenges. *World Journal of Gastroenterology*, **22** (39), pp. 8684-8697.

Gutiérrez, M.F., Alvarado, M.V., Martínez, E. and Ajami, N.J., 2007. Presence of viral proteins in drinkable water-sufficient condition to consider water a vector of viral transmission? *Water Research*, **41** (2), pp. 373-378.

- Hage, E., Liebert, U.G., Bergs, S., Ganzenmueller, T. and Heim, A., 2015. Human mastadenovirus type 70: A novel, multiple recombinant species D mastadenovirus isolated from diarrhoeal faeces of a haematopoietic stem cell transplantation recipient. *Journal of General Virology*, **96** (9), pp. 2734-2742.
- Han, T., Kim, C., Park, S., Kim, E., Chung, J. and Hwang, E., 2009. Detection of human bocavirus-2 in children with acute gastroenteritis in South Korea. *Archives of Virology*, **154** (12), pp. 1923-1927.
- Han, T., Park, S.H., Hwang, E., Reuter, G. and Chung, J., 2014. Detection of Aichi virus in South Korea. *Archives of Virology*, **159**, pp. 1835-1839.
- Hang, J., Vento, T.J., Norby, E.A., Jarman, R.G, Keiser, P.B., and Kuschner, R.A., 2017. Adenovirus type 4 respiratory infections with a concurrent outbreak of coxsackievirus A21 among United States Army basic trainees, a retrospective viral etiology study using next generation sequencing. *Journal of Medical Virology*, **89** (8), pp. 1387–94.
- Hansman, G.S., Oka, T., Li, T., Nishio, O., Noda, M. and Takeda, N., 2008. Detection of human enteric viruses in Japanese clams. *Journal of Food Protection*, **71** (8), pp. 1689-1695.
- Haramoto, E. and Kitajima, M., 2017. Quantification and genotyping of Aichi virus 1 in water samples in the Kathmandu Valley, Nepal. *Food and Environmental Virology*, **9** (3), pp. 350-353.
- Hata, A., Katayama, H., Kojima, K., Sano, S., Kasuga, I., Kitajima, M. and Furumai, H., 2014. Effects of rainfall events on the occurrence and detection efficiency of viruses in river water impacted by combined sewer overflows. *Science of the Total Environment*, **468-469**, pp. 757-763.
- Hayat, M.A., 2000. Negative staining in electron microscopy. Biological applications. 4th ed. Cambridge: Cambridge University Press, 367–99.
- Hellen, C.U.T. and Sarnow, P., 2001. Internal ribosome entry sites in eukaryotic mRNA molecules. *Genes and Development*, **15** (13), pp. 1593-1612.

Heim, A., Ebnet, C., Harste, G. and Pring-Åkerblom, P., 2003. Rapid and quantitative detection of human adenovirus DNA by real-time PCR. *Journal of Medical Virology*, **70** (2), pp. 228-239.

Henke, W., Herdel, K., Jung, K., Schnorr, D. and Loening, S.A., 1997. Betaine improves the PCR amplification of GC-rich DNA sequences. *Nucleic Acids Research*, **25** (19), pp. 3957-3958.

Hierholzer, J.C., Halonen, P.E., Dahlen, P.O., Bingham, P.G. and McDonough, M.M., 1993. Detection of adenovirus in clinical specimens by polymerase chain reaction and liquid phase hybridisation quantitated by time-resolved fluorometry. *Journal of Clinical Microbiology*, **31** (7), pp. 1886–1891.

Iaconelli, M., Divizia, M., Della Libera, S., Di Bonito, P. and La Rosa, G., 2016. Frequent detection and genetic diversity of human bocavirus in urban sewage samples. *Food and Environmental Virology*, **8** (4), pp. 289-295.

Iaconelli, M., Muscillo, M., Della Libera, S., Fratini, M., Meucci, L., De Ceglia, M., Giacosa, D. and La Rosa, G., 2017. One-year surveillance of human enteric viruses in raw and treated wastewaters, downstream river waters, and drinking waters. *Food Environmental Virology*, **9** (1), pp. 79–88.

Ibrahim, C., Hammami, S., Mejri, S., Mehri, I., Pothier, P. and Hassen, A., 2017. Detection of Aichi virus genotype B in two lines of wastewater treatment processes. *Microbial Pathogenesis*, **109**, pp. 305-312.

Imamura, S., Haruna, M., Goshima, T., Kanezashi, H., Okada, T. and Akimoto, K., 2016. Application of next-generation sequencing to investigation of norovirus diversity in shellfish collected from two coastal sites in Japan from 2013 to 2014. *Japanese Journal of Veterinary Research*, **64** (2), pp. 113-122.

Ingle, S.B. and Hinge, C.R., 2012. Gastroenteritis - Overview. *International Journal of Pharma and Bio Sciences*, **3** (2), pp. 607-613.

Iritani, N., Kaida, A., Abe, N., Kubo, H., Sekiguchi, J., Yamamoto, S.P., Goto, K., Tanaka, T. and Noda, M., 2014. Detection and genetic characterisation of human enteric viruses in oyster-associated gastroenteritis outbreaks between 2001 and 2012 in Osaka City, Japan. *Journal of Medical Virology*, **86**, pp. 2019-2025.

Ishiko, H., Shimada, Y., Konno, T., Hayashi, A., Ohguchi, T., Tagawa, Y., Aoki, Y., Ohno, S. and Yamazaki, S., 2008. Novel human adenovirus causing nosocomial epidemic keratoconjunctivitis. *Journal of Clinical Microbiology*, **46** (6), pp. 2002-2008.

Jacobs, C.S., Davison, J.A, Carr, S., Bennett, M.A., Phillpotts, R. and Wilkinson, G.W.G., 2004. Characterisation and manipulation of the human adenovirus 4 genome. *Journal of General Virology*, **85**, pp. 3361–3366

Japhet, M.O., Famurewa, O., Opaleye, O.O., Adesina, O.A., Niendorf, S., Mas Marques, A., Bock, C.-T. and Hoehne, M., 2016. Genetic diversity of 5 viruses causing diarrhoea among children 0-5 years: identification of first Aichi virus in Nigeria and detection of a novel dog astrovirus in human. Unpublished.

Jaquet, B. J., 2017. The Development of techniques for the identification of novel viruses associated with acute infantile gastroenteritis in South Africa, Rhodes University, South Africa.

Jartti, T., Hedman, K., Jartti, L., Ruuskanen, O., Allander, T. and Söderlund-Venermo, M., 2012. Human bocavirus-the first 5years. *Reviews in Medical Virology*, **22** (1), pp. 46-64.

Jiang, V., Jiang, B., Tate, J., Parashar, U.D. and Patel, M.M., 2010. Performance of rotavirus vaccines in developed and developing countries. *Human Vaccines*, **6** (7), pp. 532-542.

Jiang, S., Dezfulian, H. and Chu, W., 2005. Real-time quantitative PCR for enteric adenovirus serotype 40 in environmental waters. *Canadian Journal of Microbiology*, **51** (5), pp. 393-398.

Jin, Y., Cheng, W., Xu, Z., Liu, N., Yu, J., Li, H., Jin, M., Li, D., Zhang, Q. and Duan, Z., 2011. High prevalence of human bocavirus 2 and its role in childhood acute gastroenteritis in China. *Journal of Clinical Virology*, **52** (3), pp.251-253.

Jones, M.K., Watanabe, M., Zhu, S., Graves, C.L., Keyes, L.R., Grau, K.R., Gonzalez-Hernandez, M.B., Iovine, N.M., Wobus, C.E., Vinjé, J., Tibbetts, S.A., Wallet, S.M. and Karst, S.M., 2014. Enteric bacteria promote human and mouse norovirus infection of B cells. *Science*, **346** (6210), pp. 755-759.

- Jones II, S.M., Harrach, B., Ganac, D.R., Gozum, A.M.M., Dela Cruz, P.W., Riedel, B., Pan, C., Delwart, L.E. and Schnurr, P.D., 2007. New adenovirus species found in a patient presenting with gastroenteritis. *Journal of Virology*, **81** (11), p. 5978–5984.
- Jonsson, N., Wahlström, K., Svensson, L., Serrander, L. and Lindberg, A.M., 2012. Aichi virus infection in elderly people in Sweden. *Archives of Virology*, **157** (7), pp.1365-1369.
- Kabue, J.P., Meader, E., Hunter, P.R. and Potgieter, N., 2016. Norovirus prevalence and estimated viral load in symptomatic and asymptomatic children from rural communities of Vhembe district, South Africa. *Journal of Clinical Virology*, **84**, pp. 12-18.
- Kabue, J.P., Meader, E., Hunter, P.R. and Potgieter, N., 2017. Genetic characterisation of Norovirus strains in outpatient children from rural communities of Vhembe district/South Africa, 2014–2015. *Journal of Clinical Virology*, **94**, pp. 100-106.
- Kaikkonen, S., Räsänen, S., Rämetsä, M. and Vesikari, T., 2010. Aichi virus infection in children with acute gastroenteritis in Finland. *Epidemiology and Infection*, **138** (8), pp. 1166-1171.
- Kajon, E.A., Moseley, M.J., Metzgar, D., Huong, H.S., Wadleigh, A., Ryan, K.A.M. and Russell, L.K., 2007. Molecular epidemiology of adenovirus type 4 infections in US military recruits in the post vaccination era (1997–2003). *The Journal of Infectious Diseases*, **196** (1), pp. 67–75.
- Kantola, K., Hedman, L., Allander, T., Jartti, T., Lehtinen, P., Ruuskanen, O., Hedman, K. and Söderlund-Venermo, M., 2008. Serodiagnosis of human bocavirus infection. *Clinical Infectious Diseases*, **46** (4), pp. 540-546.
- Karamoko, Y., Ibenyassine, K., Aitmhand, R., Idaomar, M. and Ennaji, M.M., 2005. Adenovirus detection in shellfish and urban sewage in Morocco (Casablanca region) by the polymerase chain reaction. *Journal of Virological Methods*, **126**, (1-2), pp. 135–137.
- Kapikian, A.Z., Wyatt, R.G., Dolin, R., Thornhill, T.S., Kalica, A.R. and Chanock, R.M., 1972. Visualisation by immune electron microscopy of a 27-nm particle associated with acute infectious nonbacterial gastroenteritis. *Journal of Virology*, **10** (5), pp. 1075-1081.

Kapoor, A., Simmonds, P., Slikas, E., Li, L., Bodhidatta, L., Sethabutr, O., Triki, H., Bahri, O., Oderinde, B.S., Baba, M.M., Bukbuk, D.N., Besser, J., Bartkus, J. and Delwart, E., 2010. Human bocaviruses are highly diverse, dispersed, recombination prone, and prevalent in enteric infections. *Journal of Infectious Diseases*, **201** (11), pp. 1633-1643.

Kapoor, A., Slikas, E., Simmonds, P., Chieochansin, T., Naeem, A., Shaukat, S., Alam, M.M., Sharif, S., Angez, M., Zaidi, S. and Delwart, E., 2009. A newly identified bocavirus species in human stool. *Journal of Infectious Diseases*, **199** (2), pp. 196-200.

Katayama, K., Shirato-Horikoshi, H., Kojima, S., Kageyama, T., Oka, T., Hoshino, F.B., Fukushi, S., Shinohara, M., Uchida, K., Suzuki, Y., Gojobori, T. and Takeda, N., 2002. Phylogenetic analysis of the complete genome of 18 norwalk-like viruses. *Virology*, **299** (2), pp. 225-239.

Kazama, S., Masago, Y., Tohma, K., Souma, N., Imagawa, T., Suzuki, A., Liu, X., Saito, M., Oshitani, H. and Omura, T., 2016. Temporal dynamics of norovirus determined through monitoring of municipal wastewater by pyrosequencing and virological surveillance of gastroenteritis cases. *Water Research*, **92**, pp. 244-253.

Khamrin, P., Malasao, R., Chaimongkol, N., Ukarapol, N., Kongsricharoern, T., Okitsu, S., Hayakawa, S., Ushijima, H. and Maneekarn, N., 2012. Circulating of human bocavirus 1, 2, 3, and 4 in pediatric patients with acute gastroenteritis in Thailand. *Infection, Genetics and Evolution*, **12** (3), pp. 565-569.

Khamrin, P., Okame, M., Thongprachum, A., Nantachit, N., Nishimura, S., Okitsu, S., Maneekarn, N. and Ushijima, H., 2011. A single-tube multiplex PCR for rapid detection in feces of 10 viruses causing diarrhoea. *Journal of Virological Methods*, **173** (2), pp. 390-393.

Khare, R., Chen, C.Y., Weaver, E.A. and Barry, M.A., 2011. Advances and future challenges in adenoviral vector pharmacology and targeting. *Current Gene Therapy*, **11** (4), pp. 241-258.

Kidd, A.H., Jonsson, M., Garwicz, D., Kajon, A.E., Wermenbol, A.G., Verweij, M.W., De Jong, J.C., 1996. Rapid subgenus identification of human adenovirus isolates by a general PCR. *Journal of Clinical Microbiology*, **34** (3), pp. 622-627.

- Kinumaki, A., Sekizuka, T., Takamizawa, M., Igarashi, T. and Kuroda, M., 2012. Detection of abundant Human Adenovirus 41 sequences in the feces of a typical Kawasaki disease patient without gastrointestinal manifestation. Unpublished.
- Kitade, Y., Ootsuka, S., Iitsuka, O. and Saga, N., 2003. Effect of DMSO on PCR of *Porphyra yezoensis* (Rhodophyta) gene. *Journal of Applied Phycology*, **15** (6), pp. 555-557.
- Kitajima, M., Hata, A., Yamashita, T., Haramoto, E., Minagawa, H. and Katayama, H., 2013. Development of a reverse transcription-quantitative pcr system for detection and genotyping of Aichi viruses in clinical and environmental samples. *Applied and Environmental Microbiology*, **79** (13), pp. 3952-3958.
- Kitajima, M., Haramoto, E., Phanuwat, C. and Katayama, H., 2011. Prevalence and genetic diversity of Aichi viruses in wastewater and river water in Japan. *Applied and Environmental Microbiology*, **77** (6), pp. 2184-2187.
- Kitajima, M., Iker, B.C., Pepper, I.L. and Gerba, C.P., 2014. Relative abundance and treatment reduction of viruses during wastewater treatment processes - Identification of potential viral indicators. *Science of the Total Environment*, **488** (1), pp. 290-296.
- Knox, C. M., Luke, G. A., Dewar, J., de Felipe, P. and Williams, B. J., 2012. Rotaviruses and emerging picornaviruses as aetiological agents of acute gastroenteritis. *South African Journal of Epidemiological Infection*, **27** (4), pp. 141-148.
- Kobayashi, S., Sakae, K., Suzuki, Y., Ishiko, H., Kamata, K., Suzuki, K., Natori, K., Miyamura, T. and Takeda, N., 2000A. Expression of recombinant capsid proteins of Chitta virus, a genogroup II Norwalk virus, and development of an ELISA to detect the viral antigen. *Microbiology and Immunology*, **44** (8), pp. 687-693.
- Kocabas, E. and Dayar, G.T., 2015. Rotavirus vaccines. *Cocuk Enfeksiyon Dergisi*, **9** (4), pp. 166-174.
- Kogasaka, R., Akihara, M., Horino, K., Chiba, S. and Nakao, T., 1979. A morphological study of human rotavirus. *Archives of Virology*, **61** (1-2), pp. 41-48.

Kojima, S., Kageyama, T., Fukushi, S., Hoshino, F.B., Shinohara, M., Uchida, K., Natori, K., Takeda, N. and Katayama, K., 2002. Genogroup-specific PCR primers for detection of Norwalk-like viruses. *Journal of Virological Methods*, **100** (1-2), pp. 107-114.

La Rosa, G., Della Libera, S., Iaconelli, M., Donia, D., Cenko, F., Xhelilaj, G., Cozza, P. and Divizia, M., 2016. Human bocavirus in children with acute gastroenteritis in Albania. *Journal of Medical Virology*, **88** (5), pp. 906-910.

Lau, S.K.P., Yip, C.C.Y., Que, T., Lee, R.A., Au-Yeung, R.K.H., Zhou, B., So, L., Lau, Y., Chan, K., Woo, P.C.Y. and Yuen, K., 2007. Clinical and molecular epidemiology of human bocavirus in respiratory and faecal samples from children in Hong Kong. *Journal of Infectious Diseases*, **196** (7), pp. 986-993.

Lee, L.H., Phillips, C.A., South, M.A., Melnick, J.L. and Yow, M.D., 1965. Enteric virus isolation in different cell cultures. *Bulletin of the World Health Organization*, **32** (5), pp. 657-663.

Leen, A.M., Sili, U., Vanin, E.F., Jewell, A.M., Xie, W., Vignali, D., Piedra, P.A., Brenner, M.K. and Rooney, C.M., 2004. Conserved CTL epitopes on the adenovirus hexon protein expand subgroup cross-reactive and subgroup-specific CD8⁺ T cells. *Blood*, **104** (8), pp. 2432-2440.

Le Guyader, F., Neill, F.H., Estes, M.K., Monroe, S.S., Ando, T. and Atmar, R.L., 1996. Detection and analysis of a small round-structured virus strain in oysters implicated in an outbreak of acute gastroenteritis. *Applied and Environmental Microbiology*, **62** (11), pp. 4268-4272.

Le Guyader, F.S., Bon, F., DeMedici, D., Parnaudeau, S., Bertone, A., Crudeli, S., Doyle, A., Zidane, M., Suffredini, E., Kohli, E., Maddalo, F., Monini, M., Gally, A., Pompepy, M., Pothier, P. and Ruggeri, F.M., 2006A. Detection of multiple noroviruses associated with an international gastroenteritis outbreak linked to oyster consumption. *Journal of Clinical Microbiology*, **44** (11), pp. 3878-3882.

Le Guyader, F.S., Le Saux, J., Ambert-Balay, K., Krol, J., Serais, O., Parnaudeau, S., Giraudon, H., Delmas, G., Pommepuy, M., Pothier, P. and Atmar, R.L., 2008. Aichi virus, norovirus, astrovirus, enterovirus, and rotavirus involved in clinical cases from a French oyster-related gastroenteritis outbreak. *Journal of Clinical Microbiology*, **46** (12), pp. 4011-4017.

Le Guyader, F.S., Loisy, F., Atmar, R.L., Hutson, A.M., Estes, M.K., Ruvoën-Clouet, N., Pommepuy, M. and Le Pendu, J., 2006B. Norwalk virus-specific binding to oyster digestive tissues. *Emerging Infectious Diseases*, **12** (6), pp. 931-936.

Lekana-Douki, S.E., Kombila-Koumavor, C., Nkoghe, D., Drosten, C., Drexler, J.F. and Leroy, E.M., 2015. Molecular epidemiology of enteric viruses and genotyping of rotavirus A, adenovirus and astrovirus among children under 5 years old in Gabon. *International Journal of Infectious Diseases*, **34**, pp. 90-95.

Leshem, E., Gastañaduy, P.A., Trivedi, T., Laufer Halpin, A., Pringle, J., Lang, F., Gregoricus, N., Vinjé, J., Behraves, C.B., Parashar, U. and Hall, A.J., 2016. Norovirus in a United States virgin islands resort: outbreak investigation, response, and costs. *Journal of Travel Medicine*, **23** (5), pp. 1-6.

Li, Li-li., Liu, Na., Yu, Jei-mei., Ao, Yuan-yun., Li, Shan., Colin Stine, O., Duan and Zhao-jun., 2017. Analysis of Aichi virus and Saffold virus association with pediatric acute gastroenteritis. *Journal of Clinical Virology*, **87** (1), pp. 37-42.

Liu, L., Johnson, H.L., Cousens, S., Perin, J., Scott, S., Lawn, J.E., Rudan, I., Campbell, H., Cibulskis, R., Li, M., Mathers, C. and Black, R.E., 2012. Global, regional, and national causes of child mortality: An updated systematic analysis for 2010 with time trends since 2000. *The Lancet*, **379** (9832), pp. 2151-2161.

Liu, L., Qian, Y., Zhang, Y., Deng, J., Jia, L. and Dong, H., 2014. Adenoviruses associated with acute diarrhoea in children in Beijing, China. *PLoS ONE*, **9** (2), pp. 1-6.

Lodder, W.J., Rutjes, S.A., Takumi, K. and Husman, A.M.d.R., 2013. Aichi Virus in sewage and surface water, the Netherlands. *Emerging Infectious Diseases*, **19** (8), pp. 1222-1230.

- Longtin, J., Bastien, M., Gilca, R., Leblanc, E., De Serres, G., Bergeron, M.G. and Boivin, G., 2008. Human bocavirus infections in hospitalised children and adults. *Emerging Infectious Diseases Journals*, **2** (14), pp. 127-132.
- Lopman, B.A., Reacher, M.H., Van Duijnhoven, Y., Hanon, F., Brown, D. and Koopmans, M., 2003. Viral gastroenteritis outbreaks in Europe, 1995-2000. *Emerging Infectious Diseases*, **9** (1), pp. 90-96.
- Loutreul, J., Cazeaux, C., Levert, D., Nicolas, A., Vautier, S., Le Sauvage, A.L., Perelle, S. and Morin, T., 2014. Prevalence of human noroviruses in frozen marketed shellfish, red fruits and fresh vegetables. *Food and Environmental Virology*, **6** (3), pp. 157-168.
- Lukashev, A.N., Drexler, J.F., Belalov, I.S., Eschbach-Bludau, M., Baumgarte, S. and Drosten, C., 2012. Genetic variation and recombination in Aichi virus. *Journal of General Virology*, **93** (6), pp. 1226-1235.
- Mabasa, V.V., Meno, K.D., Taylor, M.B. and Mans, J., 2017. Environmental surveillance for noroviruses in selected South African wastewaters 2015–2016: Emergence of the novel GII.17. *Food and Environmental Virology*, **10** (1), pp. 16-28.
- MacIntyre, U.E. and De Villiers, F.P.R., 2010. The economic burden of diarrhoeal disease in a tertiary level hospital, Gauteng, South Africa. *Journal of Infectious Diseases*, **202** (1), pp. S116-S125.
- Madhi, S.A., Cunliffe, N.A., Steele, D., Witte, D., Kirsten, M., Louw, C., Ngwira, B., Victor, J.C., Gillard, P.H., Chevart, B.B., Han, H.H. and Neuzil, K.M., 2010. Effect of human rotavirus vaccine on severe diarrhoea in African infants. *New England Journal of Medicine*, **362** (4), pp. 289-298.
- Madupu, R., Halpin, R., Fedorova, N., Tsitritin, T., Stockwell, T., Amedeo, P., Appalla, L., Bishop, B., Edworthy, P., Gupta, N., Hoover, J., Katzel, D., Li, K., Schobel, S., Shrivastava, S., Thovarai, V., Wang, S., Dehghan, S., Singh, S., Liu, E.B., Seto, J., Jones, M.S., Kajon, A., Gray, G., Kowalski, R., Romanowski, E., Chodosh, J., Wentworth, D.E. and Seto, D., 2013. Unpublished.

Madupu, R., Halpin, R., Fedorova, N., Tsitirin, T., Stockwell, T., Amedeo, P., Appalla, L., Bishop, B., Edworthy, P., Gupta, N., Hoover, J., Katzel, D., Li, K., Schobel, S., Shrivastava, S., Thovarai, V., Wang, S., Dehghan, S., Singh, S., Liu, E.B., Seto, J., Jones, M.S., Kajon, A., Gray, G., Kowalski, R., Romanowski, E., Chodosh, J., Wentworth, D.E. and Seto, D., 2011. Unpublished.

Magwalivha, M., Wolfaardt, M., Kiulia, N.M., Van Zyl, W.B., Mwenda, J.M. and Taylor, M.B. 2010. High prevalence of species D human adenoviruses in faecal specimens from urban Kenyan Children with Diarrhoea. *Journal of Medical Virology*, **82** (1), pp. 77–84.

Mans, J., de Villiers, J.C., du Plessis, N.M., Avenant, T. and Taylor, M.B., 2010. Emerging norovirus GII.4 2008 variant detected in hospitalised paediatric patients in South Africa. *Journal of Clinical Virology*, **49** (4), pp. 258-264.

Mans, J., Murray, T.Y., Nadan, S., Netshikweta, R., Page, N.A. and Taylor, M.B., 2016. Norovirus diversity in children with gastroenteritis in South Africa from 2009 to 2013: GII.4 variants and recombinant strains predominate. *Epidemiology and Infection*, **144** (5), pp. 907-916.

Mans, J., Murray, T.Y. and Taylor, M.B., 2014. Novel norovirus recombinants detected in South Africa. *Virology Journal*, **11** (168), pp. 1-9.

Mans, J., Netshikweta, R., Magwalivha, M., Van Zyl, W.B. and Taylor, M.B., 2013. Diverse norovirus genotypes identified in sewage-polluted river water in South Africa. *Epidemiology and Infection*, **141** (2), pp. 303-313.

Martín, C.S., 2012. Latest insights on adenovirus structure and assembly. *Viruses*, **4** (5), pp. 847-877.

Mayindou, G., Ngokana, B., Sidibé, A., Moundélé, V., Koukouikila-Koussounda, F., Christevy Vouvongui, J., Kwedi Nolna, S., Velavan, T.P. and Ntoumi, F., 2016. Molecular epidemiology and surveillance of circulating rotavirus and adenovirus in Congolese children with gastroenteritis. *Journal of Medical Virology*, **88** (4), pp. 596-605.

Misigo, D., Mwaengo, D. and Mburu, D., 2014. Molecular detection and phylogenetic analysis of Kenyan human bocavirus isolates. *Journal of Infection in Developing Countries*, **8** (2), pp. 221-227.

Moore, P.L., Steele, A.D. and Alexander, J.J., 2000. Relevance of commercial diagnostic tests to detection of enteric adenovirus infections in South Africa. *Journal of Clinical Microbiology*, **38** (4), pp. 1661-1663.

Murray, T.Y., Mans, J. and Taylor, M.B., 2013. Human calicivirus diversity in wastewater in South Africa. *Journal of Applied Microbiology*, **114** (6), pp. 1843-1853.

Nagashima, S., Sasaki, J. and Taniguchi, K., 2003. Functional analysis of the stem-loop structures at the 5' end of the Aichi virus genome. *Virology*, **313** (1), pp. 56-65.

National Institute of Communicable Diseases, Annual review, 2012/2013

National Institute for Communicable Diseases (NICD), Communicable Disease Surveillance Bulletin, 2010. **8** (1).

National Institute for Communicable Diseases (NICD), Communicable Disease Surveillance Bulletin, 2010. **12** (7).

National Institute for Communicable Diseases (NICD), Communicable Disease Surveillance Bulletin, 2014. **13** (6).

National Institute of Communicable Diseases, Rotavirus Surveillance Report, 2014/ 2015.

Neske, F., Blessing, K., Tollmann, F., Schubert, J., Rethwilm, A., Kreth, HW. and Weissbrich, B., 2007. Real-Time PCR for diagnosis of human bocavirus infections and phylogenetic analysis. *Journal of Clinical Microbiolog*, **45** (7) pp. 2116–2122.

Ng, T.F.F., Marine, R., Wang, C., Simmonds, P., Kapusinszky, B., Bodhidatta, L., Oderinde, B.S., Wommack, K.E. and Delwarta, E., 2012. High variety of known and new RNA and DNA viruses of diverse origins in untreated sewage. *Journals of Virology*, **26** (22) pp. 12161-12175.

Ngabo, F., Mvundura, M., Gazley, L., Gatera, M., Rugambwa, C., Kayonga, E., Tuyishime, Y., Niyibaho, J., Mwenda, J.M., Donnen, P., Lepage, P., Binagwaho, A. and Atherly, D., 2016. The economic burden attributable to a child's inpatient admission for diarrhoeal disease in Rwanda. *PLoS ONE*, **11** (2), pp. 1-16.

- Nishida, T., Kimura, H., Saitoh, M., Shinohara, M., Kato, M., Fukuda, S., Munemura, T., Mikami, T., Kawamoto, A., Akiyama, M., Kato, Y., Nishi, K., Kozawa, K. and Nishio, O., 2003. Detection, quantitation, and phylogenetic analysis of noroviruses in Japanese oysters. *Applied and Environmental Microbiology*, **69** (10), pp. 5782-5786.
- Nielsen, A.C.Y., Gyhrs, M.L., Nielsen, L.P., Pedersen, C. and Böttiger, B., 2013. Gastroenteritis and the novel picornaviruses aichi virus, cosavirus, saffold virus, and salivirus in young children. *Journal of Clinical Virology*, **57** (3), pp. 239-242.
- Nix, W.A., Jiang, B., Maher, K., Strobert, E. and Oberste, M.S., 2008. Identification of enteroviruses in naturally infected captive primates. *Journal of Clinical Microbiology*, **46** (9), pp. 2874-2878.
- Nordgren, J., Matussek, A., Mattsson, A., Svensson, L. and Lindgren, P., 2009. Prevalence of norovirus and factors influencing virus concentrations during one year in a full-scale wastewater treatment plant. *Water Research*, **43** (4), pp. 1117-1125.
- Northill, J.A., Simmons, R.J., Moore, F.A. and Genge, D., 2012. Characterization of the first reported Aichi virus in Australia. Unpublished.
- Nunes, M.C., Kuschner, Z., Rabede, Z., Madimabe, R., Van Niekerk, N., Moloji, J., Kuwanda, L., Rossen, J.W., Klugman, K.P., Adrian, P.V. and Madhi, S.A., 2014. Clinical epidemiology of bocavirus, rhinovirus, two polyomaviruses and four coronaviruses in HIV-infected and HIV-uninfected South African children. *PLoS ONE*, **9** (2), pp. 1-12.
- Odume, O.N., Muller, W.J., Arimoro, F.O. and Palmer, C.G., 2012. The impact of water quality deterioration on macro invertebrate communities in the Swartkops River, South Africa: a multimetric approach. *African Journal of Aquatic Science*, **37** (2), pp. 191-200.
- Oh, D., Silva, P.A., Hauroeder, B., Diedrich, S., Cardoso, D.D.P. and Schreier, E., 2006. Molecular characterisation of the first Aichi viruses isolated in Europe and in South America. *Archives of Virology*, **151** (6), pp. 1199-1206.
- Okoh, A.I., Sibanda, T. and Gusha, S.S., 2010. Inadequately treated wastewater as a source of human enteric viruses in the environment. *International Journal of Environmental Research and Public Health*, **7**, pp. 2620-2637.
- Ong, D.S.Y., Schuurman, R. and Heikens, E., 2016. Human bocavirus in stool: A true pathogen or an innocent bystander? *Journal of Clinical Virology*, **74**, pp. 45-49.

Oristo, S., Ronnqvist, M., Aho, M., Sovijarvi, A., Hannila-Handelberg, T., Horman, A., Nikkari, S., Kinnunen, P.M., Maunula, L., 2016. Contamination by norovirus and adenovirus on environmental surfaces and in hands of conscripts in two Finnish garrisons. *Food and Environmental Virology*, **9** (1), pp. 62-71.

O'Ryan, M.L., Lucero, Y. and Vidal, R., 2012. Enteric viruses in wastewaters: An interesting approach to evaluate the potential impact of rotavirus vaccination on viral circulation. *Expert Review of Vaccines*, **11** (4), pp. 419-422.

Osuolale, O. and Okoh, A., 2015. Incidence of human adenoviruses and Hepatitis A virus in the final effluent of selected wastewater treatment plants in Eastern Cape Province, South Africa. *Virology Journal*, **12** (98), pp. 1-8

Oude Munnink, B.B. and Van der Hoek, L., 2016. Viruses causing gastroenteritis: The known, the new and those beyond. *Viruses*, **8** (2), pp. 1-10.

Ouédraogo, N., Kaplon, J., Bonkougou, I.J.O., Traoré, A.S., Pothier, P., Barro, N. and Ambert-Balay, K., 2016. Prevalence and genetic diversity of enteric viruses in children with diarrhoea in Ouagadougou, Burkina Faso. *PLoS ONE*, **11** (4), pp. 1-22.

Ouédraogo, N., Ngangas, S.M.T., Bonkougou, I.J.O., Tiendrebeogo, A.B., Traore, K.A., Sanou, I., Traore, A.S. and Barro, N., 2017. Temporal distribution of gastroenteritis viruses in Ouagadougou, Burkina Faso: Seasonality of rotavirus. *BMC Public Health*, **17** (274), pp. 1-8.

Ozoemena, L.C., Minor, P.D. and Afzal, M.A., 2004. Comparative evaluation of measles virus specific TaqMan PCR and conventional PCR using synthetic and natural RNA templates. *Journal of Medical Virology*, **73**, pp. 79-84.

Page, N.A., Groome, M.J., Nadan, S., Netshikweta, R., Keddy, K.H., Poonsamy, B., Moyes, J., Walaza, S., Kahn, K., Madhi, S.A., Taylor, M.B., Mans, J. and Cohen, C., 2017. Norovirus epidemiology in South African children <5 years hospitalised for diarrhoeal illness between 2009 and 2013. *Epidemiology and Infection*, **145** (9), pp. 1942-1952.

Park, G.W., Chhabra, P., Vinjé, J., 2017. Swab sampling method for the detection of human norovirus on surfaces. *Journal of Visualized Experiments*, **120**, pp. 1-11.

- Parra, G.I. and Green, K.Y., 2015. Genome of emerging norovirus GII.17, United States, 2014. *Emerging Infectious Diseases*, **21** (8), pp. 1477-1479.
- Pauly, M., Hoppe, E., Mugisha, L., Petrzalkova, K., Akoua-Koffi, C., Couacy-Hymann, E., Anoh, A.E., Mossoun, A., Schubert, G., Wiersma, L., Pascale, S., Muyembe, J.J., Karhemere, S., Weiss, S., Leendertz, S.A., Calvignac-Spencer, S., Leendertz, F.H. and Ehlers, B., 2014. High prevalence and diversity of species D adenoviruses (HAdV-D) in human populations of four Sub-Saharan countries. *Virology Journal*, **11** (25), pp. 1-9.
- Pham, N.T.K., Khamrin, P., Nguyen, T.A., Kanti, D.S., Phan, T.G., Okitsu, S. and Ushijima, H., 2007. Isolation and molecular characterisation of aichi viruses from faecal specimens collected in Japan, Bangladesh, Thailand, and Vietnam. *Journal of Clinical Microbiology*, **45** (7), pp. 2287-2288.
- Pina, S., Puig, M., Lucena, F., Jofre, J. and Girones, R., 1998. Viral Pollution in the Environment and in Shellfish: Human adenovirus detection by PCR as an index of human viruses. *Applied and Environmental Microbiology*, **9** (9), pp. 3376–3382.
- Prasad, B.V.V., Hardy, M.E., Dokland, T., Bella, J., Rossmann, M.G. and Estes, M.K., 1999. X-ray crystallographic structure of the Norwalk virus capsid. *Science*, **286** (5438), pp. 287-290.
- Prevost, B., Lucas, F.S., Goncalves, A., Richard, F., Moulin, L. and Wurtzer, S., 2015. Large scale survey of enteric viruses in river and wastewater underlines the health status of the local population. *Environment International Journals*, **79**, pp. 42–50
- Puig, M., Jofre, J., Lucena, F., Allard, A., Wadell, G., Girones, R., 1994. Detection of adenoviruses and enteroviruses in polluted waters by nested PCR amplification. *Applied Environmental Microbiology*, **60** (8), pp. 2963–2970.
- Qin, M., Dong, X., Jing, Y., Wei, X., Wang, Z., Feng, H., Yu, H., Li, J. and Li, J., 2016. A waterborne gastroenteritis outbreak caused by norovirus GII.17 in a hotel, Hebei, China, December 2014. *Food and Environmental Virology*, **8** (3), pp.180-186.
- Racaniello, V. R. (2007). *Picornaviridae: The viruses and their replication*. In: Howley, D., eds. *Fields Virology*. Philadelphia: Lippincott Williams and Wilkins, pp. 795-838.

- Reuter, G., Boldizsár, A., Papp, G. and Pankovics, P., 2009. Detection of Aichi virus shedding in a child with enteric and extraintestinal symptoms in Hungary. *Archives of Virology*, **154** (9), pp. 1529-1532.
- Rezaei, M., Sohrabi, A., Edalat, R., Siadat, S.D., Gomari, H., Rezaei, M. and Gilani, S.M., 2012. Molecular epidemiology of acute gastroenteritis caused by subgenus F (40, 41) enteric adenoviruses in inpatient children. *Labmedicine Journals*, **43** (1), pp. 1276-1294.
- Ribes, J.M., Montava, R., Téllez-Castillo, C.J., Fernández-Jiménez, M. and Buesa, J., 2010. Seroprevalence of Aichi virus in a Spanish population from 2007 to 2008. *Clinical and Vaccine Immunology*, **17** (4), pp. 545-549.
- Rigotto, C., Sinceroa, T.C.M., Simoes, C.M.O. and Barardia, C.R.M., 2005. Detection of adenoviruses in shellfish by means of conventional-PCR, nested-PCR, and integrated cell culture PCR (ICC/PCR). *Water Research Journal*, **39** (2-3), pp. 297–304.
- Risku, M., Kätkä, M., Lappalainen, S., Räsänen, S. and Vesikari, T., 2012. Human bocavirus types 1, 2 and 3 in acute gastroenteritis of childhood. *Acta Paediatrica, International Journal of Paediatrics*, **101** (9), pp. 405-410.
- Rivadulla, E., Varela, M.F. and Romalde, J.L., 2017. Low prevalence of Aichi virus in molluscan shellfish samples from Galicia (NW Spain). *Journal of Applied Microbiology*, **122** (2), pp. 516-521.
- Rodríguez-Díaz, J., Querales, L., Caraballo, L., Vizzi, E., Liprandi, F., Takiff, H. and Betancourt, W.Q., 2009. Detection and characterisation of waterborne gastroenteritis viruses in urban sewage and sewage-polluted river waters in Caracas, Venezuela. *Applied and Environmental Microbiology*, **75** (2), pp. 387-394.
- Rodriguez-Manzano, J., Hundesa, A., Calgua, B., Carratala, A., Maluquer de Motes, C., Rusiñol, M., Moresco, V., Ramos, A.P., Martínez-Marca, F., Calvo, M., Monte Barardi, C.R., Girones, R. and Bofill-Mas, S., 2014. Adenovirus and norovirus contaminants in commercially distributed shellfish. *Food and Environmental Virology*, **6** (1), pp. 31-41.
- Sahdev, S., Saini, S., Tiwari, P., Saxena, S. and Singh Saini, K., 2007. Amplification of GC-rich genes by following a combination strategy of primer design, enhancers and modified PCR cycle conditions. *Molecular and Cellular Probes*, **21** (4), pp. 303-307.

Saikruang, W., Khamrin, P., Suantai, B., Okitsu, S., Hayakawa, S., Ushijima, H. and Maneekarn, N., 2014A. Detection of diarrhoeal viruses circulating in adult patients in Thailand. *Archives of Virology*, **159** (12), pp. 3371-3375.

Saikruang, W., Khamrin, P., Suantai, B., Ushijima, H. and Maneekarn, N., 2014B. Molecular detection and characterisation of Aichi virus A in adult patients with diarrhoea in Thailand. *Journal of Medical Virology*, **86** (6), pp. 983-987.

Santos, N., Peret, T.C.T., Humphreya, C.D.D., Carolina, M., Albuquerquea, M., Cirlene-Silva, R., José-Benatia, F., Lub, X. and Erdman, D.D., 2010. Human bocavirus species 2 and 3 in Brazil. *Journal of Clinical Virology*, **48**, pp. 127–130.

Sasaki, J., Kusuhara, Y., Maeno, Y., Kobayashi, N., Yamashita, T., Sakae, K., Takeda, N. and Taniguchi, K., 2001. Construction of an infectious cDNA clone of aichi virus (a new member of the family Picornaviridae) and mutational analysis of a stem-loop structure at the 5' end of the genome. *Journal of Virology*, **75** (17), pp. 8021-8030.

Sasaki, J., Nagashima, S. and Taniguchi, K., 2003. Aichi virus leader protein is involved in viral RNA replication and encapsidation. *Journal of Virology*, **77** (20), pp. 10799-10807.

Sasaki, J. and Taniguchi, K., 2003. The 5'-end sequence of the genome of Aichi virus, a picornavirus, contains an element critical for viral RNA encapsidation. *Journal of Virology*, **77** (6), pp. 3542-3548.

Sauerbrei, A., Sehlr, K., Brandstadt, A., Heim, A., Reimer, K. and Wutzler, P. (2004). Sensitivity of human adenoviruses to different groups of chemical biocides. *Journal of Hospital Infections*, **57** (1), pp. 59–66.

Sdiri-Loulizi, K., Gharbi-Khélifi, H., De Rougemont, A., Chouchane, S., Sakly, N., Ambert-Balay, K., Hassine, M., Guédiche, M.N., Aouni, M. and Pothier, P., 2008. Acute infantile gastroenteritis associated with human enteric viruses in Tunisia. *Journal of Clinical Microbiology*, **46** (4), pp. 1349-1355.

Sdiri-Loulizi, K., Hassine, M., Aouni, Z., Gharbi-Khelifi, H., Chouchane, S., Sakly, N., Neji-Guediche, M., Pothier, P. and Ambert-Balay, K., 2010A. Detection and molecular characterisation of enteric viruses in environmental samples in Monastir, Tunisia between January 2003 and April 2007. *Journal of Applied Microbiology*, **109**, pp. 1364-5072.

Sdiri-Loulizi, K., Hassine, M., Bour, J., Ambert-Balay, K., Mastouri, M., Aho, L., Gharbi-Khelifi, H., Aouni, Z., Sakly, N., Chouchane, S., Neji-Guédiche, M., Pothier, P. and Aouni, M., 2010B. Aichi virus IgG seroprevalence in Tunisia parallels genomic detection and clinical presentation in children with gastroenteritis. *Clinical and Vaccine Immunology*, **17** (7), pp. 1111-1116.

Sdiri-Loulizi, K., Hassine, M., Gharbi-Khelifi, H., Sakly, N., Chouchane, S., Guediche, M.N., Pothier, P., Aouni, M. and Ambert-Balay, K., 2009. Detection and genomic characterisation of Aichi viruses in stool samples from children in Monastir, Tunisia. *Journal of Clinical Microbiology*, **47** (7), pp. 2275-2278.

Shimizu, H., Phan, T.G., Nishimura, S., Okitsu, S., Maneekarn, N. and Ushijima, H., 2007. An outbreak of adenovirus serotype 41 infection in infants and children with acute gastroenteritis in Maizuru City, Japan. *Infection, Genetics and Evolution*, **7** (2), pp. 279-284.

Sidhu, J.P.S., Ahmed, W. and Toze, S., 2013. Sensitive detection of human adenovirus from small volume of primary wastewater samples by quantitative PCR. *Journal of Virological Methods*, **187** (2), pp. 395-400.

Silverman, A.I., Akrong, M.O., Amoah, P., Drechsel, P. and Nelson, K.L., 2013. Quantification of human norovirus GII, human adenovirus, and faecal indicator organisms in wastewater used for irrigation in Accra, Ghana. *Journal of Water and Health*, **11** (3), pp. 473-488.

Singh, G., Robinson, M.C., Dehghan, S., Jones, S.M., Dyer, W.D., Seto, D. and Chodosha, J., 2013. Homologous recombination in E3 genes of human adenovirus species D. *Journal of Virology*, **87** (22), pp. 12481–12488.

Smit, T.K., Bos, P., Peenze, I., Jiang, X., Estes, M.K. and Steele, A.D., 1999. Seroepidemiological study of genogroup I and II calicivirus infections in south and southern Africa. *Journal of Medical Virology*, **59** (2), pp. 227-231.

Smit, T.K., Steele, A.D., Peenze, I., Jiang, X. and Estes, M.K., 1997. Study of Norwalk virus and Mexico virus infections at Ga-Rankuwa Hospital, Ga-Rankuwa, South Africa. *Journal of Clinical Microbiology*, **35** (9), pp. 2381-2385.

- Smits, S.L., Osterhaus, A.D.M.E. and Koopmans, M.P., 2016. Newly identified viruses in human gastroenteritis. *Pediatric Infectious Disease Journal*, **35** (1), pp. 104-107.
- Smuts, H. and Hardie, D., 2006. Human bocavirus in hospitalised children, South Africa. *Emerging Infectious Diseases*, **12** (9), pp. 1457-1458.
- Smuts, H.E., Workman, L.J. and Zar, H.J., 2008. Role of human metapneumovirus, human coronavirus NL63 and human bocavirus in infants and young children with acute wheezing. *Journal of Medical Virology*, **80** (5), pp. 906- 912.
- Sprengel, J., Schmitz, B., Heuss-neitzel, D., Zock, C. and Doerfler, W., 1993. Nucleotide sequence of human adenovirus type 12 DNA: Comparative functional analysis. *Journal of Virology*, **68** (1), pp. 379-389.
- Sriwana, P., Chieochansin, T., Vuthitanachot, C., Vuthitanachot, V., Theamboonlers, A. and Poovorawan, Y., 2013. Molecular characterisation of human adenovirus infection in Thailand, 2009–2012. *Virology Journal*, **10** (193), pp. 193.
- Staggemeier, R., Almeida, S.E. M. and Spilki, F.R., 2012. Methods of virus detection in soils and sediments. *Virus Reviews and Research*, **16** (1), pp.1-7.
- Statistics South Africa, 2012. Levels and trends of morbidity and mortality among children aged under-five years in South Africa, 2006–2010.
- Steele, A.D., Neuzil, K.M., Cunliffe, N.A., Madhi, S.A., Bos, P., Ngwira, B., Witte, D., Todd, S., Louw, C., Kirsten, M., Aspinall, S., Van Doorn, L.J., Bouckenooghe, A., Suryakiran, P.V. and Han, H.H., 2012. Human rotavirus vaccine Rotarix™ provides protection against diverse circulating rotavirus strains in African infants: a randomised controlled trial. *BMC Infectious Diseases*, **12** (213) pp. 1-8.
- Steele, A.D and Glass, R., 2011. Rotavirus in South Africa: From discovery to vaccine introduction. *Southern African Journal of Epidemiology and Infection*, **26** (4), pp. 184-190.
- Stewart, P.L., Chiu, C.Y., Huang, S., Muir, T., Zhao, Y., Chait, B., Mathias, P. and Nemerow, G.R., 1997. Cryo-EM visualisation of an exposed RGD epitope on adenovirus that escapes antibody neutralisation. *EMBO Journal*, **16** (6), pp. 1189-1198.
- Storch, G.A., 2000. Diagnostic virology. *Clinical Infectious Disease*, **31**, pp.739-751.

Svraka, S., Duizer, E., Vennema, H., de Bruin, E., van der Veer, B., Dorresteijn, B. and Koopmans, M., 2007. Etiological role of viruses in outbreaks of acute gastroenteritis in the Netherlands from 1994 through 2005. *Journal of Clinical Microbiology*, **45** (5), pp. 1389-1394.

Tamura, K., 1992. Estimation of the number of nucleotide substitutions when there are strong transition-transversion and G + C-content biases. *Molecular Biology and Evolution*, **9**, pp. 678-687.

Troeger, C., Forouzanfar, M., Rao, P. C., Khalil, I., Brown, A., Reiner Jr, R. C., Fullman, N., Thompson, R. L., Abajobir, A., Ahmed, M., Alemayohu, M. A., Alvis-Guzman, N., Amare, A. T. and others. 2017. Estimates of global, regional, and national morbidity, mortality, and aetiologies of diarrhoeal diseases: A systematic analysis for the Global Burden of Disease Study 2015. *The Lancet Infectious Diseases*, **17**, pp. 909-948.

Tymentsev, A., Tikunov, A., Zhirakovskaia, E., Kurilshchikov, A., Babkin, I., Klemesheva, V., Netesov, S. and Tikunova, N., 2016. Human bocavirus in hospitalised children with acute gastroenteritis in Russia from 2010 to 2012. *Infection, Genetics and Evolution*, **37** (2016), pp. 143-149.

Umesha, K.R., Bhavani, N.C., Venugopal, M.N., Karunasagar, I., Krohne, G. and Karunasagar, I., 2008. Prevalence of human pathogenic enteric viruses in bivalve molluscan shellfish and cultured shrimp in south west coast of India. *International Journal of Food Microbiology*, **122** (3), pp. 279–286.

Uršic, T., Steyer, A., Kopriva, S., Kalan, G., Krivec, U. and Petrovec, M., 2011. Human bocavirus as the cause of a life-threatening infection. *Journal of Clinical Microbiology*, **49** (3), pp. 1179-1181.

Van Alphen, L.B., Dorléans, F., Schultz, A.C., Fonager, J., Ethelberg, S., Dalgaard, C., Adelhardt, M., Engberg, J.H., Fischer, T.K. and Lassen, S.G., 2014. The application of new molecular methods in the investigation of a waterborne outbreak of norovirus in Denmark, 2012. *PLoS ONE*, **9** (9), pp. 1-9.

Van Heerden, J., Ehlers, M.M., Heim, A. and Grabow, W.O.K., 2005. Prevalence, quantification and typing of adenoviruses detected in river and treated drinking water in South Africa. *Journal of Applied Microbiology*, **99** (2), pp. 234-242.

- Van Heerden, J., Ehlers, M.M., Van Zyl, W.B. and Grabow, W.O.K., 2003. Incidence of adenoviruses in raw and treated water. *Water Research*, **37** (15), pp. 3704–3708.
- Verma, H., Chitambar, S.D. and Gopalkrishna, V., 2011. Circulation of Aichi virus genotype B strains in children with acute gastroenteritis in India. *Epidemiology and Infection*, **139** (11), pp.1687-1691.
- Vinje, J., Hamidjaja, R.A. and Sobsey, M.D., 2004. Development and application of a capsid VP1 (region D) based reverse transcription PCR assay for genotyping of genogroup I and II noroviruses. *Journal of Virological Methods*, **116** (2), pp. 109-117.
- Vinje, J. and Koopmans, M.P.G., 1996. Molecular detection and epidemiology of small round-structured viruses in outbreaks of gastroenteritis in the Netherlands. *Journal of Infectious Diseases*, **174** (3), pp. 610-615.
- Vos, H.J. and Knox, C.M., 2017. The recovery and molecular identification of HAdV-D17 in raw sewage and mussel samples collected in the Eastern Cape province of South Africa. *Southern African Journal of Infectious Diseases*, **1** (1), pp. 1–4.
- Wacker, M.J. and Godard, M.P., 2005. Analysis of one-Step and two-Step real-time RT-PCR using SuperScript III. *Journal of Biomolecular Techniques*, **16** (3), pp. 266-271.
- Wang, C., Chen, S. and Chen, K., 2015. Current status of rotavirus vaccines. *World Journal of Pediatrics*, **11** (4), pp. 300-308.
- Wang, D., Wu, Q., Yao, L., Wei, M., Kou, X. and Zhang, J., 2008. New target tissue for food-borne virus detection in oysters. *Letters in Applied Microbiology*, **47** (5), pp. 405-409.
- Wang, Y., Gonzalez, R., Zhou, H., Li, J., Li, Y., Paranhos-Baccalà, G., Vernet, G., Gou, L. and Wang, J., 2011. Detection of human bocavirus 3 in China. *European Journal of Microbiological Infectious Diseases*, **30** (6), pp. 799-805.
- Webb, A. and Starr, M., 2005. Acute gastroenteritis in children. *Australian Family Physician*, **34** (4), pp. 227-31.
- Wilhelmi, I., Roman, E. and Sánchez-Fauquier, A., 2003. Viruses causing gastroenteritis. *Clinical Microbiology and Infection*, **9** (4), pp. 247-262.

Wohlfart, C., 1988. Neutralisation of adenoviruses: Kinetics, stoichiometry, and mechanisms. *Journal of Virology*, **62** (7), pp. 2321-2328.

Wood, D.J., Bijlsma, K., De Jong, J.C. and Tonkin, C., 1989A. Evaluation of a commercial monoclonal antibody-based enzyme immunoassay for detection of adenovirus types 40 and 41 in stool specimens. *Journal of Clinical Microbiology*, **27** (6), pp. 1155-1158.

Wood, D.J., de Jong, J.C., Bijlsma, K. and van der Avoort, H.G.A.M., 1989B. Development and evaluation of monoclonal antibody-based immune electron microscopy for diagnosis of adenovirus types 40 and 41. *Journal of Virological Methods*, **25** (3), pp. 241-250.

Woods, J.W., and Burkhardt III, W., 2010. Occurrence of norovirus and Hepatitis A virus in U.S Oysters. *Food Environmental Virology*, **2** (3), pp. 176-182.

World Health Organisation, 2017. <http://www.who.int/mediacentre/factsheets/fs330/en/> (accessed 02-06-17).

World Health Organisation, 2014. <https://africacheck.org/factsheets/factsheet-the-leading-causes-of-death-in-africa/> (Accessed 02-06-17).

Wu, B., 2010. Unpublished.

Xu, W., McDonough, M.C. and Erdman., D.D., 2000. Species-specific identification of human adenoviruses by a multiplex PCR assay. *Journal of Clinical Microbiology*, **38** (11), pp. 4114–4120.

Yamashita, T., Kobayashi, S., Sakae, K., Nakata, S., Chiba, S., Ishihara, Y. and Isomura, S., 1991. Isolation of cytopathic small round viruses with BS-C-1 cells from patients with gastroenteritis. *Journal of Infectious Diseases*, **164** (5), pp. 954-957.

Yamashita, T., Sakae, K., Tsuzuki, H., Suzuki, Y., Ishikawa, N., Takeda, N., Miyamura, T. and Yamazaki, S., 1998. Complete nucleotide sequence and genetic organisation of Aichi virus, a distinct member of the Picornaviridae associated with acute gastroenteritis in humans. *Journal of Virology*, **72** (10), pp. 8408-8412.

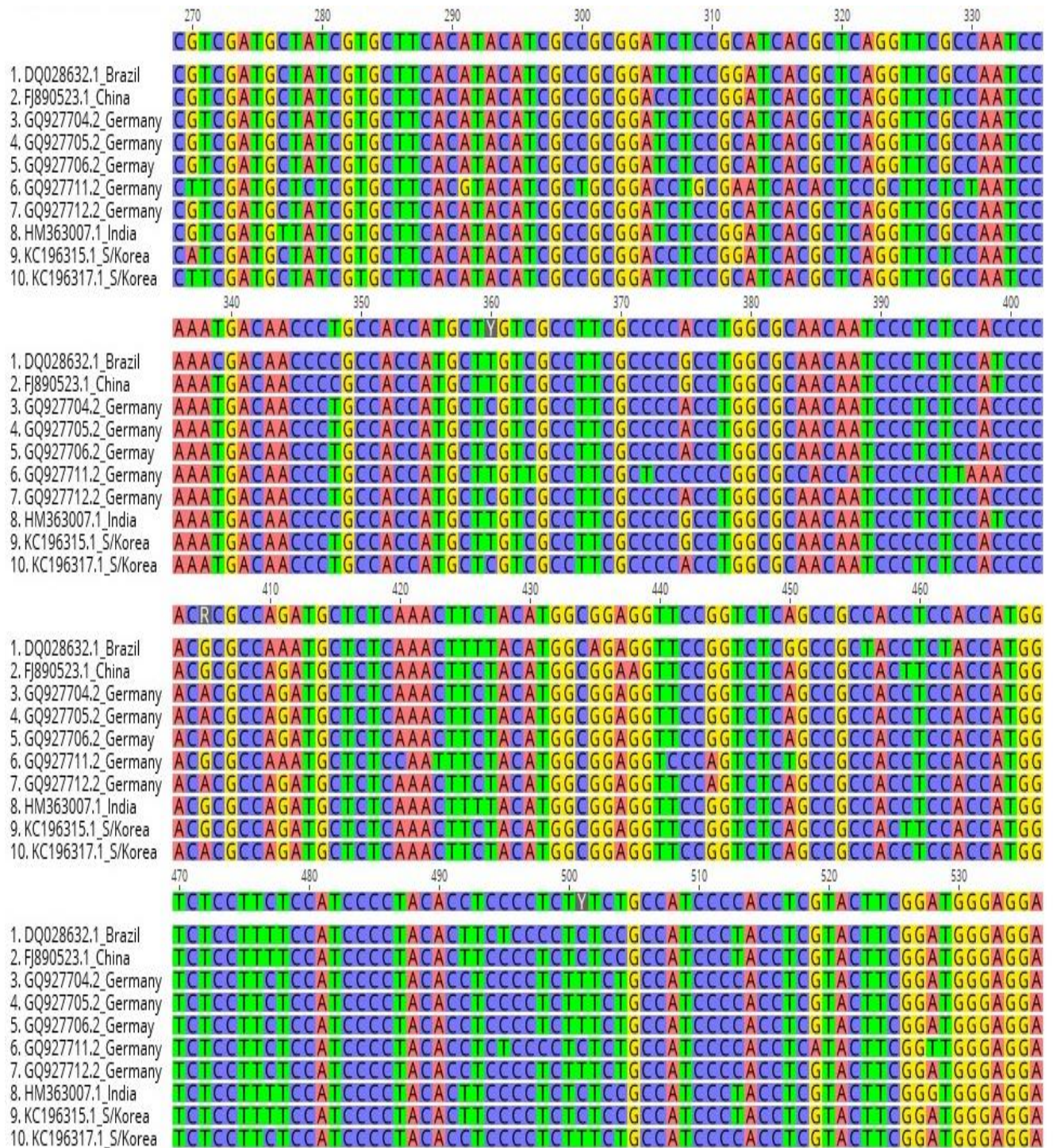
- Yamashita, T., Sugiyama, M., Tsuzuki, H., Sakae, K., Suzuki, Y. and Miyazaki, Y., 2000. Application of a reverse transcription-PCR for identification and differentiation of Aichi virus, a new member of the Picornavirus family associated with gastroenteritis in humans. *Journal of Clinical Microbiology*, **38** (8), pp. 2955-2961.
- Yang, S., Zhang, W., Shen, Q., Yang, Z., Zhu, J., Cui, L. and Hua, X., 2009. Aichi virus strains in children with gastroenteritis, China. *Emerging Infectious Diseases*, **15** (10), pp. 1703-1705.
- Yip, C.C.Y., Lo, K., Que, T., Lee, R.A., Chan, K., Yuen, K., Woo, P.C.Y. and Lau, S.K.P., 2014. Epidemiology of human parechovirus, Aichi virus and salivirus in faecal samples from hospitalised children with gastroenteritis in Hong Kong. *Virology Journal*, **11** (182), pp. 1-10.
- Yu, J., Li, D., Xu, Z., Cheng, W., Zhang, Q., Li, H., Cui, S., Miao-Jin, Yang, S., Fang, Z. and Duan, Z., 2008. Human bocavirus infection in children hospitalised with acute gastroenteritis in China. *Journal of Clinical Virology*, **42** (3), pp. 280-285.
- Zhang, D., Ma, M., Wen, W., Zhu, X., Xu, L., He, Z., He, X., Wu, J., Hu, Y., Zheng, Y., Deng, Y., Lin, C., Lu, J., Li, M. and Cao, K., 2015. Clinical epidemiology and molecular profiling of human bocavirus in faecal samples from children with diarrhoea in Guangzhou, China. *Epidemiology and Infection*, **143** (11), pp. 2315-2329.
- Zhao, B., Yu, X., Wang, C., Teng, Z., Wang, C., Shen, J., Gao, Y., Zhu, Z., Wang, J., Yuan, Z., Wu, F., Zhang, X. and Ghildyal, R., 2013. High human bocavirus viral load is associated with disease severity in children under five years of age. *PLoS ONE*, **8** (4), pp. 1-8.
- Zhou, Z., Tian, Z., Li, Q., Tian, P., Wu, Q., Wang, D. and Shi, X., 2017. In situ capture RT-qPCR: A new simple and sensitive method to detect human norovirus in oysters. *Frontiers in Microbiology*, **8** (554), pp. 1-8.
- Zhu, L., Wang, X., Ren, J., Kotecha, A., Walter, T.S., Yuan, S., Yamashita, T., Tuthill, T.J., Fry, E.E., Rao, Z. and Stuart, D.I., 2016. Structure of human Aichi virus and implications for receptor binding. *Nature Microbiology*, **1** (11), pp. 16150.

Supplementary materials

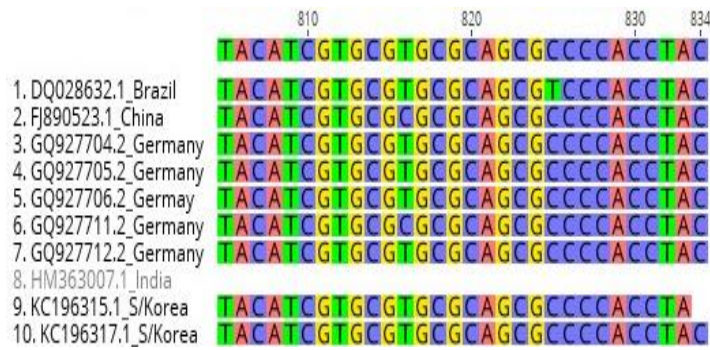
Supplementary 1

Figure 3.1S: Multiple sequence alignment of AiV-1 complete VP1 sequences used to design the VP1 primers in this study. The consensus sequence is shown on top of the alignment.









Supplementary 2

Table 3.1S: Reference AiV-1 5' UTR sequences from GenBank used in the study

Accession number	Country	Reference
JX564249.1	Taiwan	Chang <i>et al.</i> , 2013
KC167124.1	South Korea	Han <i>et al.</i> , 2014
KC167126.1	South Korea	Han <i>et al.</i> , 2014
KC196311.1	South Korea	Han <i>et al.</i> , 2014
KC167109.1	South Korea	Han <i>et al.</i> , 2014
AB040749.1	Japan	Sasaki <i>et al.</i> , 2001
DQ028632.1	Brazil	Oh <i>et al.</i> , 2006
FJ890523.1	China	Yang <i>et al.</i> , 2009
GQ927704.2	Germany	Drexler <i>et al.</i> , 2011
GQ927705.2	Germany	Drexler <i>et al.</i> , 2011
GQ927706.2	Germany	Drexler <i>et al.</i> , 2011
GQ927711.2	Germany	Drexler <i>et al.</i> , 2011

Supplementary 3

Table 3.2S: Reference AiV-1 partial 3CD sequences from GenBank used in the study

Accession number	Country	Reference
AB092827.1	Japan	Yamashita <i>et al.</i> , 2000
AB034655.1	Indonesia	Yamashita <i>et al.</i> , 2000
JN584165.1	Sweden	Jonsson <i>et al.</i> , 2012
JN584164.1	Sweden	Jonsson <i>et al.</i> , 2012
EU159251.1	France	Ambert-Balay <i>et al.</i> , 2008
EF079160.1	Thailand	Pham <i>et al.</i> , 2007
AB034657.1	Malaysia	Yamashita <i>et al.</i> , 2000
AB034653.1	Japan	Yamashita <i>et al.</i> , 2000
AB034663.1	Thailand	Yamashita <i>et al.</i> , 2000
GU459258.1	China	Wu, 2010 (unpublished)
FJ890520.1	China	Yang <i>et al.</i> , 2009
EU715251.1	Australia	Northill <i>et al.</i> , 2012 (unpublished)
JQ792245.1	Australia	Northill <i>et al.</i> , 2012 (unpublished)
NC_004421.1	Japan	Yamashita <i>et al.</i> , 2003
AB010145.1	Japan	Yamashita <i>et al.</i> , 1998
NC_011829.1	Hungary	Reuter <i>et al.</i> , 2008
KJ743982.1	Tunisia	Chourouk <i>et al.</i> , 2014 (unpublished)
FJ878794.1	Tunisia	Sdiri-Loulizi <i>et al.</i> , 2009
FJ878782.1	Tunisia	Sdiri-Loulizi <i>et al.</i> , 2009
LN612595.1	Burkina Faso	Ouédraogo <i>et al.</i> , 2016
LN612594.1	Burkina Faso	Ouédraogo <i>et al.</i> , 2016
LN612593.1	Burkina Faso	Ouédraogo <i>et al.</i> , 2016
LN612592.1	Burkina Faso	Ouédraogo <i>et al.</i> , 2016
KU860563.1	Nigeria	Japhet <i>et al.</i> , 2016 (unpublished)
DQ145759.1	Mali	Ambert-Balay <i>et al.</i> , 2008

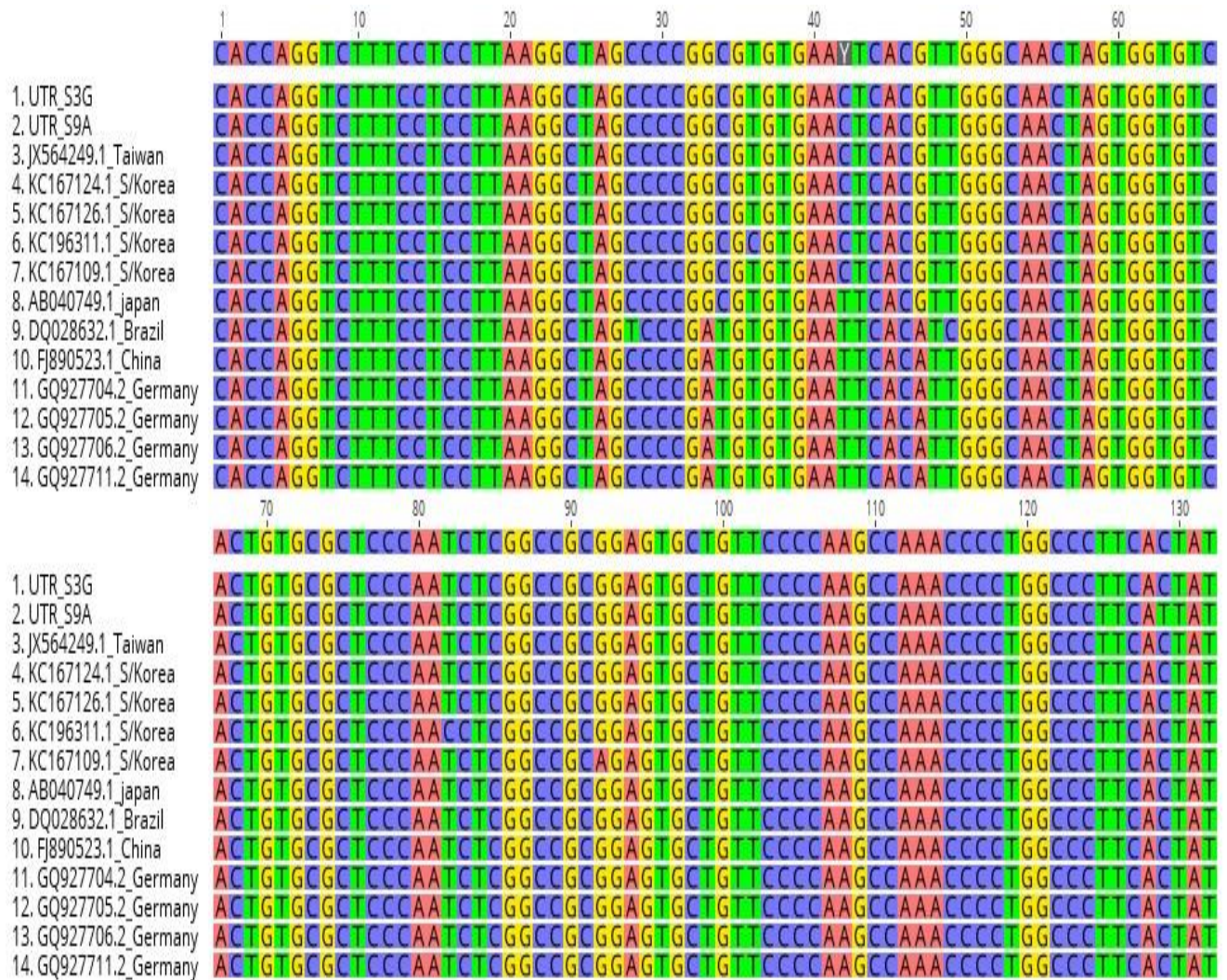
Supplementary 4

Table 3.3S: Reference AiV-1 partial VP1 sequences from GenBank used in the study

Accession number	Country	Reference
KC167094.1	South Korea	Han <i>et al.</i> , 2014
KC167087.1	South Korea	Han <i>et al.</i> , 2014
KC708818.1	Netherlands	Lodder <i>et al.</i> , 2013
KC708821.1	Netherlands	Lodder <i>et al.</i> , 2013
DQ206639.2	France	Bon <i>et al.</i> , 2005 (unpublished)
EU159253	France	Ambert-Balay <i>et al.</i> , 2008
EU159255.1	France	Ambert-Balay <i>et al.</i> , 2008
GQ927711.2	Germany	Drexler <i>et al.</i> , 2011
EU159260.1	France	Ambert-Balay <i>et al.</i> , 2008
DQ206641.1	France	Bon <i>et al.</i> , 2005 (unpublished)
JN584162.1	Sweden	Jonsson <i>et al.</i> , 2012
AB010145.1	Japan	Yamashita <i>et al.</i> , 1998
GQ927707.1	Germany	Drexler <i>et al.</i> , 2011
HM363006.1	India	Verma <i>et al.</i> , 2011
FJ890523.1	China	Yang <i>et al.</i> , 2009
EU159259.1	France	Ambert-Balay <i>et al.</i> , 2008
NC_004421.1	Japan	Yamashita <i>et al.</i> , 2003

Supplementary 5

Figure 3.2S: Multiple sequence alignment of AiV-1 5' UTR sequences for isolates from the present study and reference isolates from GenBank. The consensus sequence is shown on top of the alignment.



140 150 160 170 180 190

GTGCTGGCAAGCATATCTGAGAAGGTGTTCCGCTGTGGCTGCCAGCCTGGTAACAGGTGCCCCAG

1. UTR_S3G
 2. UTR_S9A
 3. JX564249.1_Taiwan
 4. KC167124.1_S/Korea
 5. KC167126.1_S/Korea
 6. KC196311.1_S/Korea
 7. KC167109.1_S/Korea
 8. AB040749.1_japan
 9. DQ028632.1_Brazil
 10. FJ890523.1_China
 11. GQ927704.2_Germany
 12. GQ927705.2_Germany
 13. GQ927706.2_Germany
 14. GQ927711.2_Germany

200 210 220 230 240 250 260

TGTGCGTAAACCTTCTTCCGCTCTTCGGACGGTAGTGATTGGTTAAGATTTGGTGTAAAGGTTTCATGTG

1. UTR_S3G
 2. UTR_S9A
 3. JX564249.1_Taiwan
 4. KC167124.1_S/Korea
 5. KC167126.1_S/Korea
 6. KC196311.1_S/Korea
 7. KC167109.1_S/Korea
 8. AB040749.1_japan
 9. DQ028632.1_Brazil
 10. FJ890523.1_China
 11. GQ927704.2_Germany
 12. GQ927705.2_Germany
 13. GQ927706.2_Germany
 14. GQ927711.2_Germany

270 280 290 300 310 320 330

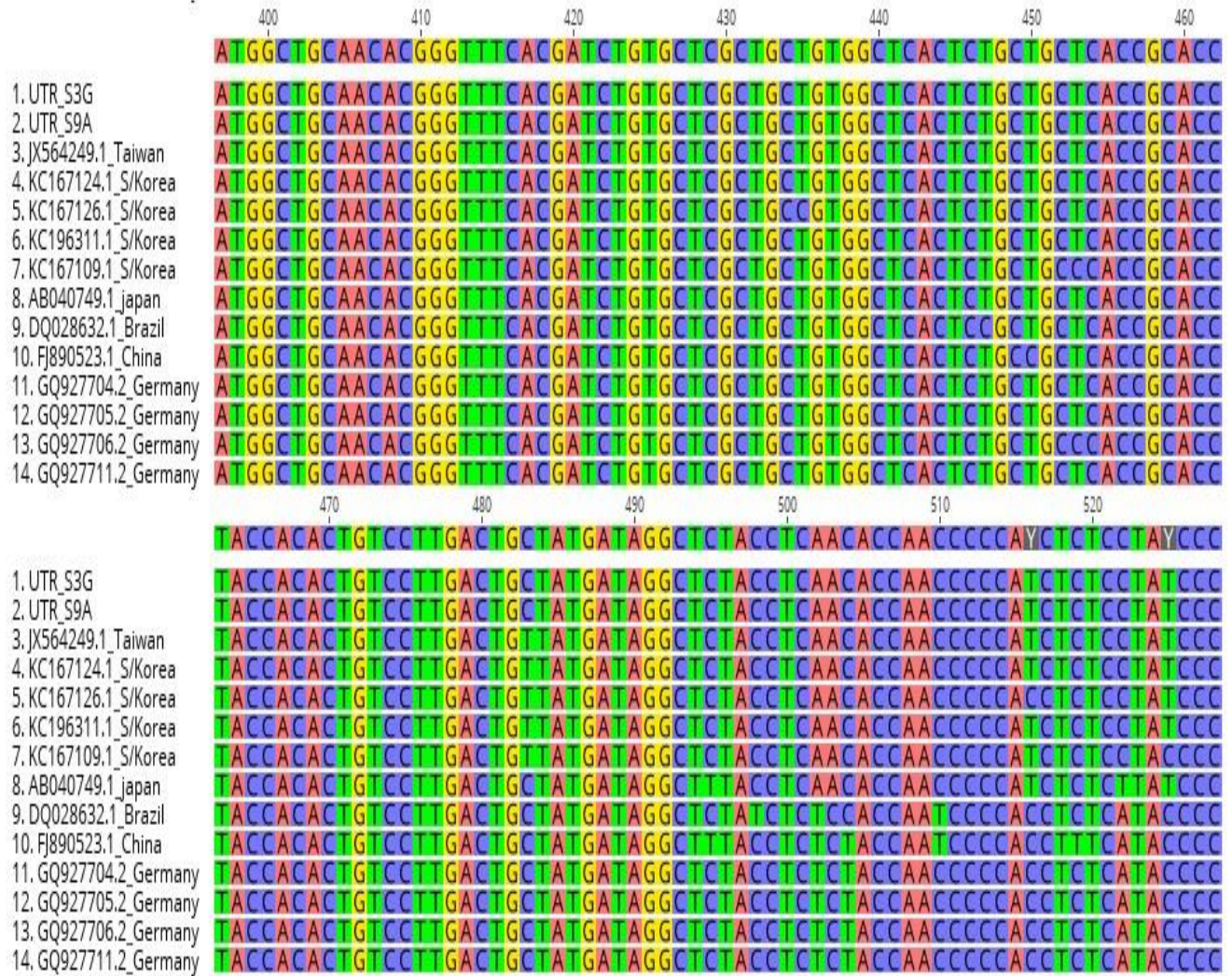
1. UTR_S3G
 2. UTR_S9A
 3. JX564249.1_Taiwan
 4. KC167124.1_S/Korea
 5. KC167126.1_S/Korea
 6. KC196311.1_S/Korea
 7. KC167109.1_S/Korea
 8. AB040749.1_japan
 9. DQ028632.1_Brazil
 10. FJ890523.1_China
 11. GQ927704.2_Germany
 12. GQ927705.2_Germany
 13. GQ927706.2_Germany
 14. GQ927711.2_Germany

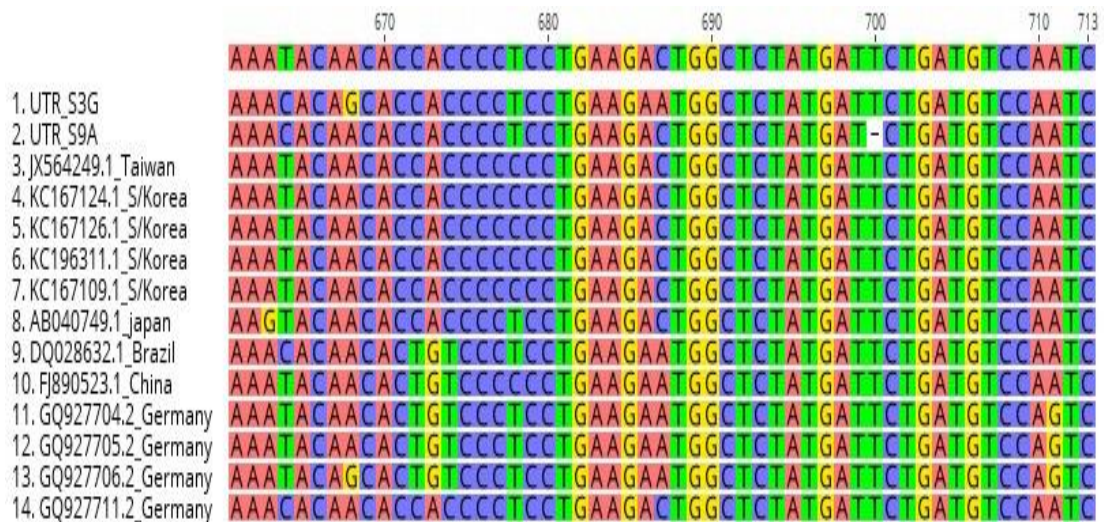
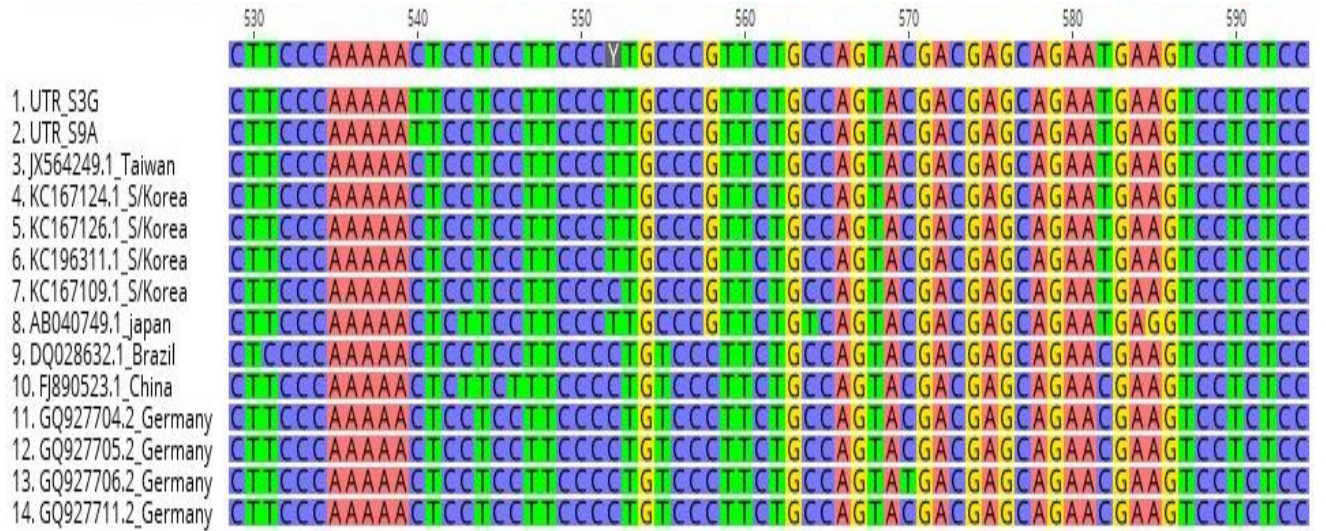
CC AACGCCCTGTGCGGGATGAAACCTCTACTGCCCTAGGAATGCCAGGCAGGTACCCACCTTCGG
 CC AACGCCCTGTGCGGGATGAAACCTCTACTGCCCTAGGAATGCCAGGCAGGTACCCACCTTCGG
 CC AACGCCCTGTGCGGGATGAAACCTCTACTGCCCTAGGAATGCCAGGCAGGTACCCACCTTCGG
 CC AACGCCCTGTGCGGGATGAAACCTCTACTGCCCTAGGAATGCCAGGCAGGTACCCACCTTCGG
 CC AACGCCCTGTGCGGGATGAAACCTCTACTGCCCTAGGAATGCCAGGCAGGTACCCACCTTCGG
 CC AACGCCCTGTGCGGGATGAAACCTCTACTGCCCTAGGAATGCCAGGCAGGTACCCACCTTCGG
 CC AACGCCCTGTGCGGGATGAAACCTCTACTGCCCTAGGAATGCCAGGCAGGTACCCACCTTCGG
 CC AACGCCCTGTGCGGGATGAAACCTCTACTGCCCTAGGAATGCCAGGCAGGTACCCACCTTCGG
 CC AACGCCCTGTGCGGGATGAAACCTCTACTGCCCTAGGAATGCCAGGCAGGTACCCACCTTCGG
 CC AACGCCCTGTGCGGGATGAAACCTCTACTGCCCTAGGAATGCCAGGCAGGTACCCACCTTCGG
 CC AACGCCCTGTGCGGGATGAAACCTCTACTGCCCTAGGAATGCCAGGCAGGTACCCACCTTCGG
 CC AACGCCCTGTGCGGGATGAAACCTCTACTGCCCTAGGAATGCCAGGCAGGTACCCACCTTCGG
 CC AACGCCCTGTGCGGGATGAAACCTCTACTGCCCTAGGAATGCCAGGCAGGTACCCACCTTCGG
 CC AACGCCCTGTGCGGGATGAAACCTCTACTGCCCTAGGAATGCCAGGCAGGTACCCACCTTCGG
 CC AACGCCCTGTGCGGGATGAAACCTCTACTGCCCTAGGAATGCCAGGCAGGTACCCACCTTCGG
 CC AACGCCCTGTGCGGGATGAAACCTCTACTGCCCTAGGAATGCCAGGCAGGTACCCACCTTCGG

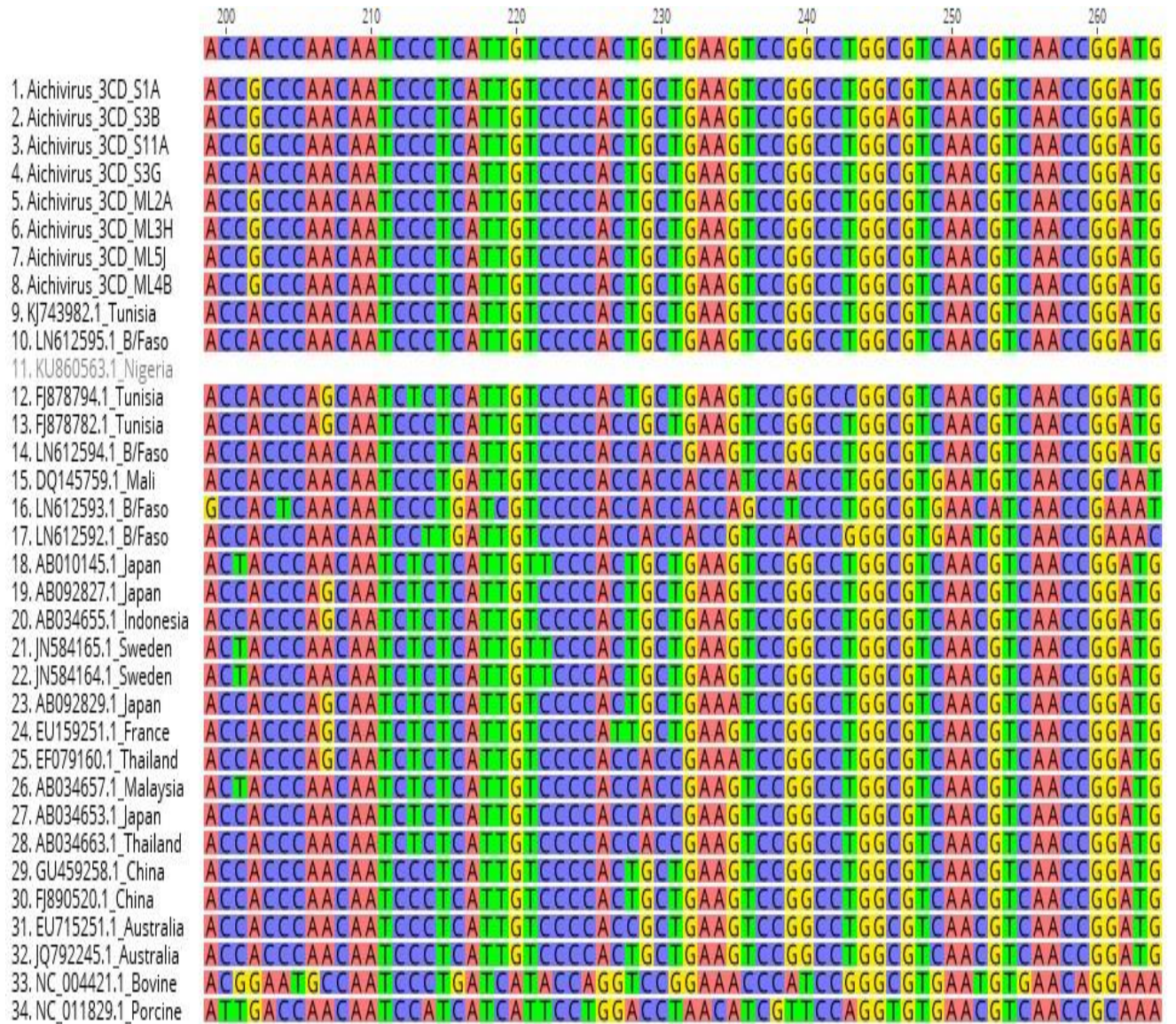
340 350 360 370 380 390

1. UTR_S3G
 2. UTR_S9A
 3. JX564249.1_Taiwan
 4. KC167124.1_S/Korea
 5. KC167126.1_S/Korea
 6. KC196311.1_S/Korea
 7. KC167109.1_S/Korea
 8. AB040749.1_japan
 9. DQ028632.1_Brazil
 10. FJ890523.1_China
 11. GQ927704.2_Germany
 12. GQ927705.2_Germany
 13. GQ927706.2_Germany
 14. GQ927711.2_Germany

GTGGGATCTGAGCCTGGGCTAATTGTCTACGGGTAGTTTCATTTCCAAATCTTTATGTGCGGAGTCT
 GTGGGATCTGAGCCTGGGCTAATTGTCTACGGGTAGTTTCATTTCCAAATCTTTATGTGCGGAGTCT
 GTGGGATCTGAGCCTGGGCTAATTGTCTACGGGTAGTTTCATTTCCAAATCTTTATGTGCGGAGTCT
 GTGGGATCTGAGCCTGGGCTAATTGTCTACGGGTAGTTTCATTTCCAAATCTTTATGTGCGGAGTCT
 GTGGGATCTGAGCCTGGGCTAATTGTCTACGGGTAGTTTCATTTCCAAATCTTTATGTGCGGAGTCT
 GTGGGATCTGAGCCTGGGCTAATTGTCTACGGGTAGTTTCATTTCCAAATCTTTATGTGCGGAGTCT
 GTGGGATCTGAGCCTGGGCTAATTGTCTACGGGTAGTTTCATTTCCAAATCTTTATGTGCGGAGTCT
 GTGGGATCTGAGCCTGGGCTAATTGTCTACGGGTAGTTTCATTTCCAAATCTTTATGTGCGGAGTCT
 GTGGGATCTGAGCCTGGGCTAATTGTCTACGGGTAGTTTCATTTCCAAATCTTTATGTGCGGAGTCT
 GTGGGATCTGAGCCTGGGCTAATTGTCTACGGGTAGTTTCATTTCCAAATCTTTATGTGCGGAGTCT
 GTGGGATCTGAGCCTGGGCTAATTGTCTACGGGTAGTTTCATTTCCAAATCTTTATGTGCGGAGTCT
 GTGGGATCTGAGCCTGGGCTAATTGTCTACGGGTAGTTTCATTTCCAAATCTTTATGTGCGGAGTCT
 GTGGGATCTGAGCCTGGGCTAATTGTCTACGGGTAGTTTCATTTCCAAATCTTTATGTGCGGAGTCT
 GTGGGATCTGAGCCTGGGCTAATTGTCTACGGGTAGTTTCATTTCCAAATCTTTATGTGCGGAGTCT
 GTGGGATCTGAGCCTGGGCTAATTGTCTACGGGTAGTTTCATTTCCAAATCTTTATGTGCGGAGTCT
 GTGGGATCTGAGCCTGGGCTAATTGTCTACGGGTAGTTTCATTTCCAAATCTTTATGTGCGGAGTCT

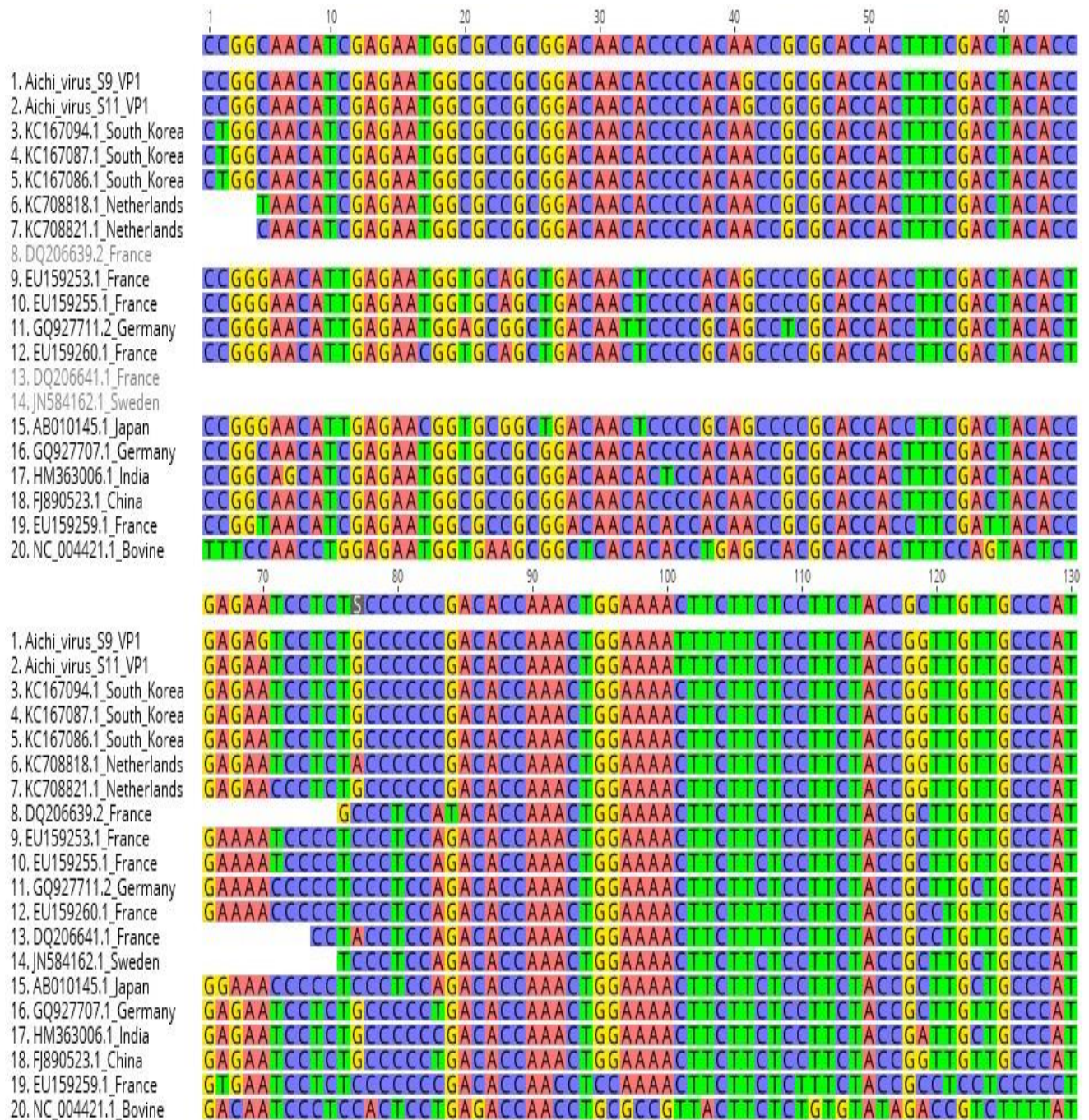


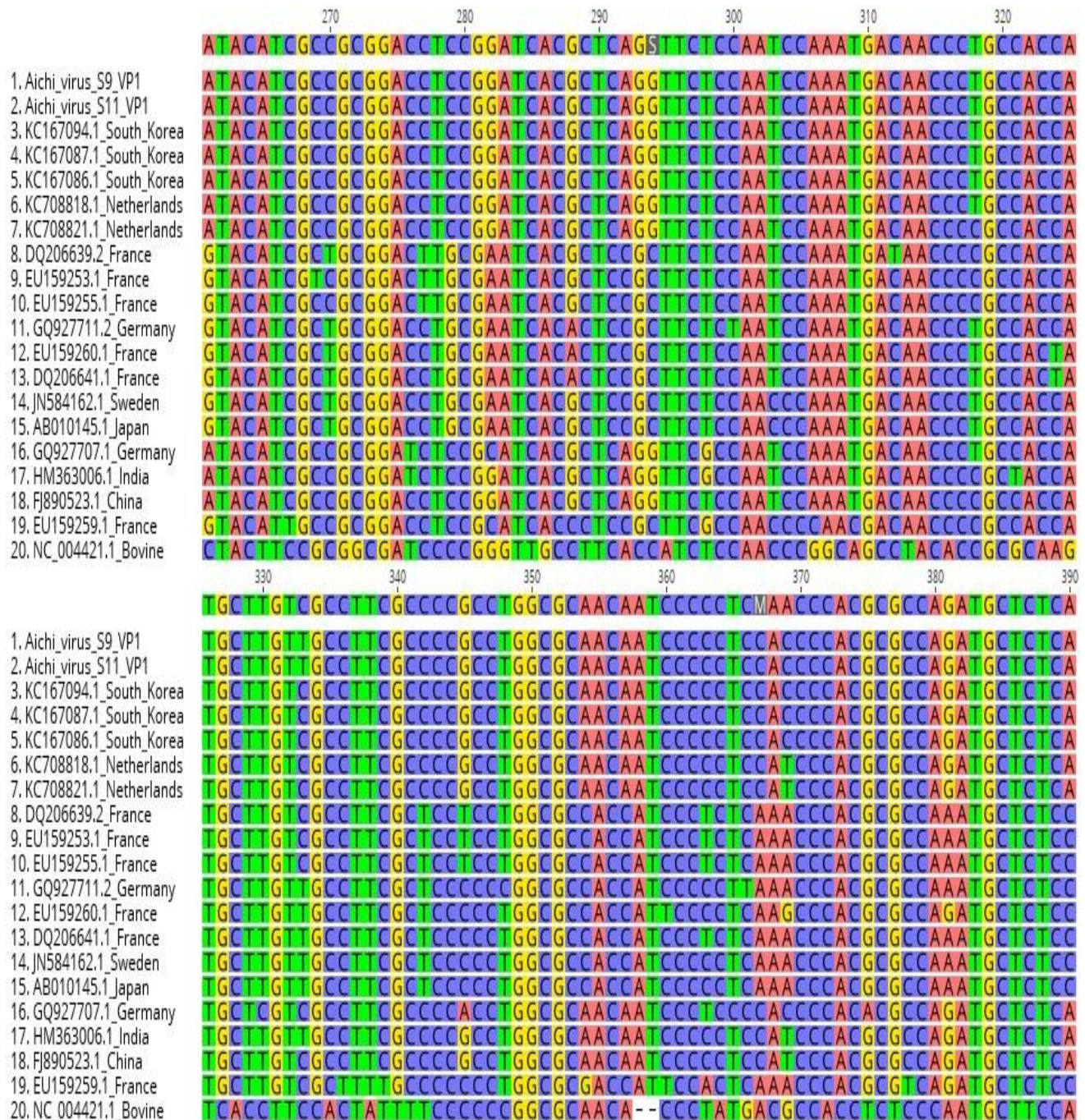




Supplementary 7

Figure 3.4S: Multiple sequence alignment of AiV-1 partial VP1 coding region for isolates from the present study and reference isolates from GenBank. The consensus sequence is shown on top of the alignment.





Supplementary 8

Table 4.1S: Reference HBoV isolates from GenBank used in the study

Accession number	Genotype	Country	Reference
JX887481.1	1	China	Wang <i>et al.</i> , 2012
HQ288043.1	1	Kenya	Misigo <i>et al.</i> , 2014
DQ317559.1	1	South Africa	Smuts and Hardie, 2006
DQ317557.1	1	South Africa	Smuts and Hardie, 2006
EU189108.1	1	South Africa	Smuts <i>et al.</i> , 2008
FJ973558.1	2	Tunisia	Kapoor <i>et al.</i> , 2010
GQ506584.1	2A	Nigeria	Kapoor <i>et al.</i> , 2010
LN890355.1	2	Albania	La Rosa <i>et al.</i> , 2016
FJ948860.1	2	Australia	Arthur <i>et al.</i> , 2009
FJ170278.1	2	Pakistan	Kapoor <i>et al.</i> , 2009
GU048662.1	2	Thailand	Chieochansin <i>et al.</i> , 2010
GQ506629.1	3	Tunisia	Kapoor <i>et al.</i> , 2010
GQ506602.1	3	Nigeria	Kapoor <i>et al.</i> , 2010
HM132056.1	3	China	Wang <i>et al.</i> , 2011
NC_012564.1	3	Australia	Arthur <i>et al.</i> , 2009
JN086998.1	3	USA	Kapoor <i>et al.</i> , 2011
GQ867666.1	3	Brazil	Santos <i>et al.</i> , 2010
FJ973561.2	4	Nigeria	Kapoor <i>et al.</i> , 2010
GQ506632.1	4	Tunisia	Kapoor <i>et al.</i> , 2010

1. ML4A
2. ML6C
3. S4A
4. S4C
5. S6A
6. S6B
7. FJ973558.1_HBoV_2a_Tunisia
8. GQ506629.1_HBoV_3_Tunisia
9. GQ506632.1_HBoV_4_Tunisia
10. GQ506584.1_HBoV_2A_Nigeria
11. GQ506602.1_HBoV_3_Nigeria
12. LN890355.1_HBoV_2_Albania
13. FJ948860.1_HBoV_2_Australia
14. FJ170278.1_HBoV_2c_Pakistan
15. GU048662.1_HBoV_2_Thailand
16. HM132056.1_HBoV_3_China
17. NC_012564.1_HBoV_3_Australia
18. JN086998.1_HBoV_3_USA
19. GQ867666.1_HBoV_3_Brazil
20. HQ288043.1_HBoV_1_Kenya
21. DQ317559.1_HBoV_1_S/Africa
22. DQ317557.1_HBoV_1_S/Africa
23. EU189108.1_HBoV_1_S/Africa
24. JX887481.1_HBoV_1_China
25. FJ973561.2_HBoV_4_Nigeria

```

      130           140           150           160           170           180
TGGAAAAAATCCTTACTTGT -- ATTTCAATAAAGCTGATGAAAAATTCATTGACGATTTGAA
TGGAAAAAATCCTTACTTGT -- ATTTCAATAAAGCTGATGAAAAATTCATTGACGATTTGAA
TGGAAAAAATCCTTACTTGT -- ATTTCAATAAAGCTGATGAAAAATTCATTGACGATTTGAA
TGGAAAGAATCCTTACTTAT -- ATTTCAATAAAGCTGATGAAAAATTCATTGACGATTTGAA
TGGAAAGAATCCTTACTTAT -- ATTTCAATAAAGCTGATGAAAAATTCATTGACGATTTGAA
TGGAAAGAATCCTTACTTAT -- ATTTCAATAAAGCTGATGAAAAATTCATTGACGATTTGAA
TGGAAAGAATCCTTACTTAT -- ATTTCAATAAAGCTGATGAAAAATTCATTGACGATTTGAA
TGGAAAAAATCCTTACTTGT -- ATTTCAATAAAGCTGATGAGAAAATTCATTGACGATTTGAA

```

1. ML4A
2. ML6C
3. S4A
4. S4C
5. S6A
6. S6B
7. FJ973558.1_HBoV_2a_Tunisia
8. GQ506629.1_HBoV_3_Tunisia
9. GQ506632.1_HBoV_4_Tunisia
10. GQ506584.1_HBoV_2A_Nigeria
11. GQ506602.1_HBoV_3_Nigeria
12. LN890355.1_HBoV_2_Albania
13. FJ948860.1_HBoV_2_Australia
14. FJ170278.1_HBoV_2c_Pakistan
15. GU048662.1_HBoV_2_Thailand
16. HM132056.1_HBoV_3_China
17. NC_012564.1_HBoV_3_Australia
18. JN086998.1_HBoV_3_USA
19. GQ867666.1_HBoV_3_Brazil
20. HQ288043.1_HBoV_1_Kenya
21. DQ317559.1_HBoV_1_S/Africa
22. DQ317557.1_HBoV_1_S/Africa
23. EU189108.1_HBoV_1_S/Africa
24. JX887481.1_HBoV_1_China
25. FJ973561.2_HBoV_4_Nigeria

```

TGGAAAAAATCCTTACTTGT -- ATTTCAATAAAGCTGATGAGAAAATTCATTGACGATTTGAA
TGGAAAAAATCCTTACTTGT -- ATTTCAATAAAGCTGATGATAAAATTCATTGACGATTTGAA
TGGAAAAAATCCTTACTTGT -- ATTTCAATAAAGCTGATGAAAAATTCATTGACGATTTGAA
TGGAAAAAATCCTTACTTGT -- ATTTCAATAAAGCTGATGAAAAATTCATTGACGATTTGAA
TGGAAAAAATCCTTACTTAT -- ATTTCAATAAAGCTGATGAAAAATTCATTGACGATTTGAA
TGGAAAAAATCCTTACTTAT -- ATTTCAATAAAGCTGATGAAAAATTCATTGACGATTTGAA
TGGAAAAAATCCTTACTTAT -- ATTTCAATAAAGCTGATGAAAAATTCATTGACGATTTGAA
TGGAAAAAATCCTTACTTAT -- ATTTCAATAAAGCTGATGAAAAATTCATTGACGATTTGAA
TGGAAAAAATCCTTACTTAT -- ATTTCAATAAAGCTGATGAAAAATTCATTGACGATTTGAA
TGGAAAAAATCCTTACTTAT -- ATTTCAATAAAGCTGATGAAAAATTCATTGACGATTTGAA
GATGACAGGACCTGGCCTGCTCAGTGCACAGAGAGTAGGACCACAGTCATCAGACACTGCTC
GATGACAGGACCTGGCCTGCTCAGTGCACAAAGAGTAGGACCACAGTCATCAGACACTGCTC
GATGACAGGACCTGGCCTGCTCAGTGCACAAAGAGTAGGACCACAGTCATCAGACACTGCTC
GATGACAGGACCTGGCCTGCTCAGTGCACAAAGAGTAGGACCACAGTCATCAGACACTGCTC
GATGACAGGACCTGGCCTGCTCAGTGCACAAAGAGTAGGACCACAGTCATCAGACACTGCTC
TGGAAAAAATCCTTACTTAT -- ATTTCAATAAAGCTGATGAAAAATTCATTGACGATTTGAA

```

```

      190           200           210           220           230           240
AAACGACTGGTCTCTGGTGGCATTATTGGCTCAAGTTTCTTAAACTTAAGCGCGCCGTGG
AAACGACTGGTCTCTGGTGGCATTATTGGCTCAAGTTTCTTAAACTTAAGCGCGCCGTGG
AAACGACTGGTCCCTGGTGGCATTATTGGCCCAAGTTTCTTAAACTTAAGCGCGCCGTGG
AAACGACTGGTCTCTGGTGGCATTATTGGCTCAAGTTTCTTAAACTTAAGCGCGCCGTGG
AAACGACTGGTCTCTGGTGGCATTATTGGCTCAAGTTTCTTAAACTTAAGCGCGCCGTGG
AAACGACTGGTCTCTGGTGGCATTATTGGCTCAAGTTTCTTAAACTTAAGCGCGCCGTGG
AAACGACTGGTCTCTGGTGGCATTATTGGCTCAAGTTTCTTAAACTTAAGCGCGCCGTGG
AAACGACTGGTCTCTGGTGGCATTATTGGCTCAAGTTTCTTAAACTTAAGCGCGCCGTGG

```

```

AAACGACTGGTCTCTAGTGGCATTATTGGCTCAAGTTTCTTAAACTTAAGCGCGCCGTGG
AAACGACTGGTCTCTGGTGGCATTATTGGCTCAAGTTTCTTAAACTTAAGCGCGCCGTGG
AAACGACTGGTCTCTGGTGGCATTATTGGCTCAAGTTTCTTAAACTTAAGCGCGCCGTGG
AAACGACTGGTCTCTGGTGGCATTATTGGCTCAAGTTTCTTAAACTTAAGCGCGCCGTGG
AAACGACTGGTCTCTGGTGGCATTATTGGCTCAAGTTTCTTAAACTTAAGCGCGCCGTGG
AAACGACTGGTCTCTGGTGGCATTATTGGCTCAAGTTTCTTAAACTTAAGCGCGCCGTGG
AAACGACTGGTCTCTGGTGGCATTATTGGCTCAAGTTTCTTAAACTTAAGCGCGCCGTGG
AAACGACTGGTCTCTGGTGGCATTATTGGCTCAAGTTTCTTAAACTTAAGCGCGCCGTGG
AAACGACTGGTCTCTGGTAGCATTATTGGCTCAAGTTTCTTAAACTTAAGCGCGCCGTGG
CATTTCATGGTTTGCACTAACCCAGAAGGAACACACATAAACACAGG - TGCTGCAGGATTTGG
CATTTCATGGTTTGCACTAACCCAGAAGGAACACACATAAACACAGG - TGCTGCAGGATTTGG
CATTTCATGGTTTGCACTAACCCAGAAGGAACACACATAAACACAGG - TGCTGCAGGATTTGG
CATTTCATGGTTTGCACTAACCCAGAAGGAACACACATAAACACAGG - TGCTGCAGGATTTGG
CATTTCATGGTTTGCACTAACCCAGAAGGAACACACATAAACACAGG - TGCTGCAGGATTTGG
AGACGATGGTCTCTGGTGGCATTATTGGCTCAAGTTTCTTAAACTTAAGCGCGCCGTGG

```


380

389

	G A A A A T G A A A T C C A A G A
1. ML4A	G A A A A T G A A A T T C A A G A
2. ML6C	G A A A A T G A A A T T C A A G A
3. S4A	G A A A A T G A A A T C C A A G A
4. S4C	G A A A A T G A A A T C C A A G A
5. S6A	G A A A A T G A A A T C C A A G A
6. S6B	G A A A A T G A A A T C C A A G A
7. FJ973558.1_HBoV_2a_Tunisia	G A A A A T G A A A T C C A A G A
8. GQ506629.1_HBoV_3_Tunisia	G A A A A T G A A A T T C A A G A
9. GQ506632.1_HBoV_4_Tunisia	G A A A A T G A A A T T C A A G A
10. GQ506584.1_HBoV_2A_Nigeria	G A A A A T G A A A T C C A A G A
11. GQ506602.1_HBoV_3_Nigeria	G A A A A T G A A A T T C A A G A
12. LN890355.1_HBoV_2_Albania	
13. FJ948860.1_HBoV_2_Australia	G A A A A T G A A A T C C A A G A
14. FJ170278.1_HBoV_2c_Pakistan	G A A A A T G A A A T C C A A G A
15. GU048662.1_HBoV_2_Thailand	G A A A A T G A A A T C C A A G A
16. HM132056.1_HBoV_3_China	G A A A A T G A A A T T C A A G A
17. NC_012564.1_HBoV_3_Australia	G A A A A T G A A A T T C A A G A
18. JN086998.1_HBoV_3_USA	G A A A A T G A A A T T C A A G A
19. GQ867666.1_HBoV_3_Brazil	G A A A A T G A A A T T C A A G A
20. HQ288043.1_HBoV_1_Kenya	A T G C T T A G A G A C C A A C T
21. DQ317559.1_HBoV_1_S/Africa	A T G C T T A G A G A C C A A C T
22. DQ317557.1_HBoV_1_S/Africa	A T G C T T A G A G A C C A A C T
23. EU189108.1_HBoV_1_S/Africa	A T G C T T A G A G A C C A A C T
24. JX887481.1_HBoV_1_China	A T G C T T A G A G A C C A A C T
25. FJ973561.2_HBoV_4_Nigeria	G A A A A T G A A A T T C A A G A

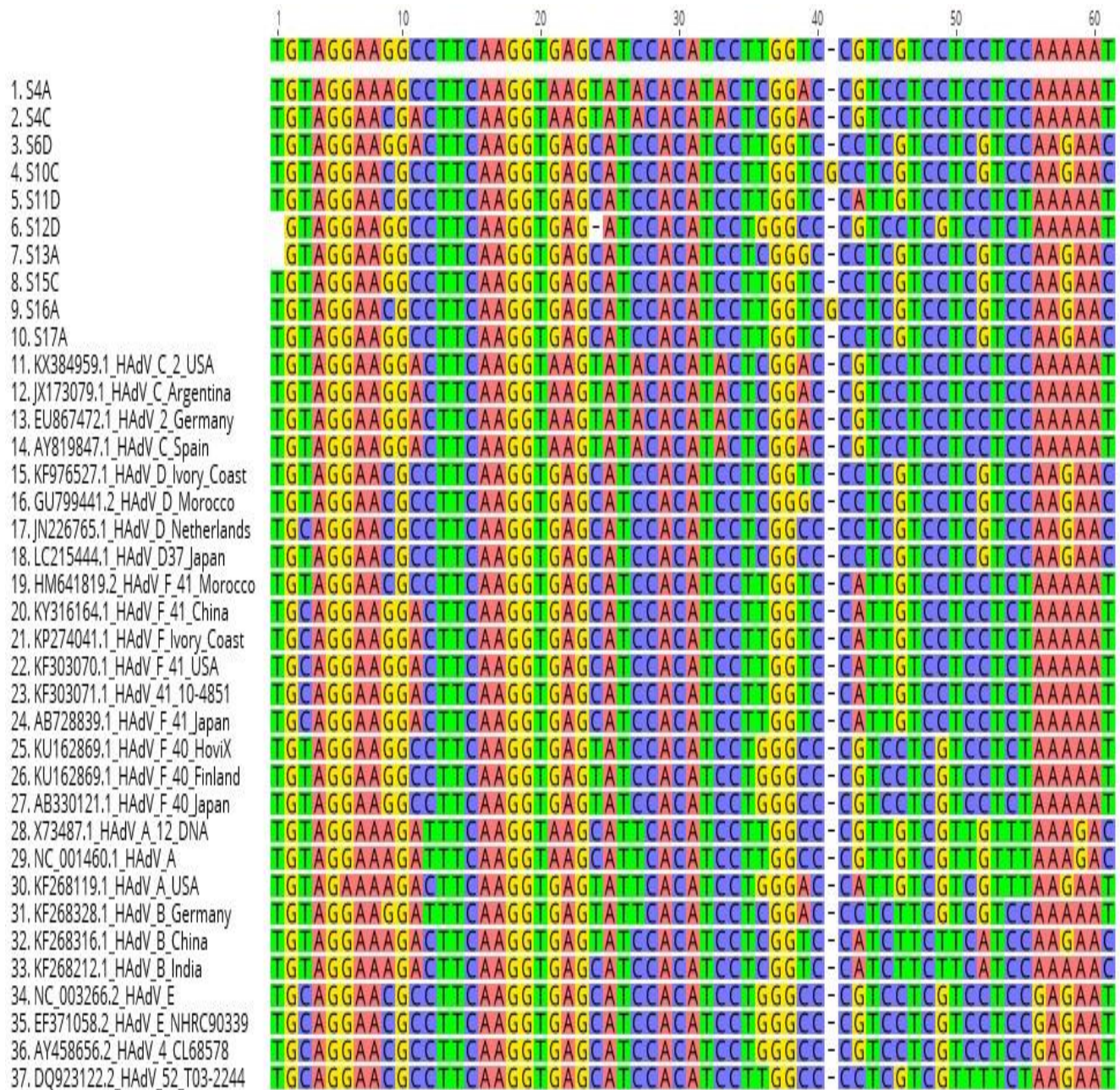
Supplementary 10

Table 5.1S: Reference HAdV sequences from GenBank used in the study

Accession number	Country	Reference
KX384959.1	USA	Hang <i>et al.</i> , 2017 (unpublished)
JX173079.1	Argentina	Madupu <i>et al.</i> , 2011 (unpublished)
EU867472.1	Germany	Biere and Schweiger, 2008
AY819847.1	Spain	Casas <i>et al.</i> , 2005
KF976527.1	Ivory Coast	Pauly <i>et al.</i> , 2014
GU799441.2	Morocco	Amdiouni <i>et al.</i> , 2012
JN226765.1	Netherlands	Singh <i>et al.</i> , 2013
HM641819.2	Morocco	Nourlil <i>et al.</i> , 2010
KY316164.1	Morocco	Yang <i>et al.</i> , 2016
KP274041.1	Ivory Coast	Pauly <i>et al.</i> , 2014
KF303070.1	USA	Lamson <i>et al.</i> , 2013
KF303071.1	USA	Lamson <i>et al.</i> , 2013
AB728839.1	Japan	Kinumaki <i>et al.</i> , 2012 (unpublished)
KU162869.1	Finland	Pacesa <i>et al.</i> , 2015 (unpublished)
EF371058.2	USA	Kajon <i>et al.</i> , 2007
AB330121.1	Japan	Ishiko <i>et al.</i> , 2008
X73487.1		Tolun <i>et al.</i> , 1979
NC_001460.1	USA	Sprengel <i>et al.</i> , 1994
KF268119.1	USA	Madupu <i>et al.</i> , 2013 (unpublished)
KF268328.1	Germany	Madupu <i>et al.</i> , 2013 (unpublished)
KF268316.1	China	Madupu <i>et al.</i> , 2013 (unpublished)
KF268212.1	India	Madupu <i>et al.</i> , 2013 (unpublished)
NC_003266.2		Jacobs <i>et al.</i> , 2004
AY458656.2	USA	Houng <i>et al.</i> , 2006
DQ923122.2	USA	Jones <i>et al.</i> , 2007

Supplementary 11

Figure 5.1S: Multiple sequence alignment of HAdV partial hexon coding region for isolates from the present study and reference isolates from GenBank. The consensus sequence is shown on top of the alignment.



1. S4A
2. S4C
3. S6D
4. S10C
5. S11D
6. S12D
7. S13A
8. S15C
9. S16A
10. S17A
11. KX384959.1_HAdV_C_2_USA
12. JX173079.1_HAdV_C_Argentina
13. EU867472.1_HAdV_2_Germany
14. AY819847.1_HAdV_C_Spain
15. KF976527.1_HAdV_D_Ivory_Coast
16. GU799441.2_HAdV_D_Morocco
17. JN226765.1_HAdV_D_Netherlands
18. LC215444.1_HAdV_D37_Japan
19. HM641819.2_HAdV_F_41_Morocco
20. KY316164.1_HAdV_F_41_China
21. KP274041.1_HAdV_F_Ivory_Coast
22. KF303070.1_HAdV_F_41_USA
23. KF303071.1_HAdV_41_10-4851
24. AB728839.1_HAdV_F_41_Japan
25. KU162869.1_HAdV_F_40_HoviX
26. KU162869.1_HAdV_F_40_Finland
27. AB330121.1_HAdV_F_40_Japan
28. X73487.1_HAdV_A_12_DNA
29. NC_001460.1_HAdV_A
30. KF268119.1_HAdV_A_USA
31. KF268328.1_HAdV_B_Germany
32. KF268316.1_HAdV_B_China
33. KF268212.1_HAdV_B_India
34. NC_003266.2_HAdV_E
35. EF371058.2_HAdV_E_NHRC90339
36. AY458656.2_HAdV_4_CL68578
37. DQ923122.2_HAdV_52_T03-2244

